Contribution à la modélisation et à la simulation des écoulements complexes : application à la rentrée atmosphérique et aux interactions particules-fluide

Julien Mathiaud

UNIVERSITÉ DE BORDEAUX

MÉMOIRE PRÉSENTÉ EN VUE DE
L' HABILITATION À DIRIGER DES RECHERCHES

Contribution à la modélisation et à la simulation des écoulements complexes : application à la rentrée atmosphérique et aux interactions particules-fluide

---

Author:
Julien MATHIAUD (CEA)

Soutenue devant le jury composé de:

M. Groppi (rapporteur), professeur (université de Parme)
R. Loubère (rapporteur), directeur de recherches au CNRS (université de Bordeaux)
T. Magin (rapporteur), professeur au Von Karman Institute (Bruxelles)
S. Bernard, ingénieur/chercheur (CEA/DAM, Bruyères-le-Châtel)
B. Desjardins, directeur scientifique (Modélisation, Mesures et Applications,Paris)
L. Desvillettes, professeur (université Paris Diderot)
P. Lafitte-Godillon, professeur (Ecole Centrale de Paris)
L. Mieussens, professeur (université de Bordeaux)
D. Vanderhaegen, directeur du programme simulation (CEA/DAM)
P. Villedieu, directeur scientifique (DMPE, ONERA, Toulouse)

1st of June 2018

To Naël,
Ewen, Maïa, Ethan and Gilliane
with all my love.

"Try not to become a man of success, but rather try to become a man of value."

Albert Einstein

Abstract

Julien MATHIAUD (CEA)

Contribution à la modélisation et à la simulation des écoulements complexes : application à la rentrée atmosphérique et aux interactions particules-fluide

This manuscript is devoted to the presentation of the different studies that I have done since 2003 and the beginning of my Phd at the French Atomic Agency (CEA). I will try to put in perspective all the things done since then and give guidelines of what I should explore later. The works presented here essentially deal with the physics of atmospheric reentry and fluid-particles interactions. For these two mains applications we focus on models, mathematical properties, numerical results and experimental results.

Acknowledgements

This manuscript represents fifteen years of work at the French Atomic Agency. All the work presented could not have been done without my colleagues in Bruyères-le-Châtel and Le Barp: it is also their manuscript.

I first want to thank all the members of the jury for reading the manuscript and coming to the defence, especially the three referees Maria Groppi, Raphaël Loubère and Thierry Magin. It has also been a pleasure to have Pauline Laffitte-Godillon as a president of the jury and Philippe Villedieu, Stéphane Bernard and Daniel Vanderhaegen as members of the jury.

I am grateful to Benoît Desjardins and Laurent Desvillettes to still be there ten years after my phd with their advices: I owe them a lot and I hope they are proud of the result.

Finally I want to thank Luc Mieussens and Céline Baranger: without them the rarefied gas dynamics part of the manuscript would not exist. Luc has always look anxious when I come with another "idea" but every time we managed to polish that idea so that it could be used. Concerning Céline, she has always been there since my phd and I want to thank her for that: friendship and human relationships are crucial in our field and nothing can be done without that in the good and bad moments.

I want also to thank people with whom I have worked along these years: L. Boudin, P. Congedo, F. James, F. Lagouttière, F. Salvarani, N. Vauchelet and G. Vignoles outside the CEA, Claire B. , Corinne A. , Thierry P. , Jean-Philippe P., Vincent R., Christophe F., Laurent S. , Marina O., Jean C. , Marielle V. inside. This manuscript owes a lot to the careful reading of Xavier Carlotti and Pierre-Henri Maire: they made me come to Bordeaux and I hope the result is worth it. I want to thank David Goudin and Anne-Pascale Leroux for helping me in organizing this defence and not only for that.

To end up, this manuscript is for **Naël** and my whole family: Ewen, Maïa, Ethan and Gilliane.

Contents

Part I

Introduction

Context

This manuscript deals with ten years of research that have been done at the French Atomic Agency (CEA) as a Phd student and later on as an engineer and an associate professor at Bordeaux INP (Enseirb/Matmeca). It was made possible through internal collaborations and also with people at CMLA (ENS Cachan), at LJLL (Jussieu, Paris), IMB (Bordeaux) and LCTS (Bordeaux). The models, results and numerics that are presented here are generally linked with applications at CEA. Three main topics have appeared during these ten years:

- rarefied gas dynamics,
- turbulence and interaction fluid/solid,
- spray interactions.

These three main topics are principally connected with two domains of applications:

- atmospheric reentry (for the first two topics),
- fluid/particle interactions (for the third one).

In this manuscript we give the advances made during these years concerning:

- models,
- theoretical results (on these models),
- numerical methods,
- model validation.

These four subjects are of equal importance for the engineer who needs models that have correct physical and mathematical backgrounds and that can be numerically solved and validated through robust methods. Of course the works presented here have different levels of complexity but they all have the same objective: go further in the comprehension of the phenomena we will encounter.

Some physics

We now briefly describe the physics that is encountered in the manuscript.

Physics of reentry

During the atmospheric reentry of a vehicle of several meters, it encounters several layers in atmosphere (thermosphere, mesosphere, stratosphere and troposphere: see figure 1). At the beginning ($> 120km$) atmosphere is very rarefied so that free transport of molecules of dioxygen and nitrogen essentially governs the behavior of the flow . Then some collisions between molecules appear when atmosphere is less rarefied ($> 70km$) and chemistry phenomena appear: Boltzmann equation rules the phenomena. Finally when atmosphere is dense enough the flow is controlled by Navier-Stokes equation (in laminar regime and closer to the ground in turbulent regime).

All these flows are characterized by high temperatures ($> 1000K$) and high Mach numbers: these two phenomena are hard to emulate by ground facilities so that validation is always difficult to

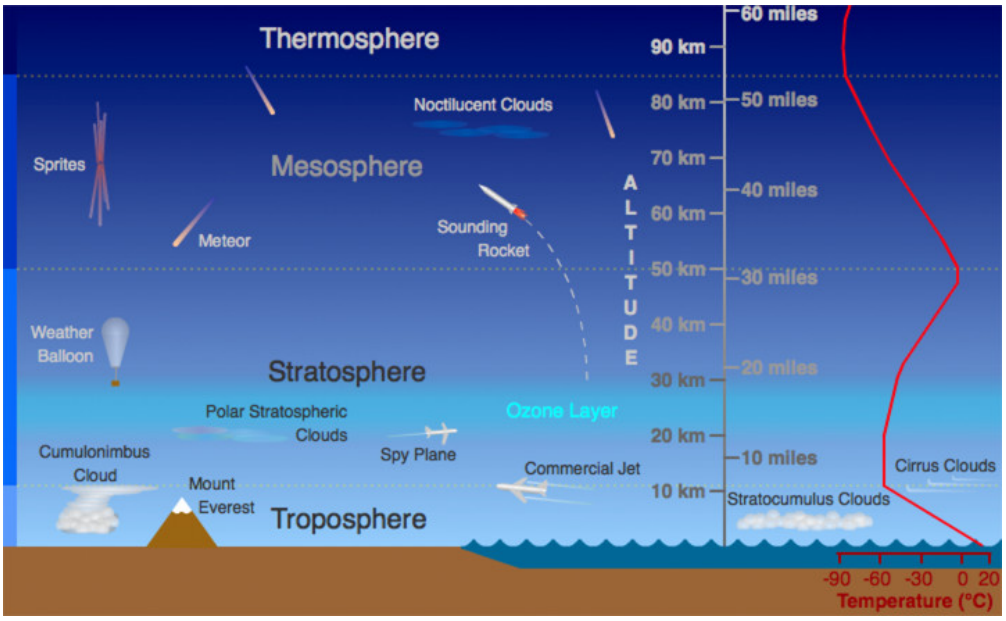

FIGURE 1: Atmosphere layers (credit: UCAR)

perform. Moreover the kind of entry (lifting or ballistic as it can be seen in figure (2)) leads to different phenomena to study with high velocities at stake included near the ground.

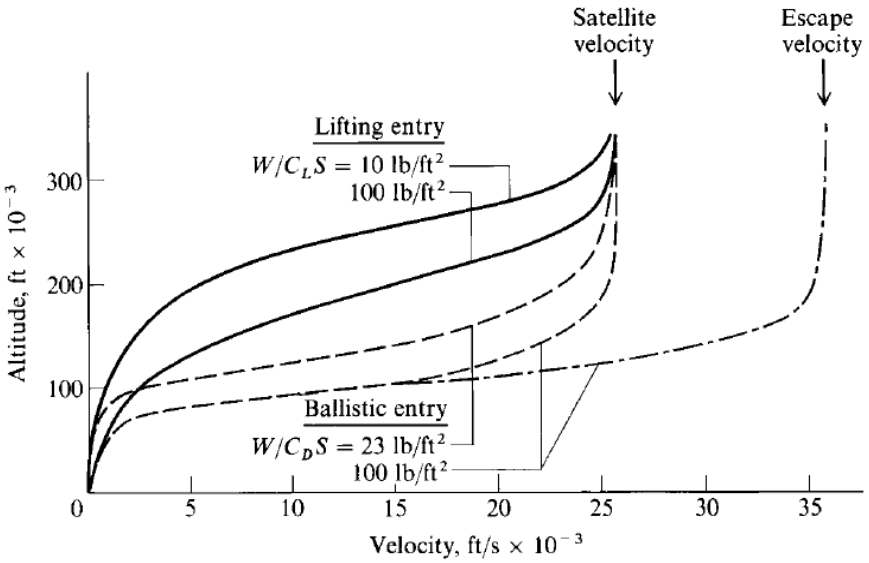

FIGURE 2: Reentry flight: [And06]

In this manuscript we essentially deals with rarefied regime and turbulent Navier-Stokes regime especially in a supersonic regime.

Physics of fluid/particles interactions

Fluid/particles interactions occur in a lot of applications: Diesel motor, spray in lungs, Ariane motors. They are generally associated to complex physics of the particles (collisions, break-up, drag force, thermal exchanges, vaporization...). Besides various models exist in the literature to

tackle with this problem. Some people will prefer to deal with two-phase flows models whereas other will try to deal with kinetic/fluid models. In this manuscript both approaches are tested. The crossing of jet presented in figure 3 show a computation by the two approaches of a crossing jet.

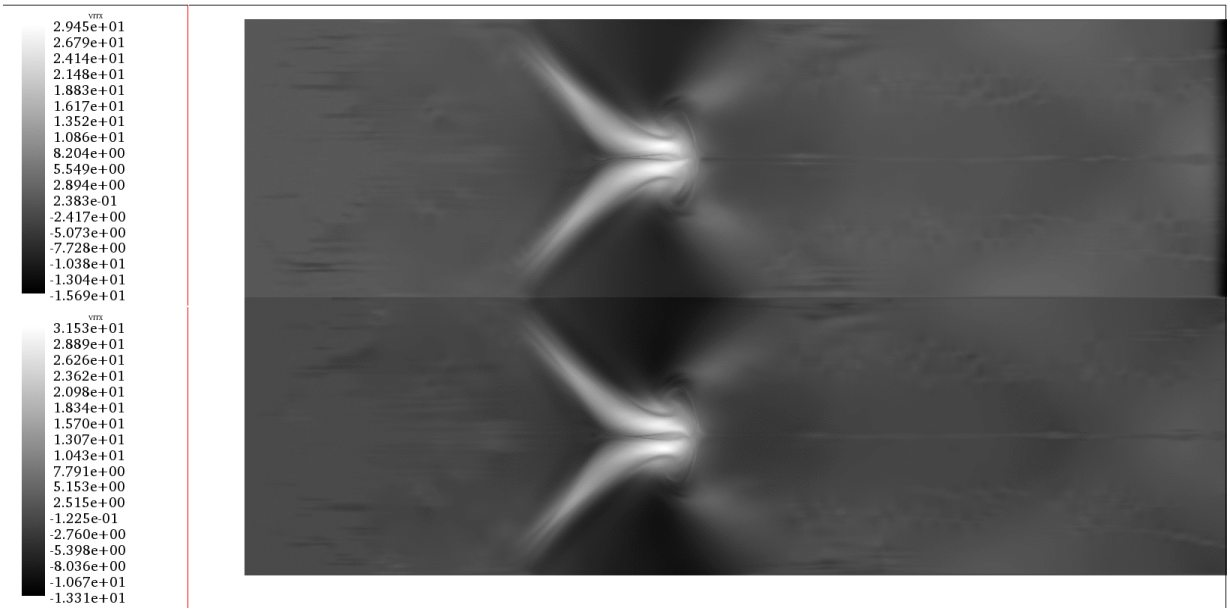

FIGURE 3: Crossing of two jets of particles in a gas (velocity in $m.s^{-1}$): kinetic/fluid approach (top) vs. fluid/fluid approach (bottom)

.

Guidelines for the manuscript

We have chosen to follow the physics and the three main topics presented before to construct this manuscript so that it is divided in three parts. In the first one we deal with rarefied gas dynamics. Then we deal with turbulence and interaction wall/fluid during an atmospheric reentry. We will essentially propose new models for reentry with "good" physical properties. Finally we study gas-particle interactions: it will include some physics, theoretical results and numerics.

This manuscript is based on the following papers and reports:

[*BM*12*a*] Laurent Boudin and Julien Mathiaud. "A numerical scheme for the one-dimensional pressureless gases system". In: Numerical Methods for Partial Differential Equations 28.6 (Sept. 2012), pp. 1729–1746. DOI: 10.1002/num.20700. URL: https://hal.archives- ouvertes.fr/hal-00537145.

[*BM*12*b*] Laurent Boudin and Julien Mathiaud. "Asymptotic behavior of a diffusive scheme solving the inviscid one-dimensional pressureless gases system". In: HYP'2012 - Fourteenth International Conference on Hyperbolic Problems. Vol. 8. AIMS Series on Applied Mathemat- ics - Hyperbolic Problems: Theory, Numerics, Applications. Padova, Italy: AIMS, June 2012, p. 1066. URL: https://hal.inria.fr/hal-00765620.

[*Bar* + 18] Baranger,C., Marois,G., Mathé,J., Mathiaud, J. and Mieussens,L. "A BGK model for high temperature rarefied gas flows". In: Work in progress (2018).

[*CDM*10] Aude Champmartin, Laurent Desvillettes, and Julien Mathiaud. "A BGK-type model for inelastic Boltzmann equations with internal energy." In: Rivista di Matematica della Università di Parma 1.2 (Dec. 2010). final version available on Riv. Mat. Univ. Parma, Volume 1 - Number 2 - 2010., pp. 271–305. .

[*DM*10] Laurent Desvillettes and Julien Mathiaud. "Some Aspects of the Asymptotics Leading fromGas-Particles Equations Towards Multiphase Flows Equations". In: Journal of Statistical Physics 141.1 (Oct. 2010), pp. 120–141. ISSN: 1572-9613. DOI: 10.1007/s10955-010- 0044-3.
URL: https://doi.org/10.1007/s10955-010-0044-3.

[*Lev* + 17] C. Levet, B. Helber, J. Couzi, J. Mathiaud, J.-B. Gouriet, O. Chazot and G.L. Vignoles "Microstructure and gas-surface interaction studies of a 3D carbon/carbon composite in atmospheric entry plasma". In: Carbon 114.Supplement C (2017), pp. 84–97.
ISSN : 0008-6223. DOI : https://doi.org/10.1016/j.carbon.2016.11.054.
URL : http://www.sciencedirect.com/science/article/pii/S0008622316310284.

[*Mat* + 08] Julien Mathiaud. "Local smooth solutions of the incompressible k-epsilon model and the low turbulent diffusion limit". In: Communications in Mathematical Sciences 6.2 (2008),pp. 361–383.

[*Mat*03] J. Mathiaud. "Différents aspects du modèle k-epsilon". MA thesis. ENS Lyon, 2003.

[*Mat*06] J. Mathiaud. "Etude de systèmes de type gaz-particules." PhD thesis. CMLA, Ecole normale supérieure de Cachan, 2006.

[*Mat*07] Julien Mathiaud. Ordres de grandeur pour le passage d'un modèle gaz-particules vers un modèle HEM. Tech. rep. CEA DAM DIF, 2007.

[*Mat*10] Julien Mathiaud. "Local smooth solutions of a thin spray model with collisions". In:Mathematical Models and Methods in Applied Sciences 20.02 (2010), pp. 191–221. DOI: 10. 1142 / S0218202510004192. eprint: http : / / www . worldscientific . com / doi / pdf / 10 .1142/S0218202510004192. .

[*MM*16] J. Mathiaud and L. Mieussens. "A Fokker–Planck Model of the Boltzmann Equation with Correct Prandtl Number". In: Journal of Statistical Physics 162.2 (Jan. 2016), pp. 397–414. ISSN : 1572-9613. DOI : 10.1007/s10955-015-1404-9. URL : https://doi.org/10.1007/ s10955-015-1404-9.

[*MM*17] J. Mathiaud and L. Mieussens. "A Fokker–Planck Model of the Boltzmann Equation with Correct Prandtl Number for Polyatomic Gases". In: Journal of Statistical Physics 168.5 (Sept. 2017), pp. 1031–1055. ISSN: 1572-9613. DOI: 10.1007/s10955- 017- 1837- 4.

[*MM*18] J. Mathiaud and L. Mieussens. "Vibrational models of Boltzmann equation with correct second principle: BGK and Fokker-Planck". In: Work in progress (2018).

[*MR*16] Julien Mathiaud and Xavier Roynard. "Local Smooth Solutions of the Incompressible k-omega Model". In: Acta Applicandae Mathematicae 146.1 (Dec. 2016), pp. 1–16. DOI: 10.1007/s10440-016-0054-5. URL: https://doi.org/10.1007/s10440-016-0054-5.

[*Ola* + 17] M Olazabal-Loumé et al. "Study on k-omega shear stress transport model corrections applied to rough wall turbulent hypersonic boundary layers". In Proceedings Eucass (2017).

Part II

Atmospheric reentry: Rarefied Gas Dynamics

Context and Boltzmann equation

There are various ways to represent a flow. The most common way is to look at it at a macroscopic level using Navier-Stokes equations. Only space and time are used as variables in this context. In this chapter we want to look at a more discrete level when the molecules are numerous enough not to be treated individually but are not numerous enough to be considered as a continuum: each molecule will have its own velocity, internal energy... By adding more variables, one can describe more precisely what happens at this molecular/microscopic level ([Bir94]; [And06]). The master equation associated with these problems is Boltzmann equation ([Cer88]; [CC70]): it combines free transport of particles and collisions between them. From now on we use the term of rarefied gas flow to describe this regime. To understand when one has to use this equation, we need to define the Knudsen number Kn which compares the mean free path λ of the molecules in the flow (that is the distance traveled by a particle between two collisions) with a characteristic length L of the flow. The Knudsen number is defined through: $Kn = \frac{\lambda}{L}$. The diagram (4) explains the different regimes available according to the value of the Knudsen number. The more important the Knudsen number is, the more rarefied the flow is. For instance a satellite of size $1m$ which is coming back from earth orbit to the ground encounters different regimes of flows according to the altitude:

- when the altitude is greater than $120km$, the flow is in a collision less regime ($Kn \gg 1$),
- between $120km$ and $70km$, collisions appear so that Boltzmann equation rules ($Kn \approx 1$),
- under $70km$, we go back to macroscopic flows ($Kn \ll 1$).

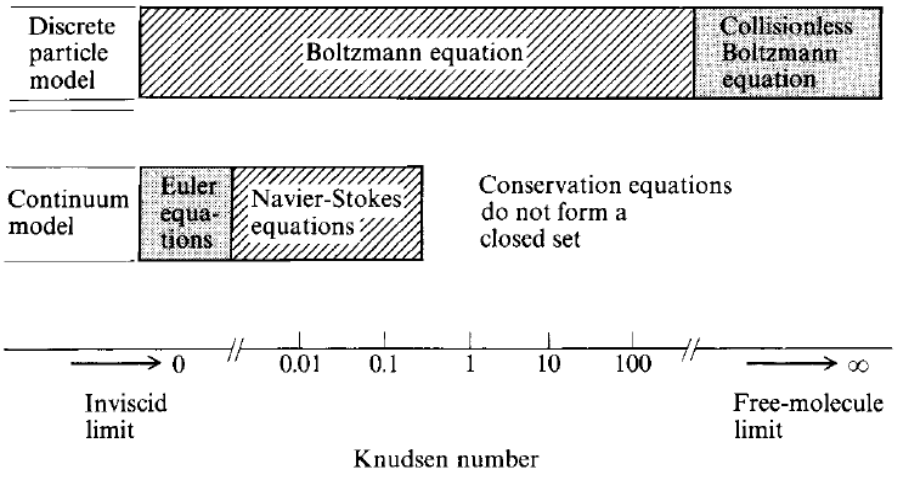

FIGURE 4: Regimes according to Knudsen number: discrete/continuous models ([And06])

As shown in the diagram, there is a zone (near $60km$) when both Navier-Stokes equation and Boltzmann equation can be used. By using what is called an hydrodynamic limit it can be proved that Euler or Navier-Stokes equations can arise from Boltzmann equation ([Cer88]). Besides we can add rarefied boundary conditions on Navier-Stokes equations to be able to use them up to a Knudsen of order 0.1 ([Aok+17]).

Boltzmann equation

In 1872, Ludwig Boltzmann wrote down his famous equation for rarefied gas dynamics ([Bol64]). From then, the model has been extended for several problems. We now present the Boltzmann equation in two cases: the one for mono-atomic gases and the one for diatomic gases. These two models can describe the behavior of perfect mono-atomic and diatomic-gases. As far as we know they cannot describe more complex effects such as high-temperature that can occur in atmospheric reentry without some modifications that we explain later.

Mono-atomic case

Let us turn to the model for mono-atomic gases. We consider a gas described by particle density function $f(t,x,v)$ that at time t have the position x and the velocity v (note that both position x and velocity v are scalar). The corresponding macroscopic quantities are $(\rho, \rho u, E) = \left\langle (1, v, \frac{1}{2}|v|^2) f \right\rangle$, where ρ, ρu, and E are the mass, momentum, and energy densities, and $\langle \phi \rangle = \int_{\mathbb{R}^3} \phi(v)\, dv$ for any velocity dependent function. The temperature T of the gas is defined by relation $E = \frac{1}{2}\rho|u|^2 + \frac{3}{2}\rho RT$, where R is the gas constant, and the pressure is $p = \rho RT$. The evolution of the gas is governed by the following Boltzmann equation (for a hard-sphere cross -section):

$$\partial_t f + v \cdot \nabla_x f = Q(f,f), \tag{1}$$

with

$$Q(f,f)(v) = \int_{v_* \in \mathbb{R}^3} \int_{\sigma \in S^2} \left(f(v'_*)\, f(v') - f(v_*)\, f(v) \right) r^2\, |v - v_*|\, d\sigma\, dv_*,$$

and

$$v' = \frac{v + v_*}{2} + \frac{|v - v_*|}{2}\,\sigma \ , \ v'_* = \frac{v + v_*}{2} - \frac{|v - v_*|}{2}\,\sigma.$$

The cross-section is important to determine the value of viscosities or heat conductivity of the fluid of molecules as functions of the temperature. It is well known that this operator conserves the mass, momentum, and energy, and that the local entropy $H(f) = \langle f \log f \rangle$ is locally non-increasing (H-theorem). As before this operator makes the distribution f relax towards its own local Maxwellian distribution, which is defined by

$$M(f)(v) = \frac{\rho}{(2\pi RT)^{3/2}} \exp\left(\frac{|v-u|^2}{2RT} \right). \tag{2}$$

Polyatomic case

The Boltzmann equation can be extended for polyatomic molecules through the Borgnakke-Larsen model ([BL75]; [Bou+94]): we consider a gas described by the mass density of particles $f(t,x,v,I)$ that at time t have the position x, the velocity v and an internal energy parameter I (note that both position x and velocity v are vectors and that I is a scalar). The internal energy of a particle is equal to $\varepsilon(I) = I^{\frac{2}{\delta}}$, δ being linked to the number of degrees of freedom of the polyatomic gas ($\delta = 2$ for diatomic gases). The corresponding macroscopic quantities are $(\rho, \rho u, E) = \left\langle (1, v, \left(\frac{1}{2}|v|^2\right) + \varepsilon(I)) f \right\rangle$, where ρ, ρu, and E are the mass, momentum, and energy densities, and $\langle \phi \rangle = \int_{\mathbb{R}^3} \phi(v, I)\, dv dI$ for any velocity dependent function. The temperature T of the gas is defined by relation $E = \frac{1}{2}\rho|u|^2 + \frac{3+\delta}{2}\rho RT$, where R is the gas constant, and the pressure is $p = \rho RT$.

We can also define a translational energy E_{tr}, a translational temperature T_{tr}, an internal energy E_{int} and an internal energy temperature T_{int} through:

$$\left\langle \tfrac{1}{2}|v|^2 f \right\rangle = E_{tr} = \frac{3}{2}\rho R T_{tr}, \tag{3}$$

$$\langle \varepsilon(I) \rangle f = E_{int} = \frac{\delta}{2}\rho R T_{int}, \tag{4}$$

$$\text{so that:} \qquad T = \frac{3}{3+\delta}T_{tr} + \frac{\delta}{3+\delta}T_{int}. \tag{5}$$

The polyatomic operator conserves the mass, momentum, and energy, and the local entropy $H(f) = \langle f \log f \rangle$ is still locally non-increasing. This means that the effect of this operator is to make the distribution f relax towards its own local Maxwellian distribution, which is defined by

$$M_p(f) = \frac{\rho \Lambda_\delta}{(2\pi)^{3/2}(RT)^{\frac{3+\delta}{2}}} \exp\left(-\frac{(v-u)^2 + I^{2/\delta}}{2RT}\right), \tag{6}$$

with $\Lambda_\delta = \left(\int_{\mathbb{R}} \exp(-I^{2/\delta})dI\right)^{-1}$.

Hydrodynamic limit of Boltzmann equation

Thanks to the second principle, one can obtain hydrodynamic limits for both Boltzmann equations: when the density of molecules is important enough (when the Knudsen number tends to zero) the particle density function f tends towards its equilibrium. At order zero in terms of Knudsen number, one gets Euler equations for mono-atomic/polyatomic perfect gases (Hilbert expansion, 1912). At order one, Navier-Stokes equations can be obtained (Chapmman-Enskog expansion: Chapmann 1916, Enskog 1917). For almost one century these problems have been purely formal; recently, Golse and Saint Raymond managed to mathematically prove some results for Euler ([Sai03]) and Navier-Stokes ([GS04]). Finally one gets the following limits ([Cer88]) for mono-atomic and diatomic gases:

Mono-atomic limit: *The solution of the kinetic model (1) satisfies, up to $O(Kn^2)$, the Navier-Stokes equations*

$$\begin{aligned} &\partial_t \rho + \nabla \cdot (\rho u) = 0, \\ &\partial_t \rho u + \nabla \cdot (\rho u \otimes u) + \nabla p = -\nabla \cdot \sigma, \\ &\partial_t E + \nabla \cdot (E+p)u = -\nabla \cdot q - \nabla \cdot (\sigma u), \end{aligned} \tag{7}$$

where the shear stress tensor and the heat flux are given by

$$\sigma = -\mu\left(\nabla u + (\nabla u)^T - \frac{2}{3}\nabla \cdot u\right), \quad \textit{and} \quad q = -\kappa \nabla \cdot T, \tag{8}$$

with μ viscosity and κ heat conductivity depending on the cross-section through a function of temperature,

$$p = \rho R T. \tag{9}$$

Generally the Prandtl number $Pr = \frac{\mu C_p}{\lambda}$ is close to $2/3$ for monoatomic perfect gases (C_p is the specific heat at constant pressure).

Diatomic limit: *The solution of the diatomic Boltzmann equation satisfies, up to $O(Kn^2)$, the Navier-Stokes equations*

$$\begin{aligned} &\partial_t \rho + \nabla \cdot \rho u = 0, \\ &\partial_t \rho u + \nabla \cdot (\rho u \otimes u) + \nabla p = -\nabla \cdot \sigma, \\ &\partial_t E + \nabla \cdot (E + p)u = -\nabla \cdot q - \nabla \cdot (\sigma u), \end{aligned} \tag{10}$$

where the shear stress tensor and the heat flux are given by

$$\sigma = -\mu\big(\nabla u + (\nabla u)^T - \alpha \nabla \cdot u\big), \quad \textit{and} \quad q = -\kappa \nabla \cdot T, \tag{11}$$

with μ viscosity, α second viscosity, κ heat conductivity depending on the expression of the cross-section through a function of temperature,

$$p = \rho RT = (\gamma - 1)\rho e.$$

Generally the Prandtl number $Pr = \frac{\mu C_p}{\lambda}$ is close to $5/7$ for diatomic perfect gases.

Towards other models: vibrations, high-temperature models

The Boltzmann equations that have been presented here cannot take into account the whole physics of reentry on earth. When the reentry is hypersonic, the gas no longer remains a perfect gas: chemistry is activated and molecules start to vibrate. Worse at very high temperature, plasma phenomena appear ([And06]) as it can be seen in figure (5). We will see how to take into account these phenomena in the next chapters.

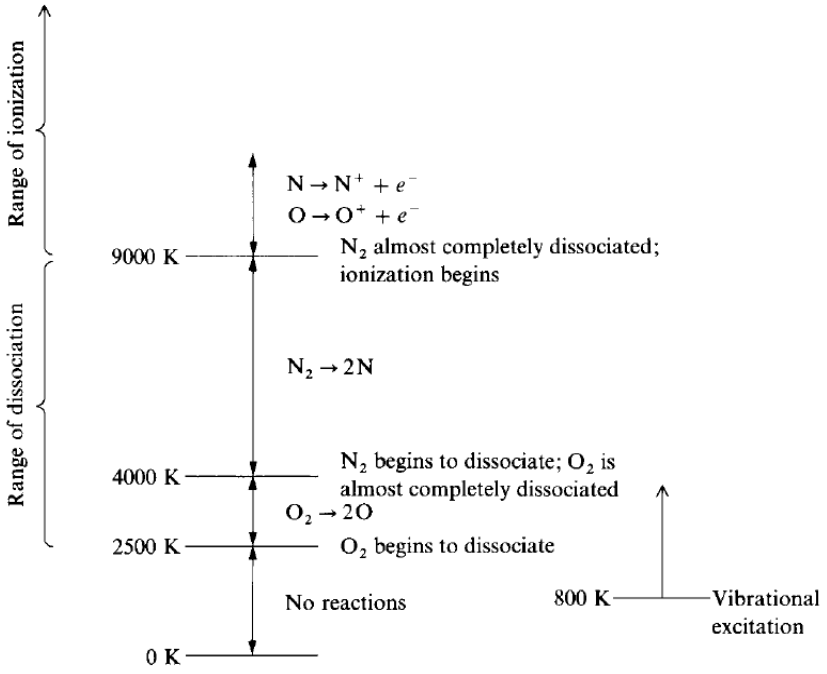

FIGURE 5: Chemistry of air according to temperature ([And06])

Objectives and main results

In this part we will present some new models to better capture the physics of rarefied supersonic high-enthalpy flows (flows at high Mach number with temperatures of several thousands of degrees) without having the complexity of Boltzmann kernel of collisions. We first present recent works on BGK (P.L. Bhatnagar, E.P. Gross, M. Krook) models to increase the domain of validity of the BGK equation. then we study another simple approach: new Fokker-Planck models which are able to capture correct hydrodynamic limits for low temperatures as well as vibration phenomena. We present the results from ([MM16]; [MM17]) and works in progress ([Bar+18]; [MM18]). The high-temperature BGK model comes from a work with Jordane Mathé (post-doc).

Chapter 1

BGK Models

The BGK model (P.L. Bhatnagar, E.P. Gross, M. Krook) has been widely used instead of Boltzmann equation because of the qualitatively satisfactory results it provides at relatively low computational cost ([GBK54]). This model emulates the relaxation of the particle density function (p.d.f.) towards its Maxwellian equilibrium, like does Boltzmann equation. This model is widely used and provides very fast results ([DL13]). Nonetheless for very rarefied or anisotropic flows it can fail or at least be rather inaccurate ([Mie99]). It was first proposed for mono-atomic gases and naturally extended to polyatomic gases:

Zoology of BGK /ESBGK models

- mono-atomic BGK model:

  The original BGK model given in [GBK54] describes the evolution of the distribution of particles of a mono-atomic gas by the following equation:

  $$\partial_t f + v \cdot \nabla_x f = \frac{M_{mo}[f] - f}{\tau},$$

  where:
  -v is the microscopic velocity of the particles,
  -$\tau = \frac{\mu}{P}$ is a relaxation time (μ dynamic viscosity, P pressure),
  -$M_{mo}[f](v) = \frac{\rho}{\sqrt{2\pi RT}^3} \exp\left(-\frac{|u-v|^2}{2RT}\right)$ is the local Maxwellian equilibrium.

  This equilibrium is defined *via* the macroscopic properties of f, *i.e.* the mass density $\rho = \langle f \rangle_v$, the impulsion $\rho u = \langle fv \rangle_v$ and the temperature $T = \frac{1}{3\rho R} \langle |v-u|^2 f \rangle_v$, where we use the notation $\langle \cdot \rangle_v = \int_{\mathbb{R}^3} \cdot \, \mathrm{d}v$.
  One of the main properties of $M_{mo}[f]$ is that it has the same moments as f in the space of microscopic velocities, *i.e.*

  $$\langle M_{mo}[f] \rangle_v = \langle f \rangle_v , \quad \langle M_{mo}[f] v \rangle_v = \langle fv \rangle_v \quad \text{and} \quad \langle |v-u|^2 M_{mo}[f] \rangle_v = \langle |v-u|^2 f \rangle_v .$$

It is also well-known that the stress tensor and the heat flux of $M_{mo}[f]$ are respectively

$$\langle (v-u)\otimes(v-u)M_{mo}[f]\rangle_v = \rho RT\, Id\,, \tag{1.1}$$

$$\left\langle \frac{|v-u|^2}{2}(v-u)M_{mo}[f]\right\rangle_v = 0\,. \tag{1.2}$$

- polyatomic BGK model:

In order to take into account the extra degrees of freedom (DoF) of a polyatomic molecule, we introduce the internal energy variable of the particle, denoted by ε and δ the number of degrees of freedom of the molecule. Then the polyatomic distribution function $g(t,x,v,\varepsilon)$ describes at time t the number of particles with position x, velocity v and internal energy ε. It satisfies the following equations:

$$\partial_t g + v\cdot\nabla g = \frac{M[g]-g}{\tau}\,, \tag{1.3}$$

where the Maxwellian equilibrium is $M[g]=M[\rho,u,e]$ defined by

$$M[g](v,\varepsilon) = \frac{\rho}{\sqrt{2\pi RT}^3}\exp\left(-\frac{|u-v|^2}{2RT}\right)\Lambda(\delta)\left(\frac{\varepsilon}{RT}\right)^{\frac{\delta}{2}-1}\frac{1}{RT}\exp\left(-\frac{\varepsilon}{RT}\right). \tag{1.4}$$

The macroscopic quantities are given by

$$\rho = \langle\langle g\rangle\rangle\,, \tag{1.5}$$

$$u = \frac{1}{\rho}\langle\langle gv\rangle\rangle\,, \tag{1.6}$$

$$\frac{3+\delta}{2}RT = \frac{1}{\rho}\left\langle\left\langle\left(\frac{|v-u|^2}{2}+\varepsilon\right)g\right\rangle\right\rangle, \tag{1.7}$$

with the notation $\langle\langle\cdot\rangle\rangle = \int\int_{\mathbb{R}^3\times\mathbb{R}^+}\cdot\,\mathrm{d}v\mathrm{d}\varepsilon$, and the closure relation on the pressure (1.29). The constant $\Lambda(\delta)$ comes from the normalization on the space of internal energy. Its definition is:

$$\Lambda(\delta) = \left(\int_{\mathbb{R}^+} y^{\frac{\delta}{2}-1}\exp(-y)\mathrm{d}y\right)^{-1}. \tag{1.8}$$

- ESBGK models:

The classical BGK models cannot capture the correct hydrodynamic limits so that a correction of the model was constructed ([Low66]; [And+00c]) to assess correctly the Prandtl number (Pr). The mono-atomic model then reads

$$\partial_t f + v\cdot\nabla_x f = \frac{G_{mo}[f]-f}{\tau}\,,$$

with

$$G_{mo}(f) = \frac{\rho}{\sqrt{\det(2\pi\Pi)}}\exp\left(-\frac{(v-u)\Pi^{-1}(v-u)}{2}\right), \tag{1.9}$$

$$\Theta := \frac{1}{\rho}\langle(v-u)\otimes(v-u)f\rangle\,,\Pi = (1-\nu)RTId + \nu\Theta, \tag{1.10}$$

with ν a parameter between $-1/2$ and 1.

The function G_{mo} has the same 5 first moments as f

$$\left\langle (1, v, \tfrac{1}{2}|v|^2) G_{mo}(f) \right\rangle = (\rho, \rho u, E),$$

and has the temperature tensor $\langle (v-u) \otimes (v-u) G(f) \rangle = \Pi$.

It was extended later on for polyatomic gases. These models still conserve mass, momentum and energy. Furthermore the second principle is still satisfied.

In this chapter we present works to capture better physics (thermodynamics essentially) with BGK models. We first try to understand how vibrations in molecules can affect the relaxation towards equilibrium for diatomic gases and then how we can capture real gas effects during re-entry (chemistry at equilibrium essentially). What is at stake behind these two problems is to capture the correct energy balance so that at the wall of the re-entry vehicles fluxes are well captured.

1.1 Vibrational BGK model for a diatomic gas

As we have seen before a reentry vehicle that comes back to earth will encounter high-enthalpy flows. At temperature $1000K$ in the air, diatomic molecules start to vibrate ([And06]; [Bir94]). In this section we create a new BGK model taking into account vibrations (this work is in progress ([MM18])).

1.1.1 Vibrations

Atoms of a molecule can vibrate with respect to an equilibrium location in the molecule ([And06]). So that an energy of vibration can be defined. Like translational or rotational energy it is defined at a discrete level. The main difference is that translational energy becomes continuous at very low temperature ($1K$ for air), rotational energy at low temperatures ($10K$ for air) whereas the distribution in vibrational energies is continuous for larger temperature ($2000K$ for dioxygen and $3300K$ for nitrogen).

In this work we want to deal with flows up to $3000K$ around the reentry vehicles so that we will consider continuous translational and rotational energies but discrete levels of energy for the vibrations.

If a gas is supposed to be at local thermodynamic equilibrium, the equilibrium can now be defined as:

$$M_{vib}[f](v, \varepsilon, i) = \frac{\rho}{\sqrt{2\pi RT}^3} \exp\left(-\frac{|u-v|^2}{2RT}\right) \Lambda(\delta_{rot}) \left(\frac{\varepsilon}{RT}\right)^{\frac{\delta_{rot}}{2}-1} \frac{1}{RT} \exp\left(-\frac{\varepsilon}{RT}\right) (1 - e^{-T_0/T}) e^{-iT_0/T}, \tag{1.11}$$

with i , $i-th$ level of vibrational energy, T_0 characteristic vibrational temperature of the molecule (see [Bir94]). The vibrational energy of the $i-th$ level is iRT_0. ρ is the density of the gas, T its temperature of equilibrium and u its mean velocity. $\delta_{rot} = 2$ is the constant number of degrees of freedom of rotations for a diatomic gas.

$$\Lambda(\delta_{rot}) = \left(\int_{\mathbb{R}^+} y^{\frac{\delta_{rot}}{2}-1} \exp(-y) \mathrm{d}y \right)^{-1} = 1 \,. \tag{1.12}$$

Now that the equilibrium is defined it is easy to define the corresponding BGK model.

1.1.2 A BGK model with vibrations

We now define $f(t,x,v,\varepsilon,i)$ the particle density function of particles whose position is x, velocity is v, internal energy is ε and whose vibrational energy is iRT_0. The natural BGK equation coming from the equilibrium is:

$$\partial_t f + v \cdot \nabla f = \frac{M_{vib}[f] - f}{\tau} \,, \tag{1.13}$$

This equilibrium is defined *via* the macroscopic properties of f, *i.e.* the mass density $\rho = \sum_i \langle f \rangle_{v,\varepsilon}$, the momentum $\rho u = \sum_i \langle fv \rangle_{v,\varepsilon}$ and the internal energy $e = \frac{1}{\rho} \sum_i \left\langle \left(\frac{1}{2}|v-u|^2 + \varepsilon + iRT_0 \right) f \right\rangle_{v,\varepsilon}$, where we use the notation $\langle \cdot \rangle_{v,\varepsilon} = \int_{\mathbb{R}^3,\mathbb{R}^3} \cdot \, \mathrm{d}v\mathrm{d}\varepsilon$. The characteristic time τ is still $\frac{\mu}{p}$. It remains to understand the link between the internal energy e and the temperature. Some fast computations lead to the relation:

$$e(T) = \frac{3+\delta(T)}{2} RT, \tag{1.14}$$

with $\delta(T) = \delta_{rot} + \dfrac{2T_0/T}{e^{T_0/T}-1}$.

Immediate computations leads to a unique T for a given e (the function $T \to e(T)$ is monotonic). One can note that $\delta_{rot} \leq \delta(T) \leq \delta_{rot} + 2$. We will note T^{-1} the function that gives T according to e.

Moreover we have the following properties (proofs are immediate):
Property 1.1.1 (Conservation, Second principle)**.**

- *Mass, momentum and total energy are conserved by the BGK operator.*
- *Furthermore if one defines the entropy as* $H(f) = \sum_i \langle f \log(f) \rangle_{v,\varepsilon}$*, it is a non increasing function.*

1.1.3 A reduced BGK model with vibrations

By adding the vibrational energy we have increased the dimension of the space phase and consequently the numerical cost to simulate the BGK model. One classical technique is often used to pass over this flaw: a two particle density functions approach in a reduced space phase as it is done for the polyatomic BGK model ([And+00c]). We can define the following set of equations:

$$\partial_t F + v \cdot \nabla_x F = \frac{1}{\tau}\left(M_{vib}[F,G] - F\right), \tag{1.15}$$

$$\partial_t G + v \cdot \nabla_x G = \frac{1}{\tau}\left(\frac{\delta(T)}{2} RT M_{vib}[F,G] - G\right). \tag{1.16}$$

with:

$$F = \sum_i f(t,x,v,\varepsilon,i), \tag{1.17}$$

$$G = \sum_i iRT_0 f(t,x,v,\varepsilon,i), \tag{1.18}$$

$$M_{vib}[F,G] = \frac{\rho}{\sqrt{2\pi RT}^3} \exp\left(-\frac{\rho|u-v|^2}{2p}\right) \Lambda(\delta_{rot}) \left(\frac{\varepsilon}{RT}\right)^{\frac{\delta_{rot}}{2}-1} \frac{1}{RT} \exp\left(-\frac{\varepsilon}{RT}\right), \tag{1.19}$$

$$\rho = \langle F \rangle_{v,\varepsilon}, \tag{1.20}$$

$$\rho u = \langle Fv \rangle_{v,\varepsilon}, \tag{1.21}$$

$$\rho e = \left\langle F\left(\frac{1}{2}(v-u)^2 + \varepsilon\right)\right\rangle_{v,\varepsilon} + \langle G \rangle_{v,\varepsilon}, \tag{1.22}$$

$$T = T^{-1}(e). \tag{1.23}$$

We no longer have discrete levels: F and G only depend on t, x, v, ε; these equations are continuous. Moreover we immediately recover the conservation of the mass, momentum and energy. The most difficult part is to recover the second principle. Minimization techniques leads to the following definition for the entropy:

Remark 1.1.1. The entropy $H(F,G)$ of the reduced model is the following:

$$H(F,G) = \left\langle F\log(F) + F\log\left(\frac{RT_0F}{RT_0F+G}\right) + \frac{G}{RT_0}\log\left(\frac{G}{RT_0F+G}\right)\right\rangle_{v,\varepsilon}. \tag{1.24}$$

Using convex analysis as in [And+00c] one can prove the following proposition.
Proposition 1.1.1. *The function $H(F,G)$ is a non increasing function so that the second principle holds.*

1.1.4 Hydrodynamic limit of the reduced system

Using Chapman-Enskog analysis on the reduced model, one will get the following proposition
Proposition 1.1.2. *Let (F,G) be solutions of BGK equations up to $O(\mathrm{Kn}^2)$. Then the moments of (F,G) satisfy the following Navier-Stokes equations up to $O(\mathrm{Kn}^2)$:*

$$\begin{cases} \partial_t \rho + \nabla_x \cdot (\rho u) = 0 \\ \partial_t(\rho u) + \nabla_x \cdot (\rho u \otimes u) + \nabla_x p = -\nabla_x \cdot (\sigma) + O(\mathrm{Kn}^2) \\ \partial_t E + \nabla_x \cdot ((E+p)u) = -\nabla_x \cdot (q) - \nabla_x \cdot (\sigma u) + O(\mathrm{Kn}^2), \end{cases} \tag{1.25}$$

with:

$$E = \left\langle \left(\frac{1}{2}|v|^2 + \varepsilon\right) F + G \right\rangle_{v,\varepsilon} = \rho e + \frac{1}{2}\rho|u|^2, \tag{1.26}$$

$$\sigma = -\mu\left(\nabla_x u + \nabla_x u^T - \mathcal{C}\nabla_x \cdot (u) Id\right), \tag{1.27}$$

$$q = -\mu\nabla_x h, \tag{1.28}$$

where $h = e(T) + RT$ *is the enthalpy of the system and* $\mathcal{C} = \partial_e(RT) = R\partial_e(T) = \dfrac{R}{C_v(T(e))}$. *The specific heat (at constant volume) is equal to* $C_v(T) = \dfrac{5}{2}R + \dfrac{(T_0/T)^2 e^{T_0/T}}{(e^{T_0/T}-1)^2}R$. *If one defines* $C_p = C_v + R$ *the specific heat at constant pressure then one gets* $q = -\mu C_p \nabla_x T$ *so that as usual only a gas with a Prandtl number of one is obtained for this BGK model.*

1.1.5 Comments

This work is very recent so we need to understand all the implications it could have. At the beginning we only wanted to create a Fokker-Planck model with vibrations to extend our models of Fokker-Planck. We managed to do it only once it was done for the BGK thanks to a reduced model ([MM18]).

1.2 High temperature BGK model

The nature of the gas seems to play an important role, especially in the hypersonic regime (Mach number higher than five). For these regimes, the air is a mixture of mono-atomic and polyatomic gases, in which occurs chemical reactions when the temperature is high enough. Moreover the characteristics of the gas mixture (viscosities and specific heats) also depend on its temperature (see [NBK86]).

One way to take into account this variability is to use an approximate equation of state for air. This approximation permits to compute, for example, all thermodynamical quantities (pressure, entropy, temperature, specific heats) in terms of density and internal energy. To do such a thing, one has to assume that the gas is at local chemical equilibrium. In the case of a local thermodynamic equilibrium, the temperature is implicitly given by the internal energy of the mixture (see [And06]). Either, one can use a constitutive law based on empirical considerations, like the one given in [Han60]. In the framework of fluids dynamics, this kind of law consists of a closure of the compressible Navier-Stokes equations and it can be used for simulations in the domain of small Knudsen number (see, for example, [Mon+88]).

For rarefied gases, this macroscopic point of view on the effects of real gas are not often been studied. To our knowledge, the first attempt to introduce this kind of law into a kinetic model has recently been published in [RS16]. In this article, the authors define the constant volume specific heat c_v as a third-order polynomial function of the temperature of the gas. Another way to take into account the variation of behavior of the gas in a kinetic model is to model it as a mixture of polyatomic gases ([BC16]). This approach seems to be more precise in terms of physics, but the cost in terms of numerical resources is also much higher. Besides high temperatures that can appear for reentry problems are not studied in these papers.

The aim of the present work is to propose a kinetic model based on BGK collision kernel ([GBK54]) including the effects of real gas in a more general way than the one chosen in [RS16]. We first construct an extended BGK model.Then using Chapman-Enskog expansion, we prove that this model reduces to Navier-Stokes equations with appropriate constitutive laws and transport coefficients when the Knudsen number is small enough. Under the hypothesis of an enthalpy only depending on the temperature, we prove that our model provides correct viscosity and thermal conductivity in the corresponding Navier-Stokes equations when the Prandtl number is equal to one (it is a restriction of BGK models [And+00b]; [And+00a]; [GTJ11]; [GJ12]; [MM16]; [MM17]). Finally we show how the model has been developed and validated in a deterministic BGK code([DM99]; [Mie00]): we will focus on a non reacting mixture of two vibrating diatomic perfect gases.

This work is a first attempt to capture the correct physics at high temperatures and should be extended to an ES-BGK like models (as introduced in [And+00b]), in a further work, so that it provides realistic Prandtl number.

1.2.1 A generalized BGK model for polyatomic gases

Our goal is to study high enthalpy rarefied flows (temperatures up to $10000K$). When one considers dense flows, the Navier-Stokes equations which are used have to be completed with a constitutive law, which gives the pressure and the temperature as functions of its density ρ and its internal energy e:

$$p = p(\rho, e)\,, \tag{1.29}$$
$$T = T(\rho, e)\,. \tag{1.30}$$

A classical constitutive law is the one of perfect gases $p = \rho RT$, where R is the constant of the gas. In this case, we speak about *thermally perfect gas*. But when one works with air at high temperatures, it does not behave like a thermally perfect gas and there is no obvious relation between p and T. This remark has no impact on the formulation of the Navier-Stokes equations, nor on its numerical resolution. Besides the BGK (Gross, Bhatnagar and Krook) model is historically designed for perfect mono-atomic gases and is only defined through (ρ, u, T) the pressure being $p = \rho RT$ ([GBK54]). It was extended to polyatomic non vibrating gases ([And+00b]). In this section, we extend the BGK model for a gas which has general closure relations (1.29) and (1.30). This expansion is developed with the objective to have correct transport coefficients in the Navier-Stokes equations obtained by Chapman-Enskog expansion, which is performed in section 1.2.2.

The generalized polyatomic BGK model

In order to take into account the extra degrees of freedom (DoF) of a polyatomic molecule, we introduce the internal energy variable of the particle, denoted by ε: this variable contains all the energy of the molecule that is no translational energy (rotational, vibrational, chemical ...). It is already a reduction of model since all these various energies are put into only one variable. Then the polyatomic distribution function $g(t, x, v, \varepsilon)$ describes at time t the number of particles with position x, velocity v and internal energy ε. Our extended BGK model satisfies the following equations:

$$\partial_t h + v \cdot \nabla h = \frac{M[h] - h}{\tau}\,, \tag{1.31}$$

where the Maxwellian equilibrium is $M[h] = M[\rho, u, e]$ defined by

$$M[h](v,\varepsilon) = \frac{\rho}{\sqrt{2\pi\frac{p}{\rho}}^3} \exp\left(-\frac{\rho|u-v|^2}{2p}\right) \Lambda(\delta) \left(\frac{\rho\varepsilon}{p}\right)^{\frac{\delta}{2}-1} \frac{\rho}{p} \exp\left(-\frac{\rho\varepsilon}{p(\rho,e)}\right). \tag{1.32}$$

The macroscopic quantities are given by

$$\rho = \langle\langle h \rangle\rangle, \tag{1.33}$$

$$u = \frac{1}{\rho} \langle\langle hv \rangle\rangle, \tag{1.34}$$

$$e = \frac{1}{\rho} \left\langle \left\langle \left(\frac{|v-u|^2}{2} + \varepsilon \right) h \right\rangle \right\rangle, \tag{1.35}$$

with the notation $\langle\langle \cdot \rangle\rangle = \int\int_{\mathbb{R}^3 \times \mathbb{R}^+} \cdot \, \mathrm{d}v\mathrm{d}\varepsilon$, and the closure relation on the pressure (1.29). The constant $\Lambda(\delta)$ comes from the normalization on the space of internal energy. Its definition is:

$$\Lambda(\delta) = \left(\int_{\mathbb{R}^+} y^{\frac{\delta}{2}-1} \exp(-y) \mathrm{d}y \right)^{-1}. \tag{1.36}$$

As we will see in the next subsection, the number of DoF δ is defined by

$$\delta(\rho, e) = \frac{2\rho e}{p(\rho, e)} - 3, \tag{1.37}$$

to capture the correct conservation of total energy for the system. It is not a real degree of freedom (it is not always an integer).

Finally one has to note there is no longer a temperature in the Maxwellian. It is replaced by p/ρ: of course if p is defined through a perfect gases law p/ρ is equal to RT the classical BGK model is recovered. We will see that using this replacement ensure to capture Euler equations at order 0 in the Chapman expansion.

Main properties of the Maxwellian equilibrium

We now explain the properties satisfied by the extended BGK model. First note that the Maxwellian $M[g]$ (defined by (1.32)) is a product of two distributions, the first being the "mono-atomic" equilibrium (or translational equilibrium) and the second one the distribution in internal energy. To simplify the forthcoming computations, we adopt the following notations:

$$M[h](v,\varepsilon) = M_{mo}[h](v) M_{di}[h](\varepsilon), \tag{1.38}$$

$$M_{mo}[h](v) = \frac{\rho}{\sqrt{2\pi\frac{p}{\rho}}^3} \exp\left(-\frac{\rho|u-v|^2}{2p}\right), \tag{1.39}$$

$$M_{di}[h](\varepsilon) = \Lambda(\delta) \left(\frac{\rho\varepsilon}{p}\right)^{\frac{\delta}{2}-1} \frac{\rho}{p} \exp\left(-\frac{\rho\varepsilon}{p}\right). \tag{1.40}$$

Because of the separation of variables one directly obtains:

$$\langle (v-u)\otimes(v-u)M_{mo}[h]\rangle_v = p\,Id\,, \tag{1.41}$$

$$\left\langle \frac{|v-u|^2}{2}(v-u)M_{mo}[h]\right\rangle_v = 0\,, \tag{1.42}$$

Furthermore, thanks to the definition (1.36) of $\Lambda(\delta)$ and easy calculation, one can remark that

$$\langle M_{di}[h]\rangle_\varepsilon = \int_{\mathbb{R}^+} M_{di}[h]\mathrm{d}\varepsilon = 1\,, \tag{1.43}$$

$$\langle M_{di}[h]\varepsilon\rangle_\varepsilon = \int_{\mathbb{R}^+} M_{di}[h]\varepsilon\mathrm{d}\varepsilon = \frac{\delta}{2}\,\frac{p}{\rho}\,. \tag{1.44}$$

Now we give the moments of $M[h]$ and compare it to those of h.
Proposition 1.2.1. *The Maxwellian equilibrium $M[g]$ defined by (1.32) satisfies the following equalities:*

$$\langle\langle M[g]\rangle\rangle = \rho = \langle\langle h\rangle\rangle\,, \tag{1.45}$$

$$\langle\langle M[h]v\rangle\rangle = \rho u = \langle\langle hv\rangle\rangle\,, \tag{1.46}$$

$$\left\langle\left\langle M[h]\left(\frac{|u-v|^2}{2}+\varepsilon\right)\right\rangle\right\rangle = \tfrac{3+\delta}{2}p = \rho e = \left\langle\left\langle h\left(\frac{|u-v|^2}{2}+\varepsilon\right)\right\rangle\right\rangle. \tag{1.47}$$

1.2.2 Asymptotic properties and local entropy dissipation

Chapman-Enskog expansion

We begin this section with the general definitions of the stress tensor and the heat flux for any distribution on the phase space (t,x,v,ε).
Definition 1.2.1. The stress tensor $\Sigma(H)$ of a function $H(t,x,v,\varepsilon)$ is defined by

$$\Sigma(H) = \langle\langle (v-u)\otimes(v-u)H\rangle\rangle\,. \tag{1.48}$$

The heat flux $q(H)$ of a function $H(t,x,v,\varepsilon)$ is given by

$$q(H) = \left\langle\left\langle\left(\frac{|v-u|^2}{2}+\varepsilon\right)(v-u)H\right\rangle\right\rangle. \tag{1.49}$$

Thanks to the result of proposition 1.2.1, one can show that the moments of the solution g of equation (1.31) satisfy the following conservation laws:

$$\begin{cases} \partial_t\rho + \nabla_x\cdot(\rho u) = 0\,,\\ \partial_t(\rho u) + \nabla_x\cdot(\rho u\otimes u + \Sigma(h)) = 0\,,\\ \partial_t E + \nabla_x\cdot(Eu + \Sigma(h)u + q(h)) = 0\,, \end{cases} \tag{1.50}$$

where $E = \left\langle\left\langle\left(\frac{|v|^2}{2}+\varepsilon\right)h\right\rangle\right\rangle = \rho e + \frac{1}{2}\rho|u|^2$. The goal of the Chapman-Enskog analysis is to find an approximation of $\Sigma(h)$ and $q(h)$ up to second order with respect to the Knudsen number Kn (defined below). Doing so, we find the equivalent Navier-Stokes equations of the model with the expressions of the viscosities and the heat transfer coefficient as functions of (ρ,u,p) and their derivatives.

Before we begin this procedure, we give a non-dimensional form of the model. To do so, let x_*, p_* and e_* be respectively a length, a pressure and an energy of reference. Then we can derive reference values of all other quantities: mass density $\rho_* = p_*/e_*$, velocity $v_* = \sqrt{e_*}$, time $t_* = x_*/v_*$, distribution function $h_* = \rho_*/e_*^{5/2}$. We also assume we have a reference value for the relaxation time $\tau_* = \tau$. If we denote by $w' = w/w_*$ the non-dimensional form of any variable w of the model, the equation reads

$$\partial_{t'} h' + v' \cdot \nabla_{x'} h' = \frac{1}{\mathrm{Kn}} (M'[h'] - h') \,,$$

with $M'[h'] = \dfrac{M[h]}{h_*}$ and $\mathrm{Kn} = \dfrac{\tau}{t_*}$.

Using classical Chapman expansion one gets the following result:

Proposition 1.2.2. *Let h be the solution of BGK equation up to $O(\mathrm{Kn}^2)$. Then the moments of g satisfy the following Navier-Stokes equations up to $O(\mathrm{Kn}^2)$:*

$$\begin{cases} \partial_t \rho + \nabla_x \cdot (\rho u) = 0 \\ \partial_t (\rho u) + \nabla_x \cdot (\rho u \otimes u) + \nabla_x p = -\nabla_x \cdot (\sigma) + O(\mathrm{Kn}^2) \\ \partial_t E + \nabla_x \cdot ((E+p)u) = -\nabla_x \cdot (q) - \nabla_x \cdot (\sigma u) + O(\mathrm{Kn}^2) \,, \end{cases} \tag{1.51}$$

with

$$E = \left\langle \left\langle \left(\frac{1}{2}|v|^2 + \varepsilon \right) g \right\rangle \right\rangle = \rho e + \frac{1}{2}\rho |u|^2 \,, \tag{1.52}$$

$$\sigma = -\mu \left(\nabla_x u + \nabla_x u^T - \mathcal{C} \nabla_x \cdot (u) Id \right) \,, \tag{1.53}$$

$$q = -\mu \nabla_x h \,, \tag{1.54}$$

where $h = \dfrac{5+\delta}{2} \dfrac{p}{\rho}$ is the enthalpy of the system and $\mathcal{C} = \frac{\rho}{p} \left(\partial_1 p + \frac{p}{\rho^2} \partial_2 p - \frac{p}{\rho} \right)$, in which the notation $\partial_1 p$ (resp. $\partial_2 p$) is the partial derivative of p with respect to the first (resp. the second) variable (i.e. ρ (resp. e)).

Remark 1.2.1.

- The dynamic viscosity μ is given thanks to the relaxation time τ and depends on $T(\rho, e)$.
- The second viscosity λ is proportional to μ, with coefficient $\mathcal{C}$. In the particular case where δ is constant, this coefficient is given by $\mathcal{C} = \frac{2}{3+\delta}$.
- When the enthalpy satisfies $h = h(T)$, the thermal transfer coefficient κ is equal to μc_p ($c_p = h'(T)$), so that $\mathrm{Pr} = \frac{\mu c_p}{\kappa} = 1$.

Local entropy dissipation

Another critical point to check for any kinetic model is if it satisfies the second principle or not. With our model, if we look at a relative entropy function, then we can prove the local dissipation but not the global dissipation in the general case.

Proposition 1.2.3. *Let g be the solution of the BGK equation. Then the following inequality is satisfied:*

$$\left\langle \left\langle (M-h) \ln \left(\frac{h}{\frac{\delta}{2} \left(\frac{\rho \varepsilon}{p} \right)^{\frac{\delta}{2}-1}} \right) \right\rangle \right\rangle \leq 0 \,. \tag{1.55}$$

Remark 1.2.2. This result does not imply in the general case the dissipation of the global entropy, except, for example, if δ is constant. There still remains some work to understand if there is any second principle with respect to the model for the whole space in x.

1.2.3 Numerical validation

We now present our first numerical tests on a reduced model which has the same properties as the original but which does not need a full discretization in internal energy. Then we explain how it was implemented in our deterministic BGK code. Finally we show some results on an hypersonic test case when the gas is a mixture of two vibrating perfect diatomic gases (nitrogen and dioxygen).

Reduced polyatomic model with two distribution functions

For the polyatomic model, the phase space is of dimension 7 for 2D simulations and 8 for 3D simulations, which is one more (the one of the internal energy) than in the mono-atomic case. So numerical simulations for this model are very expensive. That is why a simpler formalism has been introduced in [DM99], which gives the same macroscopic variables with two distribution functions on a phase space of the dimension of the mono-atomic model. More precisely, it defines one distribution function for the mass (f) and one for the internal energy (g) by

$$f(t,x,v) = \langle h \rangle_\varepsilon \quad \text{and} \quad g(t,x,v) = \langle \varepsilon h \rangle_\varepsilon \,, \tag{1.56}$$

where g is the solution of the equation (1.31). We can obtain the macroscopic quantities of g from (f,g):

$$\rho = \langle f \rangle_v \,, \qquad \rho u = \langle f v \rangle_v \,, \qquad \rho e = \left\langle \frac{|v-u|^2}{2} f + g \right\rangle_v .$$

The pressure p, which is a function of ρ and e, is also defined from (f,g). Furthermore, the associated Maxwellian distribution $M[f,g]$ is given by the mono-atomic part of $M[g]$ defined by the relation (1.39):

$$M[f,g](v) = M_{mo}[g](v) = \frac{\rho}{\sqrt{2\pi\frac{p}{\rho}}^3} \exp\left(-\frac{\rho|u-v|^2}{2p}\right) . \tag{1.57}$$

The BGK system governing the evolution of (f,g) is obtained from (1.31) by integration in $\mathrm{d}\varepsilon$ and $\varepsilon \mathrm{d}\varepsilon$. Thanks to (1.43) and (1.44), these calculations yield:

$$\partial_t f + v \cdot \nabla_x f = \frac{1}{\tau}\left(M[f,g] - f\right) , \tag{1.58}$$

$$\partial_t g + v \cdot \nabla_x g = \frac{1}{\tau}\left(\frac{\delta}{2}\frac{p}{\rho} M[f,g] - g\right) . \tag{1.59}$$

Some words on the numerical solving and the existing code

To solve the problem, we have a deterministic BGK code developed by L. Mieussens and al.([Mie99]; [Bar+13]): it uses Cartesian or AMR grids in velocity and finite volumes in physical space phase.

The scheme is of order 2 (including boundary conditions). The set of equations which is solved is

$$\partial_t f + v \cdot \nabla_x f = \frac{1}{\tau}\left(M[f,g] - f\right), \tag{1.60}$$

$$\partial_t g + v \cdot \nabla_x g = \frac{1}{\tau}\left(\frac{\delta}{2} RTM[f,g] - g\right), \tag{1.61}$$

so that it is very close to our new model.

The solving of the problem (eq.1.60 - 1.61) is made possible thanks to the use of the entropic variable α (a vector) which is defined through: $M[f,g] = \exp(\alpha \cdot m(v))$ where $m(v)$ is the vector $(1, v, \frac{1}{2}v^2)$. Numerically a Newton method is used to determine α (see [Mie99]) by looking for α such that:

$$\rho = < f >, \tag{1.62}$$

$$\rho u = < fv >, \tag{1.63}$$

$$\rho\left[\frac{1}{2}u^2 + e\right] = =< f\frac{1}{2}v^2 > + < g >, \tag{1.64}$$

$$\rho = < \exp(\alpha \cdot m(v)) >, \tag{1.65}$$

$$\rho u = < \exp(\alpha \cdot m(v))v >, \tag{1.66}$$

$$\rho\left[\frac{1}{2}u^2 + e\right] = < \exp(\alpha \cdot m(v))\frac{1}{2}v^2 > + \frac{\delta}{2} RT < \exp(\alpha \cdot m(v)) > . \tag{1.67}$$

Modifications of the code for the new model

We have chosen to adapt our code to the new model (equations (1.58) and (1.59)). In order to do so, we have to modify equation (1.67) since we modify the definition of g in our model: to capture the new α we first compute the moments of f and g as before through:

$$\rho = < f >, \tag{1.68}$$

$$\rho u = < fv >, \tag{1.69}$$

$$\rho\left[\frac{1}{2}u^2 + e\right] = =< f\frac{1}{2}v^2 > + < g > . \tag{1.70}$$

This gives us ρ and e so that through the equation of state we get $p = p(\rho, e)$ and $\delta = \delta(\rho, e) = \dfrac{2\rho e}{p(\rho, e)} - 3$. Now we can find α solution of

$$\rho = < \exp(\alpha \cdot m(v)) >, \tag{1.71}$$

$$\rho u = < \exp(\alpha \cdot m(v))v >, \tag{1.72}$$

$$\rho\left[\frac{1}{2}u^2 + e\right] = < \exp(\alpha \cdot m(v))\frac{1}{2}v^2 > + \frac{\delta}{2}\frac{p}{\rho} < \exp(\alpha \cdot m(v)) > . \tag{1.73}$$

Numerically integrals are replaced by sums other all the velocities in each cell of the mesh in x variable and α is the numerical solution on the discrete grid of velocities.

A first test case of validation

We test the model on a mixture of two vibrating gases(N_2 and O_2) for an hypersonic flow over a cylinder with diffusive boundary conditions(figure 1.1). At the inlet, the following data are used:

Mass concentration of N_2 (c_{N_2})	0.75
Mass concentration of O_2 (c_{O_2})	0.25
Mach number of the mixture	10
Velocity of the mixture	$2267 m.s^{-1}$
Density of the mixture	$3.059 \times 10^{-4} kg.m^{-3}$
Pressure of the mixture	$11.22 Pa$
Temperature of the mixture	$127.6 K$
Temperature of the cylinder	$293 K$
Radius of the cylinder	$0.1 m$

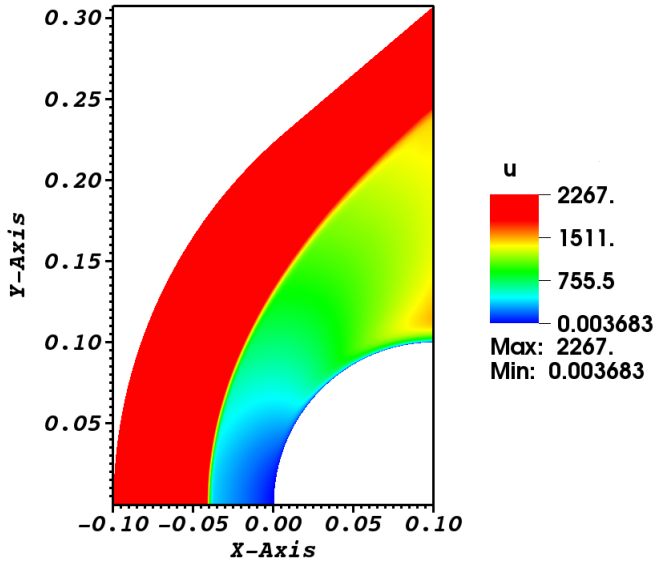

FIGURE 1.1: Flow over a cylinder at Mach 10 (velocity field)

Pressure and energy laws We consider a mixture of two perfect vibrating gases so that the pressure laws reads:

$$P = \rho RT \tag{1.74}$$

with $R = c_{O_2} R_{O_2} + c_{N_2} R_{N_2}$. The energy equation for two vibrating perfect gases reads:

$$\begin{aligned} e &= c_{O_2} e_{O_2} + c_{N_2} e_{N_2} \\ &= c_{O_2} \frac{3 + \delta_{O_2}(T)}{2} R_{O_2} T + c_{N_2} \frac{3 + \delta_{N_2}(T)}{2} R_{N_2} T \\ &= \frac{3}{2} RT + \frac{1}{2} (c_{O_2} \delta_{O_2}(T) R_{O_2} + c_{N_2} \delta_{N_2}(T) R_{N_2}) T \end{aligned} \tag{1.75}$$

where the internal energy of the dioxygen (resp. nitrogen) is e_{O_2} (resp. e_{N_2}). The number of degrees of freedom activated for dioxygen and nitrogen are respectively defined as :

$$\delta_{O_2}(T) = 2 + 2 \frac{T^{vib}_{O_2}/T}{\exp(T^{vib}_{O_2}/T) - 1}, \delta_{N_2}(T) = 2 + 2 \frac{T^{vib}_{N_2}/T}{\exp(T^{vib}_{N_2}/T) - 1},$$

with the following vibrational temperatures: $T^{vib}_{O_2} = 2256.K$ and $T^{vib}_{N_2} = 3373.K$. Consequently, the corresponding δ function for the mixture is:

$$\delta(\rho,T) = \frac{c_{O_2}\delta_{O_2}(T)R_{O_2} + c_{N_2}\delta_{N_2}(T)R_{N_2}}{R} = 2 + 2\frac{c_{O_2}R_{O_2}\frac{T^{vib}_{O_2}/T}{\exp(T^{vib}_{O_2}/T)-1} + c_{N_2}R_{N_2}\frac{T^{vib}_{N_2}/T}{\exp(T^{vib}_{N_2}/T)-1}}{R}$$

The only thing to know is that for a given energy of the mixture e there exists a unique temperature T. Furthermore, $e(T)$ is a monotonic function so that one can recover easily T from e numerically using a fixed point method and then compute δ.

Results The test case presented here is set so that vibrations occur in molecules (as seen in figure 1.67) but no chemical reactions are active (temperatures go up to $3000K$ whereas chemical reactions occur at $5000K$ at pressure $P = 1atm$): our thermodynamical approach is then licit. Since the test case is dense enough (Knudsen number of order 0.01) we can compare the new model with a Navier-Stokes code (a 2D structured code with finite volumes). To do it properly one has to choose the same law of viscosity (μ) for the two codes. Once it is done you have to define the law of conductivity (λ) in the Navier Stokes by $\lambda = \frac{\mu C_p}{Pr} = \mu C_p$ (C_p: specific heat at constant pressure) since BGK models only provide Prandtl numbers (Pr) equal to one. To validate the new model we have made four types of computations for the mixture:

- a Navier-Stokes computation without taking into account vibrations (called $NS1$),
- a Navier-Stokes computation taking into account vibrations (called $NS2$),
- a BGK computation without taking into account vibrations (called $BGK1$),
- a BGK computation taking into account vibrations (called $BGK2$).

We make three different comparisons :

- the first is between $NS1$ and $BGK1$ to show that they agree (we are dense enough): it validates that viscosity and conductivity law are the same. As it can be seen in figure 1.2, the results agree very well for non vibrating gases.
- the second one one is between $NS2$ and $BGK2$ to show that for another physics (vibrations) we still have a good agreement. This is what we observe in figure 1.3. One can observe that due to vibrations The temperature has fallen from $2682K$ to $2358K$ for Navier-Stokes and from $2695K$ to $2365K$ for BGK.
- the last one is between $BGK1$ and $BGK2$ to show what we gain by using our model in terms of physical relevancy. We can observe that the shock is no longer at the same position. Since there is a transfer of energy into vibrations the maximum temperature is lower and the shock slightly goes back to the cylinder (figure 1.4). If we make a cut along the axis of the temperature we clearly see the difference between the two physics (figure 1.5).

1.2.4 Conclusion

In this work, we have proposed a generalized BGK model to capture more physics for high temperatures. The study of this model is motivated by the necessity to take into account the fact that, for polyatomic gases, some internal degrees of freedom are partially excited with a level of excitation depending on the temperature. Namely, the goal is to simulate a flow of a polyatomic gas

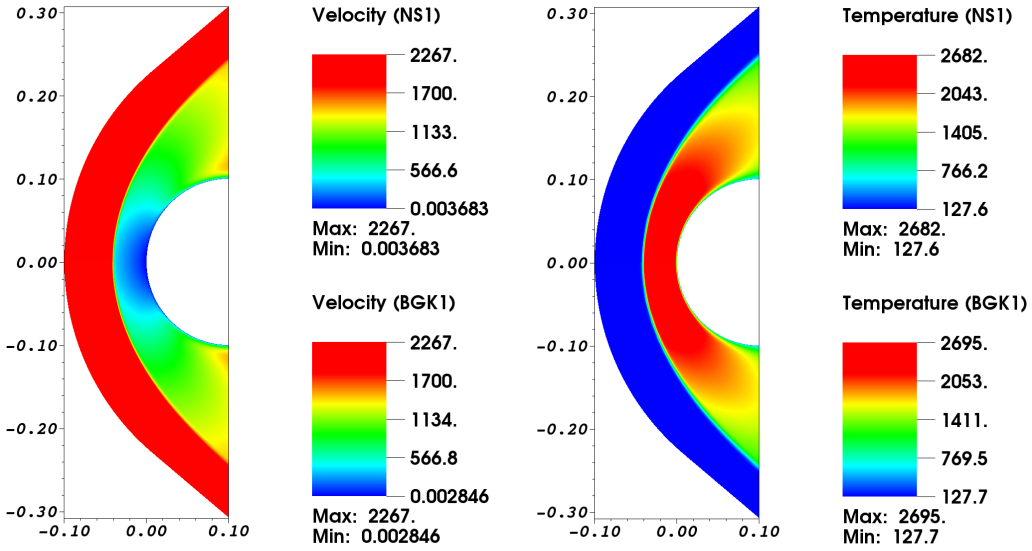

FIGURE 1.2: Velocity field and Temperature field (Top: NS1, bottom: BGK1)

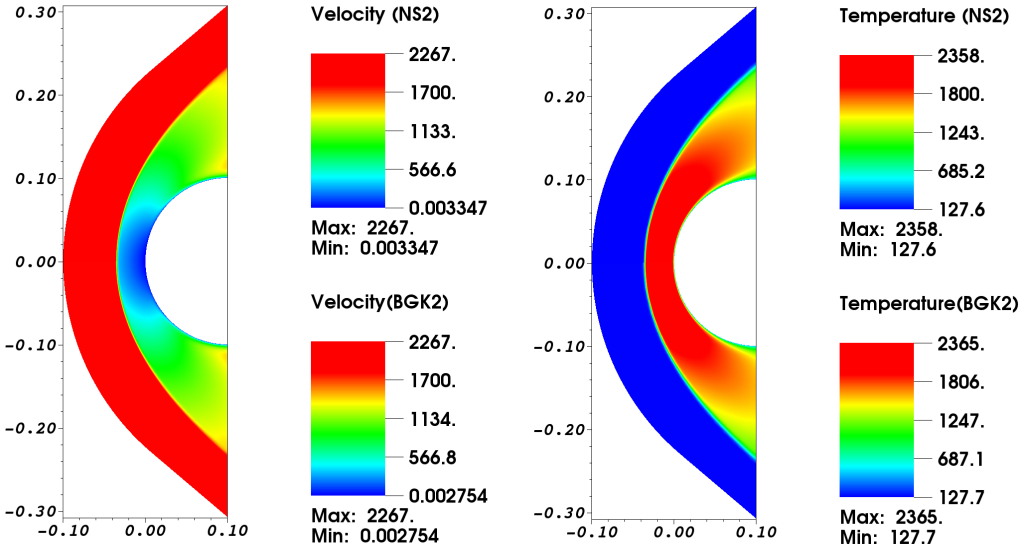

FIGURE 1.3: Velocity field and Temperature field (Top: NS2, bottom: BGK2)

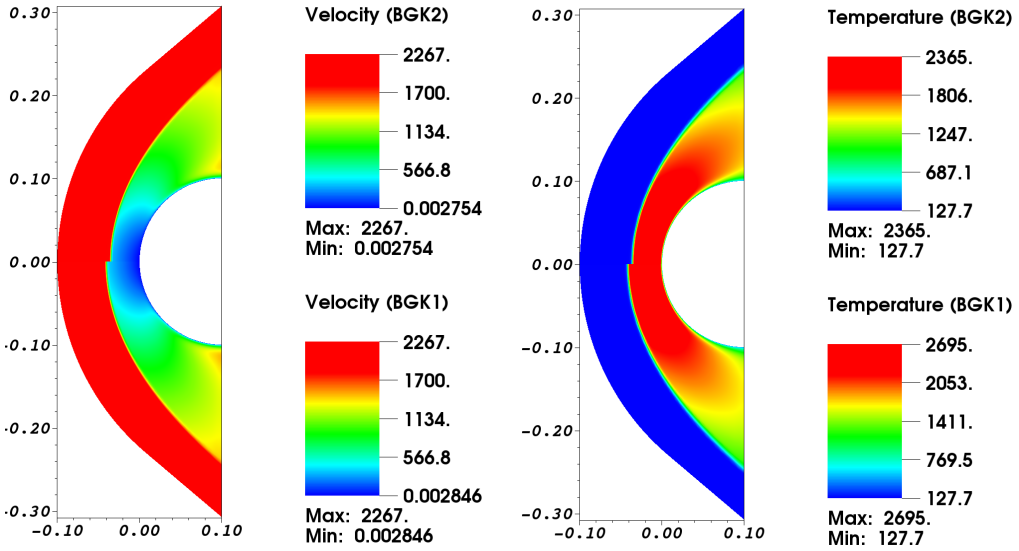

FIGURE 1.4: Velocity field and Temperature field (Top: BGK2, bottom: BGK1)

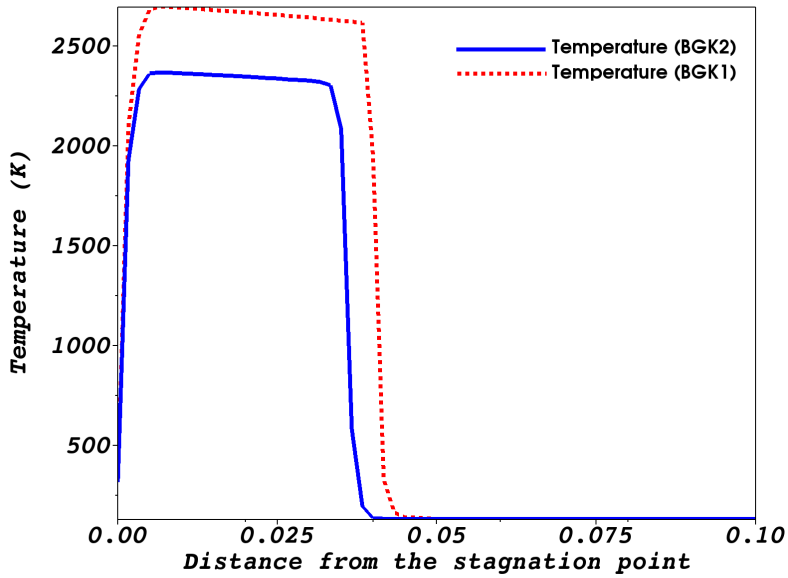

FIGURE 1.5: Temperature along the axis

with non-constant specific heat $C_p = C_p(T)$. Under low hypothesis, we have given the Chapman-Enskog expansion of order 1 of the model, *i.e.* the Navier-Stokes equations, in which the viscosities and heat transfer coefficient are explicitly expressed. Furthermore, we have proved the local entropy dissipation of the model. A description with two distribution functions has been also given in order to compute faster numerical simulations. Finally, some numerical results have been computed and compared successfully to those of the corresponding Navier-Stokes simulations. The next step of the study is the extension to ES-BGK model of these results to recover the correct Prandtl number in the hydrodynamic limit.

Chapter 2

Fokker-Planck models

Numerical simulations of rarefied gas flows are fundamental tools to study the behavior of a gas in a system which length is of same order of magnitude as the mean free path of the gas molecules. For instance, these simulations are used in aerodynamics to estimate the heat flux at the wall of a re-entry space vehicle at high altitudes; numerical simulations are also used to estimate the attenuation of a micro-accelerometer by the surrounding gas in a micro-electro-mechanical system; a last example is when one wants to estimate the pumping speed or compression rate of a turbo-molecular pump. Very recently, in a series of paper [JTH10]; [GTJ11]; [GJ12]; [GJ13], Jenny et al. proposed a very different and innovative approach: they proposed to use a different model equation known as the Fokker-Planck model to design a rarefied flow solver. In this model, the collisions are taken into account by a diffusion process in the velocity space. Like the model equations mentioned above, this equation also satisfy the main properties of the Boltzmann equation, even the H-theorem. Instead of using a direct discretization of this equation, the authors used the equivalent stochastic interpretation of this equation (the Langevin equations for the position and velocity of particles) that are discretized by a standard stochastic ordinary differential equation numerical scheme. This approach turned out to be very efficient, in particular in the transition regime, since it is shown to be insensitive to the number of simulated particles, as opposed to the standard DSMC. However, this Fokker-Planck model is parametrized by a single parameter, like the BGK model, and hence cannot give the correct transport coefficients in near equilibrium regimes: this is often stated by showing that the Prandtl number–which is the ratio of the viscosity to the heat transfer coefficient–has an incorrect value. The authors have proposed a modified model that allow to fit the correct value of the Prandtl number [GTJ11], and then have extended it to more complex flows (multi-species [GJ12] and diatomic [GJ13]). However, even if the results obtained with this approach seem very accurate, it is not clear that these models still satisfy the H-theorem. In this part, we propose another kind of modification of the Fokker-Planck equation to get a correct Prandtl number: roughly speaking, the diffusion coefficient (which is the equilibrium temperature) is replaced by a non diagonal temperature tensor. This approach is closely related to the way the BGK model is extended to the ES-BGK model, and we call our model the ES-Fokker Planck (ES-FP) model. Then, we are able to prove that this model satisfies the H-theorem. For illustration, we also show numerical experiments that confirm our analysis, for a space homogeneous problem. We present here the papers [MM16] and [MM17] which deal with monoatomic and polyatomic models.

2.1 Mono-atomic model

We consider a gas described by the mass density of particles $f(t,x,v)$ that at time t have the position x and the velocity v. The corresponding macroscopic quantities are $(\rho,\rho u,E)=\left\langle (1,v,\frac{1}{2}|v|^2)f\right\rangle$,

where ρ, ρu, and E are the mass, momentum, and energy densities, and $\langle \phi \rangle = \int_{\mathbb{R}^3} \phi(v)\, dv$ for any velocity dependent function. The temperature T of the gas is defined by relation $E = \frac{1}{2}\rho|u|^2 + \frac{3}{2}\rho RT$, where R is the gas constant, and the pressure is $p = \rho RT$. The evolution of the gas is governed by the following Boltzmann equation

$$\partial_t f + v \cdot \nabla_x f = Q(f, f), \tag{2.1}$$

where the collision operator is, in the hard-sphere case,

$$Q(f,f)(v) = \int_{v_* \in \mathbb{R}^3} \int_{\sigma \in S^2} \Big(f(v'_*)\, f(v') - f(v_*)\, f(v) \Big)\, r^2\, |v - v_*|\, d\sigma\, dv_*,$$

with

$$v' = \frac{v + v_*}{2} + \frac{|v - v_*|}{2}\,\sigma, v'_* = \frac{v + v_*}{2} - \frac{|v - v_*|}{2}\,\sigma,$$

and r is the radius of the molecules. It is well known that this operator conserves the mass, momentum, and energy, and that the local entropy $H(f) = \langle f \log f \rangle$ is locally non-increasing. This means that the effect of this operator is to make the distribution f relax towards its own local Maxwellian distribution, which is defined by

$$M(f)(v) = \frac{\rho}{(2\pi RT)^{3/2}} \exp\left(\frac{|v - u|^2}{2RT} \right).$$

For the sequel, it is useful to define another macroscopic quantity, which is not conserved: the temperature tensor, defined by

$$\Theta := \frac{1}{\rho} \left\langle (v - u) \otimes (v - u) f \right\rangle. \tag{2.2}$$

In an equilibrium state (that is to say when $f = M(f)$), Θ reduces to the isotropic tensor RTI.

2.1.1 The ES-Fokker Planck model

The standard Fokker-Planck model for the Boltzmann equation is (see [Cer88]):

$$\partial_t f + v \cdot \nabla_x f = \frac{1}{\tau} \nabla_v \cdot \big((v - u) f + RT \nabla_v f \big), \tag{2.3}$$

Our model is obtained in the same spirit as the ES model is obtained from a modification of the BGK equation: the temperature that appears in (2.3), as a diffusion coefficient, is replaced by a tensor Π so that we obtain

$$\partial_t f + v \cdot \nabla_x f = D(f), \tag{2.4}$$

where the collision operator is defined by

$$D(f) = \frac{1}{\tau} \nabla_v \cdot \big((v - u) f + \Pi \nabla_v f \big), \tag{2.5}$$

where τ is a relaxation time, and Π is a convex combination between the temperature tensor Θ and its equilibrium value RTI, that is to say:

$$\Pi = (1 - \nu) RTI + \nu \Theta, \tag{2.6}$$

with ν a parameter. According to [And+00b], Π is symmetric positive definite if $\nu \in]-\frac{1}{2}, 1]$. In fact, this condition is too restrictive and we have the following result.

Proposition 2.1.1 (Condition of positive definiteness of Π)**.**

The tensor Π is symmetric positive definite for every tensor Θ if, and only if,

$$-\frac{RT}{\lambda_{max} - RT} < \nu < \frac{RT}{RT - \lambda_{min}}, \tag{2.7}$$

where λ_{max} and λ_{min} are the (positive) maximum and minimum eigenvalues of Θ. Moreover Π is positive definite independently of the eigenvalues of Θ as long as:

$$-\frac{1}{2} < \nu < 1, \tag{2.8}$$

The operator D has two other equivalent formulations:

$$D(f) = \frac{1}{\tau}\nabla_v \cdot \left(\Pi G(f) \nabla_v \frac{f}{G(f)}\right), \tag{2.9}$$

and

$$D(f) = \frac{1}{\tau}\nabla_v \cdot \left(\Pi f \nabla_v \log\left(\frac{f}{G(f)}\right)\right), \tag{2.10}$$

where $G(f)$ is the anisotropic Gaussian defined by

$$G(f) = \frac{\rho}{\sqrt{\det(2\pi\Pi)}} \exp\left(-\frac{(v-u)\Pi^{-1}(v-u)}{2}\right), \tag{2.11}$$

which has the same 5 first moments as f

$$\left\langle (1, v, \tfrac{1}{2}|v|^2) G(f) \right\rangle = (\rho, \rho u, E),$$

and has the temperature tensor $\langle (v-u) \otimes (v-u) G(f) \rangle = \Pi$.

Now, we state that D has the same conservation and entropy properties as the Boltzmann collision operator Q ([MM16]).

Proposition 2.1.2. *We assume ν satisfies (2.29) and that $\nu < 1$. The operator D conserves the mass, momentum, and energy:*

$$\left\langle (1, v, \tfrac{1}{2}|v|^2) D(f) \right\rangle = 0, \tag{2.12}$$

it satisfies the dissipation of the entropy:

$$\langle D(f) \log f \rangle \leq 0,$$

and we have the equilibrium property:

$$D(f) = 0 \Leftrightarrow f = G(f) \Leftrightarrow f = M(f).$$

2.2 Polyatomic model

We consider a gas described by the mass density of particles $f(t, x, v, I)$ that at time t have the position x, the velocity v and an internal energy parameter I (note that both position x and velocity v are vectors and that I is a scalar). The internal energy of a particle is equal to $\varepsilon(I) = I^{\frac{2}{\delta}}$, δ being

linked to the number of degrees of freedom of the polyatomic gas ($\delta = 2$ for diatomic gases). The corresponding macroscopic quantities are $(\rho, \rho u, E) = \left\langle (1, v, \left(\frac{1}{2}|v|^2\right) + \varepsilon(I)) f \right\rangle$, where ρ, ρu, and E are the mass, momentum, and energy densities, and $\langle \phi \rangle = \int_{\mathbb{R}^3} \phi(v, I)\, dvdI$ for any velocity dependent function. The temperature T of the gas is defined by relation $E = \frac{1}{2}\rho|u|^2 + \frac{3+\delta}{2}\rho RT$, where R is the gas constant, and the pressure is $p = \rho RT$. We can also define a translational energy E_{tr}, a translational temperature T_{tr}, an internal energy E_{int} and an internal energy temperature T_{int} through:

$$E_{tr} = \frac{3}{2}\rho R T_{tr} = \left\langle \tfrac{1}{2}|v-u|^2 f \right\rangle, \tag{2.13}$$

$$E_{int} = \frac{\delta}{2}\rho R T_{int} = \langle \varepsilon(I) f \rangle, \tag{2.14}$$

so that:

$$T = \frac{3}{3+\delta} T_{tr} + \frac{\delta}{3+\delta} T_{int}. \tag{2.15}$$

The evolution of the gas can be governed by the following Boltzmann equation (if we do not take into account exchanges in internal energy)

$$\partial_t f + v \cdot \nabla_x f = Q(f, f), \tag{2.16}$$

where $Q(f, f)$ is for instance the Borgnakke-Larsen kernel of collision described in ([Des97b]; [DMS05]) which allows reversible exchanges of energy between internal energy and translational energy of the particles.

It is well known that this operator conserves the mass, momentum, and energy, and that the local entropy $H(f) = \langle f \log f \rangle$ is locally non-increasing. This means that the effect of this operator is to make the distribution f relax towards its own local Maxwellian distribution, which is defined by

$$M_p(f)(v, I) = \frac{\rho \Lambda_\delta}{(2\pi)^{3/2} (RT)^{(3+\delta)/2}} \exp\left(-\frac{|v-u|^2}{2RT} - \frac{I^{2/\delta}}{RT} \right), \tag{2.17}$$

where $\Lambda_\delta = \left(\int_0^{+\infty} \exp(-I^{2/\delta}) dI \right)^{-1}$.

For the sequel, it is useful to define another macroscopic quantity, which is not conserved: the "temperature" tensor, defined by

$$\Theta := \frac{1}{\rho} \left\langle (v-u) \otimes (v-u) f \right\rangle. \tag{2.18}$$

In an equilibrium state (that is to say when $f = M(f)$), Θ reduces to the isotropic tensor RTI.

2.2.1 The ES-Fokker-Planck model for polyatomic gases

Our extension of the previous model to polyatomic gases is based on two ideas. First, the variation of the internal energy of the particles due to collisions are taken into account by an additional diffusion term (with respect to the internal energy variable) in the collision operator. Then, the transfers between translational and internal energies are taken into account by an additional parameter

θ, like in the construction of the ESBGK model for polyatomic gases proposed in [And+00b]. This leads to our ES-Fokker-Planck model for polyatomic gases:

$$\partial_t f + v \cdot \nabla_x f = D(f), \tag{2.19}$$

where the collision operator is defined by

$$D(f) = \frac{1}{\tau}\left(\nabla_v \cdot \left((v-u)f + \Pi \nabla_v f\right) + \partial_I(\delta f I + \frac{\delta^2}{2} R T_{rel} I^{2-\frac{2}{\delta}} \partial_I f)\right), \tag{2.20}$$

with τ its relaxation time, and Π the following combination between the temperature tensor Θ, the translational temperature tensor $RT_{tr}Id$ and its equilibrium value $RTId$:

$$\Pi = (1-\theta)\left((1-\nu)RT_{tr}Id + \nu\Theta\right) + \theta RTId, \tag{2.21}$$

where the coefficients ν and θ are some free parameters, and the temperature T_{rel} is defined by

$$T_{rel} = (1-\theta)T_{int} + \theta T. \tag{2.22}$$

This model is the natural extension of the monoatomic ESFP model to get the polyatomic anisotropic Gaussian as equilibrium for polyatomic gases, as it was done for the ESBGK model for polyatyomic gases (see [And+00b]).

Now, we give a few comments about parameters θ and δ. First, it can be seen that θ governs the reversible exchanges between internal and translational energies. Indeed, for a space homogeneous problem (we neglect the space dependence of the problem), it can easily be seen the relaxation time of exchanges between internal energies and translational energies is $\frac{3+\delta}{2\delta\theta}\tau$, and a relaxation collision number on the collision rate time-scale τ (see [Bir94]) can be defined by $Z = \frac{3+\delta}{2\delta\theta}$ which is clearly parametrized by θ. Consequently, it is clear that when $\theta = 0$ we no longer have exchanges between internal and translational energies. Note that this model is compatible with the monoatomic model: indeed, when $\delta = 0$ we immediately recover the monoatomic model since in this case $T_{tr} = T$.

For the following, it is usefull to rewrite model (2.19) a bit differently. We define the generalized tensor Ω by

$$\Omega = \left(\begin{array}{c|c} \Pi & 0 \\ \hline 0 & \frac{\delta^2}{2} R T_{rel} I^{2-\frac{2}{\delta}} \end{array}\right), \tag{2.23}$$

so that the collision operator of (2.19) reads

$$D(f) = \frac{1}{\tau}\nabla_{v,I} \cdot \left(\begin{pmatrix} v-u \\ \delta I \end{pmatrix} f + \Omega \nabla_{v,I} f\right),$$

where $\nabla_{v,I}$ denotes the derivative operator with respect to both v and I variables. We can now define the generalized Gaussian $G_p(f)$ for polyatomic gases as:

$$G_p(f) = \frac{\rho \Lambda_\delta}{\sqrt{\det(2\pi\Pi)}(RT_{rel})^{\delta/2}} \exp\left(-\frac{1}{2}\begin{pmatrix} v-u \\ \delta I \end{pmatrix}^T \Omega^{-1} \begin{pmatrix} v-u \\ \delta I \end{pmatrix}\right). \tag{2.24}$$

One can note that contrary to the case of monoatomic gases the tensor Ω depends on the variables of the phase space through the internal parameter. The generalized Maxwellian $M_p(f)$ of

equilibrium for polyatomic gases (2.17) can also be defined as:

$$M_p(f) = \frac{\rho\Lambda_\delta}{(2\pi)^{3/2}(RT)^{\frac{3+\delta}{2}}} \exp\left(-\begin{pmatrix} \frac{v-u}{\sqrt{2RT}} \\ \frac{I^{1/\delta}}{\sqrt{RT}} \end{pmatrix}^T \begin{pmatrix} \frac{v-u}{\sqrt{2RT}} \\ \frac{I^{1/\delta}}{\sqrt{RT}} \end{pmatrix}\right) \tag{2.25}$$

We now look for the properties of the collision kernel $D(f)$ as it was done in the monoatomic case.
Proposition 2.2.1. *The operator D has two other equivalent formulations:*

$$D(f) = \frac{1}{\tau}\nabla_{v,I} \cdot \left(\Omega G_p(f)\nabla_{v,I}\frac{f}{G_p(f)}\right), \tag{2.26}$$

and

$$D(f) = \frac{1}{\tau}\nabla_{v,I} \cdot \left(\Omega f\nabla_{v,I}\log\left(\frac{f}{G_p(f)}\right)\right), \tag{2.27}$$

Moreover G_p has the same 5 first moments as f

$$\left\langle (1, v, \tfrac{1}{2}|v|^2 + I^{2/\delta})G_p(f)\right\rangle = (\rho, \rho u, \rho E),$$

and has its translationnal temperature tensor equal to $\left\langle (v-u)\otimes(v-u)G_p(f)\right\rangle/\rho = \Pi$.
Proposition 2.2.2 (Condition of definite positiveness of Π)**.**

Assume $0 < \theta < 1$, the tensor Π is symmetric positive definite if, and only if,

$$-\frac{RT_{tr} + \frac{\theta}{1-\theta}RT}{\lambda_{max} - RT_{tr}} < \nu < \frac{RT_{tr} + \frac{\theta}{1-\theta}RT}{RT_{tr} - \lambda_{min}}, \tag{2.28}$$

for every tensor Θ (λ_{max} and λ_{min} being its (positive) maximum and minimum eigenvalues). Moreover Π is positive definite independently of the eigenvalues of Θ as long as:

$$-\frac{1}{2} < \nu < 1, \tag{2.29}$$

Now, we state that D has the same conservation and entropy properties as the Boltzmann collision operator Q.
Proposition 2.2.3. *We assume ν satisfies (2.28) and that $\nu < 1$. The operator D conserves the mass, momentum, and energy:*

$$\left\langle (1, v, \tfrac{1}{2}|v|^2 + I^{2/\delta})D(f)\right\rangle = 0, \tag{2.30}$$

it satisfies the dissipation of the entropy:

$$\langle D(f)\log f\rangle \leq 0,$$

and we have the equilibrium property:

$$D(f) = 0 \Leftrightarrow f = G_p(f) \Leftrightarrow f = M_p(f).$$

2.2.2 Equation on internal energy

While the formulation of our model with the internal energy parameter I is useful to prove the H-theorem, using the internal energy $\varepsilon(I) = I^{2/\delta}$ turns out to be more convenient for numerical

simulations. If we denote by $g(t,x,v,\varepsilon)$ the corresponding distribution function (that is to say, such that $g\,d\varepsilon = f\,dI$), we get the following equation

$$\partial_t g + v\cdot\nabla_x g = \mathcal{D}(g), \tag{2.31}$$

where the collision operator is defined by

$$\mathcal{D}(g) = \frac{1}{\tau}\left(\nabla_v\cdot\left((v-u)g + \Pi\nabla_v g\right) + \nabla_\varepsilon\left(2(\varepsilon - \frac{\delta}{2}RT_{rel})g + \nabla_\varepsilon 2(RT_{rel}\varepsilon g)\right)\right). \tag{2.32}$$

The equilibrium and its Gaussian extension are now

$$\mathcal{M}(g) = \frac{\rho\Lambda_g}{(2\pi)^{3/2}}\frac{\varepsilon^{\frac{\delta-2}{2}}}{(RT)^{\frac{\delta}{2}}}\exp\left(-\frac{\frac{1}{2}(v-u)^2+\varepsilon}{RT}\right)$$

and

$$\mathcal{G}(g) = \frac{\rho\Lambda_g}{\sqrt{\det(2\pi\Pi)}}\frac{\varepsilon^{\frac{\delta-2}{2}}}{(RT_{rel})^{\frac{\delta}{2}}}\exp\left(-\frac{1}{2}(v-u)^t\Pi^{-1}(v-u) - \frac{\varepsilon}{RT_{rel}}\right)$$

with

$$\Lambda_g = \left(\int_{\mathbb{R}}\varepsilon^{\frac{\delta-2}{2}}\exp(-\varepsilon)d\varepsilon\right)^{-1}.$$

When one deals with diatomic gases ($\delta = 2$) one recovers the same equation as before since $\varepsilon(I)$ is equal to I. The main difference with the ε-formulation of the problem is that the entropy inequality is transformed into a relative entropy inequality, that is

$$\left\langle D_g(g)\log\left(\frac{g}{\varepsilon^{\frac{\delta-2}{2}}}\right)\right\rangle \le 0,$$

due to the change of variables.

2.3 Hydrodynamic limits

2.3.1 The monoatomic case

From (2.3) and (2.30), the moments of f satisfy the conservation laws

$$\begin{aligned}
&\partial_t\rho + \nabla_x\cdot\rho u = 0,\\
&\partial_t\rho u + \nabla_x\cdot(\rho u\otimes u) + \nabla_x\cdot\Sigma(f) = 0,\\
&\partial_t E + \nabla_x\cdot(Eu + \Sigma(f)u + q(f)) = 0,
\end{aligned} \tag{2.33}$$

where $\Sigma(f)$ and $q(f)$ denote the stress tensor and the heat flux, defined by

$$\Sigma(f) = \langle(v-u)\otimes(v-u)f\rangle \qquad q(f) = \left\langle\tfrac{1}{2}(v-u)|v-u|^2 f\right\rangle. \tag{2.34}$$

The Chapman-Enskog procedure consists in looking for an approximation of $\Sigma(f)$ and $q(f)$ up to second order with respect to the Knudsen number Kn which is defined below.

To do so, we now write our model in a non-dimensional form. Assume we have some reference values of length x_*, pressure p_*, and temperature T_*. With these reference values, we can derive

reference values for all the other quantities: mass density $\rho_* = p_*/RT_*$, velocity $v_* = \sqrt{RT_*}$, time $t_* = x_*/v_*$, distribution function $f_* = \rho_*/(RT_*)^{3/2}$. We also assume we have a reference value for the relaxation time τ_*. By using the non-dimensional variables $w' = w/w_*$ (where w stands for any variables of the problem), our model can be written

$$\partial_t f + v \cdot \nabla_x f = \frac{1}{\varepsilon} D(f), \tag{2.35}$$

where $Kn = \frac{v_* \tau_*}{x_*}$ is the Knudsen number. Note that since we always work with the non-dimensional variables from now on, these variables are not written with the $'$ in (2.35).

Note that an important consequence of the use of these non-dimensional variables is that RT has to be replaced by T in every expressions given before. Namely, now Π is defined by

$$\Pi = (1-\nu)TI + \nu\Theta, \tag{2.36}$$

the temperature is now defined by

$$E = \tfrac{1}{2}\rho|u|^2 + \tfrac{3}{2}\rho T,$$

and the Maxwellian of f now is

$$M(f) = \frac{\rho}{(2\pi T)^{3/2}} \exp\left(\frac{|v-u|^2}{2T}\right).$$

Now, it is standard to look for the deviation of f from its own local equilibrium, that is to say to set $f = M(f)(1 + Kng)$. However, this requires the linearization of the collision operator D around $M(f)$, which is not very easy. At the contrary, it will be shown that it is much simpler to look for the deviation of f from the anisotropic Gaussian $G(f)$ defined in (2.24). Since it can easily be seen that $M(f)$ and $G(f)$ are close up to $O(Kn)$ terms, this expansion is sufficient to get the Navier-Stokes equations: we will then prove the following result.

Proposition 2.3.1. *The moments of the solution of the kinetic model (2.3) satisfy, up to $O(Kn^2)$, the Navier-Stokes equations*

$$\begin{aligned} &\partial_t \rho + \nabla \cdot \rho u = 0, \\ &\partial_t \rho u + \nabla \cdot (\rho u \otimes u) + \nabla p = -\nabla \cdot \sigma, \\ &\partial_t E + \nabla \cdot (E+p)u = -\nabla \cdot q - \nabla \cdot (\sigma u), \end{aligned} \tag{2.37}$$

where the shear stress tensor and the heat flux are given by

$$\sigma = -\mu\big(\nabla u + (\nabla u)^T - \frac{2}{3}\nabla \cdot u\big), \quad \textit{and} \quad q = -\kappa \nabla \cdot T, \tag{2.38}$$

with the following values of the viscosity and heat transfer coefficients

$$\mu = \frac{\tau p}{2(1-\nu)}, \quad \textit{and} \quad \kappa = \frac{5}{6}\tau p R. \tag{2.39}$$

Moreover, the corresponding Prandtl number is

$$\mathrm{Pr} = \frac{3}{2(1-\nu)},$$

and Kn is the Knudsen number defined below.

The ES-Fokker Planck model with a non constant ν

We establish how we deal with the Prandtl number in all cases.

Some limits of the model with a constant ν In the previous section, we have found that the Prandtl number obtained for the ES-Fokker Planck model is

$$\mathrm{Pr} = \frac{\mu}{\kappa}\frac{5R}{2} = \frac{3}{2(1-\nu)}, \tag{2.40}$$

and can be adjusted to various values by choosing a corresponding value of the parameter ν.

Moreover, we have seen that the model is well defined (that is to say that the tensor Π is positive definite for every f) if, and only if $-\frac{1}{2} < \nu < 1$. This last condition leads to the following limitations for the Prandtl number:

$$1 < Pr < +\infty,$$

so that the correct Prandtl number for monoatomic gases (which is equal to $\frac{2}{3}$) cannot be obtained. In the next section, we show that this analysis, which is based on the inequality (2.29) is too restrictive, and that there is a simple way to adjust the correct Prandtl number.

Recovering the good Prandtl number The previous analysis relies on inequality (2.29) of proposition 2.2.2 that does not take into account the distribution f itself: this inequality ensures the positive definiteness of Π independently of f. However, proposition 2.2.2 also indicates that Π is positive definite for a given f if ν satisfies (2.28). This inequality is less restrictive, since it depends on f via the temperature T and the extreme eigenvalues of Θ.

Now, our first idea is that ν can be set to a non constant value (it may depend on time and space): it just has to lie in the interval $[-\frac{RT}{\lambda_{max}-RT}, 1]$, so that it satisfies the assumptions of proposition 2.2.3. The second idea is that the Prandtl number makes sense when the flow is close to the equilibrium, that is to say when f is close to its own local Maxwellian $M(f)$: in such case, $\Theta = RTI + O(Kn)$, and all the eigenvalues of Θ are close to RT up to $O(Kn)$ terms, which implies $\lambda_{max} = RT + CKn$. Consequently, the value of ν now lies in $[-\frac{RT}{RCKn}, 1]$ which shows that ν can take any arbitrary value between $-\infty$ and 1 when Kn is small enough, and in particular the value $\nu = -\frac{5}{4}$ that gives the correct Prandtl number $\mathrm{Pr} = \frac{2}{3}$ can be used.

In other words, by defining ν as a non constant value that satisfies (2.28) and is lower than 1, we can adjust the correct Prandtl number provided that ν can be set to $-\frac{5}{4}$ near the equilibrium regime.

This analysis suggests a very simple definition of ν : we propose to use the smallest negative ν such that:

- Π remains strictly definite positive,
- $\nu \geq -\frac{5}{4}$.

This leads to the following definition:

$$\nu = \max\left(-\frac{5}{4}, -\frac{RT}{\lambda_{max} - RT}\right). \tag{2.41}$$

Note that in most realistic cases ν is equal to $-\frac{5}{4}$. Indeed, $\nu \neq -\frac{5}{4}$ implies $\lambda_{max} > 1.8RT$ which can only happen in case of highly non equilibrium flow with strong directional non isotropy: such cases are very specific and are usually not observed in aerodynamical flows, for instance.

2.3.2 The diatomic case

From (2.19) and (2.30), it can easily be shown that the moments of f satisfy the following conservation laws

$$\begin{aligned} &\partial_t \rho + \nabla_x \cdot \rho u = 0, \\ &\partial_t \rho u + \nabla_x \cdot (\rho u \otimes u) + \nabla_x \cdot \Sigma(f) = 0, \\ &\partial_t E + \nabla_x \cdot (Eu + \Sigma(f)u + q(f)) = 0, \end{aligned} \tag{2.42}$$

where $\Sigma(f)$ and $q(f)$ denote the stress tensor and the heat flux, defined by

$$\Sigma(f) = \langle (v-u) \otimes (v-u) f \rangle \qquad q(f) = \left\langle (\tfrac{1}{2}|v-u|^2 + I^{2/\delta})(v-u) f \right\rangle . \tag{2.43}$$

Once more we proceed to a Chapman-Enskog procedure (as it was done for the mono-atomic case) and prove the following proposition:

Proposition 2.3.2. *The moments of the solution of the kinetic model (2.35) satisfy, up to $O(Kn^2)$, the Navier-Stokes equations*

$$\begin{aligned} &\partial_t \rho + \nabla \cdot \rho u = 0, \\ &\partial_t \rho u + \nabla \cdot (\rho u \otimes u) + \nabla p = -\nabla \cdot \sigma, \\ &\partial_t E + \nabla \cdot (E + p)u = -\nabla \cdot q - \nabla \cdot (\sigma u), \end{aligned} \tag{2.44}$$

where the shear stress tensor and the heat flux are given by

$$\sigma = -\mu\big(\nabla u + (\nabla u)^T - \alpha \nabla \cdot u\big), \quad \textit{and} \quad q = -\kappa \nabla \cdot T, \tag{2.45}$$

with the following values of the viscosity and heat transfer coefficients (in dimensional variables)

$$\mu = \frac{\tau p}{2(1-(1-\theta)\nu)}, \quad \alpha = (\gamma - 1) - \frac{(1-\nu)(1-\theta)}{\theta}\left(\frac{5}{3} - \gamma\right) \quad \textit{and} \quad \kappa = \frac{5+\delta}{6}\tau p R, \tag{2.46}$$

and $\gamma = \frac{\delta+5}{\delta+3}$. Moreover, the corresponding Prandtl number is

$$\mathrm{Pr} = \frac{3}{2(1-(1-\theta)\nu)}. \tag{2.47}$$

Note that we still have to adjust the Prandtl number following the procedure proposed for monoatomic gases ([MM16]) just before: it can be read in ([MM17]).

2.4 Numerical results

2.4.1 Numerical method

We use a DSMC method to solve these different problems. For homogeneous cases, the probability density function in the mono-atomic case) is approximated with N numerical particles so that

$$f(t,v) \simeq \alpha \sum_i^N \omega_i \delta_{V_i(t)},$$

where ω_i is the numerical weight of numerical particle i and $\delta_{V_i(t)}$ is the Dirac function at the particle velocity $V_i(t)$. Moreover α is defined through the constant density $\rho = \int_{\mathbb{R}^3} f(t,v)dv$ by

$$\rho = \alpha \sum_i^N \omega_i.$$

In the test cases presented here, all numerical weights ω_i are equal, and we just have to define the dynamics of the numerical particles. To solve diffusive problems, it is well-known that using Brownian motion is a good way to proceed (see [Lap+98]): the corresponding stochastic ordinary differential equation is called the Ornstein-Uhlenbeck process that reads

$$dV_i(t) = -\frac{dt}{\tau}\left(V_i(t) - u\right) + AdB(t), \tag{2.48}$$

for each $1 \leq i \leq N$. The quantity $dB(t)$ is a three dimensional Brownian process. The matrix A has to satisfy $AA^T = \Pi$. Several choices are available for A. The obvious one would be to use the square root of Π (which is a positive definite matrix): this requires to compute the eigenvectors of Π and may lead to expensive computations. We find it simpler to use the Cholesky decomposition because of the simplicity of the algorithm. For the time discretization we use a backward Euler method. The complete algorithm is the following:

1. Approximate the initial data $f(0,v)$ by $\sum_i^N \omega \delta_{V_i(t)}$, where N is the number of numerical particles and ω a constant numerical weight. The velocities are chosen randomly according to the particle density function $f(0,.)$.
2. Compute the tensor Θ
3. Compute the three real eigenvalues the positive definite tensor Θ with Cardan's formula.
4. Compute the Cholesky factorization $\Pi = A^T A$ of Π.
5. For i from 1 to N, advance the velocity V_i^n through the process:

$$V_i^{n+1} = \left(1 - \frac{\Delta t}{\tau}\right)\left(V_i^n - u\right) + \sqrt{\frac{2\Delta t}{\tau}} A \begin{pmatrix} B_1 \\ B_2 \\ B_3 \end{pmatrix}$$

   where $\Delta t = t^{n+1} - t^n$, B_1, B_2, B_3 are random numbers chosen through a standard normal law. Since the scheme is explicit we enforce $\frac{\Delta t}{\tau} \leq 0.1$ to ensure stability: this leads to around $\frac{T_f}{0.1 \times \tau}$ time steps to reach the final time T_f.

The scheme we propose here preserves mass but does not preserve momentum and energy, like most DSMC methods. However, these quantities are preserved in a statistical way. Moreover at

the end of each time step, the distribution is renormalized to keep the mean velocity constant and to decrease the error in Θ.

We extended the approach for the polyatomic case through

$$f(t,v,e) \simeq \alpha \sum_i^N \omega_i \delta_{V_i(t),\varepsilon_i(t)},$$

where ω_i is the numerical weight of numerical particle i and $\delta_{V_i(t)}$ is the Dirac function at the particle velocity $V_i(t)$ and particle internal energy $\varepsilon_i(t)$. Moreover α is defined through the constant density $\rho = \int_{\mathbb{R}^3} f(t,v)dv$ by

$$\rho = \alpha \sum_i^N \omega_i.$$

The Ornstein-Uhlenbeck process now reads

$$dV_i(t) = -\frac{dt}{\tau}\left(V_i(t) - u\right) + A_v dB_v(t), \tag{2.49}$$

$$d\varepsilon_i(t) = -\frac{2dt}{\tau}\left(\varepsilon_i(t) - \frac{\delta}{2}RT_{rel}\right) + 2\sqrt{RT_{rel}\varepsilon_i(t)}\, dB_\varepsilon(t), \tag{2.50}$$

for each $1 \leq i \leq N$. The quantities $dB_v(t)$ and $dB_\varepsilon(t)$ respectively are three dimensional and one dimensional Brownian processes.

We now focus on the internal energy equation. Since the diffusion coefficient depends on the square root of the internal energy, this latter variable must remain positive, and hence a simple Euler algorithm cannot work in this case. We will adapt the Milshtein scheme (see [Lap+98]) that reads on our problem:

$$\varepsilon_i^{n+1} = \left(\left(\sqrt{\varepsilon_i^n} + \sqrt{\frac{dt}{\tau}RT_{rel}}B_\varepsilon\right)^2 + (\delta - 1)RT_{rel}\frac{dt}{\tau}\right) / \left(1 + \frac{2dt}{\tau}\right), \tag{2.51}$$

with B_ε a random number chosen from a standard normal law.

2.4.2 Numerical results

Simulations that are presented here were done with one million particles. One way to validate the model is to recover the correct relaxation times for the flux and the directional temperatures (see [MM16]; [MM17]). We only show results without corrections on ν.

mono-atomic case

We choose three independent laws for the three components of velocity of the numerical particles:

- the first component is equal to $100s^4 - 20$ where s follows a uniform law between $[0,1]$,
- the second and third components of the velocity follow a uniform law between $[-50,50]$,

The choice for the first component seems a little bit strange but we need to have a non zero heat flux at the beginning of the computations to be able to capture a characteristic time of variation

for q. However, we have chosen distributions whose variances are of the same order so that the ν which is used all along this computation is equal to $-\frac{5}{4}$. The final time is set to 1.

As expected, we observe the convergence of the directional temperatures $T_{i,i}$ (the diagonal elements of Θ) towards the temperature and the relaxation towards the Maxwellian (figure 2.1). Moreover, all along the computation, the correction of ν is not activated and hence the Prandtl number defined by (2.40) is always equal to $\frac{2}{3}$ (figure 2.2). Finally, the Prandtl number is computed by using linear regression on the logarithm curves of $\Theta(t)$ and $q(t)$ (figure 2.2). We get a numerical Prandtl number $Pr_n = \frac{2.8971}{4.5001} = 0.6428$, which is close to $\frac{2}{3}$.

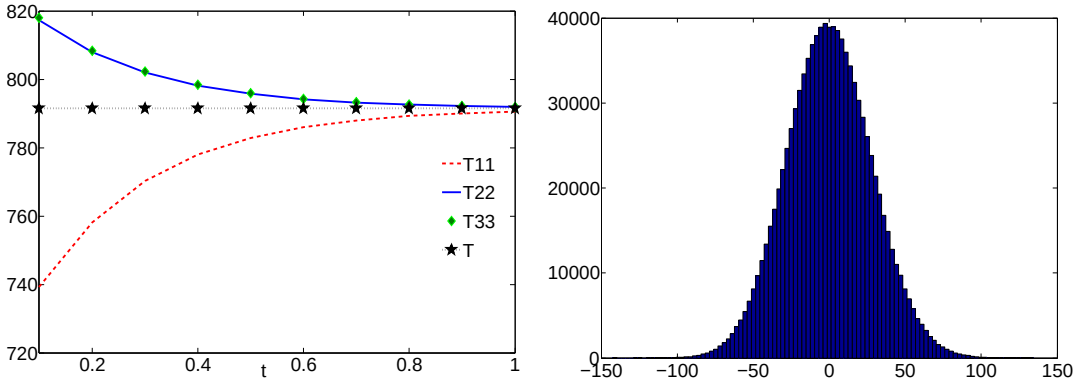

FIGURE 2.1: Left: time evolution of the diagonal components T_{11}, T_{22}, T_{33} of the tensor Θ and of its trace T. Right: histogram of the first component of velocity at final time $t = 1$.

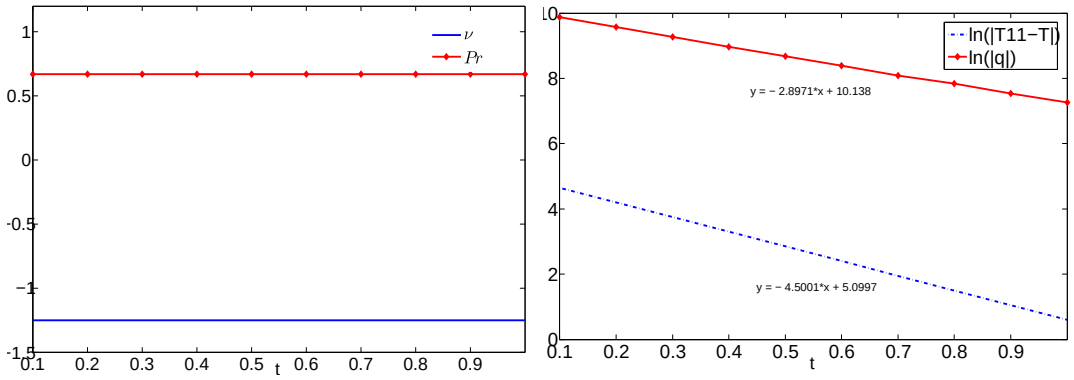

FIGURE 2.2: Left: time evolution of ν (defined by (2.41)) and Pr (defined by (2.40)). Right: time history of $\log|T - T_{11}|$ and $\log|q|$.

diatomic case

In this test case, we use air whose Prandtl number is approximately 0.71. We take the standard value $\theta = 0.2$, and the Prandtl number is adjusted with $\nu_{air} = -1.3908$. The initial data is not too anisotropic so that the correction on ν is not active.

We use 2 million particles. We choose three independent laws for the three components of velocity of the numerical particles:

- the first component is equal to $1000s^4 - 200$ where s follows a uniform law between $[0, 1]$,

- the second component of velocity is equal to $1000s - 500$ where s follows a uniform law between $[0, 1]$,
- the second component of velocity is equal to $1000s - 500$ where s follows a uniform law between $[0, 1]$.

The internal energies are defined by $40.000s + 40.000$ where s follows a uniform law between $[0, 1]$.

The time step is set to 0.02. The final simulation time is 10τ, where the relaxation time is set to $\tau = 1$ to capture the relaxation towards equilibrium for velocities and internal energies (whose characteristic time is 5τ).

On figure 2.3 we can observe after some time the convergence of the directional translational temperatures T_{11}, T_{22}, T_{33} (diagonal components of Θ). towards the same translational temperature T_{tr}, and later the convergence of all these temperatures with the internal energy temperature T_{int} to the equilibrium temperature T.

At convergence we recover the Maxwellian distribution on velocities (figure 2.4) and the exponential one on internal energies (figure 2.5).

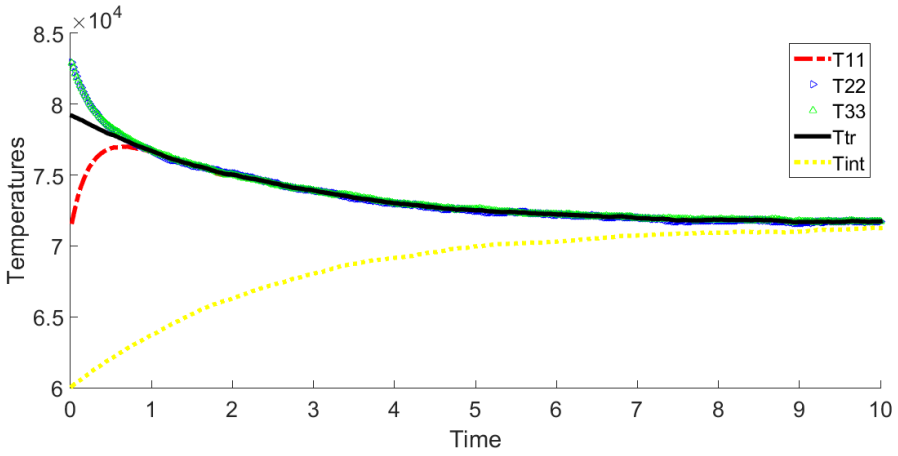

FIGURE 2.3: Convergence of the directional translational temperatures and the internal temperature to their equilibrium value.

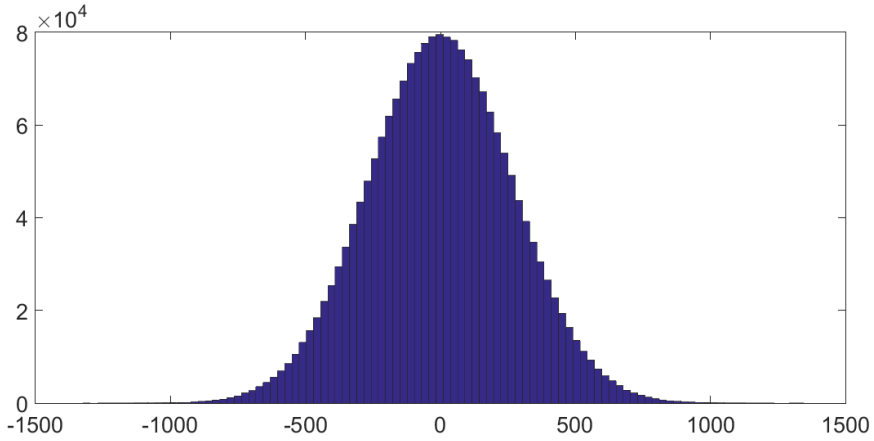

FIGURE 2.4: Maxwellian equilibrium for the distribution of the first component of the velocities, at time $t = 10s$: number of numerical particles on the y axis as a function of the V_x component

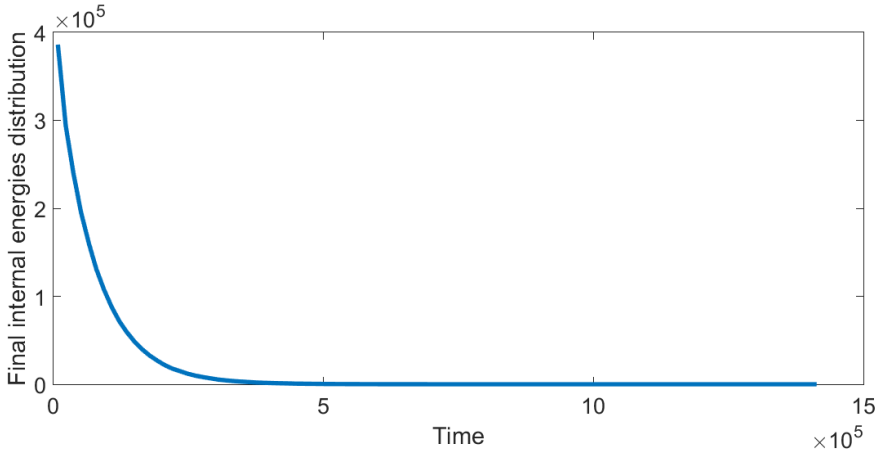

FIGURE 2.5: Distribution of the internal energies at time $t = 10$: exponential equilibrium.

2.5 Conclusions

In this chapter we propose several ways to emulate Boltzmann equation with a Fokker-Planck model. All the results are very encouraging but there remains to code the model in non homogeneous codes to compare with BGK models and Boltzmann equation.

Chapter 3

Conclusions and perspectives

In this part we have presented several new models to deal with rarefied gas dynamics. These models still need some validations. We will try to provide numerical results in the next years to comfort our approach: for instance we should get experiments at Mach 20 in the ICARE facility (CNRS Orléans) in collaboration with V. Lago. There remains also to extend our new BGK models to ESBGK models in order to capture the correct heat fluxes.

Part III

Atmospheric reentry: turbulence and interactions with the wall

Introduction

In this part we present some first results that have been obtained around turbulence and the interaction between a wall and a fluid for a supersonic flow. In the first chapter we describe some RANS (Reynolds Averaged Navier-Stokes) models and explain the difficulties which arise from them. We also look at mathematical solutions for this model. This work has lead to two theoretical papers in which we construct smooth solutions for the models ([Mat08]; [MR16]). Then in a second chapter we present some experiments around the fluid/wall interaction during reentry for a laminar/turbulent flow: these works have been done through a Phd (Cyril Levet at LCTS (Bordeaux) with G. Vignoles (LCTS) and J. Couzi(CEA)) and the masters thesis of F. Danvin(CEA) with M. Olazabal-Loumé and B. Aupoix(Onera).

Chapter 4

RANS models: theoretical results and application to turbulent supersonic flows

4.1 RANS models

Turbulence has always been a stumbling block for understanding the behavior of flows. It appears almost everywhere: astrophysics, aerodynamics, FCI ... A lot of progress has been made to compute turbulence for the last decades. Although more precise and costly methods are now used (DNS(Direct numerical simulations),LES (Large Eddy simulations,ZDES (Zonal Detached Eddy Simulation)...), industrials still rely on "old methods" to simulate the phenomenon. The classical way to do so is the use of Reynolds Averaged Navier-Stokes equations (RANS): these methods have been developed for years now on ([MP94]). They have proved their efficiency but it is generally admitted that the use of RANS models is not very accurate in complex compressible flows (RANS models were first constructed fo incompressible flows): having no model for turbulence is worse (300% of error for reentry problems on the heat flux). In this chapter we present some works around the RANS models. There are several models available in the literature (Spalart-Allmaras ([SA92]), Baldwin-Lomax ([BB90]), $k-\omega$ model ([Wil94], $k-\omega$ SST model ([Men92]). Theoretical results which are proved are based on incompressible models which are easier to tackle with from a mathematical viewpoint whereas we will deal with applications for compressible fluids in next chapter. This part is a sum up of theoretical results, numerical implementation and works in progress around models of physics (which need a lot of experiments to be validated).

4.2 Theoretical results for some RANS models: the $k-\varepsilon$ model

We recall the results that were obtained in [Mat08]. Although the original application was turbulence for supernova, the theoretical result still remains true for other applications. We re-use the original article but only keep the main results. The existence and uniqueness of solutions are principally obtained through maximum principle and the use of Sobolev spaces.

4.2.1 Introduction

The k-ε model is widely used in various physical models to assess isotropic turbulence effects (see [MP94]). It is based on two scalar quantities characterizing turbulence: the kinetic turbulent energy and the rate of dissipation of turbulent energy. This model, proposed by Launder and Spalding ([LS72]), was designed to model the evolution of large turbulent structures

and their effect on the large scale mean velocity flow. Its main applications can be found in Aerodynamics, for instance to study the influence of turbulence on airfoils boundary layers (cf. [Cou89] and [GHP91]). It is also considered for modeling turbulent mixing induced by Rayleigh–Taylor, Kelvin–Helmholtz and Richtmyer–Meshkov instabilities, for instance in Astrophysical framework.

As a matter of fact, observations of the famous supernova 1987A have indicated that radioactive cobalt is far more thoroughly distributed among the explosive debris in the envelope than was predicted by model calculations of thin-shell nucleosynthesis in the pre-supernova star. It suggests the occurrence of large-scale mixing in the ejecta during the explosion [Kum+89] [Arn+89]. The most promising mechanism for explaining mixing in the ejecta is a combination of the Rayleigh-Taylor and Kelvin-Helmholtz instabilities. The Rayleigh-Taylor instability can arise in the supernova envelope when the outwardly moving shock wave from the initial explosion propagates through layers of the star with radial stratification of the heavy elements. As the shock passes through the composition interfaces (i.e., oxygen/silicon, helium/carbon+oxygen and hydrogen/helium), a rarefaction front moves back into the star, resulting in an effective reversal of gravity as low-density composition is pressure-accelerated into the underlying high-density composition. Any perturbation at the interface (i.e., velocity perturbation or spatial perturbation) will get amplified by the Rayleigh-Taylor and Richtmyer-Meshkov instabilities and result in the overturning of light and heavy elements. This results in the mixing of heavy elements throughout the envelope of the supernova remnant, with associated observational consequences in the light curve. A further mixing will occur as the dense "tongues" of the heavy elements experience differential shear with the lighter elements, resulting in Kelvin-Helmholtz instabilities. Thus the fingers of heavy and light fluid that developed initially get far more distorted and the mixing layer increases its width. Eventually these instabilities become so nonlinear that the mixing layer appears to become fully turbulent. The properties of turbulently mixed layers may be equally important in understanding how interstellar clouds get reprocessed back into the interstellar medium. Efficient mixing of cloud and inter-cloud matter has been shown to occur after clouds get crushed by the interaction of strong shocks from supernova remnants [KMC90] [KMC94].

Here we study the mathematical properties of the incompressible model. Let us emphasize that this model is widely used in industrial codes because of its physical relevance and its simplicity. In order to introduce the mathematical setting and write the model equations, let us first introduce some notations. The domain will be a 3–dimensional box $\mathbb{T}^3 = \mathbb{R}^3/(2\pi\mathbb{Z})^3$ with periodic boundary conditions in order to avoid additional difficulties (specific physical modeling and mathematical tools are needed to handle boundaries but here we choose not to deal with boundary layers for sake of simplicity). The system of equations can be written as follows (cf.[MP94]):

$$\frac{\partial U}{\partial t} + U\cdot\nabla U + \nabla P - \nu\Delta U - \nabla\cdot R = 0, \tag{4.1}$$

$$\nabla\cdot U = 0, \tag{4.2}$$

$$\frac{\partial k}{\partial t} + U\cdot\nabla k - \frac{c_\mu}{2}\frac{k^2}{\varepsilon}|\nabla U + \nabla U^T|^2 - \nabla\cdot\left(c_\mu\frac{k^2}{\varepsilon}\nabla k\right) + \varepsilon = 0, \tag{4.3}$$

$$\frac{\partial \varepsilon}{\partial t} + U\cdot\nabla \varepsilon - \frac{c_1}{2}k|\nabla U + \nabla U^T|^2 - \nabla\cdot\left(c_\varepsilon\frac{k^2}{\varepsilon}\nabla \varepsilon\right) + c_2\frac{\varepsilon^2}{k} = 0, \tag{4.4}$$

$$U(0,x) = U^0(x), \quad k(0,x) = k^0(x), \quad \varepsilon(0,x) = \varepsilon^0(x), \tag{4.5}$$

where $U := U(t,x) \in \mathbb{R}^3$ denotes the large scale flow, $k := k(t,x)$ the kinetic turbulent energy, $\varepsilon := \varepsilon(t,x)$ its dissipation rate. $P = P(t,x)$ stands for the mean pressure of the fluid; as usual in incompressible fluid models, it may be interpreted as a lagrangian multiplier of the constraint

(4.27). Moreover $R := R(t,x)$ denotes the Reynolds stress tensor given by,

$$R = -\frac{2}{3}kI + c_\mu \frac{k^2}{\varepsilon}(\nabla U + \nabla U^T). \tag{4.6}$$

Finally, ν denotes the constant positive molecular viscosity of the fluid, while c_1, c_2, c_μ and c_ε are given positive constants that allow to capture the large scale features of turbulence (typical numerical values taken in realistic computations are: $c_1 = 0.126$, $c_2 = 1.92$, $c_\mu = 0.09$ and $c_\varepsilon = 0.07$).

For a survey about uniqueness and existence results concerning the Navier – Stokes equation without the k–ε extension, we refer to [Lio96]. Some inequalities on k and ε can be found in [Lew93] and [MP94]: they are extended here using the same ideas. There also exist some results on a modified k–ε model (the so-called ϕ–θ model) given by Mohammadi and Lewandowski ([LM93]) when U is supposed to be known so that one has only to solve the equations on ϕ and θ (which are very close to (4.28) and (4.29)); nonetheless the solutions which are found are more general than the ones found here - in a weaker sense- and still unique. More recently, the elliptic problem associated to k and ε has been studied ([GO01]): this problem arises in geophysics when one intends to study stationary mean flows. Weak solutions have been found: the main difficulty is to deal with the control of the singularity of the turbulent viscosity $c_\mu \frac{k^2}{\varepsilon}$, when k and ε both tend to zero, as we will also see in this paper.

As far as we know, it is the first result on smooth solutions for the **coupled equations** (4.1)-(4.5).

The aim of this article is to provide a first study of this problem:

1. First we prove the following result for short enough time:
   Theorem 4.2.1 (existence and uniqueness of smooth solutions)**.**

   The following two results hold:

   (a) Let the initial data U^0, k^0, ε^0 be in H^s for $s > 4 + 3/2$ ($s \in \mathbb{N}$) with k^0 and ε^0 bounded away from zero by a positive constant. Then there exists a positive T and a strong[1] solution (U,k,ε) to system (4.1)-(4.5) on $[0,T]$ which belongs to $\mathcal{C}([0,T];H^s(\mathbb{T}^3)) \cap \mathcal{C}^1([0,T];H^{s-2}(\mathbb{T}^3))$, such that k and ε remain positive on $[0,T]$.

   (b) Moreover let (U_1,k_1,ε_1) and (U_2,k_2,ε_2) be two solutions of system (4.1)-(4.5) in the sense of distributions. We suppose that they belong to $\mathcal{C}([0,T];H^2(\mathbb{T}^3)) \cap \mathcal{C}^1([0,T];L^2(\mathbb{T}^3))$ and that k_1, ε_1, k_2 and ε_2 are positive functions.

   If $U_1^0 = U_2^0$, $k_1^0 = k_2^0$, $\varepsilon_1^0 = \varepsilon_2^0$, then $U_1 = U_2$, $k_1 = k_2$, $\varepsilon_1 = \varepsilon_2$ on $[0,T]$.

2. Then we study a particular regime when turbulent diffusion effects are small compared with dissipation and when the mean flow is supposed to be at rest (so that U is considered to be identically 0). Rescaling the $k-\varepsilon$ system is classical in order to obtain further information. For instance S. Lasserre provides a study of the system depending on the couple of variables $(k, ln(k^{\sigma_k}/\sigma_\varepsilon/\varepsilon))$ ([Las05]) to study compact solutions but here we want to stay as close as possible to the original equations to preserve the parabolic behavior and also to be in accordance with physical data. We consider the following non dimensional system (see the

[1] By strong we mean a classical $\mathcal{C}_t^1(C_x^2)$ solution

beginning of subsection 4.2.4):

$$\frac{\partial k}{\partial t} - \eta\nabla\cdot\left(\frac{k^2}{\varepsilon}\nabla k\right) + A\varepsilon = 0, \tag{4.7}$$

$$\frac{\partial \varepsilon}{\partial t} - \eta\nabla\cdot\left(\frac{c_\varepsilon}{c_\mu}\frac{k^2}{\varepsilon}\nabla\varepsilon\right) + c_2 A\frac{\varepsilon^2}{k} = 0, \tag{4.8}$$

with $A = \varepsilon^0 T/k^0$, $\eta = c_\mu (k^0)^2 T/(\varepsilon^0 L^2)$, k^0 denoting the typical kinetic turbulent energy, ε^0 the rate of kinetic turbulent energy dissipation, T and L the typical time and length scales of the physical situation.

We make an asymptotic expansion with respect to η for this model since for some typical physical set of values, η is negligible while A's value is of order 1. The difference between the solution (k,ε) of equations (4.7)–(4.8) and the first terms of its η expansion ($k_0+\eta k_1$, $\varepsilon_0+\eta\varepsilon_1$) can be controlled through the following result:

Theorem 4.2.2 (Asymptotic expansion)**.** *Let k^0, ε^0 belong to $H^7(\mathbb{T}^3))$ and be bounded away from zero by positive constants, k and ε be positive solutions of (4.7) and (4.8) bounded away from zero in $C^1([0,T];H^5(\mathbb{T}^3))$. Then there exist a positive time $T' \leq T$ and a constant C such that for all $t \leq T'$:*

$$\|k - k_0 - \eta k_1\|_{L^\infty(\mathbb{T}^3)}(t) \leq C\,\eta^{\frac{3}{2}}, \qquad \|\varepsilon - \varepsilon_0 - \eta\varepsilon_1\|_{L^\infty(\mathbb{T}^3)}(t) \leq C\,\eta^{\frac{3}{2}},$$

where $k_0, k_1, \varepsilon_0, \varepsilon_1$ are solutions of the following ordinary differential and partial differential equations systems:

1. *Zero-th order system*

$$\frac{\partial k_0}{\partial t} + A\varepsilon_0 = 0, \quad k_0(0,.) = k^0(.),$$
$$\frac{\partial \varepsilon_0}{\partial t} + c_2 A\frac{\varepsilon_0^2}{k_0} = 0, \quad \varepsilon_0(0,.) = \varepsilon^0(.).$$

2. *First order system*

$$\frac{\partial k_1}{\partial t} - \nabla\cdot\left(\frac{k_0^2}{\varepsilon_0}\nabla k_0\right) + A\varepsilon_1 = 0, \quad k_1(0,.) = 0,$$
$$\frac{\partial \varepsilon_1}{\partial t} - \nabla\cdot\left(\frac{c_\varepsilon}{c_\mu}\frac{k_0^2}{\varepsilon_0}\nabla\varepsilon_0\right) + c_2 A\left(\frac{2\varepsilon_0\varepsilon_1}{k_0} - \frac{\varepsilon_0^2 k_1}{k_0^2}\right) = 0, \quad \varepsilon_1(0,.) = 0.$$

From a mathematical viewpoint, the main difficulty in the proof of Theorems 1 and 2 is the control of the positivity of k and ε since the mathematical model degenerates when k or ε vanish: because of the ε (resp. $c_2\varepsilon^2/k$) term in equation (4.28) (resp.(4.29)) we cannot ensure strict positivity of k (resp. ε).

Three classical mathematical tools are used all along the article to carry on the study. The first one is the maximum principle for parabolic PDE's. The second one is the use of energy methods for parabolic PDE's to obtain *a priori* estimates. The last one is the use of Sobolev embeddings (see [Bre83] and [Tay96a]) and Gagliardo-Niremberg inequalities in order to control the different norms. Since we need smoothness of the solutions in order to be able to use these inequalities, our study is for data which belong to H^s with $\mathbf{s > 4 + 3/2}$ so that the L^∞-norms of the gradients of the data are bounded by the H^s-norms.

In subsection 4.2.2 we give an *a priori* estimate and in subsection 4.2.3, we solve the problem of existence and uniqueness of solutions of (4.26)–(4.36), proving the first theorem; in Section 4.2.4 we perform the expansion with respect to η and prove the second theorem. All the results are given for small times since there is no hope in controlling the strict positivity of k and ε for long times.

4.2.2 Preliminary results

We establish *a priori* estimates on U, k and ε solutions of system (4.26)–(4.36). In all the computations, we consider solutions (U,k,ε) belonging to $C([0,T];H^s(\mathbb{T}^3))\cap C^1([0,T];H^{s-2}(\mathbb{T}^3))$ for some $T>0$ for s integer such that $s>4+3/2$ (and consequently to $C^2([0,T];H^{s-4}(\mathbb{T}^3))$ at least). All the integrals are computed on $\mathbb{T}^3$; k and ε are supposed to be strictly positive quantities for $t\in[0,T]$. We systemically use Sobolev embedding $H^s(\mathbb{T}^3)\hookrightarrow \mathcal{C}^{s-2}(\mathbb{T}^3)$ so that the $(s-2)^{th}$ space derivatives of U, k and ε are L^∞–bounded by the H^s norm of U, k and ε (see [Bre83]) in dimension 3.

A priori estimates on the Navier–Stokes equations

We obtain the following estimates on smooth solutions of the incompressible Navier–Stokes equation:

Property 4.2.1 (Estimates on U). *Let U, k and ε be solutions of (4.26)-(4.36) which belong to $C([0,T];H^s(\mathbb{T}^3))\cap C^1([0,T];H^{s-2}(\mathbb{T}^3))$, with k and ε strictly positive and $s\geq 4+3/2$. We have:*

$$\frac{d}{dt}||U||^2_{H^s}\leq C\ Q_{4s+8}(U,k,\varepsilon)(t),$$

where C is a generic constant and $Q_1,\dots,Q_n$ are functions defined by:

$$Q_1(U,k,\varepsilon)(t)=1+||U(t)||_{H^s}+||k(t)||_{H^s}+||\varepsilon(t)||_{H^s}+\frac{1}{k_{min}(t)}+\frac{1}{\varepsilon_{min}(t)},$$
$$Q_n=(Q_1)^n,$$

where we note

$$k_{min}(t)=\min_{x\in\mathbb{T}^3}k(t,x),\quad k_{max}(t)=\max_{x\in\mathbb{T}^3,0\leq s\leq t}k(s,x),$$
$$\varepsilon_{min}(t)=\min_{x\in\mathbb{T}^3,0\leq s\leq t}\varepsilon(s,x),\quad \varepsilon_{max}(t)=\max_{x\in\mathbb{T}^3,0\leq s\leq t}(\varepsilon(s,x)),$$

and D^ih denote the i^{th} derivative of a function h.

A priori estimates on k and ε

We are now able to control positive lower bounds k and ε through the following lemma.

Lemma 4.2.1 (Maximum principle). *Let U, k and ε be solutions of System (4.26)-(4.36) which belong to $C([0,T];H^s(\mathbb{T}^3))\cap C^1([0,T];H^{s-2}(\mathbb{T}^3))$, with k and ε bounded below by a strictly positive constant. Let k^0, ε^0 belong to $H^s(\mathbb{T}^3))$ and be bounded away from zero by strictly positive constants. We have for all*

$t \geq 0$:

$$\frac{1}{k_{min}(t)} - \frac{1}{k_{min}(0)} \leq C \frac{t}{k^2_{min}(t)} \sup_{0\leq t'\leq t} ||\varepsilon(t',.)||_{H^s},$$
$$\frac{1}{\varepsilon_{min}(t)} - \frac{1}{\varepsilon_{min}(0)} \leq C \frac{t}{k_{min}(t)\varepsilon^2_{min}(t)} \sup_{0\leq t'\leq t} ||\varepsilon(t',.)||^2_{H^s}.$$

In addition, we obtain the following estimates for k and ε (strict positivity of both k and ε is necessary for the inequalities).

Property 4.2.2 (a priori estimates on k and ε)**.** *Let U, k and ε be solutions of (4.26)-(4.36) which belong to $C([0,T];H^s(\mathbb{T}^3)) \cap C^1([0,T];H^{s-2}(\mathbb{T}^3))$, with k and ε strictly positive and $s \geq 4+3/2$. We have:*

$$\frac{d}{dt}||k||^2_{H^s} \leq C\, Q_{4s+9}(U,k,\varepsilon), \qquad \frac{d}{dt}||\varepsilon||^2_{H^s} \leq C\, Q_{4s+9}(U,k,\varepsilon).$$

Positive lower bounds for k and ε

We establish an *a priori* estimate for the turbulent fields k and ε and then prove that solutions of the system can be controlled locally in time.

Property 4.2.3. *Let $s \in \mathbb{N}$ such that $s \geq 4+3/2$ and U, k and ε be smooth solutions of (4.26)–(4.36) in $C([0,T];H^s(\mathbb{T}^3)) \cap C^1([0,T];H^{s-2}(\mathbb{T}^3))$. Let k^0, ε^0 belong to $H^s(\mathbb{T}^3))$ and be bounded away from zero by strictly positive constants. Then there exists a positive time T' ($T' \leq T$) such that k, ε remain strictly positive on $[0,T']$ (bounded below by a strictly positive constant) and such that U, k and ε have finite H^s norm.*

4.2.3 Existence and uniqueness of solutions for the whole system

Thanks to the ideas used to obtain the *a priori* estimates, we are able to prove Theorem 4.3.1.

Existence:

We only give a sketch of proof for the existence. We use an iterative method to obtain the result. We note U^n, k^n and ε^n (k^n and ε^n are supposed to be strictly positive) the $n-th$ iterate of U, k and ε which are defined on $[0,t_n]$: the time of existence depends on n; we have to prove that it can be bounded below. U^0, k^0 and ε^0 are the initial data defined above.

Iterative process We obtain U^{n+1}, k^{n+1} and ε^{n+1} through the following iterative process:

$$\frac{\partial U^{n+1}}{\partial t} + U^n \cdot \nabla U^{n+1} + \nabla P^{n+1} - \nu \Delta U^{n+1} = \nabla \cdot \left(-\frac{2}{3} k^n I + c_\mu \frac{(k^n)^2}{\varepsilon^n} (\nabla U^{n+1} + \nabla U^{n+1^T}) \right) \quad (4.9)$$

$$\nabla \cdot U^{n+1} = 0 \quad (4.10)$$

$$\frac{\partial k^{n+1}}{\partial t} + U^{n+1}\cdot\nabla k^{n+1} - \nabla\cdot\left(c_\mu \frac{(k^n)^2}{\varepsilon^n}\nabla k^{n+1}\right) = \frac{c_\mu}{2}\frac{(k^n)^2}{\varepsilon^n}|\nabla U^{n+1} + \nabla U^{n+1^T}|^2 - \varepsilon^n \quad (4.11)$$

$$\frac{\partial \varepsilon^{n+1}}{\partial t} + U^{n+1}\cdot\nabla \varepsilon^{n+1} - \nabla\cdot\left(c_\varepsilon \frac{(k^n)^2}{\varepsilon^n}\nabla \varepsilon^{n+1}\right) = \frac{c_1}{2}k^n|\nabla U^{n+1} + \nabla U^{n+1^T}|^2 - c_2\frac{(\varepsilon^n)^2}{k^n} \quad (4.12)$$

$$U^{n+1}(0,x) = U^0(x) \quad (4.13)$$
$$k^{n+1}(0,x) = k^0(x) \quad (4.14)$$
$$\varepsilon^{n+1}(0,x) = \varepsilon^0(x) \quad (4.15)$$

In the article [Mat08], we prove that all iterates exist and can be controlled through the previous estimates.

Passing to the limit Finally, it can be proven by decreasing the time T, if necessary, that the iterative scheme converges using that for this time,

$$\sum_{n\geq 1}\Big(||U^n - U^{n+1}||^2_{L^\infty([0,T];L^2)} + ||\varepsilon^n - \varepsilon^{n+1}||^2_{L^\infty([0,T];L^2)} + ||k^n - k^{n+1}||^2_{L^\infty([0,T];L^2)}\Big) < +\infty. \quad (4.16)$$

(see the proof below).

The convergence of the series ensures that U_n, k_n and ε_n converge in $L^\infty([0,T];L^2)$ and consequently in $\mathcal{C}([0,T];L^2)$ since all the terms are continuous. They also converge in $\mathcal{C}([0,T];H^{s'})$ for $s' < s$ as they are bounded in $L^\infty([0,T];H^s)$ (one can prove that using Gagliardo-Niremberg inequality -see [Maj84]-) Using classical arguments on the regularity of Sobolev spaces (see [Maj84] or [Ser96a])) and distribution theory, we see that the limits of the sequences U_n, k_n and ε_n are solutions of the problem in $\mathcal{C}([0,T];H^s(\mathbb{T}^3)) \cap \mathcal{C}^1([0,T];H^{s-2}(\mathbb{T}^3))$: for instance, since $H^{s'}$ and $H^{s'-1}$ are algebra for s' near enough $s > 4 + \frac{3}{2}$, in the k equation we get that $U^{n+1}\cdot\nabla k^{n+1}$ converges in $L^\infty([0,T];H^{s'-1}))$ towards $U\cdot\nabla k$ and consequently converges in a distribution sense.

Concerning the pressure term, it can be recovered from the Navier–Stokes equations as usual (see [CF88] for instance: the series of pressure is also bounded since U, k and ε are bounded). Therefore, the theorem is finally proven.

We can prove that the series is indeed convergent for T small enough

Uniqueness

As the solutions are regular enough (they belong indeed to the functional space $\mathcal{C}([0,T];H^2(\mathbb{T}^3)) \cap \mathcal{C}^1([0,T];L^2(\mathbb{T}^3))$), the $U\cdot\nabla U$ term does not prevent us from proving uniqueness. So adapting

the proofs of uniqueness of parabolic equations (see [Tay96b] and Navier–Stokes equations (see [Lio96]) leads to uniqueness.

4.2.4 Study of a simplified k–ε model

Here we simplify the model by assuming the system is initially at rest so that $U = 0$ - as it is the case for instance in the early development of a Rayleigh–Taylor or Richtmyer–Meshkov mixing layer (see [DLY99])-. Consequently we only take account of the following simplified k–ε equations:

$$\frac{\partial k}{\partial t} - \nabla_x \cdot \left(c_\mu \frac{k^2}{\varepsilon} \nabla k \right) + \varepsilon = 0, \quad k(0,x) = k^0(x) \in H^7(\mathbb{T}^3), \tag{4.17}$$

$$\frac{\partial \varepsilon}{\partial t} - \nabla \cdot \left(c_\varepsilon \frac{k^2}{\varepsilon} \nabla \varepsilon \right) + c_2 \frac{\varepsilon^2}{k} = 0, \quad \varepsilon(0,x) = \varepsilon^0(x) \in H^7(\mathbb{T}^3), \tag{4.18}$$

We make a dimensional analysis which leads us to compute an asymptotic expansion.

Dimensional analysis

We analyze the different terms of the equations by making a change of variables:

- $x \hookrightarrow \tilde{x} = \dfrac{x}{L}$ with L: typical length scale
- $t \hookrightarrow \tilde{t} = \dfrac{t}{T}$ with T: typical time scale
- $\varepsilon \hookrightarrow \tilde{\varepsilon} = \dfrac{\varepsilon}{\varepsilon^0}$ with ε^0: typical rate of dissipation of turbulent energy scale
- $k \hookrightarrow \tilde{k} = \dfrac{k}{k^0}$ with k^0: typical turbulent energy scale

Thanks to the change of variable we obtain:

$$\frac{\partial k}{\partial t} - \eta \nabla . \left(\frac{k^2}{\varepsilon} \nabla k \right) + A\varepsilon = 0 \ , \ \frac{\partial \varepsilon}{\partial t} - \eta \nabla \cdot \left(\frac{c_\varepsilon}{c_\mu} \frac{k^2}{\varepsilon} \nabla \varepsilon \right) + c_2 A \frac{\varepsilon^2}{k} = 0,$$

with: $A = \dfrac{\varepsilon^0 T}{k^0}$ and $\eta = c_\mu \dfrac{(k^0)^2 T}{\varepsilon^0 L^2}$ dimensionless numbers.

For instance we have the following numerical data (in c.g.s. system) for Rayleigh-Taylor instabilities in dense hot plasma (see [Tha+00]: $k^0 = 10^{16} cm^2/s' T = 10^{-3} s, A = 0.5, \varepsilon^0 = 5.10^{18} cm^2/s^3, L = 10^7 cm, \eta \sim 10^{-5}$

As it can be noticed η is small for the physical applications we study. This is why we expand ε and k in formal series (see next subsubsection).

We can also write η as: $c_\mu A (\dfrac{(k^0)^{\frac{3}{2}}}{\varepsilon^0 L})^2$ with $\dfrac{(k^0)^{\frac{3}{2}}}{\varepsilon^0}$ representing the typical length of turbulent vortices (see [LB03]). So a small η is equivalent to neglect diffusion of vortices because they are too small. Another equivalent approach is to say (writing η as $\dfrac{c_\mu}{A} \times (T \dfrac{\sqrt{k^0}}{L})^2$) that the typical time of creation of the vortices $\dfrac{L}{\sqrt{k^0}}$ is large enough so that vortices cannot diffuse turbulence.

Bounds for k and ε

We obtain bounds for the solutions of the simplified system which are independent of η and which allow us to control nonlinear terms.

Property 4.2.4 (Maximum principle for k and ε)**.** *Let k^0, ε^0 belong to $H^7(\mathbb{T}^3)$ and be bounded below by a strictly positive constant. Let k and ε be strictly positive solutions of (4.7) and (4.8) and belong to $C^1([0,T];H^5(\mathbb{T}^3))$. Then we get that $\forall x \in \mathbb{T}^3$ and $\forall t \in [0,T]$*

$$k(t,x) \leq k_{max}(0)$$

$$\varepsilon(t,x) \leq \varepsilon_{max}(0)$$

$$k(t,x) \geq k_{min}(0) - A\,\varepsilon_{max}(0)\,t$$

$$\varepsilon(t,x) \geq \varepsilon_{min}(0) \Big/ \left(1 - c_2 \frac{\varepsilon_{min}(0)}{\varepsilon_{max}(0)} \log\left(1 - \frac{t\,A\,\varepsilon_{max}(0)}{k_{min}(0)}\right)\right)$$

Let us observe that we obtain a time of strict positivity T independent of η whose value is $k_{min}/(A\varepsilon_{max})$ and for which k and ε remain positive. Nonetheless this time is of the same order of the typical time (see numerical data above).

Asymptotic analysis of the system

The values used in physics lead to make an asymptotic expansion in $\eta-$series (η tends to zero) in order to approach the real solution; we write k and ε as:

$$k = \sum_{n=0}^{\infty} k_n \eta^n, \qquad \varepsilon = \sum_{n=0}^{\infty} \varepsilon_n \eta^n.$$

We first establish properties on the differential systems obtained by expanding in $\eta-$series. Then the real solution is compared with the truncated series. Moreover we obtain that the more η decreases the more the real solution remains positive. Replacing k and ε by their expansion we get the following systems. We limit our study to second order even if it can be extended further: although the main result concerns only zero-th and first order systems, we need the second order to prove it.

Zero-th order system

$$\frac{\partial k_0}{\partial t} + A\varepsilon_0 = 0, \quad k_0(0,.) = k^0(.),$$
$$\frac{\partial \varepsilon_0}{\partial t} + c_2 A \frac{\varepsilon_0^2}{k_0} = 0, \quad \varepsilon_0(0,.) = \varepsilon^0(.).$$

First order system

$$\frac{\partial k_1}{\partial t} - \nabla \cdot \left(\frac{k_0^2}{\varepsilon_0} \nabla k_0\right) + A\varepsilon_1 = 0, \quad k_1(0,.) = 0,$$
$$\frac{\partial \varepsilon_1}{\partial t} - \nabla \cdot \left(\frac{c_\varepsilon}{c_\mu} \frac{k_0^2}{\varepsilon_0} \nabla \varepsilon_0\right) + c_2 A \left(\frac{2\varepsilon_0 \varepsilon_1}{k_0} - \frac{\varepsilon_0^2 k_1}{k_0^2}\right) = 0, \quad \varepsilon_1(0,.) = 0.$$

Second order system

$$\begin{aligned}
&\frac{\partial k_2}{\partial t} - \nabla\cdot\left(\frac{k_0^2}{\varepsilon_0}\nabla k_1 + \frac{2k_0k_1}{\varepsilon_0}\nabla k_0 \ - \frac{k_0^2\varepsilon_1}{\varepsilon_0^2}\nabla k_0\right) + A\varepsilon_2 = 0,\\
&\frac{\partial \varepsilon_2}{\partial t} - \frac{c_\varepsilon}{c_\mu}\nabla\cdot\left(\frac{k_0^2}{\varepsilon_0}\nabla \varepsilon_1 + \frac{2k_0k_1}{\varepsilon_0}\nabla \varepsilon_0 \ - \frac{k_0^2\varepsilon_1}{\varepsilon_0^2}\nabla \varepsilon_0\right)\\
&\qquad\qquad + c_2A\left(\frac{2\varepsilon_0\varepsilon_2}{k_0} - \frac{\varepsilon_0^2k_2}{k_0^2} - 2\frac{\varepsilon_0\varepsilon_1k_1}{k_0^2} + \frac{\varepsilon_0^2k_1^2}{k_0^3} + \frac{\varepsilon_1^2}{k_0}\right) = 0,\\
&k_2(0,.) = 0, \qquad \varepsilon_2(0,.) = 0.
\end{aligned}$$

After some computations we obtain the following solutions of these systems.

Property 4.2.5 (Solutions of the systems)**.** *Let k^0, ε^0 belong to H^7 and be strictly positive. Let's define k_0 and ε_0 as:*

$$k_0(t,x) = k^0(x)\left(1 + (c_2-1)A\frac{\varepsilon^0(x)}{k^0(x)}t\right)^{\frac{1}{1-c_2}}$$

$$\varepsilon_0(t,x) = \varepsilon^0(x)\left(1 + (c_2-1)A\frac{\varepsilon^0(x)}{k^0(x)}t\right)^{\frac{c_2}{1-c_2}}$$

k_0 et ε_0 are solutions of the zero-order system, belong to C^∞([0,∞[; $H^7(\mathbb{R})$) and remain strictly positive.
k_1 and ε_1 exist, are unique and belong to C^∞([0,∞]; $H^5(\mathbb{R})$). Moreover their growth and those of their derivatives is at worst polynomial in time.
k_2 and ε_2 exist, are unique and belong to C^∞([0,∞]; $H^3(\mathbb{R})$). Moreover their growth and those of their derivatives is at worst polynomial in time.

A priori estimates

We now compare k and ε with their second order expansion with respect to η in H^2-norm. Let us define

$$K = k - \sum_{n=0}^{2}\eta^n k_n \qquad \text{and} \qquad E = \varepsilon - \sum_{n=0}^{2}\eta^n\varepsilon_n.$$

We obtain the following equations for K and E:

$$\frac{\partial K}{\partial t} + \eta\nabla\cdot(F1) + AE = 0\ ,\ K(0,.) = 0 \tag{4.19}$$

$$\frac{\partial E}{\partial t} + \frac{c_\varepsilon}{c_\mu}\eta\nabla\cdot(F2) + c_2A\times(F3) = 0\ ,\ E(0,.) = 0 \tag{4.20}$$

with:

$$(F1) \ = \ \left(\frac{k_0^2}{\varepsilon_0}\nabla k_0 + \eta\left(\frac{k_0^2}{\varepsilon_0}\nabla k_1 + (\frac{2k_0k_1}{\varepsilon_0} - \frac{k_0^2\varepsilon_1}{\varepsilon_0^2})\nabla k_0\right) - \frac{k^2}{\varepsilon}\nabla k\right),$$

$$(F2) \ = \ \left(\frac{k_0^2}{\varepsilon_0}\nabla \varepsilon_0 + \eta\left(\frac{k_0^2}{\varepsilon_0}\nabla \varepsilon_1 + \frac{2k_0k_1}{\varepsilon_0}\nabla \varepsilon_0 \ - \frac{k_0^2\varepsilon_1}{\varepsilon_0^2}\nabla \varepsilon_0\right) - \frac{k^2}{\varepsilon}\nabla \varepsilon\right),$$

$$(F3) = \left(\frac{\varepsilon^2}{k} - \frac{\varepsilon_0^2}{k_0} + \eta\Big(\frac{\varepsilon_0^2 k_1}{k_0^2} - \frac{2\varepsilon_0\varepsilon_1}{k_0}\Big) + \eta^2\Big(\frac{\varepsilon_0^2 k_2}{k_0^2} - \frac{\varepsilon_1^2}{k_0} - \frac{2\varepsilon_0\varepsilon_2}{k_0} + 2\frac{\varepsilon_0\varepsilon_1 k_1}{k_0^2} - \frac{\varepsilon_0^2 k_1^2}{k_0^3}\Big)\right).$$

We define $T \mapsto B(T)$ by

$$B(T)^{-1} = \inf_{0\le t\le T, x\in\mathbb{T}^3}(k(t,x), k_0(t,x), \varepsilon(t,x), \varepsilon_0(t,x))$$

which is bounded as k and ε are bounded and strictly positive on $[0,T]$.

We assess the norm of the different terms to obtain energy estimates or the whole system. To simplify computations we suppose $\eta < 1$ (η tends to zero..). We get:

Lemma 4.2.2. *Let k^0, ε^0 belong to H^7 and be strictly positive. Let k and ε be strictly positive solutions of (4.7) and (4.8) and belong to $C^1([0,T];H^5(\mathbb{T}^3))$. There exists a positive function f depending in a polynomial way of time [2] but independent of η such that:*

$$\begin{aligned}
|(F1)(t,x)| + |(F2)(t,x)| &\le B(T)^5 f(T)\left[(\|K\|_{H^2} + \|E\|_{H^2})^6 + \eta^2\right]\\
|D^1(F1)(t,x)| + |D^1(F2)(t,x)| &\le B(T)^5 f(T)\Big[\eta^2\\
&\quad + \Big(1 + |D^2K(t,x)| + |D^2E(t,x)|\Big)\\
&\quad \times\Big(||K||_{H^2} + ||E||_{H^2}\Big)^7\Big]\\
|(F3)(t,x)| + |D^1(F3)(t,x)| &\le B(T)^5 f(T)\left[\Big(\|K\|_{H^2} + \|E\|_{H^2}\Big)^6 + \eta^3\right]\\
|D^2(F3)(t,x)| &\le B(T)^5 f(T)\Big[\eta^3\\
&\quad + \Big(1 + |D^2K|(t,x) + |D^2E(t,x)|\Big)\\
&\quad \times\Big(\|K\|_{H^2} + \|E\|_{H^2}\Big)^7\Big]
\end{aligned}$$

Property 4.2.6 (H^2 estimates)**.** *Let k^0, ε^0 belong to H^7 and be strictly positive. Let k and ε be strictly positive solutions of (4.7) and (4.8) and belong to $C^1([0,T];H^5(\mathbb{T}^3))$. There exists f depending in a polynomial way of time but independent of η such that:*

$$\frac{d}{dt}||D^2K||_{L^2}^2 \le B(T)^5 f(t)\left[\left(\|K\|_{H^2}^2 + \|E\|_{H^2}^2\right)^9 + \eta^3\right], \tag{4.21}$$

$$\frac{d}{dt}||D^2E||_{L^2}^2 \le B(T)^5 f(t)\left[\left(\|K\|_{H^2}^2 + \|E\|_{H^2}^2\right)^9 + \eta^3\right], \tag{4.22}$$

$$\frac{d}{dt}(\|K\|_{H^2}^2 + \|E\|_{H^2}^2) \le B(T)^5 f(t)\left[\left(\|K\|_{H^2}^2 + \|E\|_{H^2}^2\right)^9 + \eta^3\right]. \tag{4.23}$$

Thanks to these results one obtains the following proof for the theorem:

[2] by this we mean $f \le C(1+t)^n$ for some integer n

Proof of theorem 4.2.2 Let's define $S(t) = \|K\|^2_{H^2}(t) + \|E\|^2_{H^2}(t)$. Note that $S(0) = 0$. Thanks to Proposition 4.2.6, there exists f function of time bounded by $C(1+t)^n$ such that we have (we recall that we have already supposed that $\eta \leq 1$):

$$\begin{aligned} S'(t) &\leq B(T)^5 f(t) \left[S(t)^9 + \eta^3\right] \\ &\leq H(T) \left[S(t)^9 + \eta^3\right] \\ &\leq H(T) \left[S(t)^9 + 1\right] \end{aligned} \tag{4.24}$$

with $H(T) = B(T)^5 \sup_{0\leq t\leq T} f(t)$.

Let T_1 be the first time such as $S(T_1) = 1$ ($T1$ is independent of η thanks to inequality 4.24). For all $t \leq T_1$, $S^9(t) \leq S(t)$ and $S'(t) \leq H(T)\left[S(t) + \eta^3\right]$ so that,

$$\forall t \leq T_1\,,\ S(t) \leq \eta^3(\exp(H(T)t) - 1) \quad \text{(using Gronwall lemma)}, \tag{4.25}$$

So we get:

$$\begin{aligned} \forall t \leq T_1\,,\ \|K\|_{H^2}(t) &\leq \sqrt{\exp(H(T)t) - 1}\,\eta^{\frac{3}{2}}, \\ \forall t \leq T_1\,,\ \|E\|_{H^2}(t) &\leq \sqrt{\exp(H(T)t) - 1}\,\eta^{\frac{3}{2}}. \end{aligned}$$

Then using Sobolev embeddings, as $H^2(\mathbb{T}^3) \hookrightarrow L^\infty(\mathbb{T}^3)$, one gets:

$$\begin{aligned} \forall t \leq T_1\,,\ \|k - k_0 - \eta k_1 - \eta^2 k_2\|_\infty(t) &\leq C\sqrt{\exp(H(T)t) - 1}\,\eta^{\frac{3}{2}} \leq C\,\eta^{\frac{3}{2}} \\ \forall t \leq T_1\,,\ \|\varepsilon - \varepsilon_0 - \eta\varepsilon_1 - \eta^2\varepsilon_2\|_\infty(t) &\leq C\sqrt{\exp(H(T)t) - 1}\,\eta^{\frac{3}{2}} \leq C\,\eta^{\frac{3}{2}} \end{aligned}$$

Using the fact that k_2 and ε_2 are bounded by a polynomial function of time which are bounded on $[0, T]$(see prop 4.2.5), one gets the theorem.

4.3 Theoretical results for some RANS models: the $k-\omega$ model

In this section we prove existence and uniqueness of solutions to the $k-\omega$ model.

The main difference with the results on the $k-\varepsilon$ result is that we have to deal with infinite space so that the control of the solutions is trickier for the maximum principle. Other difficulties are tackled as it was done for the $k-\varepsilon$. The original article was done with X. Roynard a former masters student ([MR16]). Since the way of constructing solutions is very similar to the one of the $k-\varepsilon$ model we only recall the result.

Turbulence is a key-point for modeling complex flows in aerodynamics ([Cou89]). Under turbulence, fluxes and viscosity can be strongly modified. There are different level of complexity in turbulence modeling from the algebraic models which introduce a variable viscosity (e.g. the Baldwin-Lomax model ([BB90])) on the Navier-Stokes equations to the more complex one-equation models (e.g. Spalart and Allmaras model([SA92]) and the two-equations models (e.g. $k-\varepsilon$ and $k-\omega$ models) and even second-order models (also called Stress-Transport models).

In this work we deal with the $k-\omega$ model because of its relevance for aerodynamics applications ([Wil94]; [Wil93]; [Wil08]; [Men92]) and because no mathematical results are known up to now for

this model. In this context we focus on the local well posedness of the $k-\omega$ model in the three dimensional space $\mathbb{R}^3$.

Here we study the mathematical properties of the incompressible model. Let us emphasize that this model is widely used in industrial codes because of its physical relevance and its simplicity. In order to introduce the mathematical setting and write the model equations, let us first introduce some notations. The domain will be the 3-dimensional space $\mathbb{R}^3$. The system of equations can be written as follows ([Wil94]).

$$\frac{\partial U}{\partial t} + U \cdot \nabla U + \nabla P - \nu \Delta U - \nabla \cdot R = 0, \tag{4.26}$$

$$\nabla \cdot U = 0, \tag{4.27}$$

$$\frac{\partial k}{\partial t} + U \cdot \nabla k - \frac{k}{\omega} \left| \frac{\nabla U + \nabla U^T}{2} \right|^2 - \nabla \cdot ((\nu + \sigma \nu_T) \nabla k) + \beta \omega k = 0, \tag{4.28}$$

$$\frac{\partial \omega}{\partial t} + U \cdot \nabla \omega - \left| \frac{\nabla U + \nabla U^T}{2} \right|^2 - \nabla \cdot ((\nu + \sigma \nu_T) \nabla \omega) + \beta^\star \omega^2 = 0, \tag{4.29}$$

with the boundary conditions k^b and ω^b:

$$\forall t \in \mathbb{R}^+, \quad U(t,x) \underset{\|x\| \to +\infty}{\longrightarrow} 0, \tag{4.30}$$

$$k(t,x) \underset{\|x\| \to +\infty}{\longrightarrow} k^b, \tag{4.31}$$

$$\omega(t,x) \underset{\|x\| \to +\infty}{\longrightarrow} \omega^b, \tag{4.32}$$

and the initial data U^0, k^0 and ω^0 (which satisfy the previous conditions, take $t = 0$):

$$\forall x \in \mathbb{R}^3, \quad U(0,x) = U^0(x), \tag{4.33}$$

$$k(0,x) = k^0(x), \tag{4.34}$$

$$\omega(0,x) = \omega^0(x), \tag{4.35}$$

where $U = U(t,x) \in \mathbb{R}^3$ denotes the large scale flow, $k = k(t,x)$ the kinetic turbulent energy and $\omega = \omega(t,x)$ a characteristic frequency of turbulence. $P = P(t,x)$ stands for the mean pressure of the fluid; as usual in incompressible fluid models, it may be interpreted as a Lagrangian multiplier of the constraint (4.27). And there is a constant $C > 0$ such that $k^0 > C$, $\omega^0 > C$, $k^b > C$ and $\omega^b > C$. Moreover $R = R(t,x)$ denotes the Reynolds stress tensor given by,

$$R = -\frac{2}{3} k I + \nu_T \left(\frac{\nabla U + \nabla U^T}{2} \right). \tag{4.36}$$

Finally, ν denotes the constant positive molecular viscosity of the fluid, while $\sigma = \frac{1}{2}$, $\nu_T = \frac{k}{\omega}$, and β and $\beta^\star$ are given positive constants that allow to capture the large scale features of turbulence (typical numerical values taken in realistic computations are $\beta = 9/125$ and $\beta^\star = 9/100$ according to [Wil94]).

As far as we know, it was the first result for smooth solutions for the **coupled equations** (4.26)-(4.36) on the whole 3-D domain.

The aim of this paper is to provide a first study of this problem : we prove the following result for short enough time :
Theorem 4.3.1 (existence and uniqueness of smooth solutions)**.**

The following two results holds :

(a) Let the initial data U^0, k^0 and ω^0 be in H^s for $s > 4 + 3/2$ ($s \in \mathbb{N}$) with k^0 and ω^0 bounded away from zero by a positive constant. And the boundary conditions k^b and ω^b be strictly positive constants.

Then there exists a positive T and a strong[3] solution $(U, k - k^b, \omega - \omega^b)$ to system (4.26)-(4.36) on $[0,T]$ which belongs to $\mathcal{C}([0,T]; H^s(\mathbb{R}^3)) \cap \mathcal{C}^1([0,T]; H^{s-2}(\mathbb{R}^3))$, such that k and $\omega - \omega$ remain positive on $[0,T]$.

(b) Moreover let $(U_1, k_1 - k^b, \omega_1 - \omega^b)$ and $(U_2, k_2 - k^b, \omega_2 - \omega^b)$ be two solutions of system (4.26)-(4.36) in the sense of distributions. We suppose that they belong to $\mathcal{C}([0,T]; H^s(\mathbb{R}^3)) \cap \mathcal{C}^1([0,T]; H^{s-2}(\mathbb{R}^3))$ and that k_1, ω_1, k_2 and ω_2 are positive functions.

If $U_1^0 = U_2^0$, $k_1^0 = k_2^0$ and $\omega_1^0 = \omega_2^0$, then $U_1 = U_2$, $k_1 = k_2$ and $\omega_1 = \omega_2$.

From a mathematical viewpoint, the main difficulty in the proof of Theorem 4.3.1 is the control of positivity of k and ω since the mathematical model degenerates when k or ω vanishes: because of the $\beta\omega k$ (resp. $\beta^\star\omega^2$) term in equation (4.28) (resp. (4.29)) we cannot ensure strict positivity of k (resp. ω).

Three classical mathematical tools are used all along the article to carry on the study. The first one is the maximum principle for parabolic PDE's. The second one is the use of energy methods for parabolic PDE's to obtain *a priori* estimates. The last one is the use of Sobolev embeddings (see [Bre83] and [Tay96a]) and Gagliardo-Nirenberg inequalities in order to control the different norms. Since we need smoothness of the solutions in order to be able to use these inequalities, our study is for data which belong to H^s with $\mathbf{s > 4 + 3/2}$ so that the L^∞-norms of the gradients of the data are bounded by the H^s-norms (practically s is an integer such that $s > 6$).

4.4 A numerical implementation of a modified $k-\omega$ model

We now show some numerics around turbulence. The results were presented at the Multimat Conference in 2013 in San Francisco.

4.4.1 Introduction and model

Since we are interested in atmospheric reentry at high Mach numbers, we need to use a compressible RANS model. We chose to use the $k-\omega$ Wilcox model of 1998 ([Wil08]) to assess its efficiency for supersonic test cases. The main difference with the model presented just before is that we need to solve the mass equation on density ρ. The global system to solve is the following

[3] By strong we mean a classical $\mathcal{C}_t^1(\mathcal{C}_x^2)$ solution

$$\partial_t(\rho) + \nabla \cdot (\rho U) = 0, \tag{4.37}$$

$$\partial_t(\rho U) + \nabla (\rho U \otimes U) + \nabla \left(P + \frac{2}{3}\rho k \right) = \nabla \cdot \left[\rho (\nu + \nu_t) \left(\nabla U + \nabla U^T - \frac{2}{3}(\nabla \cdot U)\mathbf{I} \right) \right], \tag{4.38}$$

$$\partial_t(\rho E) + \nabla \left(\left(\rho E + P + \frac{2}{3}\rho k \right) U \right) - \nabla \cdot \left(\left(\lambda + \frac{\rho \nu_t C_p}{Pr_t} \right) \nabla T \right) = \nabla \cdot \left[\rho (\nu + \nu_t) \left(\nabla U + \nabla U^T - \frac{2}{3}(\nabla \cdot U)\mathbf{I} \right) U \right] + \nabla \cdot \left[\rho (\nu + \sigma^* \nu_t) \nabla k \right], \tag{4.39}$$

$$\partial_t(\rho k) + \nabla \cdot (\rho k U) = -f_c \rho R : \nabla U - \beta^*_{new} \rho k \omega + \nabla \cdot \left[\rho (\nu + \sigma^* \nu_t) \nabla k \right], \tag{4.40}$$

$$\partial_t(\rho \omega) + \nabla \cdot (\rho \omega U) = -\alpha f_c \rho R : \nabla U - \beta_{new} \rho \omega^2 + \nabla \cdot \left[\rho (\nu + \sigma \nu_t) \nabla \omega \right], \tag{4.41}$$

$$\nu_t = \alpha^* \frac{k}{\omega}, \nu = \frac{\mu}{\rho}, \tag{4.42}$$

$$S = \frac{\nabla U + \nabla U^T}{2}, \Omega = \frac{\nabla U - \nabla U^T}{2}, R = \nu_t \left(2S - \frac{2}{3}(\nabla \cdot U)\mathbf{I} \right) - \frac{2}{3} k \mathbf{I}, \tag{4.43}$$

with the following constants:

$$f_c = 1.7, Re_t = \frac{k}{\nu \omega}, \sigma = \sigma^* = 0.5, \beta_0 = \frac{9}{125}, \beta^*_0 = \frac{9}{100}, \alpha^*_0 = \frac{1}{3}\beta_0, \alpha_0 = \frac{1}{9}, \tag{4.44}$$

$$\alpha^* = \frac{\alpha^*_0 + Re_t/R_k}{1 + Re_t/R_k}, \alpha = \frac{13}{25}\frac{\alpha_0 + (Re_t/R_\omega)}{1 + (Re_t/R_\omega)}(\alpha^*)^{-1}, \tag{4.45}$$

$$\beta = \beta_0 \frac{4/15 + (Re_t/R_\beta)^4}{1 + (Re_t/R_\beta)^4} f_\beta, \beta^* = \beta^*_0 f_\beta, \tag{4.46}$$

$$\beta^*{}_{new} = \beta^* - 1.5 \max(Ma_t^2 - Ma_{t_0}^2, 0)\beta \qquad \text{with} \quad Ma_{t_0} = 0.5 \tag{4.47}$$

$$\beta_{new} = \beta(1 + 1.5 \max(Ma_t^2 - Ma_{t_0}^2, 0)) \tag{4.48}$$

$$R_\beta = 8\,,\ R_k = 6\,,\ R_\omega = 6 \tag{4.49}$$

$$f_\beta = \frac{1 + 70\chi_\omega}{1 + 80\chi_\omega} \qquad \text{with} \quad \chi_\omega = \left| \frac{(\Omega \otimes \Omega) : S}{(\beta_0 \omega)^3} \right|, \tag{4.50}$$

$$f^*_\beta = \begin{cases} 1 & , \quad \chi_k \leq 0 \\ \dfrac{1 + 680\chi_k^2}{1 + 400\chi_k} & , \quad \chi_k \geq 0 \end{cases} \quad , \quad \chi_k = \frac{1}{\omega^3} \nabla k \nabla \omega, \tag{4.51}$$

$$Pr_t = 0.7. \tag{4.52}$$

As one can see corrections on turbulent the Reynolds number (Re_t) are added to the basic model in order to capture as best as possible the boundary layer. Besides we modified the production term by a factor f_c to improve the results. Some corrections are also added for supersonic flows ([Wil08]) by taking account of the turbulent Mach number. As usual what is difficult to tackle with with such a complex model is the validation of all terms especially when turbulence becomes a non linear phenomena.

4.4.2 Solving and Numerical results

Solving

The solving of these equations is based on a Roe solver (finite volumes) developed at the French Atomic Agency. We want to deal with stationary test cases so we use a Time-Marching method ([And06]; [Wil08]).

Numerical results

What is important in aerodynamics is the assessment of the following quantities at the boundaries on the object:

- C_p defined as:

$$C_p = \frac{P - P_\infty}{\frac{1}{2}\rho_\infty V_\infty^2},$$

  the pressure coefficient (P_∞: pressure far from the ramp, V_∞: velocity far from the ramp, ρ_∞: density far from the ramp)

- the Stanton number defined as:

$$St = \frac{\lambda \nabla T \cdot \overrightarrow{n}}{\rho_\infty V_\infty C \left(T_\infty (1 + \frac{\gamma-1}{2} M_\infty^2) - T_p \right)},$$

  which assess thermal fluxes (M_∞: Mach number far from the ramp, T_∞: temperature far from the ramp).

The following problem was solved (ramp of Delery (1990):see [DC91]):

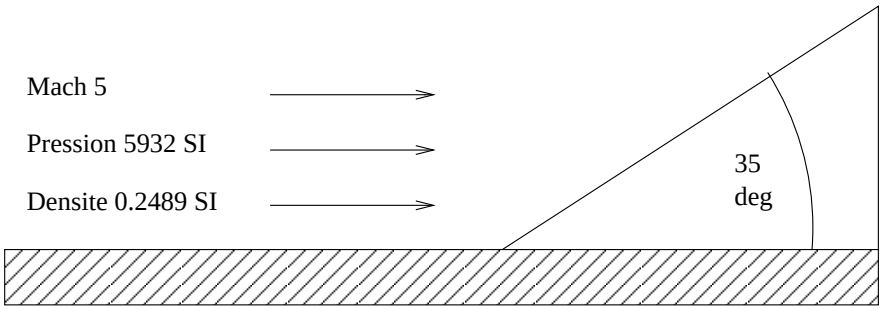

FIGURE 4.1: Ramp at Mach 5

It is a ramp of compression which creates a zone of recirculation when the geometry changes.

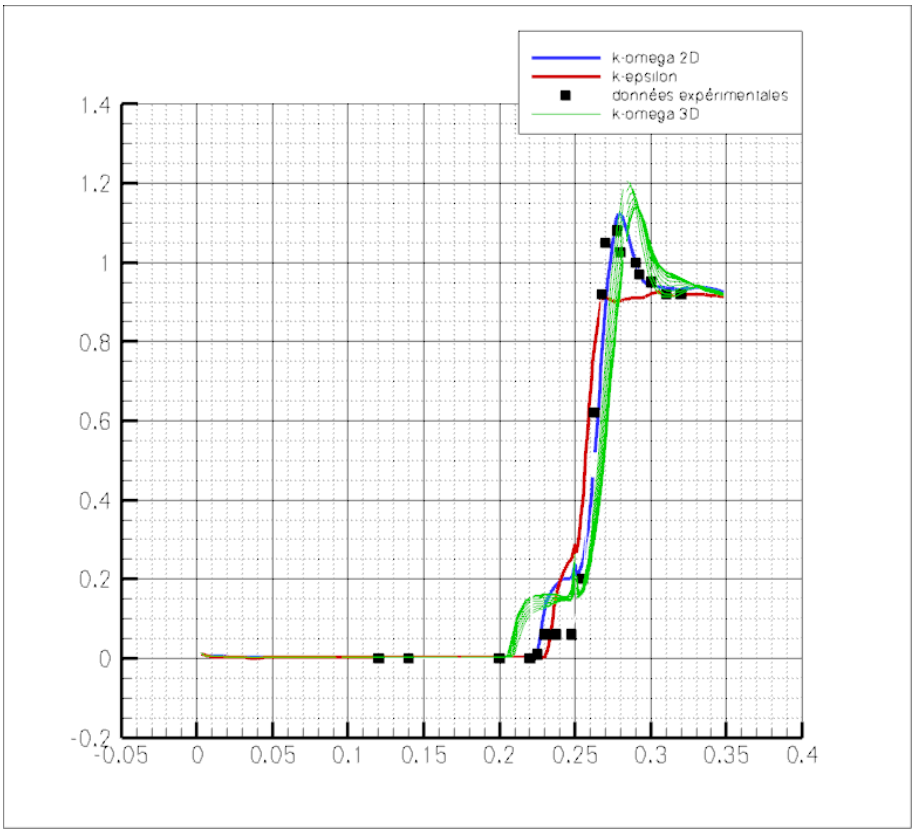

FIGURE 4.2: C_p on the wall.

In figure 4.2 and 4.3, we compare the pressure coefficient for the $k-\omega$ model in 2D and in 3D (several cuts in green) with results from the $k-\epsilon$ model and experimental data ("données expérimentales"). As one can see, results with the $k-\omega$ model agree well with the experiments on this test case.

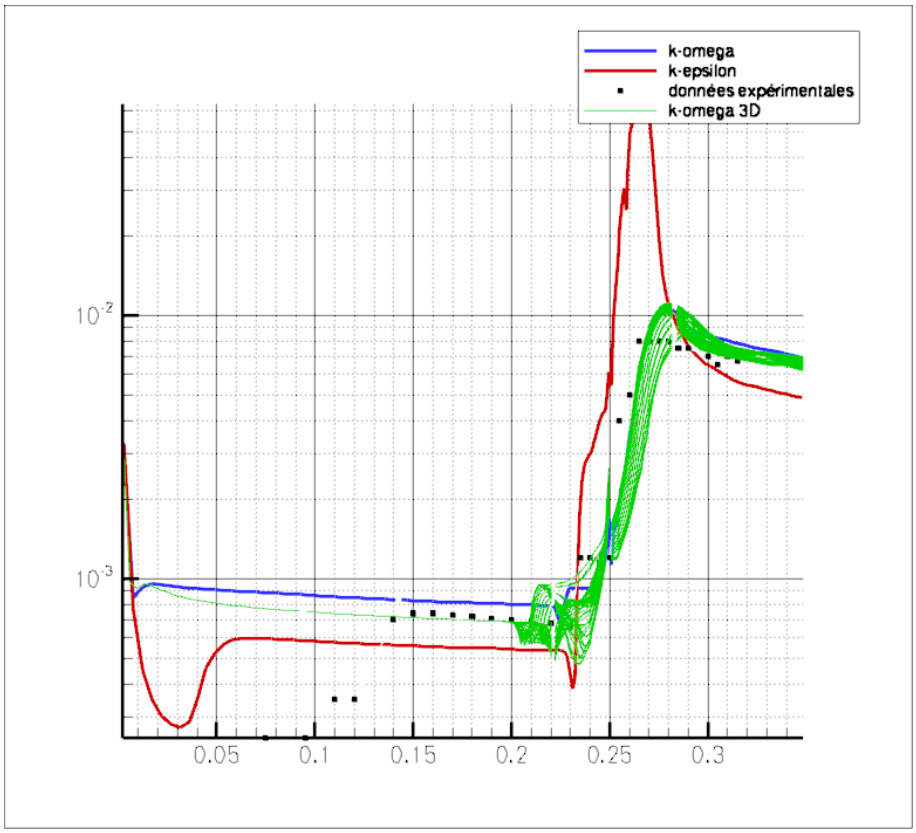

FIGURE 4.3: Stanton number at the wall (logarithm scale).

4.4.3 Conclusions and perspectives

The aim of this chapter is just to show that we have developed and assessed some RANS models in our code at the French atomic agency. The complex part is to come in next chapters: we want to couple these widely used models with ablation and roughness.

Chapter 5

Roughness and ablation

During a reentry phase, an object which is going to the ground will encounter very high fluxes. To be able to land, the object has to be protected through a TPS (Thermal Protection System). Selection and thickness definition of the Thermal Protection Material (TPM) are key performance parameters in TPS design. Prediction inaccuracies can be fatal for the re-entry vehicle. In this chapter we show the two sides of the problem. From a solid viewpoint we want to be able to describe the ablation according to the fluxes and chemistry seen by the solid. From a fluid viewpoint we want to know the impact of ablation on the fluid through the modification of the surface. It is generally admitted that roughness of the TPS surface can increase by a factor 3 the fluxes and turbulence can also multiply fluxes by the same factor. So a gain up to 9 can be obtained, putting in danger the re-entry vehicle. In a first section we study ablation (at a laminar level; note that a thesis for the transition regime (X. Lamboley at LCTS) has begun after the thesis of C. Levet). in a second section we study the impact of roughnesses on the the fluxes for supersonic/hypersonic re-entry regimes.

5.1 Interaction with the wall: the solid viewpoint (ablation)

In this section we rapidly present some results around ablation ([Vig+10]; [DAA13]) which were done during the Phd of C. Levet (2013-20116) at the LCTS in Bordeaux ([Lev17]; [Lev+17]).

5.1.1 Introduction

Carbon-fiber reinforced carbon composites (CFRC, CFC, Carbon/ Carbon) are dedicated to high technology structural and thermal applications in aggressive environments. They are used as thermostructural protections in various applications such as atmospheric re-entry, rocket propulsion, aircraft braking systems and plasma facing elements of the Tokamak. In the first two applications, the composites are progressively destroyed by oxidation, nitridation, sublimation, and, up to a certain extent, thermo-mechanical erosion. These phenomena are collected in the generic term of ablation. They are usually globally endothermic, transforming the thermal energy into mass loss and surface recession, whilst the remaining solid material insulates the vehicle substructure. Selection and thickness definition of the Thermal Protection Material (TPM) are key performance parameters in Thermal Protection System (TPS) design.

5.1.2 Some experimental results

In this subsection, we briefly report new data to improve the understanding of the behavior of dense composites during atmospheric re-entry and to feed multi-scale models of ablation. In order to reproduce the aero-thermodynamic environment of atmospheric entry in the boundary layer, the subsonic 1.2 MW Inductively Coupled Plasma (ICP) torch of the Plasmatron facility of the von Karman Institute (VKI) has been used. It allows the use of a wide range of pressures and heat fluxes ([Lev+17]). For instance under oxidation we got the following results at the facility:

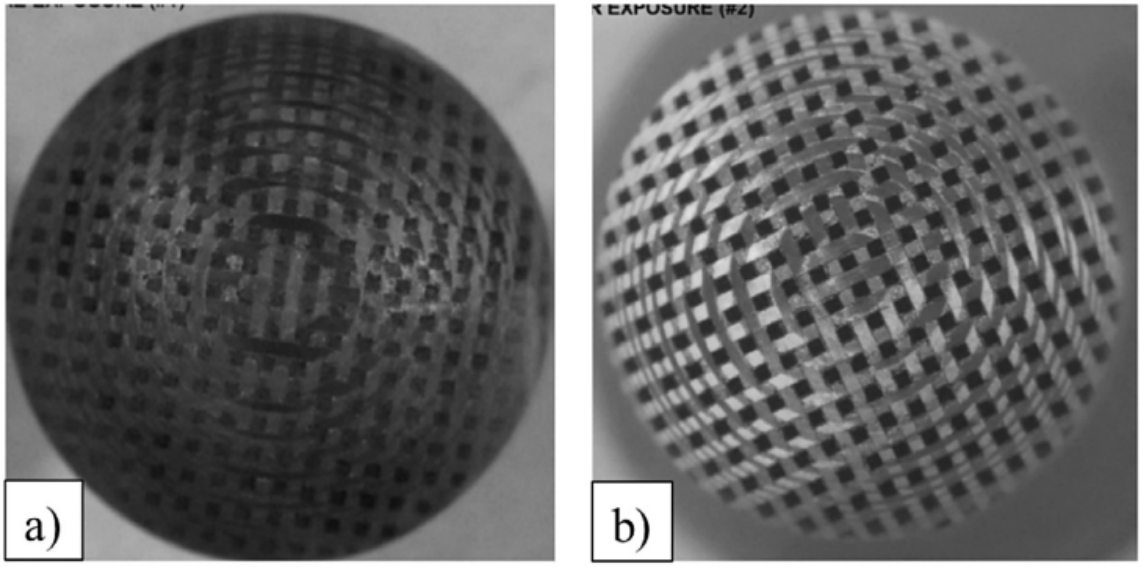

Micrographs of the *Oxidation HS* sample before (a) and after (b) ablation on the Plasmatron.

FIGURE 5.1: Samples of composites before/after oxidation at the plasmatron

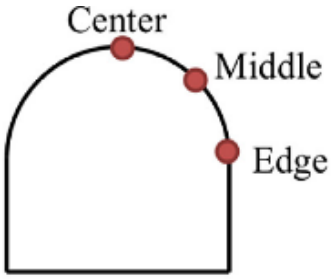

(a) Scheme of HS sample locations

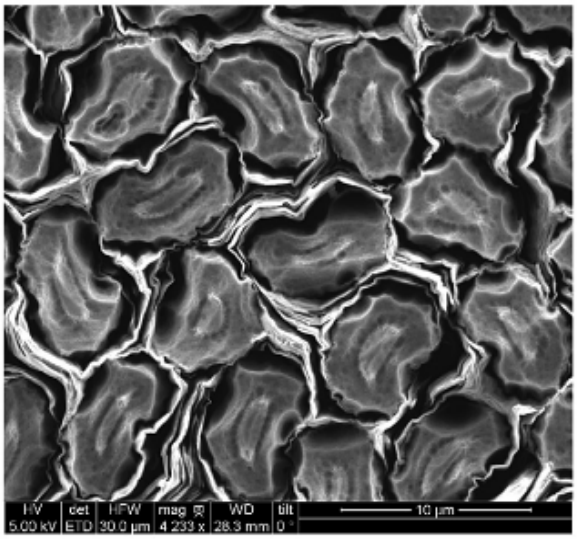

(b) *Oxidation ST*

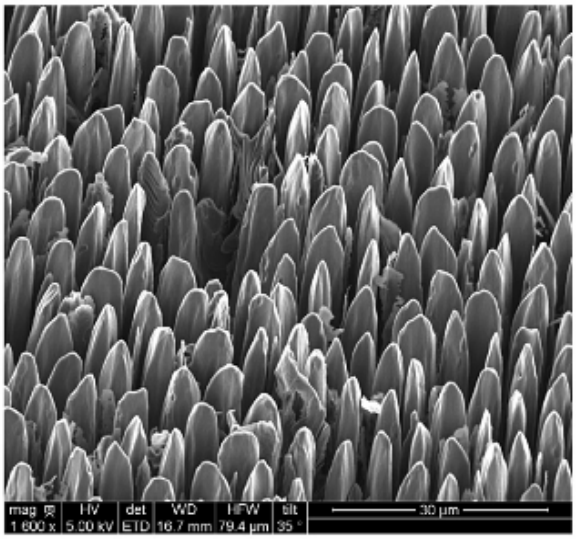

(c) *Oxidation HS center*

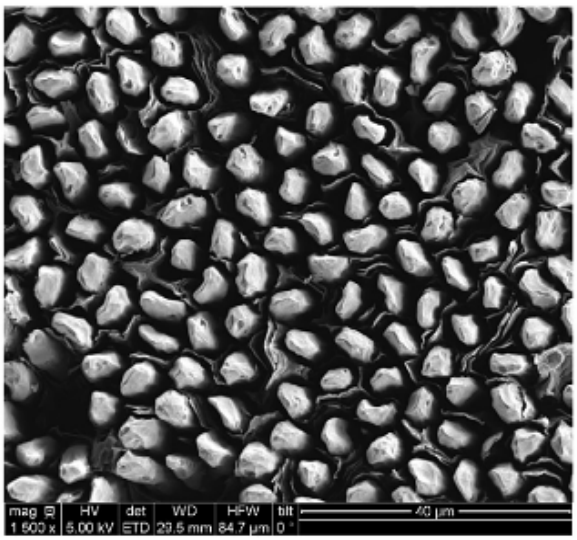

(d) *Oxidation HS middle*

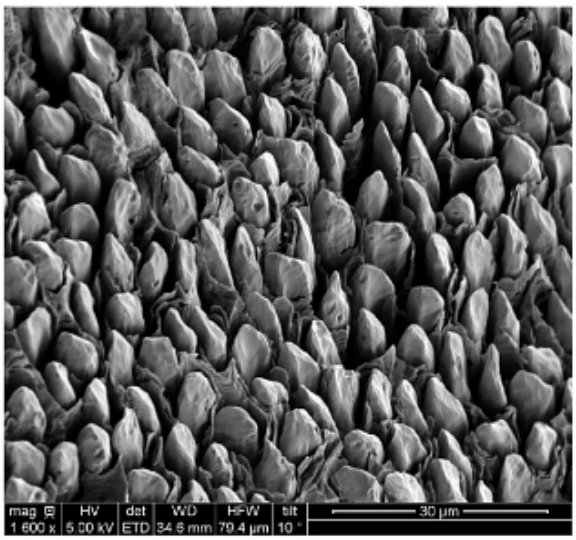

(e) *Oxidation HS edge*

FIGURE 5.2: SEM (Scanning Electron Microscopy) pictures of fiber bundles perpendicular to the surface for ST(standard) and HS(hemispheric) samples ablated under air. A scheme of the observations locations on HS samples is presented in a)

What can be seen in these kind of experiments which were done in supersonic conditions for the flow is that roughnesses can be very different according to the chemistry which is at stake in the flow. We will see later that the form of roughnesses can influence the increase in fluxes (in next chapter). A code (AMA) has been developed during the Phd of C. Levet to emulate the process of ablation based on the works of G. Vignoles at LCTS (Bordeaux). This code is still being improved during the Phd of X. Lamboley.

5.2 Interaction with the wall: the fluid viewpoint (roughness)

We briefly present some results that were obtained during the master of F. Danvin (CEA) with the help of M. Olazabal-Loumé (CEA) and B. Aupoix (ONERA). The results were shown at EUCASS 2017 ([Ola+17]).

5.2.1 Introduction

During a supersonic/hypersonic reentry flight, heating may damage the vehicle body causing rough surface state. In the low atmospheric layers, roughness effects on the turbulent flows have to be accounted for in CFD (Computational Fluid Dynamics) code simulations. Indeed, roughness is known to increase the skin friction and heat flux on the wall causing a dramatic modification of the aerodynamic coefficients. Usually, for such applications, turbulence effects are modeled using RANS (Reynold Averaged Navier-Stokes) approaches. Two-equation models like the $k-\omega$ Shear Stress Transport (SST) ([Men92]) model are being commonly used in aeronautic applications requiring accurate treatment of the near wall turbulent flow. For studying the roughness effect with numerical simulation, different approaches have been developed. In the direct numerical simulation (DNS), roughness elements have to be included in the initial geometry. The accuracy of the flow simulation around them and computational cost may be prohibiting for complex and /or huge size geometries. The discrete element method consists in directly include some roughness corrective terms into the Navier-Stokes or boundary layer equations. This method includes a form drag term and a blockage coefficient as a ratio between the volume accessible by the fluid over the total volume. It accounts for corrections related to both drag and heat-transfer around the roughness elements. This method has been widely used to describe the interaction between well-defined distributed roughness patterns and the turbulent flow. Nevertheless, it needs considerable modifications of the original equations. The equivalent sand-grain approach consists in bringing any kind of 3-D roughness to an equivalent sand-grain height to reproduce a turbulence level in the skin friction. As this method is non intrusive for an existing code, it appears to be the most suitable for industrial purposes. Several formulations were developed to be applied to RANS turbulence models. Such corrections for the $k-\omega$ SST model were recently proposed to take into account roughness effects on the skin friction and thermal flux ([Aup15b]; [Aup15a]). They were widely validated on low Mach number experiment data. This paper presents the first application of these corrections to hypersonic flows using a Navier-Stokes (N-S) code.

5.2.2 Turbulent flow modeling on a rough wall

Equivalent sand grain approach

Nikuradse's experiment study ([Nik50]) , on the effect of distributed sand grain roughness on pressure loss in cylindrical pipes constitutes a reference work. It was observed that the roughness influence on the flow field depends on a non-dimensional sand grain height The effect of roughness on the flow field can be decomposed into three regimes:

- Hydraulically smooth : The effect of roughness is not influencing the flow field. The wall skin friction remains unchanged.
- Transient Drag is generated both by viscous forces and by the pressure exerting on the roughness elements.
- Fully rough : Skin friction increases and the effects of roughness are independent from the Reynolds number. The viscous effects become negligible.

The given bounds can differ according to the authors. It is worth noticing that the equivalent sand-grain approach is not physical in the sense that it doesn't allow to describe the interaction between specific roughness elements and the flow. However, several correlations were proposed to calculate values from real roughness geometries and enable to reproduce the effect of roughness on the skin friction.

A few years later, Schlichting ([Sch37]) proposed for the completely rough regime to assimilate any kind of roughness to an equivalent sand grain (of height), which would generate the same skin friction increase as in Nikuradse's experiments. Importance of both roughness element form and density were pointed out. This approach is advantageous thanks to its ease of implementation and its cheap additional computational cost. Nevertheless, the method is quite sensitive to the equivalent sand-grain height estimate.

Roughness effect on the turbulent boundary layer

To study velocity variations inside the boundary layer, it is a common practice to use the non dimensional variables $u+$ and $y+$. It is worth reminding that a turbulent boundary layer on a smooth wall can be decomposed into three different regions ([Cou89]). In the viscous sublayer, where the viscous forces prevail due to the no-slip condition at the wall, the velocity profile can be approximated by $y+ < 11$. Then, the log layer corresponds to a turbulence development zone with a decrease of viscous effects. The velocity profile follows the so-called logarithmic law. The third region is the defect layer related to the boundary layer edge state.

On a rough wall, the boundary layer structure is modified: the roughness element presence tends to suppress viscous effects in the wall vicinity. Moreover, the flow characteristics may be different above roughness elements and in the troughs between them. According to Nikuradse ([Nik50]) and confirmed by others authors, the velocity fluctuates from the roughness trough until two to five times the actual roughness height before being able to define a mean velocity. Roughness effect is then described by introducing a $\Delta U+$ shift in the velocity profile logarithmic law towards lower velocities along the relation. Nikuradse's work also evidenced the $\delta U+$ dependency regarding the non dimensional sand grain height . Grigson's study ([Gri92]) exhibited a law on $\delta U+$ in order to fit Colebrook's data ([Col37].

5.2.3 Application to the $k-\omega$ SST turbulence model

The $k-\omega$ SST model was proposed by Menter ([Men92]) to mitigate some lack in the framework of two-equation turbulence models. It combines the suitability of Wilcox's $k-\omega$ model ([Wil94]) to near wall turbulent flow capture and the $k-\omega$ model properties in the far from wall field. This is achieved using a coupling function so that the compressible equations of kinetic turbulent energy and specific dissipation rate conservation.

Dynamic corrections

Several dynamic corrections applicable to the $k-\omega$ SST model were studied by Aupoix ([Aup15b]), in order to improve the predictions in the transient and fully rough regimes. ONERA-type corrections applied to Colebrook's data were selected, firstly because they overestimate skin-friction in the transient rough regime, and secondly due to their consistency with the Von Karman's constant, which provides a fine fluid representation in the fully rough regime. These modifications applied to the $k-\omega$ SST turbulence model consist in changing the boundary conditions on k and ω. The velocity shift is achieved thanks to an increase in the turbulence level at the wall and an increase in wall heat fluxes.

Thermal corrections

The proportional increase of wall heat fluxes with respect to drag increase, which is called Reynolds analogy, does not necessarily hold for rough walls as observed in several experiments. In reference ([Aup15a]), it is suggested to account for this phenomenon by including some corrections applicable to the equivalent sand grain approach. The discrete element method was used to study different roughness element density and shape effects on heat fluxes. This database served to the construction of thermal corrections suitable to the equivalent sand grain approach to improve the wall heat flux prediction. These thermal corrections are based on a modification of the turbulent Prandtl number in order to lower the wall heat fluxes. The turbulent Prandlt number correction depends on the equivalent sand grain height (ks), on the roughness height (h), and on a corrected wetted surface (Scorr).

5.2.4 Hill experiment simulation

The paper by Hill et al. ([HVW80]) reports the realization and the analysis of wind tunnel tests on a 7-degrees half-angle sharp and blunt cones at Mach 10. Nitrogen gas was used and experiment data were obtained for smooth and rough wall with three different roughness patterns. Wall temperature is 311 K. Simulations of the experiment using the N-S code and CLICET are performed for the sharp cone using the approximation of air gas and perfect gas assumption. Both dynamic and thermal corrections are used in simulations.

Equivalent sand grain height evaluation

To evaluate the equivalent sand grain height, one has to refer to Finson's study ([ML82]) where averaged roughness patterns were defined to analyse Hill's experiment data. They are based on profilometer measurements and on the assumption of identical roughness elements with uniform density to be suitable to the discrete element type method used. In the present study, due to a lack

of detailed information on the real surface state in experiment tests, these averaged patterns are used to evaluate the equivalent sand grain height and the corrected surface needed in dynamic and thermal correction evaluations.. Moreover, different correlations can lead to different rough regime identification. Note also that free-stream conditions vary from one test to another and two of them correspond to smooth wall tests.

Comparison between experiment data and simulations

Simulations are performed with the N-S code and the boundary layer code CLICET. For this, boundary layer edge quantities are extracted from the N-S simulations using a criterium of 99.5 to 99.8 % of the freestream total enthalpy which is conserved through the shock wave. Unfortunately, they are not so many detailed results presented in the original Hill's paper. Figure (5.4) presents the boundary layer velocity profile for the smooth wall and the 65mil rough wall case. N-S simulations reproduce correctly the experiment data for both cases. In Figure (5.4), Stanton number from Finson's paper ([ML82]) are compared with N-S simulations. The Stanton number is evaluated using the boundary layer edge quantities.

Simulations match well with experiment data in the case of smooth wall and rough wall with weak equivalent sand grain height (11mil case with Dirling correlation). For higher ks values, corresponding to transient and fully rough regimes, a difference is noticeable between simulations and experiment data, including the 65mil case for which velocities profiles are comparable. Simulations give overestimated values of the Stanton number (40% to 70%). N-S results are then compared to CLICET simulations showing a good agreement in wall heat flux evaluations for all the roughness patterns. The maximal difference observed on heat flux is of 5% for the 37mil and 65mil cases while it reaches 9% for the 11mil case with W-K correlation. Figures (5.3,5.4,5.5) show the resulting heat flux respectively for 65mil, 11mil and 37mil cases. To interpret these discrepancies in the Stanton values, several potential origins can be pointed out: first, some uncertainties may come from the use of modeled roughness instead of real surface patterns and the application of correlations to evaluate ks. We noticed that the ks value needed to retrieve the Stanton data level is of order of 5 x 10-4 m for the 65mil case. However, it seems inconsistent with the reasonable agreement found for boundary layer velocity profiles shown in figure (5.3). Another point is the application of Stanton formulae based on the boundary layer outer edge quantities. However, smooth wall Stanton numbers are well reproduced by simulations. Even accounting for the fact that slight modifications in N-S simulations could be found between smooth and rough cases, the uncertainty on outer edge quantity evaluation may not be sufficient to explain such discrepancies. In this experiment configuration, wall roughness and thermal combined effects are expected to play an important role in the final heat flux level, according to the Reynolds analogy failure. It is worth noticing that in simulations, a weak 5% to 10% difference was found applying dynamic corrections only or both dynamic and thermal corrections. These simulations of Hill's experiments constitute a first step of the validation of Aupoix's $k-\omega$ SST corrections applied to hypersonic flows. While dynamic corrections provided reasonable results, deeper investigation is needed in the application of the thermal corrections to high Mach flows. This validation is being pursued on the base of additional experiment data.

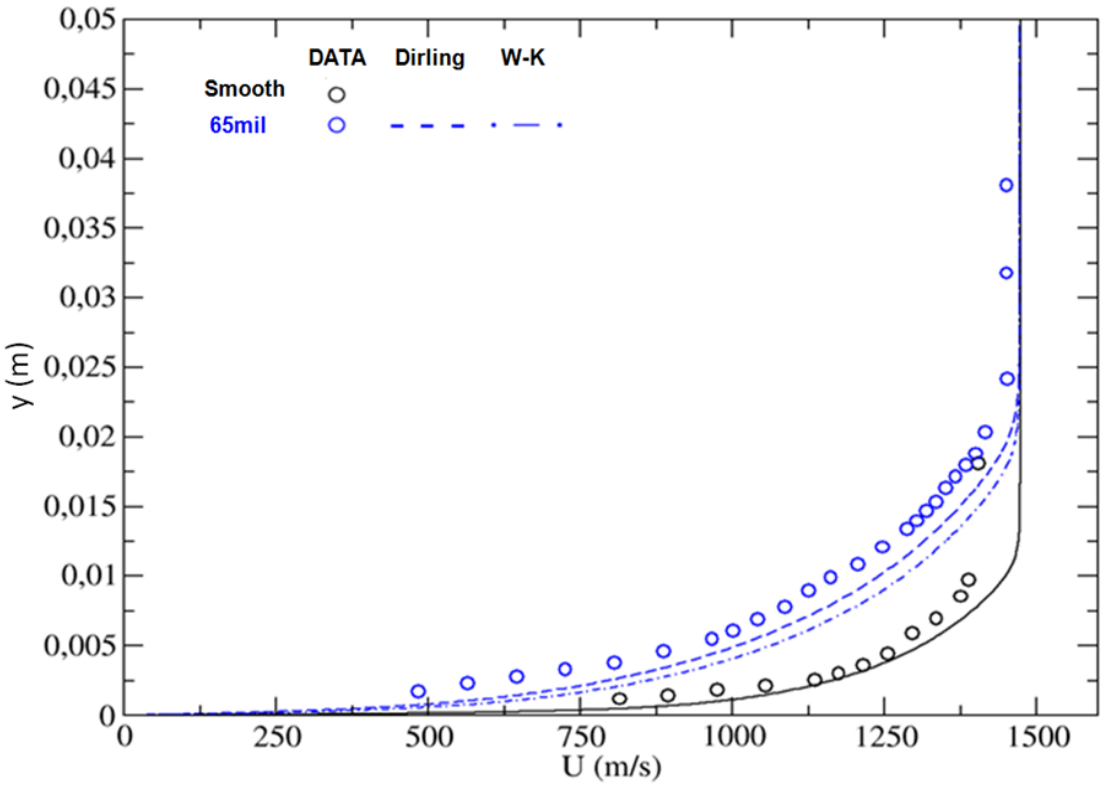

FIGURE 5.3: Boundary layer velocity profiles, experiment data (dots) from Hill's paper ([HVW80]) and N-S simulations (plain) for smooth wall and 65mil rough wall case

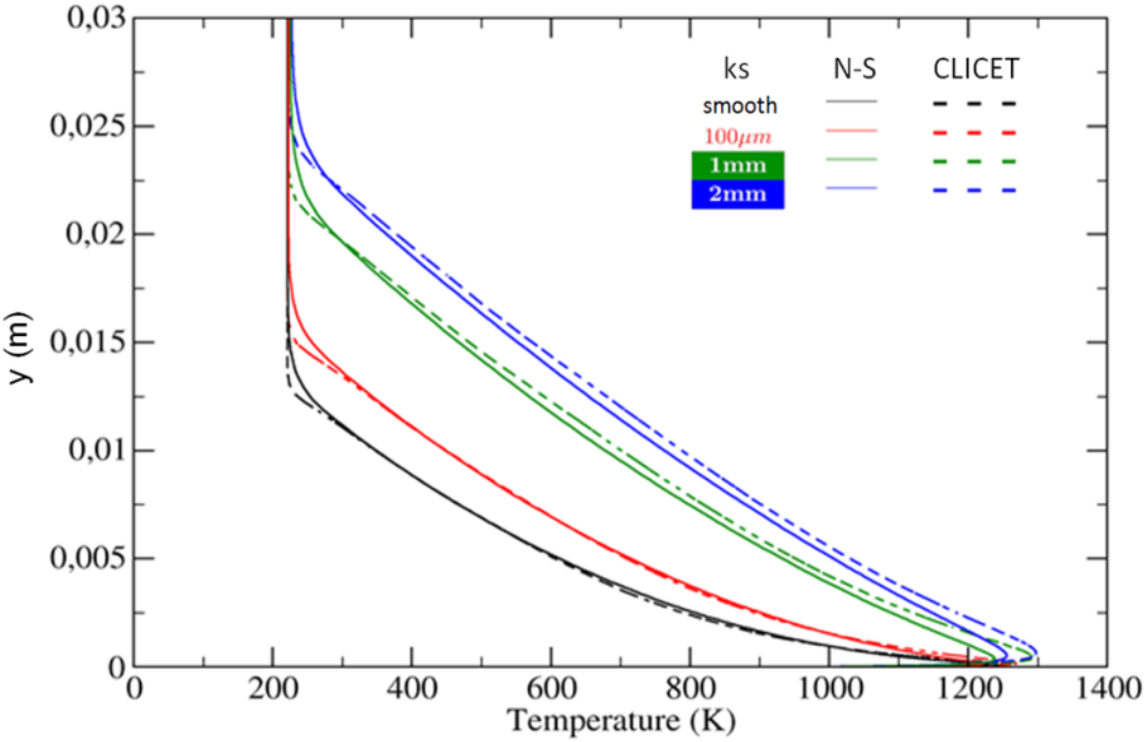

FIGURE 5.4: Stanton number obtained with N-S simulations and experiment data (dots/squares) given in ref. ([HVW80])

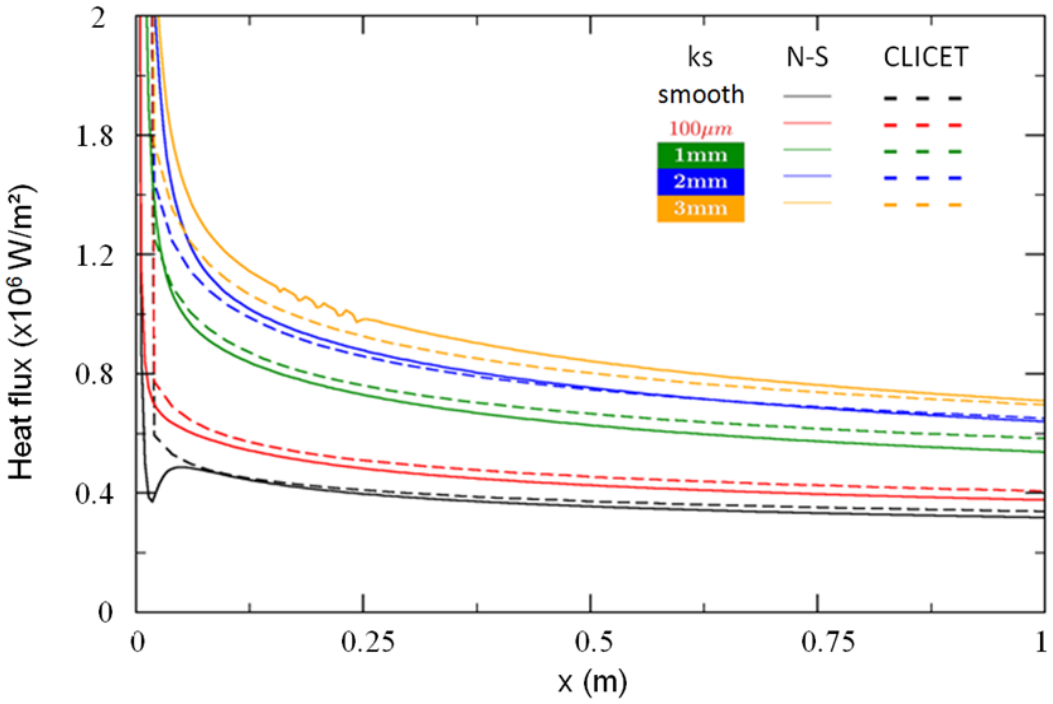

FIGURE 5.5: N-S and CLICET simulations - Heat flux at the wall for the 65mil case

Chapter 6

Conclusions and Perspectives

Several aspects of turbulence and ablation have been presented in this part. Although it has not been the essential task of my research work there is still a lot to do on the subjects. For instance RANS models need to be enriched by more subtle models such as DNS or LES as soon as it is possible to get more precise results. For ablation, transition to turbulence has to be studied to characterize as much as possible the size and distribution of roughnesses since we have shown their importance in understanding the fluxes. Of course it can be made possible if and only if experiments are available...

Part IV

Interactions between particles and fluid

Spray models

Fluid-particles flows (or equivalently sprays) are complex flows to model. They can be found in various applications (combustion, medicine, dusts in Mars atmosphere...). One can describe them using partial differential equations. They are mainly two ways to describe them.

The first one will use a continuous approach (Eulerian/Eulerian approach) using two phase flow models ([Sai95],[Bou98], [Rov06], et [GHS04]) considering that the characteristics of the spray (radius, energy, velocity) are not too dispersed (see chapter 8 for instance). The second one is based on a kinetic approach using Vlasov-Boltzmann equation to describe the behavior of the particles [ORo81], [MV01], [Hyl99], [VH97], [Lau02], [Bar04], [Duf05] , [HF92] et [HF95]).

In this part we will study both approaches form various viewpoints: theoretical results, models and asymptotic as well as numerics. Through an asymptotic limit we will also establish the link between the two kinds of models.

Chapter 7

Spray with collisions

In this chapter we study models of sprays with collisions. We will first look at mathematical solutions of the problem, then try to understand what happens when collisions are very numerous so that the spray regime is near to two-phase flow regimes and finally try to explore another model of collision in this dense regime to decrease the numerical cost in computations. These works are based on the papers ([Mat10]; [DM10]; [CDM10]) and can also be found with more details in the Phds [Mat03] and [Cha11].

7.1 Existence and uniqueness of solutions

We now present a work on existence and uniqueness of solutions for sprays with collisions. We go into details of the proof to illustrate the difficulty to deal with complex flows from a mathematical viewpoint.

The gas is described through compressible Euler equations: it evolves at high Reynolds numbers (like in the model proposed for instance in [BDM03]). The density ρ_g, the velocity u_g and the internal energy e_g characterize the behavior of the gas (considered as a perfect gas for the sake of simplicity).

The particles are described via a particle density function (p.d.f.) f which satisfies a Vlasov-Boltzmann equation. The parameters of the p.d.f. are the time t, the position x, the velocity v and the internal energy e. The collision kernel corresponds to **hard spheres**.

The coupling between the two phases is made through the drag force and thermal exchanges. Although viscosity is neglected in the gas equations, the drag force (which is proportional to viscosity) has to be taken into account because particles can be very small compared with the length scale of the gas (the Reynolds numbers of the particles are not very high)).

From a mathematical viewpoint, existence and uniqueness results exist for both Boltzmann equation and Euler equations taken independently. Concerning the Boltzmann equation, there exists global renormalized solutions ([DL89]), perturbative solutions near gaussians ([UA82], [MP97], [Guo03]) or vacuum ([IS84], [BT85]). Some of these results can be extended to the Vlasov-Boltzmann equation when the force acting on the particles has a specific form ([Lio94]). For the compressible Euler equations, only local smooth solutions are known ([Maj84]) in all dimensions. Global solutions with small total variation also exist in 1D ([Ser96b]).

Some mathematical results have already been proved for sprays. For instance, Domelevo and Roquejoffre have shown the existence and uniqueness of regular solutions for a coupling of the

viscous (1D) Burgers equation with Vlasov equation (see [DR99]). Hamdache proved the existence of solutions for large times for a coupling of the Stokes equation with a Vlasov equation ([Ham98]). Recently Baranger and Desvillettes proved the existence and uniqueness of local in time $\mathcal{C}^1$ solutions for a coupling of 3D compressible isentropic Euler equations with a Vlasov equation ([BD06]). The present work is the next step towards thick sprays, where the volume fraction occupied by the particles is explicitly appearing in the equations. It is also the first work which deals with the energies of the two phases, and also the first mathematical work where collisions are taken into account in the context of a coupling between fluid and kinetic equations. **Furthermore, it is the coupling through drag force which allows us to solve the problem.**

We now write down the system of equations:

$$\partial_t \rho_g + \nabla_x \cdot (\rho_g u_g) = 0\,, \tag{7.1}$$

$$\partial_t u_g + (u_g \cdot \nabla_x) u_g + \frac{\nabla_x p}{\rho_g} = -\frac{1}{\rho_g} \iint_{v,e} m_p F f dv de\,, \tag{7.2}$$

$$\partial_t e_g + u_g \cdot \nabla_x e_g + \frac{p}{\rho_g} \nabla_x \cdot u_g = \frac{1}{\rho_g} \iint_{v,e} m_p \left(F \cdot (u_g - v) - \phi\right) f dv de, \tag{7.3}$$

$$\partial_t f + v \cdot \nabla_x f + \nabla_v \cdot (fF) + \partial_e (f\phi) = Q(f,f)\,, \tag{7.4}$$

$$F = D_p(u_g - v)\,, \tag{7.5}$$

$$\phi = \frac{4\pi r}{m_p} \lambda Nu (T_g - T_p)\,, \tag{7.6}$$

$$p = (\gamma - 1)\rho_g e_g, \tag{7.7}$$

$$T_g = \frac{e_g}{C_{vg}}\,, \tag{7.8}$$

$$T_p = \frac{e}{C_{vp}}. \tag{7.9}$$

We define the constants of the model in this way: D_p is the drag coefficient (one can note that, in some models, D_p is proportional to the density of the gas ([BD06]): our theorem still holds in this case), the quantity C_{vg} (resp. C_{vp}) is the specific heat at constant volume of the gas (resp. particles), λ is the thermal conductivity of the gas, Nu is the Nusselt number, and finally γ is the specific heat ratio of the gas. The particles are supposed to have the same mass m_p and radius r. All these data are supposed to be constant.

Equations (7.1)-(7.3) are balance laws for the density $\rho_g := \rho_g(t,x)$, the velocity $u_g := u_g(t,x)$ and the internal energy (per mass unit) $e_g := e_g(t,x)$ of the gas, while equation (7.4) is a Vlasov-Boltzmann equation for the particle density function $f := f(t,x,v,e)$ of the particles. The gas is supposed to be perfect (equations (7.7) and (7.8)).

The coupling between (7.1)-(7.3) on one hand, and (7.4) on the other hand is made through the source terms in (7.2) and (7.3), an through the divergence terms in velocity and energy in (7.4). In these source terms appear the force $m_p\Gamma$ and the term of energy exchange $m_p\phi$. The whole system is closed by the thermodynamic laws (7.7), (7.8) and (7.9).

Finally, $Q(f,f)$ is a suitable hard-sphere type collision kernel taking into account internal energies:

$$Q(f,f)(t,x,v,e) = \iiint_{\sigma\in\mathbb{S}^2, v_*\in\mathbb{R}^3, e_*\in\mathbb{R}^+} \left(f'_* f' - f_* f\right) r^2 |v - v^*| d\sigma dv_* de_*, \tag{7.10}$$

with,

- σ: vector in $\mathcal{S}^2$,
- $v' = \frac{v+v_*}{2} + \frac{|v-v_*|}{2}\sigma$: post-collisional velocity,
- $v'_* = \frac{v+v_*}{2} - \frac{|v-v_*|}{2}\sigma$: post-collisional velocity,
- $e' = e$: post-collisional internal energy,
- $e'_* = e_*$: post-collisional internal energy.
- $f'_* = f(t, x,' v'_*, e'_*)$
- $f' = f(t, x, v', e')$
- $f_* = f(t, x, v_*, e_*)$
- $f = f(t, x, v, e)$

From now on, the constants λ, C_{vg},C_{vp}, D_p, m_p, r are taken equal to 1 for mathematical purposes, and γ is such that $\gamma > 1$. Nu is chosen so that $\frac{4\pi r}{m_p}\lambda Nu = 1$ in order to simplify computations.

We can now write down the final form of the system that we shall study. The unknowns are $\rho_g := \rho_g(t,x) \geq 0$, $u_g := u_g(t,x) \in \mathbb{R}^3$, $e_g := e_g(t,x) \geq 0$, and $f := f(t,x,v,e) \geq 0$, and they satisfy:

$$\partial_t \rho_g + \nabla_x \cdot (\rho_g u_g) = 0\,, \tag{7.11}$$

$$\partial_t u_g + (u_g \cdot \nabla_x) u_g + \frac{\nabla_x p}{\rho_g} = -\frac{1}{\rho_g} \iint_{v,e} F f dv de\,, \tag{7.12}$$

$$\partial_t e_g + u_g \cdot \nabla_x e_g + \frac{p}{\rho_g} \nabla_x \cdot u_g = \frac{1}{\rho_g} \iint_{v,e} \left(F \cdot (u_g - v) - \phi\right) f dv de\,, \tag{7.13}$$

$$\partial_t f + v \cdot \nabla_x f + \nabla_v \cdot (fF) + \partial_e (f\phi) = Q(f,f)\,, \tag{7.14}$$

$$F = u_g - v\,, \tag{7.15}$$

$$\phi = e_g - e\,, \tag{7.16}$$

$$p = (\gamma - 1)\rho_g e_g, \tag{7.17}$$

where $Q(f,f)$ is defined by (7.10) (with $r = 1$).

Functional space and norms

We now define the space of functions for f. We denote by $||g||$ the L^2-norm and by $||g||_w$ the weighted-L^2 norm ($w = (1 + |v|^2)$),

$$||g|| = \left(\iiint_{x,v,e} g^2 dedvdx \right)^{\frac{1}{2}},$$

$$||g||_w = \left(\iiint_{x,v,e} g^2 w dedvdx \right)^{\frac{1}{2}}.$$

We define $|g|$ and $|g|_w$ the local L^2-norms,

$$|g| = \left(\iint_{v,e} g^2 dedv \right)^{\frac{1}{2}}, \; |g|_w = \left(\iint_{v,e} g^2 w dedv \right)^{\frac{1}{2}}.$$

Sobolev spaces $W^{s,2}$ are denoted by H^s.

We write down $\partial_\alpha^{\beta,\gamma} := \partial_x^\alpha \partial_v^\beta \partial_e^\gamma$. Let s be an integer such that $s > 4$. Using Guo's Energy method, we define the energy of a function as

$$\mathcal{E}_{s,\varepsilon}(g)(t) = \sum_{|\alpha|+|\beta|+|\gamma|\leq s} \left[\frac{1}{2} \left|\left| \partial_\alpha^{\beta,\gamma} g \right|\right|^2 (t) + \int_0^t 2(1-\varepsilon) \left|\left| \partial_\alpha^{\beta,\gamma} g \right|\right|_w^2 (u) du \right], \tag{7.18}$$

where ε is a constant which satisfies $0 < \varepsilon < 1$ (cf. [Guo02]; [Guo03]).

We define $E_{s,\varepsilon,T}$ as the intersection of the nonnegative functions and the functional space made of the functions f in $\mathcal{C}([0,T], H^s(\mathbb{R}^3 \times \mathbb{R}^3 \times \mathbb{R}^+))$ such that

$$\sup_{0\leq t\leq T} \mathcal{E}_{s,\varepsilon}(f)(t)^{\frac{1}{2}} < +\infty.$$

The norm associated with $E_{s,\varepsilon,T}$ is denoted $||.||_{E_{s,\varepsilon,T}}$ and defined through

$$||f||_{E_{s,\varepsilon,T}} = \sup_{0\leq t\leq T} \mathcal{E}_{s,\varepsilon}(f)(t)^{\frac{1}{2}}.$$

The space $E_{s,\varepsilon,T}$ is complete since it is the intersection of a complete functional space and the cone of positive functions.

7.1.1 Outline of the work

We first establish an a priori estimate for the Boltzmann equation, thanks to the use of a simple change of unknown in the equation. We define $g := f \times \exp(v^2 + e)$ using Guo's method ([Guo03]). The function g satisfies

$$\partial_t g + v \cdot \nabla_x g + \nabla_v \cdot (gF) + \partial_e (g\phi) - 2v \cdot gF - g\phi = \Gamma(g,g), \tag{7.19}$$

where Γ is defined through

$$\begin{aligned} & \Gamma[g_1,g_2](t,x,v,e) \\ = \; & \Gamma^+[g_1,g_2](t,x,v,e) - \Gamma^-[g_1,g_2](t,x,v,e) \\ = \; & \iiint_{\mathbb{R}^3\times\mathbb{R}^+\times S^2} |v-v_*| \exp(-({v_*}^2 + e_*)) g_1(t,x,v'_*,e'_*) g_2(t,x,v',e') dv_* de_* d\sigma \\ - \; & g_2(t,x,v,e) \iiint_{\mathbb{R}^3\times\mathbb{R}^+\times S^2} |v-v_*| \exp(-({v_*}^2 + e_*)) g_1(t,x,v_*,e_*) dv_* de_* d\sigma. \end{aligned}$$

We prove that $||g||_{E_{s,\varepsilon,T}}$ remains bounded for small T, using the fact that the "new" collision kernel Γ can be controlled by the term coming from the drag force $-2v \cdot gF$.

Then, we establish a result of existence and uniqueness for a given u_g, e_g for equation (7.19). In order to do so, we use Picard's fixed point theorem and estimates based on the characteristics method (as in [BD06]). More precisely, we prove the following result:

Theorem 7.1.1 (Existence and uniqueness for equation (7.19))**.** *We suppose that e_g is a strictly positive function. Furthermore, we assume that u_g and $\tilde{e}_g = e_g - 1$ belong to $\mathcal{C}([0,T], H^s(\mathbb{R}^3)) \cap \mathcal{C}^1([0,T], H^{s-1}(\mathbb{R}^3))$ for some $T > 0$ and s integer such that $s \geq 5$. We suppose that $g_0 := f_0 \exp(v^2 + e)$ satisfies*

$$\sum_{|\alpha|+|\beta|+|\gamma|\leq s} \frac{1}{2} \left|\left|\partial_\alpha^{\beta,\gamma}(g_0)\right|\right|^2 < +\infty.$$

Then:

1. *One can find $T' > 0$ such that there exists a solution g to equation (7.19) with g_0 for initial data (and F and ϕ given by (7.15) and (7.16)). Besides, g remains positive and*

$$\mathcal{E}_{s,\frac{1}{2}}(g(t,.)) = \sum_{|\alpha|+|\beta|+|\gamma|\leq s} \left[\frac{1}{2}\left|\left|\partial_\alpha^{\beta,\gamma} g\right|\right|^2(t) + \int_0^t \left|\left|\partial_\alpha^{\beta,\gamma} g\right|\right|_w^2(u)du\right]$$

remains bounded on $[0,T']$. Finally, T' is controlled through

$$T' \geq \frac{3}{8C\left[1 + \sup_{0\leq t\leq T}||u_g||_{H^s}^2 + \sup_{0\leq t\leq T}||\tilde{e}_g||_{H^s} + \frac{3}{2}||g_0||_{H^s}^2\right]} \tag{7.20}$$

with C strictly positive constant depending only on s.

Moreover, g lies in $\mathcal{C}([0,T], H^s(\mathbb{R}^3 \times \mathbb{R}^3 \times \mathbb{R}^+)) \cap \mathcal{C}^1([0,T], H^{s-1}(\mathbb{R}^3 \times \mathbb{R}^3 \times \mathbb{R}^+))$.

2. *If g_1 and g_2 are two positive solutions of eq. (7.19) in $\mathcal{C}([0,T], H^s(\mathbb{R}^3 \times \mathbb{R}^3 \times \mathbb{R}^+)) \cap \mathcal{C}^1([0,T], H^{s-1}(\mathbb{R}^3 \times \mathbb{R}^3 \times \mathbb{R}^+))$ with same initial data - ρ_g, u_g and $\tilde{e}_g$ being fixed- and such that $\sup_{0\leq t\leq T} \mathcal{E}_{s,\frac{1}{2}}(g_1(t,.)) < +\infty$ and $\sup_{0\leq t\leq T} \mathcal{E}_{s,\frac{1}{2}}(g_2(t,.)) < +\infty$, then $g_1 = g_2$.*

The main point of the proof is the control of the loss of moments due to the collision operator.

Then we tackle the global system (7.11)-(7.17). Using an iterative scheme based on the symmetrization of the hyperbolic equations for the gas and theorem 7.1.1 for the particles, we prove the following result:

Theorem 7.1.2. *We consider $I =]0, +\infty[\times \mathbb{R}^3 \times]0, +\infty[$, $s \in \mathbb{N}$ such that $s \geq 5$, and I_1, I_2 open sets of I such that $\overline{I_1} \subset I_2$, and such that $\overline{I_1}$, $\overline{I_2}$ are compact in I. Let $(\rho_{g_0}, u_{g_0}, e_{g_0}) : \mathbb{R}^3 \to I_1$ be functions satisfying $\tilde{\rho}_{g_0} = \rho_{g_0} - 1 \in H^s(\mathbb{R}^3)$, $u_{g_0} \in H^s(\mathbb{R}^3)$ and $\tilde{e}_{g_0} = e_{g_0} - 1 \in H^s(\mathbb{R}^3)$. Let also $g_0 = f_0 \exp(v^2 + e) : \mathbb{R}^3 \times \mathbb{R}^3 \times \mathbb{R}^+ \to \mathbb{R}^+$ be a function of $H^s(\mathbb{R}^3 \times \mathbb{R}^3 \times \mathbb{R}^+)$.*

Then, one can find $T > 0$ such that there exists a solution $(\rho_g, u_g, e_g; f)$ to system (7.11) - (7.17) belonging to $C^1([0,T] \times \mathbb{R}^3, \overline{I_2}) \times C^1([0,T] \times \mathbb{R}^3 \times \mathbb{R}^3 \times \mathbb{R}^+, \mathbb{R}^+)$. Moreover, $\tilde{\rho}_g (= \rho_g - 1)$, u_g, $\tilde{e}_g (= e_g -$

$1) \in \mathcal{C}([0,T], H^s(\mathbb{R}^3)) \cap \mathcal{C}^1([0,T], H^{s-1}(\mathbb{R}^3))$, $\tilde{f} = f\exp(v^2+e) \in \mathcal{C}([0,T], H^s(\mathbb{R}^3\times\mathbb{R}^3\times\mathbb{R}^+)) \cap \mathcal{C}^1([0,T], H^{s-1}(\mathbb{R}^3\times\mathbb{R}^3\times\mathbb{R}^+))$.

Finally, if $(\tilde{\rho}_{g_1}, u_{g_1}, \tilde{e}_{g_1}; f_1)$ *and* $(\tilde{\rho}_{g_2}, u_{g_2}, \tilde{e}_{g_2}; f_2)$ *are in* $(\mathcal{C}([0,T], H^s(\mathbb{R}^3)) \cap \mathcal{C}^1([0,T], H^{s-1}(\mathbb{R}^3)))$ $\times$ $(\mathcal{C}([0,T], H^s(\mathbb{R}^3\times\mathbb{R}^3\times\mathbb{R}^+)) \cap \mathcal{C}^1([0,T], H^{s-1}(\mathbb{R}^3\times\mathbb{R}^3\times\mathbb{R}^+)))$, *if* $(\rho_{g_1}, u_{g_1}, e_{g_1}; f_1)$ *and* $(\rho_{g_2}, u_{g_2}, e_{g_2}; f_2)$ *belong to* $C^1([0,T]\times\mathbb{R}^3, \overline{I_2})$ $\times$ $C^1([0,T]\times\mathbb{R}^3\times\mathbb{R}^3\times\mathbb{R}^+, \mathbb{R}^+)$ *and they satisfy (7.11)-(7.17), then* $\rho_{g_1} = \rho_{g_2}$, $u_{g_1} = u_{g_2}$, $e_{g_1} = e_{g_2}$ *and* $f_1 = f_2$.

We first establish a priori estimates for the p.d.f. . Then we give the proof of theorem 7.1.1. Finally, we establish the main result (theorem 7.1.2) in the last section.

7.1.2 A priori estimates on the p.d.f. equation

We now study the following equation,

$$\partial_t f + v\cdot\nabla_x f + \nabla_v\cdot(fF) + \partial_e(f\phi) = Q(f,f), \tag{7.21}$$

with F, ϕ, Q given by $(7.14) - (7.16)$

We suppose that u_g and $\tilde{e}_g = e_g - 1$ are in $\mathcal{C}([0,T], H^s(\mathbb{R}^3)) \cap \mathcal{C}^1([0,T], H^{s-1}(\mathbb{R}^3))$ for some $T > 0$ and s integer such that $s \geq 5$ (typical space for hyperbolic problems -cf [Maj84]-): the gas is at rest at infinity. Moreover we suppose that $f_0\exp(v^2+e)$ is in $H^s(\mathbb{R}^3\times\mathbb{R}^3\times\mathbb{R}^+)$.

Rewriting Boltzmann equation

We define g as the following function: $g : (t,x,v,e) \hookrightarrow f(t,x,v,e)\exp(v^2+e)$. Putting g in the Vlasov-Boltzmann equation, one obtains

$$\partial_t g + v\cdot\nabla_x g + \nabla_v\cdot(gF) + \partial_e(g\phi) - 2v\cdot gF - g\phi = \Gamma(g,g), \tag{7.22}$$

where Γ is defined through

$$\begin{aligned} & \Gamma[g_1,g_2](t,x,v,e) \\ = \; & \Gamma^+[g_1,g_2](t,x,v,e) - \Gamma^-[g_1,g_2](t,x,v,e) \\ = \; & \iiint_{\mathbb{R}^3\times\mathbb{R}^+\times S^2} |v-v_*|\exp(-({v_*}^2+e_*))g_1(t,x,v'_*,e'_*)g_2(t,x,v',e')dv_*de_*d\sigma \\ - \; & g_2(t,x,v,e)\iiint_{\mathbb{R}^3\times\mathbb{R}^+\times S^2} |v-v_*|\exp(-({v_*}^2+e_*))g_1(t,x,v_*,e_*)dv_*de_*d\sigma. \end{aligned} \tag{7.23}$$

The form of Γ is obtained by noticing that both kinetic and internal energy are conserved during collisions.

We only recall the two main a priori estimates: the one on the collision kernel which needs a lot of computations to be proved and the one on the drag force term which counterbalances the loss of moment in velocity due to the hard sphere cross section in the kernel of collision.

Collision kernel

We now consider the modified collision operator introduced in (7.23), and present a formula for its derivatives of any order. The collision kernel is defined by:

$$\begin{aligned}
&\Gamma[g_1,g_2](t,x,v,e)\\
=\;&\Gamma^+[g_1,g_2]-\Gamma^-[g_1,g_2]\\
=\;&\iiint_{\mathbb{R}^3\times\mathbb{R}^+\times\mathbb{S}^2}|v-v_*|\exp(-({v_*}^2+e_*))g_1(t,x,v'_*,e'_*)g_2(t,x,v',e')dv_*de_*d\sigma\\
-\;&g_2(t,x,v,e)\iiint_{\mathbb{R}^3\times\mathbb{R}^+\times\mathbb{S}^2}|v-v_*|\exp(-({v_*}^2+e_*))g_1(t,x,v_*,e_*)dv_*de_*d\sigma.
\end{aligned}\tag{7.24}$$

Using the change of variables $v_* \hookrightarrow v_*+v$ in the integral, and the fact that collisions do not change internal energy, one gets:

$$\begin{aligned}
&\Gamma[g_1,g_2](t,x,v,e)\\
=\;&\Gamma^+[g_1,g_2](t,x,v,e)-\Gamma^-[g_1,g_2](t,x,v,e)\\
=\;&\iiint_{\mathbb{R}^3\times\mathbb{R}^+\times\mathbb{S}^2}|v_*|\exp(-((v_*+v)^2+e_*))g_1(t,x,v+\frac{1}{2}(v_*-|v_*|\sigma),e_*)\\
&\times g_2(t,x,v+\frac{1}{2}(v_*+|v_*|\sigma),e)dv_*de_*d\sigma\\
-\;&\iiint_{\mathbb{R}^3\times\mathbb{R}^+\times\mathbb{S}^2}|v_*|\exp(-((v_*+v)^2+e_*))g_1(t,x,v_*+v,e_*)dv_*de_*d\sigma.\\
&\times g_2(t,x,v,e)
\end{aligned}\tag{7.25}$$

Using this form of the kernel, one can differentiate this expression (see [Guo03]) and, using the change of variables backwards, one gets

$$\begin{aligned}
\partial_\alpha^{\beta,\gamma}\Gamma(g_1,g_2)=\;&\sum\; C(|\alpha|,|\alpha_1|,|\alpha_2|,|\beta|,|\beta_0|,|\beta_1|,|\beta_2|,|\gamma|,|\gamma_0|,|\gamma_1|,|\gamma_2|)\\
&\times\Gamma_0\left[\partial_{\alpha_1}^{\beta_1,\gamma_1}g_1,\partial_{\alpha_2}^{\beta_2,\gamma_2}g_2\right],
\end{aligned}\tag{7.26}$$

the summation being over $\beta=\beta_0+\beta_1+\beta_2$, $\alpha=\alpha_1+\alpha_2$ and $\gamma=\gamma_0+\gamma_1+\gamma_2$. The coefficients $C(...)$ are integers that we do not compute and Γ_0 is defined as

$$\begin{aligned}
&\Gamma_0\left[\partial_{\alpha_1}^{\beta_1,\gamma_1}g_1,\partial_{\alpha_2}^{\beta_2,\gamma_2}g_2\right]\\
=\;&\Gamma_0^+\left[\partial_{\alpha_1}^{\beta_1,\gamma_1}g_1,\partial_{\alpha_2}^{\beta_2,\gamma_2}g_2\right](t,x,v,e)-\Gamma_0^-\left[\partial_{\alpha_1}^{\beta_1,\gamma_1}g_1,\partial_{\alpha_2}^{\beta_2,\gamma_2}g_2\right](t,x,v,e)\\
=\;&\iiint_{\mathbb{R}^3\times\mathbb{R}^+\times\mathbb{S}^2}|v-v_*|\partial^{\beta_0,\gamma_0}[\exp(-({v_*}^2+e_*))](\partial_{\alpha_1}^{\beta_1,\gamma_1}g_1)'_*(\partial_{\alpha_2}^{\beta_2,\gamma_2}g_2)'\\
-\;&\iiint_{\mathbb{R}^3\times\mathbb{R}^+\times\mathbb{S}^2}|v-v_*|\partial^{\beta_0,\gamma_0}[\exp(-({v_*}^2+e_*))](\partial_{\alpha_1}^{\beta_1,\gamma_1}g_1)_*\partial_{\alpha_2}^{\beta_2,\gamma_2}g_2.
\end{aligned}\tag{7.27}$$

Note that in fact $\gamma_1=\gamma_0=0$, and $\gamma_2=\gamma$ for all γ since the derivatives in e are only the derivatives of g_2.

We can now prove the two different properties on the gain and loss terms of the collision kernel (note that weighted norms appear):

Lemma 7.1.1. *Let $\beta = \beta_0 + \beta_1 + \beta_2$, $\alpha = \alpha_1 + \alpha_2$ and $\gamma = \gamma_0 + \gamma_1 + \gamma_2$.*

1. *The following inequalities hold:*

$$\left| \iiint \Gamma_0^+ \left[\partial_{\alpha_1}^{\beta_1,\gamma_1} g_1, \partial_{\alpha_2}^{\beta_2,\gamma_2} g_2 \right] \partial_\alpha^{\beta,\gamma} g_3 dv de dx \right| \leq C \left[\sum_{|\delta|\leq 3} \left|\left| \partial_{\alpha_1+\delta}^{\beta_1,\gamma_1} g_1 \right|\right| \right] \left|\left| \partial_{\alpha_2}^{\beta_2,\gamma_2} g_2 \right|\right| \left|\left| \partial_\alpha^{\beta,\gamma} g_3 \right|\right|_w, \quad (7.28)$$

$$\left| \iiint \Gamma_0^- \left[\partial_{\alpha_1}^{\beta_1,\gamma_1} g_1, \partial_{\alpha_2}^{\beta_2,\gamma_2} g_2 \right] \partial_\alpha^{\beta,\gamma} g_3 dv de dx \right| \leq C \left[\sum_{|\delta|\leq 3} \left|\left| \partial_{\alpha_1+\delta}^{\beta_1,\gamma_1} g_1 \right|\right| \right] \left|\left| \partial_{\alpha_2}^{\beta_2,\gamma_2} g_2 \right|\right| \left|\left| \partial_\alpha^{\beta,\gamma} g_3 \right|\right|_w. \quad (7.29)$$

2. *The following inequalities hold:*

$$\left| \iiint \Gamma_0^+ \left[\partial_{\alpha_1}^{\beta_1,\gamma_1} g_1, \partial_{\alpha_2}^{\beta_2,\gamma_2} g_2 \right] \partial_\alpha^{\beta,\gamma} g_3 dv de dx \right| \leq C \left[\sum_{|\delta|\leq 3} \left|\left| \partial_{\alpha_2+\delta}^{\beta_2,\gamma_2} g_2 \right|\right| \right] \left|\left| \partial_{\alpha_1}^{\beta_1,\gamma_1} g_1 \right|\right| \left|\left| \partial_\alpha^{\beta,\gamma} g_3 \right|\right|_w, \quad (7.30)$$

$$\left| \iiint \Gamma_0^- \left[\partial_{\alpha_1}^{\beta_1,\gamma_1} g_1, \partial_{\alpha_2}^{\beta_2,\gamma_2} g_2 \right] \partial_\alpha^{\beta,\gamma} g_3 dv de dx \right| \leq C \left[\sum_{|\delta|\leq 3} \left|\left| \partial_{\alpha_2+\delta}^{\beta_2,\gamma_2} g_2 \right|\right| \right] \left|\left| \partial_{\alpha_1}^{\beta_1,\gamma_1} g_1 \right|\right| \left|\left| \partial_\alpha^{\beta,\gamma} g_3 \right|\right|_w. \quad (7.31)$$

Drag term

The most important result of this subsection is the following, which allows to recover the loss of moments due to the collision kernel:

Lemma 7.1.2 ($gF \cdot v$-term)**.** *For all ε such that $1 > \varepsilon > 0$,*

$$\sum_{|\alpha|+|\beta|+|\gamma|\leq s} \iiint \partial_\alpha^{\beta,\gamma} g \, \partial_\alpha^{\beta,\gamma} (gF \cdot v) dv de dx \leq -(1-\varepsilon) \sum_{|\alpha|+|\beta|+|\gamma|\leq s} ||\partial_\alpha^{\beta,\gamma} g||_w^2 + C_1 ||g||_{H^s}^2 + \frac{C_2}{\varepsilon} ||g||_{H^s}^2 ||u_g||_{H^s}^2. \quad (7.32)$$

A priori estimates

Thanks to all the previous results, we are able to get the following a priori estimate for solutions of the modified Boltzmann equation (7.19). We now sum up all the results through the following

lemma:

Lemma 7.1.3. *Let g be a nonnegative solution of (7.19) in $\mathcal{C}([0,T], H^s(\mathbb{R}^3\times\mathbb{R}^3\times\mathbb{R}^+))\cap\mathcal{C}^1([0,T], H^{s-1}(\mathbb{R}^3\times\mathbb{R}^3\times\mathbb{R}^+))$, with e_g strictly positive function and u_g and $\tilde{e}_g = e_g - 1$ belonging to $\mathcal{C}([0,T], H^s(\mathbb{R}^3))\cap\mathcal{C}^1([0,T], H^{s-1}(\mathbb{R}^3))$ for some $T>0$. For all $s\geq 5$, $1>\varepsilon>0$, we have the following a priori estimate for the energy $\mathcal{E}_{s,\varepsilon}$ defined by (7.18),*

$$\frac{d}{dt}\mathcal{E}_{s,\varepsilon} \leq \frac{C}{\varepsilon}\left(1+||u_g||^2_{H^s}+||\tilde{e}_g||_{H^s}+\mathcal{E}_{s,\varepsilon}\right)\mathcal{E}_{s,\varepsilon}. \tag{7.33}$$

where C depends only on the physical constants and s.

7.1.3 Solving the Boltzmann equation for a given gas

We now want to use lemma 7.1.3 in order to prove theorem 7.1.1. We first prove the existence of solutions thanks to an iterative scheme as it is done in [Guo03] and [BD06]. Then we prove uniqueness.

For the sake of simplicity, we shall suppose that the initial datum g_0 is $\mathcal{C}^\infty$ and compactly supported (so that integrations by parts are valid), and ρ_g, u_g, e_g are also smooth $\mathcal{C}^\infty$ functions.

Existence: iterative scheme and characteristics

We adopt the following iterative scheme in order to prove the existence of a solution to equation (7.19) in theorem 7.1.1:

$$\partial_t g^{n+1} + v\cdot\nabla_x g^{n+1} + \nabla_v\cdot(g^{n+1}F) + \partial_e(g^{n+1}\phi) = \Gamma^+(g^n,g^n) - \Gamma^-(g^n,g^{n+1}) + 2v\cdot g^{n+1}F + g^{n+1}\phi, \tag{7.34}$$

$$g(0,.,.,.) = g_0(.,.,.). \tag{7.35}$$

The first iterate g^0 of the sequel $(g^n)_{n\in\mathbb{N}}$ is equal to the constant function (in time) g_0.

There are two main reasons for using this iterative scheme. First, we ensure positiveness of all iterates if g^0 is positive by taking $\Gamma^-(g^n,g^{n+1})$. Secondly, we can use the characteristics method in order to prove the existence of all iterates (see [BD06]).

We define $X(s;x,v,e,t)$, $V(s;x,v,e,t)$, $E(s;x,v,e,t)$ as the characteristics linked to the flow of the modified Boltzmann equation (7.19). They satisfy the following equations:

$$\begin{aligned}
\frac{d}{dt}X &= V && , \quad X(s;x,v,e,s) = x,\\
\frac{d}{dt}V &= -(V-u_g(t,X)) && , \quad V(s;x,v,e,s) = v,\\
\frac{d}{dt}E &= -\left(E-e_g(t,X)\right) && , \quad E(s;x,v,e,s) = e.
\end{aligned}$$

The characteristics are well defined since ρ_g, u_g and e_g are smooth functions. We define Y as the point in the phase space (X,V,E).

Solution

We now give the expression of the solution of the linear Vlasov equation appearing in (7.34) using the characteristics. Equation (7.34) can be rewritten

$$\partial_t g^{n+1} + v \cdot \nabla_x g^{n+1} + (u_g - v) \cdot \nabla_v g^{n+1} + (e_g - e)\partial_e g^{n+1} \\ = \Gamma^+(g^n, g^n) + h(g_n) g^{n+1}, \quad (7.36)$$

where $h(g_n)$ is defined through

$$h(g_n)(t,x,v,e) = 4 + 2v \cdot (u_g - v) + (e_g - e) \\ - \iiint_{\mathbb{R}^3 \times \mathbb{R}^+ \times \mathbb{S}^2} |v - v_*| \exp(-({v_*}^2 + e_*)) g_n(t,x,v_*,e_*) dv_* de_* d\sigma. \quad (7.37)$$

The solution of the iterative scheme at step n can be written explicitly thanks to the formula

$$g^{n+1}(t,x,v,e) = \exp\left(\int_0^t h(g_n)(\tau, Y(\tau;x,v,e,t)) d\tau \right) g_0(Y(0;x,v,e,t)) \\ + \int_0^t \exp\left(\int_\tau^t h(g_n)(\tau, Y(\tau;x,v,e,t)) d\tau \right) \Gamma^+(g_n, g_n)(Y(\tau;x,v,e,t)) d\tau. \quad (7.38)$$

One can notice that all iterates are compactly supported and $\mathcal{C}^\infty$ by induction since $g^0 = g_0$ has these properties. Contrary to [BD06], we do not need to control the support of all iterates: because of collisions, we already know that the limit of the sequence g_n is not compactly supported. This formula also shows that all iterates remain positive.

Convergence of the iterative scheme, uniqueness

We prove the convergence of the scheme using Picard's fixed point theorem. We define the following application G:

$$\begin{aligned} G \quad : \quad & E_{s,1/2,T'} \cap \mathcal{C}^\infty \mapsto \mathcal{C}^\infty, \\ & k \mapsto \ell \end{aligned} \quad (7.39)$$

where ℓ is the unique solution given by formula (7.38) of the equation:

$$\partial_t \ell + v \cdot \nabla_x \ell + (u_g - v) \cdot \nabla_v \ell + (e_g - e)\partial_e \ell = \Gamma^+(k,k) + h(k)\ell, \quad (7.40)$$

$$\ell(0,.) = g(0,.) \in \mathcal{C}^\infty. \quad (7.41)$$

The operator G is well-defined: ℓ exists, is nonnegative and smooth (k is nonnegative). We recall that $E_{s,1/2,T'}$ is complete: in order to use Picard's theorem, it remains to prove that for each g_0 there exists a radius R and T' small enough, such that the application maps the ball of radius R of $E_{s,1/2,T'}$ into itself and is a contraction on this ball. Once we know that the fixed point exists, it

automatically lies in $E_{s,1/2,T'}$, and therefore in $\mathcal{C}([0,T'],H^s(\mathbb{R}^3\times\mathbb{R}^3\times\mathbb{R}^+))$. Using equation (7.19), one gets that the partial derivative in time of the fixed point will lie in $\mathcal{C}([0,T'],H^{s-1}(\mathbb{R}^3\times\mathbb{R}^3\times\mathbb{R}^+))$ so that the fixed point belongs to $\mathcal{C}^1([0,T'],H^{s-1}(\mathbb{R}^3\times\mathbb{R}^3\times\mathbb{R}^+))$.

We choose the radius R of the ball in the following way:

$$R = ||g_0||_{H^s} = 2\mathcal{E}_{s,1/2}(g_0)(0)^{\frac{1}{2}}.$$

Then, we choose T':

$$T' = \frac{3}{4C\left[1+\sup_{0\leq t\leq T}||u_g||^2_{H^s}+\sup_{0\leq t\leq T}||\tilde{e}_g||_{H^s}+2R^2\right]}, \tag{7.42}$$

for some C that is given later.

We now explain how we have obtained the time of existence given in theorem 7.1.1. For ordinary differential equations with locally Lipschitz coefficients, it is known that if the solution is bounded on $[0,T_1]$, then it can be extended for a time T_2 strictly greater than T_1 using Cauchy's theorem. The same result holds here as long as the energy of g is bounded, it can be extended and the a priori estimate given in lemma 7.1.3 controls the solution. Using this a priori estimate, we obtain the time given in theorem 7.1.1. Obviously, the uniqueness of the solution comes from the proof of the constricting behavior of G. Theorem 7.1.1 is now proved.

7.1.4 Coupling Euler and Vlasov-Boltzmann equation: existence and uniqueness of H^s-solutions

We now prove theorem 7.1.2. In order to obtain this theorem, we combine theorem 7.1.1 and results on local solutions for the hyperbolic system of Euler equations of perfect gases (see [Ser96a] and [Maj84])). The proof of theorem is close to the one in [BD06], especially for the hyperbolic part of the problem. Therefore we only describe the main steps of the proof:

- we first recall some classical results for hyperbolic systems (especially in the linearized case),
- we write down an iterative scheme based on the results obtained for the Boltzmann-Vlasov equation for a given gas (theorem 7.1.1) and on linearized hyperbolic systems,
- we finally pass to the limit in the scheme in order to obtain theorem 7.1.2.

Hyperbolic part of the system

We now recall some facts about the compressible Euler equations of perfect gases (see [Ser96a] for further details). Let's define $I=]0,+\infty[\times\mathbb{R}^3\times]0,+\infty[$ as the space in which (ρ_g,u_g,e_g) lies. The system of equations for perfect gases (7.11)-(7.12)-(7.13) can be put in a symmetrized form:

Lemma 7.1.4. *We define U_g as $U_g = {}^t(\rho_g,u_g,e_g)$, $\delta_{j,i}$ as the Kronecker's symbol, and c as the sound speed of the gas defined by $c := \sqrt{\gamma(\gamma-1)e_g}$. System (7.11)-(7.12)-(7.13) is symmetrized thanks to the following formula:*

$$S(U_g)\partial_t U_g + \sum_i (SA_i)(U_g)\partial_{x_i}U_g = S(U_g)\,b(U_g,f), \tag{7.43}$$

where S, A_i (for $i = 1, 2, 3$) and b are respectively defined by:

$$S = \begin{pmatrix} \left(\frac{(\gamma-1)e_g}{\rho_g}\right)^2 & 0 & 0 \\ 0 & \frac{1}{\gamma}c^2 & 0 \\ 0 & 0 & (\gamma-1) \end{pmatrix},$$

$$A_i = \begin{pmatrix} u_{g_i} & \rho_g\delta_{1,i} & \rho_g\delta_{2,i} & \rho_g\delta_{3,i} & 0 \\ \frac{(\gamma-1)e_g}{\rho_g}\delta_{1,i} & u_{g_i} & 0 & 0 & e_g\delta_{1,i} \\ \frac{(\gamma-1)e_g}{\rho_g}\delta_{2,i} & 0 & u_{g_i} & 0 & e_g\delta_{2,i} \\ \frac{(\gamma-1)e_g}{\rho_g}\delta_{3,i} & 0 & 0 & u_{g_i} & e_g\delta_{3,i} \\ 0 & (\gamma-1)e_g\delta_{1,i} & (\gamma-1)e_g\delta_{2,i} & (\gamma-1)e_g\delta_{3,i} & u_{g_i} \end{pmatrix},$$

$$b = \begin{pmatrix} 0 \\ -\iint \frac{1}{\rho_g} f(u_{g_1} - v)dvde \\ -\iint \frac{1}{\rho_g} f(u_{g_2} - v)dvde \\ -\iint \frac{1}{\rho_g} f(u_{g_3} - v)dvde \\ -\iint \frac{1}{\rho_g} f(e_g - e)dvde + \iint \frac{1}{\rho_g} f\left(u_g - v\right)^2 dvde \end{pmatrix}.$$

For $s \geq 5$, if $f\exp(v^2+e)(t,.)$ is in $H^s(\mathbb{R}^3\times\mathbb{R}^3\times\mathbb{R}^+)$, if moreover $\left(\rho_g - 1, u_g, e_g - 1\right)(t,.)$ is in $(H^s(\mathbb{R}^3))^5$ and belongs to I_2, then $b(t,.)$ is in $H^s(\mathbb{R}^3)$ and we have the following control:

$$\begin{aligned} & ||b(t,.)||_{H^s} \\ \leq\ & C(s,\overline{I_2})(1+||\rho_g - 1||_{H^s}) \\ \times\ & ||f\exp(v^2+e)(t,.)||_{H^s}\left(1+||e_g-1||_{H^s}+||u_g||^2_{H^s}\right). \end{aligned} \tag{7.44}$$

The constant C only depends on the compact set $\overline{I_2}$ and on the Sobolev index s. Moreover, the symmetric definite positive matrix $S(U_g)$ is a smooth function of U_g satisfying

$$d\, Id_5 \leq S(U_g) \leq d^{-1}\, Id_5, \tag{7.45}$$

when $U_g \in I_1$ (or I_2), for some constant $d > 0$ (depending on I_1 (or I_2)). Finally, all the matrices $SA_i(U_g)$ are symmetric.

In fact, we shall only consider a linearized hyperbolic problem of the type

$$S(U)\partial_t V + \sum_i (SA_i)(U)\partial_{x_i} V = S(U)\, b(U,f), \tag{7.46}$$

$$V(0,.) = U(0,.) \in I_1, \tag{7.47}$$

in the iterative scheme. Here, $U = (U_1, U_2, U_3)$ and $V = (V_1, V_2, V_3)$ are in $(\mathbb{R}^+\times\mathbb{R}^3\times\mathbb{R}^+)$. The matrices SA_i are the ones defined above.

This linear system is strictly hyperbolic as soon as $U_1 > 0$ and $U_3 > 0$. Then, if f is known and regular enough ($f \exp(v^2 + e) \in \mathcal{C}\left([0,T]; H^s(\mathbb{R}^7)\right)$), there exists a (local in time) solution to (7.46) − (7.47) since $b(t,.)$ belongs to $H^s(\mathbb{R}^3)$. This solution exists as long as f and U exist but may stay in I_2 for a shorter time. More precisely, we have the following a priori estimate for these hyperbolic systems with smooth coefficient (cf. [Maj84], [Ser96a] and [AG91]):

Lemma 7.1.5 (Control of linear hyperbolic systems)**.** *Let s be an integer such that $s \geq 5$. If $f \exp(v^2 + e)$ is in $\mathcal{C}\left([0,T]; H^s(\mathbb{R}^7)\right)$ and $U - U(0,.)$ is in $\mathcal{C}\left([0,T]; (H^s(\mathbb{R}^3))^5\right)$, then the linearized problem (7.46)-(7.47) has a solution V such that $V(t,.) - V(0,.)$ belongs to $\mathcal{C}\left([0,T]; (H^s(\mathbb{R}^3))^5\right) \cap \mathcal{C}^1\left([0,T]; (H^{s-1}(\mathbb{R}^3))^5\right)$, and such that for a strictly positive time T_p, V remains in I_2 on $[0,T_p]$. Besides, the following inequality holds:*

$$\forall t \leq T_p, ||V(t,.) - V(0,.)||_{H^s}(t) \leq Ct, \tag{7.48}$$

where C is a constant depending on the compact set $\overline{I_2}$, the Sobolev index s, $\sup_{0\leq u\leq T} ||f \exp(v^2+e)(u,.)||_{H^s}$ and $\sup_{0\leq u\leq T} ||U(u,.) - U(0,.)||_{H^s}$.

Iterative scheme

We now start the proof of theorem 7.1.2. We recall that $U_{g_0} - {}^t(1,0,0,0,1) \in H^s$ and that $f_0 exp(v^2 + e) \in H^s$. Furthermore, we recall that $U_{g_0}(x)$ is in I_1 for all x. We define R by $R := ||f_0 \exp(v^2 + e)||_{H^s}$.

We define by induction the following iterative scheme,

$$U_g{}^0(t,.) = U_{g_0}(.), \tag{7.49}$$
$$f^0(t,.) = f_0(.), \tag{7.50}$$
$$T_0 = +\infty, \tag{7.51}$$

(one can notice that $U_g{}^0$ lies in I_2 since U_{g_0} is in I_1).

Then,

$$S(U_g{}^k)\partial_t U_g{}^{k+1} + \sum_{i=1}^{N} (SA_i)(U_g{}^k)\partial_{x_i} U_g{}^{k+1} = S(U_g{}^k)\, b(U_g{}^k, f^k), \tag{7.52}$$

$$U_g{}^{k+1}(0,x) = U_0(x), \tag{7.53}$$

$$\begin{aligned} &\partial_t f^{k+1} + \nabla_x \cdot (v f^{k+1}) + \nabla_v \cdot (f^{k+1}(u_g^k - v)) + \partial_e (f^{k+1}(e_g^k - e)) \\ = \;& Q(f^{k+1}, f^{k+1}), \end{aligned} \tag{7.54}$$

$$f^{k+1}(0,x,v) = f_0(x,v). \tag{7.55}$$

We define T_{k+1} (for $k \geq 0$) as the minimum of:

- the maximal time of existence for $U_g{}^{k+1}$ (which is T_k thanks to lemma 7.1.5),

- the maximal time such that ${U_g}^{k+1}$ remains in $\overline{I_2}$,
- the maximal time such that $||{U_g}^{k+1} - U_{g_0}||_s \leq 2||U_{g_0} -^t (1,0,0,0,1)||_s$,
- the maximal time of existence for f^{k+1},
- the maximum time such that $\forall t / 0 \leq t \leq T_{k+1}$,

$$\sum_{|\alpha|+|\beta|+|\gamma|\leq s} \left[\frac{1}{2} \left|\left| \partial_\alpha^{\beta,\gamma} \left(f^{k+1} \exp(v^2+e) \right) \right|\right|^2 (t) + \int_0^t \left|\left| \partial_\alpha^{\beta,\gamma} \left(f^{k+1} \exp(v^2+e) \right) \right|\right|_w^2 (u) du \right] \leq R^2. \quad (7.56)$$

The iterates are well defined since the initial data and the first iterates $({U_g}^0, f_0)$ are in H^s. U_g^{k+1} and f^{k+1} are solved "separately". The hyperbolic part is solved using results on hyperbolic linear systems with smooth coefficients (lemma 7.1.5). The kinetic part is solved using theorem 7.1.1 for the Boltzmann equation with fixed gas: for T_{k+1} small enough strictly positive, the condition (7.56) is verified. Finally using the results of regularity in lemma 7.1.5 and theorem 7.1.1, $({\rho_g}^{k+1} - \rho_{g_0}$, u_g^{k+1}, $e_g^{k+1} - e_{g_0}) \in \mathcal{C}([0,T_{k+1}], H^s(\mathbb{R}^3)) \cap \mathcal{C}^1([0,T_{k+1}], H^{s-1}(\mathbb{R}^3))$, and $g^{k+1} = f^{k+1}\exp(v^2+e) \in \mathcal{C}([0,T_{k+1}], H^s(\mathbb{R}^3 \times \mathbb{R}^3 \times \mathbb{R}^+)) \cap \mathcal{C}^1([0,T_{k+1}], H^{s-1}(\mathbb{R}^3 \times \mathbb{R}^3 \times \mathbb{R}^+))$.

The aim is now to prove that the sequence of existence times $(T_k)_{k\in\mathbb{N}}$ has a strictly positive lower bound T.

Using the conditions giving T_k, one gets that

$$\sup_{0\leq t\leq T_k} ||{U_g}^k - U_{g_0}||_s \leq 2||U_{g_0} -^t (1,0,0,0,1)||_s. \quad (7.57)$$

Using the control on the hyperbolic system (lemma 7.1.5), we get

$$\forall t \leq T_{k+1},\ ||U_g^{k+1} - U_{g_0}||_{H^s}(t) \leq C_1 t, \quad (7.58)$$

where C_1 depends on $2||U_{g_0} -^t (1,0,0,0,1)||_s$, I_2 and R.

Moreover, using Sobolev embeddings, there exists C_2 such that

$$\begin{aligned} ||U_g^{k+1} - U_{g_0}||_{L^\infty} &\leq C_2||U_g^{k+1} - U_{g_0}||_{H^s} \\ &\leq C_1 C_2 t. \end{aligned} \quad (7.59)$$

Since $\overline{I_1} \subset I_2$, the distance $dist(fr(I_2), I_1)$ between the frontier of I_2 (called $fr(I_2)$) and I_1 is strictly positive. U_g^{k+1} remains in I_2 as long as $t \leq \frac{1}{C_1 C_2} dist(fr(I_2), I_1)$.

There remains to obtain a time for which all the iterates f_k satisfy $||f^k||^2_{E_{s,1/2,T_k}} \leq ||f_0 \exp(v^2+e)||^2_{H^s}$. Using theorem 7.1.1, one gets that f_k is at least defined for all t such that

$$\begin{aligned} t &\geq \frac{3}{8C\left(1+\sup_{0\leq t\leq T}||u_g^{k-1}||^2_{H^s}+\sup_{0\leq t\leq T}||\tilde{e}_g^{k-1}||_{H^s}+\frac{3}{2}||f_0\exp(v^2+e)||^2_{H^s}\right)} \\ &\geq \frac{3}{8C\left(1+\sup_{0\leq t\leq T}2||U_{g_0}-{}^t(1,0,0,0,1)||_s+\frac{3}{2}||f_0\exp(v^2+e)||^2_{H^s}\right)}. \end{aligned}$$

Using this inequality, one gets a time T_* independent of k (since the constants no longer depend on k) for which all iterates f^k satisfy $||f^k||^2_{E_{s,1/2,T_*}} \leq ||f_0\exp(v^2+e)||^2_{H^s}$. By defining $T := \min(T_*, \frac{dist(fr(I_2),I_1))}{C_1C_2})$, one finally gets a time T strictly positive for which the scheme is stable: all T_k are larger than T.

Passing to the limit

We pass to the limit. To begin with, the following lemma holds:

Lemma 7.1.6. *We consider the sequence T_k, U_g^k, f^k of the iterative scheme, and $T>0$ the time of stability of the scheme. Then one can find $T_* \in]0,T[$ such that (for $k\geq 2$),*

$$\sup_{0\leq t\leq T_*}|||(f^k-f^{k-1})\exp(v^2+e)|| \leq C_1(I_2,s,U_{g_0},f_0)\sup_{0\leq t\leq T_*}||U_g^{k-1}-U_g^{k-2}||, \tag{7.60}$$

$$\sup_{0\leq t\leq T_*}||U_g^{k+1}-U_g^k|| \leq \frac{1}{4}\sup_{0\leq t\leq T_*}||U_g^k-U_g^{k-1}|| + \frac{1}{4}\sup_{0\leq t\leq T_*}||U_g^{k-1}-U_g^{k-2}||. \tag{7.61}$$

Thanks to (7.61), we see that

$$\sum_k \sup_{0\leq t\leq T_*}\|U_g^{k+1}-U_g^k\| < +\infty. \tag{7.62}$$

Then, (U_g^k) is a Cauchy sequence and converges in $L^\infty([0,T_*],(L^2(\mathbb{R}^3))^5)$ towards some limit U_g which satisfies $U_g - {}^t(1,0,1) \in L^\infty([0,T_*],(L^2(\mathbb{R}^3))^5)$.

It is clear that $U_g - {}^t(1,0,0,0,1) \in C([0,T_*],(L^2(\mathbb{R}^3))^5)$ ($\forall k\geq 0$, $U_g^k - {}^t(1,0,1) \in C([0,T_*],(L^2(\mathbb{R}^3))^5)$).

Moreover, thanks to (7.60) and (7.62),

$$\sum_k \sup_{0\leq t\leq T_*}\|(f^{k+1}-f^k)\exp(v^2+e)\|_{L^2} < +\infty. \tag{7.63}$$

Using classical arguments (see[Mat06]; [Mat10]) on Sobolev embeddings one can now recover existence of solutions through Cauchy sequences.

Uniqueness of solutions is a consequence of the proof of lemma 7.1.6.

7.2 Hydrodynamic limit

We now go to the study of dense sprays when the volume fraction of particles has to be considered. We want to show that two-phase flow systems can be recovered from sprays equations. Unfortunately it has been done only at a formal level as we will see in this work. From a mathematic viewpoint, it is always difficult to tackle with the volume fraction.

We consider in this work only monodisperse sprays (that is, all the droplets in the disperse phase have the same radius r). Moreover, we shall also suppose that all droplets are incompressible and that no evaporation occurs, so that r will be in the sequel an absolute constant.

We denote by $\alpha := \alpha(t,x) \in [0,1]$ the volume fraction of gas at time $t \in \mathbb{R}_+$ and point $x \in \Omega$ (Ω being a subset of $\mathbb{R}^3$). Considering this quantity makes sense when the volume $\frac{4}{3}\pi r^3$ of a typical droplet is much smaller than a small (but macroscopic) elementary volume of fluid. We say that the spray is thick [it was first introduced in [Duk80] and then used in the KIVA code [ORo81]; [AOB89]; [AO89]; [OZS09]] when $1-\alpha(t,x)$ is not negligible in at least part of $\mathbb{R}_+ \times \Omega$ (typically $1-\alpha(t,x) >> 10^{-3}$) but not too big either (typically, $1-\alpha(t,x) \leq 0.2$ at worst). We refer to [Duk80]; [ORo81] for the concept of thick spays.

Thick sprays are modeled by a coupling of a kinetic equation and a fluid equation. This coupling is done through the volume fraction α and the drag between the two phases. We write below the set of equations described in [Duk80], with a few differences that we explain in the sequel.

We denote by $\rho_g := \rho_g(t,x) \in \mathbb{R}_+$, $p := p(t,x) \in \mathbb{R}_+$, $u_g := u_g(t,x) \in \mathbb{R}^3$, $e_g := e_g(t,x) \in \mathbb{R}_+$, $E_g := E_g(t,x) = e_g(t,x) + \frac{1}{2}|u_g(t,x)|^2 \in \mathbb{R}_+$ and $T_g := T_g(t,x) \in \mathbb{R}_+$ the respective density (of mass), pressure, velocity, internal energy (per unit of mass), total (internal + kinetic) energy (per unit of mass), and temperature of the gas. Those quantities satisfy the following balance laws:

$$\partial_t(\alpha\rho_g) + \nabla_x \cdot (\alpha\rho_g u_g) = 0\,, \tag{7.64}$$

$$\partial_t(\alpha\rho_g u_g) + \nabla_x \cdot (\alpha\rho_g u_g \otimes u_g) + \nabla_x p = -A, \tag{7.65}$$

$$\partial_t(\alpha\rho_g E_g) + \nabla_x \cdot \left(\alpha\rho_g \left(E_g + \frac{p}{\rho_g}\right) u_g\right) + p\partial_t\alpha = -B_1 - B_2, \tag{7.66}$$

where A is the momentum transferred to the (elementary volume at time t and point x of) gas by the dispersed phase and B_1, B_2 constitute the corresponding (resp. mechanical and thermal) transfer.

The density in the phase space $f := f(t,x,u_p,e_p) \geq 0$ of droplets which at time t and point x have velocity $u_p \in \mathbb{R}^3$ and internal energy $e_p \in \mathbb{R}_+$ satisfies the following Vlasov-Boltzmann equation:

$$\partial_t f + u_p \cdot \nabla_x f + \nabla_{u_p} \cdot (f\Gamma) + \partial_{e_p}(f\phi) = Q(f,f), \tag{7.67}$$

where Γ and ϕ represent the transfer of momentum and energy of the gaseous phase on a given droplet (which at time t and point x has velocity $u_p \in \mathbb{R}^3$ and internal energy $e_p \in \mathbb{R}_+$). Accordingly,

$$m_p\Gamma = -\frac{m_p}{\rho_p}\nabla_x p - D\,(u_p - u_g); \qquad m_p\phi = \Phi\,(T_g - T_p), \tag{7.68}$$

$$A = \iint_{u_p,e_p} m_p\Gamma\, f\, du_p de_p, \tag{7.69}$$

$$B_1 = \iint_{u_p,e_p} m_p \left(\Gamma + \frac{\nabla_x p}{\rho_p}\right) \cdot u_p \, f \, du_p de_p, \tag{7.70}$$

$$B_2 = \iint_{u_p,e_p} m_p \phi \, f \, du_p de_p, \tag{7.71}$$

where m_p is the mass of one droplet, ρ_p is the density of the liquid constituting the droplets ($m_p = \frac{4}{3}\pi r^3 \rho_p$, and m_p, ρ_p, r are absolute constants), and T_p is the temperature of the droplet. In (7.68), the term $D(u_p - u_g)$ models the drag. The drag coefficient D is in general a function of ρ_g, $|u_g - u_p|$ (and also r, ρ_p and the molecular viscosity of the gas [this last quantity being neglected in the equation of momentum of the gas]).

Also in (7.68), the term $\Phi(T_g - T_p)$ models the thermal exchanges between the droplets and the gas. The coefficient Φ in general depends upon the thermal viscosity of the particle and the Nusselt number (and therefore upon r, $|u_g - u_p|$, etc.).

The system is closed thanks to the constitutive equations of the gas and the liquid:

$$p(t,x) = P_1(\rho_g(t,x), e_g(t,x)), \qquad T_g(t,x) = T_1(\rho_g(t,x), e_g(t,x)), \tag{7.72}$$

$$T_p = T_2(e_p), \tag{7.73}$$

and the identity for the volume fraction of droplets:

$$1 - \alpha(t,x) = \frac{4}{3}\pi r^3 \iint_{u_p,e_p} f(t,x,u_p,e_p)\, du_p de_p. \tag{7.74}$$

The set of equations (7.64) – (7.74) is sometimes called "Gas-particles" or "Eulerian-Lagrangian". The main differences with the model proposed by Dukowicz ([Duk80]) is that we take into account collisions (they were neglected in the original model) and equations for the energy ([BDM03]).

Note that the presence of a non-infinitesimal volume fraction $1 - \alpha$ of droplets is not compatible with the presence of a non-infinite Boltzmann kernel (this is a consequence of the Boltzmann-Grad asymptotic: cf. [CIP94]). The situation in the classical work of Dukowicz [Duk80] is even worse since no collision kernel is considered there. The scaling that we propose in next section partially removes the incompatibility, since the collision kernel tends to infinity.

We provide in this work a link between eq. (7.64) – (7.74) and a different class of systems, sometimes called "Eulerian-Eulerian", which models two-phase flows (including thick sprays). Those systems are thoroughly described in [IH06]. They are obtained at a heuristic level by taking averages of Euler-type equations for both phases, and by imposing reasonable closures.

In the "Eulerian-Eulerian" approach, the phase space f of droplets is replaced by macroscopic quantities, namely: the density (of mass) $\rho := \rho(t,x) \in \mathbb{R}_+$ of liquid, its velocity $v := v(t,x) \in \mathbb{R}^3$, its internal energy (per unit of mass) $e := e(t,x) \in \mathbb{R}_+$, its total (internal + kinetic) energy (per unit of mass) $E := E(t,x) = e(t,x) + \frac{1}{2}|v(t,x)|^2 \in \mathbb{R}_+$ and its temperature $T := T(t,x) \in \mathbb{R}_+$. The equations write

$$\partial_t(\alpha\rho_g) + \nabla_x \cdot (\alpha\rho_g u_g) = 0, \tag{7.75}$$

$$\partial_t(\alpha\rho_g u_g) + \nabla_x \cdot (\alpha\rho_g u_g \otimes u_g) + \alpha\nabla_x p = -\tilde{A}, \tag{7.76}$$

$$\partial_t(\alpha\rho_g E_g) + \nabla_x \cdot \left(\alpha\rho_g \left(E_g + \frac{p}{\rho_g}\right) u_g\right) + p\partial_t\alpha = -\tilde{B}_1 - \tilde{B}_2, \tag{7.77}$$

$$\partial_t((1-\alpha)\rho) + \nabla_x \cdot ((1-\alpha)\rho v) = 0, \tag{7.78}$$

$$\partial_t((1-\alpha)\rho v) + \nabla_x \cdot ((1-\alpha)\rho v \otimes v) + (1-\alpha)\nabla_x p = \tilde{A}, \tag{7.79}$$

$$\partial_t\left((1-\alpha)\rho E\right) + \nabla_x \cdot \left((1-\alpha)\rho\left(E + \frac{p}{\rho}\right)v\right) + p\partial_t(1-\alpha) = \tilde{B_1} + \tilde{B_2}. \tag{7.80}$$

Those balance laws are completed by the constitutive equations of the gas (similar to (7.72))

$$p(t,x) = P_1(\rho_g(t,x), e_g(t,x)); \qquad T_g(t,x) = T_1(\rho_g(t,x), e_g(t,x)), \tag{7.81}$$

together with the constitutive equations of the liquid (incompressible) phase

$$T(t,x) = T_2(e(t,x)), \qquad \rho(t,x) = \rho_p. \tag{7.82}$$

Finally, the transfer terms $\tilde{A}$, $\tilde{B}_1$, $\tilde{B}_2$ of momentum and energy write

$$\tilde{A} = -(1-\alpha)\frac{\rho}{m_p}\tilde{D}\,(v - u_g), \qquad \tilde{B}_1 = -(1-\alpha)\frac{\rho}{m_p}\tilde{D}\,(v-u_g)\cdot v, \tag{7.83}$$

$$\tilde{B}_2 = -(1-\alpha)\frac{\rho}{m_p}\tilde{\Phi}\,(T - T_g). \tag{7.84}$$

The terms $\tilde{A}$, $\tilde{B}_1$, $\tilde{B}_2$ respectively represent the drag force term, its deposit in terms of energy, and the thermal exchanges. The constants $\tilde{D}$, $\tilde{\Phi}$ respectively represent the drag force coefficient and the thermal conduction coefficient. They can be fitted using experimental data and in general depend upon α, $|v - u_g|$, etc . Note that systems like (7.75) – (7.82) appear not only in the theory of sprays, but also in many other kinds of multiphase flows (stratified, churning flows, etc.), the transfer terms (like $\tilde{A}$, etc.) depend in general of the type of flows which are considered and are generally obtained by using statistical averages ([IH06]; [AOB89]; [ORo81]; [OZS09]).

Our goal in this paper is to provide a clear scaling which enables to derive "rigorously at the formal level" macroscopic equations such as (7.75) – (7.84) from "gas-particles" equations such as (7.64) – (7.74). It is clear that eq. (7.78) – (7.80) will be obtained by taking moments (with respect to v, e) of eq. (7.67). This stategy has already been used in many works concerning the modeling of sprays ([Mas96]; [Lau02]; [Duf05]), in the more complicated case when the spray is polydisperse: it uses however heuristic closures in order to derive the "Eulerian-Eulerian" equations.

Our approach, though it is restricted to the simpler case of monodisperse sprays, is quite different since:

i) It is based on a scaling of the sprays equation obtained after a non-dimensionalization of those equations;

ii) It provides *non heuristical* closures (that is, a mathematical link between A, B_1, B_2 and $\tilde{A}$, $\tilde{B}_1$, $\tilde{B}_2$);

iii) It involves the description of a new variant of the Boltzmann kernel where all the parameters are assessed.

In the scaling that we propose, the collision term Q appearing in (7.67) must be dominant. This exactly corresponds in the context of standard kinetic theory to the limit of small Knudsen number, in which $\frac{1}{\varepsilon}$ is put in front of the collision kernel, and which leads from the Boltzmann equation of rarefied gases towards the compressible Euler equations of fluid dynamics (Cf. [KMN79] for a rigorous proof in the context of very smooth solutions on a small time interval, and [Gol05] for a general survey on the question).

Our paper is structured as follows: in section 7.2.1, the gas-particles equations are specified in detail, including the collision kernel Q. Then, a non-dimensional version of those equations is provided in section 7.2.2. The distributions which cancel Q are described in section 7.2.3. Then, equations for the macroscopic quantities (for both phases) are written down and the system is closed (in section 7.2.4). Some conclusions and perspectives are presented at the end of the paper (section 7.2.5).

7.2.1 Presentation of the inelastic collision kernel

General form of the collision kernel

We now recall the main assumptions that we presented in the introduction of this work about the flow we consider.We assume that the flow is constituted of a surrounding gas and of a dispersed liquid phase. This phase is itself assumed to be of relatively small volume fraction (typically between 10^{-3} and 0.2), and to be constituted of very tiny spherical incompressible droplets having all the same radius r (that is, the spray is monodisperse). The flow inside the droplets is not modeled.

As stated in the introduction, a system which models the spray under this assumption can be written down by considering the unknown $f := f(t,x,u_p,e_p) \geq 0$ for the droplets and $\rho_g := \rho_g(t,x) \in \mathbb{R}_+$, $u_g := u_g(t,x) \in \mathbb{R}^3$, $p := p(t,x) \in \mathbb{R}_+$, $E_g := E_g(t,x) \in \mathbb{R}_+$ for the gas. The set of equations is then (7.64) – (7.74), and it remains to precisely define the collision operator Q.

The assumptions that underly the establishment of this operator are the following: First, since the spray is monodisperse, no complex phenomena of coalescence or breakup of droplets are considered. For the same reason, all collisions are supposed to be binary (that is, two droplets are present at the beginning of the collision and produce two droplets at the end of the collision).

Then, since droplets are macroscopic objects, the cross section will be that of hard spheres. For the same reason, kinetic energy conservation during the process of collision is not expected in general. As a consequence, one needs to write down a model in which part of the kinetic energy is lost: models of granular media (Cf. [BCG00]; [Vil02]; [CCC09]) provide a good solution for that.

Moreover, since the internal energy of the droplets is one of the variables in f, one needs a rule to exchange internal energy during the process of collision: models for polyatomic gases (Cf. [BL75]; [Des97a]) provide a simple solution for this physical phenomenon.

Finally, the kinetic energy which is lost has to be converted in internal energy, and to be distributed between the two outgoing droplets. Since those droplets have the same volume, we choose to divide it equally.

Collecting all those ideas, we end up with a collision kernel which writes

$$Q(f,f)(t,x,u_p,e_p) = \iiiint\limits_{\substack{\sigma\in\mathbb{S}^2,u_{p_*}\in\mathbb{R}^3\\ e_{p_*}\in\mathbb{R}^+}} \Big(\frac{1}{1-a}\frac{1}{\beta^2}\ f(t,x,'u_{p_*},'e_{p_*})\, f(t,x,'u_p,'e_p) \\ -\ f(t,x,u_{p_*},e_{p_*})\, f(t,x,u_p,e_p) \Big) \times 1_{\{'e_p,'e_p^*\geq 0\}}\ r^2\ |u_p-u_{p_*}|\, d\sigma du_{p_*} de_{p_*}, \quad (7.85)$$

where the pre-collisional velocities ${}'u_{p_*}$ and ${}'u_p$ are defined as

$$
{}'u_p = \frac{u_p + u_{p_*}}{2} - \frac{1-\beta}{4\beta}\left(u_p - u_{p_*}\right) + \frac{1+\beta}{4\beta}|u_p - u_{p_*}|\sigma,
$$

$$
{}'u_{p_*} = \frac{u_p + u_{p_*}}{2} + \frac{1-\beta}{4\beta}\left(u_p - u_{p_*}\right) - \frac{1+\beta}{4\beta}|u_p - u_{p_*}|\sigma,
$$

where σ belongs to the unit sphere $\S^2$, and $\int_{\sigma\in\S^2} d\sigma = 4\pi$. The pre-collisional internal energies ${}'e_{p_*}$ and ${}'e_p$ are defined as

$$
{}'e_p = \frac{2-a}{2-2a}\,e_p - \frac{a}{2-2a}\,e_{p_*} - \frac{1}{2}\,\Delta E,
$$

$$
{}'e_{p_*} = -\frac{a}{2-2a}\,e_p + \frac{2-a}{2-2a}e_{p_*} - \frac{1}{2}\,\Delta E,
$$

where

$$
\Delta E = \frac{1}{2}({}'u_p{}^2 + {}'u_{p_*}{}^2 - u_{p_*}{}^2 - u_p{}^2) = \left(\frac{1-\beta^2}{8\beta^2}\right)|u_p - u_{p_*}|^2 - \frac{1-\beta^2}{8\beta^2}|u_p - u_{p_*}|\left(u_p - u_{p_*}\right)\cdot\sigma \tag{7.86}
$$

is the loss of kinetic energy (or gain of internal energy) [divided by mass].

In those formulas, $\beta := \beta(|u_p - u_{p_*}|)$ is a measure of the inelasticity of the collision (the collision is elastic when $\beta = 1$), and $a := a(|u_p - u_{p_*}|)$ is the parameter which measures what part of the internal energy is exchanged during a collision (no internal energy is exchanged when $a = 0$).

Note that the prefactor $\dfrac{1}{1-a}\dfrac{1}{\beta^2}$ is related to the Jacobian of the pre-collisional transform $(u_p, e_p, u_{p_*}, e_{p_*}) \mapsto ({}'u_p, {}'e_p, {}'u_{p_*}, {}'e_{p_*})$, and to the cross section of hard spheres ([Vil06]). The model presented here is strongly reminiscent of models appearing in granular gases. The only difference is the treatment of the internal energy of the droplets.

Using the weak form of the kernel of we get the conservations of mass, momentum and total energy ([DM10]):

$$
\iint_{u_p, e_p} Q(f,f)(u_p, e_p)\, m_p\, du_p de_p = 0, \tag{7.87}
$$

$$
\iint_{u_p, e_p} Q(f,f)(u_p, e_p)\, m_p\, u_p\, du_p de_p = 0, \tag{7.88}
$$

$$
\iint_{u_p, e_p} Q(f,f)(u_p, e_p)\, \left[\frac{1}{2} m_p u_p^2 + m_p e_p\right]\, du_p de_p = 0. \tag{7.89}
$$

The equations for thick sprays being now complete, we introduce in next section a scaling based on the dimensional analysis of those equations.

7.2.2 Non dimensional form of the Vlasov-Boltzmann equation

We write down in this short section the dimensional analysis which enables to obtain a formal limit for the Vlasov-Boltzmann equation (7.67). In order to do so, we first introduce the following time/space typical quantities:

- t_g: typical time of the experiment,

- L: typical length of the experiment.

Next, we introduce quantities related to the gas and the droplets (remember that r, m_p, ρ_p are the radius, mass and density of droplets, and that D, Φ are the coefficients for drag force and thermal exchanges)

- N: typical number of droplets of the experiment,
- V: typical mean velocity of the droplets. We shall assume that it is also the typical thermal velocity of the droplets [that is, the square root of the variance of the velocity distribution], and the typical velocity of the gas. One has $V\, t_g = L$.
- I_p: typical internal energy of the droplets per mass unit,
- I_g: typical internal energy of the gas per mass unit,
- T_T: typical temperature of the droplets. We shall assume that it is also the typical temperature of the gas.
- P: Typical pressure of the gas
- $P' = \rho_p\, V^2$: this quantity has the dimension of a pressure

It is customary to introduce at this level the mean free path $\sigma = \frac{L^3}{r^2 N}$. Finally, we denote by ε the Knudsen number $\varepsilon = \dfrac{\sigma}{L}$. This quantity is at the basis of the passage from Boltzmann equation towards Euler equation. (see [Cer88] and [CC70]). We now introduce non-dimensional quantities (denoted with a tilde) for the unknowns and parameters entering eq. (7.67). That is, we consider

$$\tilde{t} = \frac{t}{t_g}, \quad \tilde{x} = \frac{x}{L}, \quad \tilde{u}_p = \frac{u_p}{V}, \quad \tilde{e}_p = \frac{e_p}{I_p}, \quad \tilde{T}_p = \frac{T_p}{T_T},$$

$$\tilde{f}(\tilde{t}, \tilde{x}, \tilde{u}_p, \tilde{e}_p) = \frac{I_p L^3 V^3}{N} f(t_g\, \tilde{t}\,,\, L\, \tilde{x}\,,\, V\, \tilde{u}_p\,,\, I_p\, \tilde{e}_p),$$

for the particles and

$$\tilde{u}_g(\tilde{t}, \tilde{x}) = \frac{u_g(t_g\, \tilde{t}\,,\, L\, \tilde{x})}{V}, \quad \tilde{T}_g(\tilde{t}, \tilde{x}) = \frac{T_g(t_g\, \tilde{t}\,,\, L\, \tilde{x})}{T_T}, \quad \tilde{e}_g(\tilde{t}, \tilde{x}) = \frac{e_g(t_g\, \tilde{t}\,,\, L\, \tilde{x})}{I_g}, \quad \tilde{P}(\tilde{t}, \tilde{x}) \frac{p(t_g\, \tilde{t}\,,\, L\, \tilde{x})}{P}$$

for the gas.

The equation satisfied by $\tilde{f}$ then becomes

$$\partial_{\tilde{t}} \tilde{f} + \tilde{u}_p \cdot \nabla_{\tilde{x}} \tilde{f} + \nabla_{\tilde{u}_p} \cdot (\tilde{f} \tilde{\Gamma}) + \partial_{\tilde{e}_p} (\tilde{f} \tilde{\phi}) = \frac{1}{\varepsilon} Q(\tilde{f}, \tilde{f}), \tag{7.90}$$

where

$$\tilde{\Gamma} = \frac{P}{P'} \nabla_{\tilde{x}} \tilde{p} + C_2 \ \left(\tilde{u}_p - \tilde{u}_g\right), \tilde{\phi} = C_3 (\tilde{T}_g - \tilde{T}_p), C_2 = \frac{D}{m_p} t_g, C_3 = \frac{\Phi T_T t_g}{m_p I_p}.$$

We shall now study the limit of eq. (7.90) when $\varepsilon \to 0$. We see that this limit makes sense when the typical parameters of the experiment under study are such that

$$1 \gg \varepsilon, \tag{7.91a}$$
$$\frac{P'}{P} \gg \varepsilon, \tag{7.91b}$$
$$\frac{m_p}{D\, t_g} \gg \varepsilon, \tag{7.91c}$$
$$\frac{m_p I_p}{\Phi T_T t_g} \gg \varepsilon. \tag{7.91d}$$

A typical situation appearing in industry where those assumptions are fulfilled is described in [Mat06]. Other scaling can be done on sprays ([GJV02]).

7.2.3 Limit of the pdf in the scaling

In order to pass to the limit (at the formal level) in eq. (7.90) when $\varepsilon \to 0$, we study the solutions of the functional equation $Q(f,f) = 0$, when collisions are truly inelastic, that is when $\beta := \beta(|u_p - u_{p_*}|) \in [0,1[$. The computation of the exchange of kinetic energy leads to

$$\iint_{u_p,e_p} Q(f,f)\ \frac{1}{2}\, m_p u_p^2\, du_p de_p \ = -\iiiint_{u_p,e_p,u_{p*},e_{p*}} \frac{1-\beta^2}{8} f f_* 4\pi r^2\, m_p |u_p - u_{p_*}|^3\, du_{p_*} de_{p_*} du_p de_p\ , \tag{7.92}$$

so that the effect of inelastic collisions is to concentrate the velocities of the droplets. Note first that when considering only the evolution of velocities, in absence of internal energy exchange, the convergence towards a Dirac mass is rigorously proven in [BCG00], [Vil02] or [FM05] for solutions of the spatially homogeneous Boltzmann equation $\partial_t f = Q(f,f)$ (for β constant).

We now wish to show, at the formal level, that when considering the evolution of both velocities and internal energies in $\partial_t f = Q(f,f)$,

$$\lim_{t\to+\infty} f(t,u_p,e_p) = G\delta_{u_p=v}(u_p) \otimes \delta_{e_p=e}(e_p), \tag{7.93}$$

with $v \in \mathbb{R}^3, G \geq 0, e > 0$.

Note that this cannot be done directly by the study of the solutions of $Q(f,f) = 0$ since all densities of the form

$$f(u_p,e_p) = \delta_{u_p=v}(u_p) \otimes \mu(e_p)$$

are such solutions (equilibria).

The case of constant coefficients of inelasticity and energy exchange

We assume in the following computation that a and β are constant, for the sake of simplicity. An extension of this computation in a case in which a and β are not constant was done (in [Mat06]).

In order to do so, we first recall Haff's law ([Haf83]): For $f := f(t,u_p)$ satisfying the spatially homogeneous equation $\partial_t f = Q(f,f)$ (with $\beta \in [0,1[$ and no exchange of energy involved), the following estimate holds:

$$\frac{m}{1+t^2} \leq T(t) \leq \frac{M}{1+t^2}, \tag{7.94}$$

where $T(t) := \dfrac{\int_{u_p} f(t,u_p)\frac{1}{3}m_p(u_p-v)^2du_p}{\int_{u_p} f(t,u_p)m_p du_p}$, and where m and M are constants depending on initial data. A rigorous proof of this result can be found in [MM06] and [MMR06] (when β is a constant).

A first hint of the proof can be found in [BCG00] when one assumes that $|v-v_*|$ is replaced by a term proportional to $\sqrt{T}$. Our goal here is to estimate the evolution of the mean internal energy along the solutions of the equation

$$\partial_t f(t,u_p,e_p) = Q(f,f)(t,u_p,e_p). \tag{7.95}$$

The computations that we provide are only approximations. They give an idea of what should be the evolution of the quantity

$$g(t) := \frac{\iint_{u_p,e_p} f(t,u_p,e_p)m_p\left(e_p-e(t)\right)^2 du_p de_p}{\iint_{u_p,e_p} f(t,u_p,e_p)m_p\, du_p de_p},$$

that is the variance of f w.r.t. e_p. They will be sustained in next subsection by numerical simulations. Note first that thanks to the conservation of mass,

$$\begin{aligned} g'(t) &= \frac{\iint Q(f,f)(t,u_p,e_p)m_p(e_p-e(t))^2du_pde_p}{\iint f(t,u_p,e_p)m_p\,du_pde_p} \\ &= \left(-a(1-\frac{a}{2})\iiiint \frac{1}{2}ff^*4\pi r^2(e_p-e_{p_*})^2|u_p-u_{p_*}|du_pdu_{p_*}de_pde_{p_*}\right. \\ &+ \left.\frac{1}{2}\iiiint 4\pi r^2ff^*\left[\frac{1}{2}\Delta E^2+\Delta E\left(e_p+e_{p_*}-2e\right)\right]|u_p-u_{p_*}|du_pdu_{p_*}de_pde_{p_*}\right) \\ &\Big/ \iint f du_p de_p\,. \end{aligned} \tag{7.96}$$

We use the following approximation based on Haff's law: in all computations we replace $|u_p - u_{p_*}|$ by $\sqrt{6T}$ (the 6 comes from the fact that we are in 3D): it is more or less the same approach as in [BCG00].

After some computations and using (according to Haff's law) the approximation $T(t) = \dfrac{c_1^2}{(1+c_2 t)^2}$ where c_1 and $c_2 > 0$, we obtain (except in the exceptional case when $\dfrac{3}{r}(1-\alpha)\dfrac{c_1}{c_2}\sqrt{6}a(1-a/2) = 4$):

$$g(t) \sim \frac{g(0)}{(1+c_2 t)^{\frac{3}{r}(1-\alpha)\frac{c_1}{c_2}\sqrt{6}a(1-a/2)}} + \frac{1}{4}\left(\frac{1-\beta^2}{4}\right)^2 \frac{\left(\sqrt{6}c_1\right)^5 / c_2}{\frac{3}{r}(1-\alpha)\frac{c_1}{c_2}\sqrt{6}a(1-a/2) - 4}\left[(1+c_2 t)^{-4} - (1+c_2 t)^{-\frac{3}{r}(1-\alpha)\frac{c_1}{c_2}\sqrt{6}a(1-a/2)}\right]. \quad (7.97)$$

We now discuss the behavior of g according to the sign of $\dfrac{3}{r}(1-\alpha)\dfrac{c_1}{c_2}\sqrt{6}\,a(1-a/2) - 4$.

- When $4 < \dfrac{3}{r}(1-\alpha)\dfrac{c_1}{c_2}\sqrt{6}a(1-a/2)$: we get

$$g(t) \sim \frac{Cst}{(1+c_2 t)^4}. \quad (7.98)$$

  This is the situation when thermal exchanges are predominant: $\sqrt{g(t)}$ then converges to zero as rapidly as the temperature $T(t)$ (note that $\sqrt{g}$ has the same dimension as an energy).

- When $4 > \dfrac{3}{r}(1-\alpha)\dfrac{c_1}{c_2}\sqrt{6}a(1-a/2)$, we get

$$g(t) \sim \frac{Cst}{(1+c_2 t)^{\frac{3}{r}(1-\alpha)\frac{c_1}{c_2}\sqrt{6}a(1-a/2)}},$$

  so that $\sqrt{g(t)}$ still converges towards 0, but this convergence is slower than that of the temperature $T(t)$. It can even be very slow when a is close to 0 (that is, when the exchanges of internal energy are of small amplitude).

Note finally that the exceptional case $\dfrac{3}{r}(1-\alpha)\dfrac{c_1}{c_2}\sqrt{6}\,a(1-a/2) = 4$ leads to a formula close to (7.98) [but with a logarithmic correction].

The previous computations show (although not rigorously) that the only stable equilibrium in the case of inelastic collisions for $\partial_t f = Q(f,f)$ ($\beta \in [0,1[$) are functions defined by (7.93).

We now detail a numerical simulation which confirms the approximate computations presented above. We present some numerical tests for the spatially homogeneous Boltzmann equation $\partial_t f = Q(f,f)$, when Q is the inelastic collision kernel defined by (7.85), with a and β fixed constants. The computations are performed thanks to a particle method (Cf. [Bar04]; [PR04]), where the density $f := f(t, u_p, e_p)$ is approximated by a sum of Dirac masses with the same numerical weight (that is, $f(t,u_p,e_p) \sim w \sum_{i=1}^N \delta_{u_p=u_{pi};e_p=e_{pi}}$). This set of numerical particles then evolves according to Bird's method (Cf. [Bir94]). The tests which are presented correspond to the following parameters:

$$r = 10^{-4}, \qquad f(0,u_p,e_p) = Cst\, 1_{u_p \in [-10^4,10^4]^3; e_p \in [5.10^5, 5.10^6]}.$$

About 10^4 numerical particles are used.

First test: *Convergence towards the Dirac mass w.r.t. velocity; Haff's law*

We check that Haff's law holds for $a = 1$ and $\beta = 0.99, 0.95, 0.8$: we plot the results in logarithm scale: we expect to get a (asymptotically) straight line whose slope is -2 (since Haff's law means that $T(t) \sim t^{-2}$).

It is indeed what we observe in the figure below. Note also that, as expected, the convergence is slower when β increases.

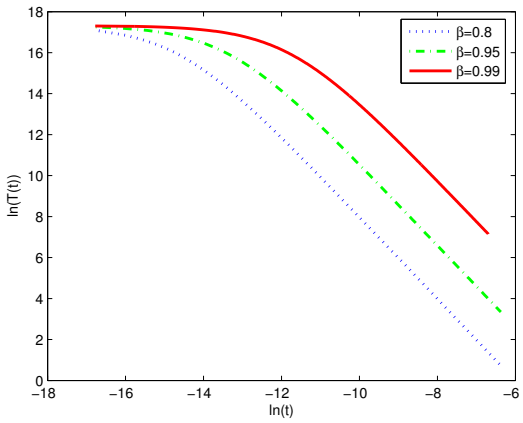

FIGURE 7.1: Behavior of kinetic temperature: $\ln T$ as a function of $\ln t$ for different β

Second test: *Convergence towards the Dirac mass w.r.t. the internal energy*

We now check the convergence towards the Dirac mass w.r.t internal energy. We fix $\beta = 0.99$ and let a vary between 0.01 and 1.0. We plot

$$W = \ln\left(\iint f(t,u_p,e_p)|e_p - e(t)|de_p du_p / \iint f(t,u_p,e_p)de_p du_p\right)$$

as a function of $ln(t)$. As can be seen in figure 7.2, the more a increases, the more the coefficients

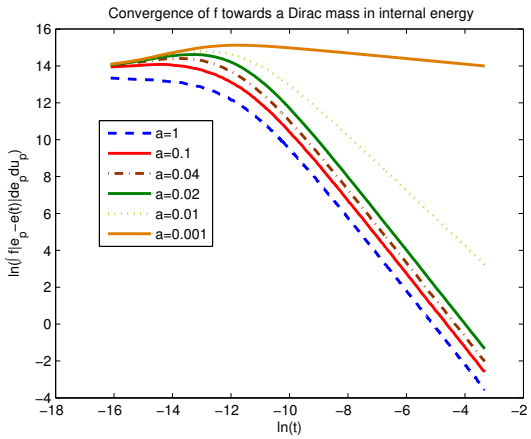

FIGURE 7.2: Convergence in internal energy: $\ln\left(\iint f(t,u_p,e_p)|e_p - e(t)|de_p du_p / \iint f(t,u_p,e_p)de_p du_p\right)$ as a function of $\ln t$ for various values of parameters

of the asymptotic straight line tend to -2. More precisely (in accordance with the theoretical

computation), we see that there exists a critical a (around 0.06) which separates a zone in which the behavior of W seems to be in t^{-2}, and a zone in which it is rather in $t^{-\theta}$, with $\theta \in]0,2[$ depending on a. Finally, we observe that for small a, the function W increases during a certain amount of time: thermal exchanges are then not significant enough to completely counterbalance the positive term in equation (7.96) (that is, the transfer of kinetic energy to internal energy) at all times.

7.2.4 Fluid of particles:

According to the dimensional analysis of section 7.2.2, we end up with the following set of scaled equations for the spray:

$$\partial_t(\alpha^\varepsilon \rho_g^\varepsilon) + \nabla_x \cdot (\alpha^\varepsilon \rho_g^\varepsilon u_g^\varepsilon) = 0\,, \tag{7.99}$$

$$\partial_t(\alpha^\varepsilon \rho_g^\varepsilon u_g^\varepsilon) + \nabla_x \cdot (\alpha^\varepsilon \rho_g^\varepsilon u_g^\varepsilon \otimes u_g^\varepsilon) + \nabla_x p^\varepsilon = -A^\varepsilon, \tag{7.100}$$

$$\partial_t(\alpha \rho_g^\varepsilon E_g^\varepsilon) + \nabla_x \cdot \left(\alpha^\varepsilon \rho_g^\varepsilon \left(E_g^\varepsilon + \frac{p^\varepsilon}{\rho_g^\varepsilon} \right) u_g^\varepsilon \right) + p^\varepsilon \partial_t \alpha^\varepsilon = -B_1^\varepsilon - B_2^\varepsilon, \tag{7.101}$$

$$\partial_t f^\varepsilon + u_p^\varepsilon \cdot \nabla_x f^\varepsilon + \nabla_{u_p} \cdot (f^\varepsilon \Gamma^\varepsilon) + \partial_{e_p}(f^\varepsilon \phi^\varepsilon) = \frac{1}{\varepsilon} Q(f^\varepsilon, f^\varepsilon), \tag{7.102}$$

where

$$m_p \Gamma^\varepsilon = -\frac{m_p}{\rho_p} \nabla_x p^\varepsilon - D(u_p - u_g^\varepsilon); \qquad m_p \phi^\varepsilon = \Phi\,(T_g^\varepsilon - T_p), \tag{7.103}$$

$$A^\varepsilon = \iint_{u_p, e_p} m_p \Gamma^\varepsilon f^\varepsilon \, du_p de_p, \tag{7.104}$$

$$B_1^\varepsilon = \iint_{u_p, e_p} m_p \, (\Gamma^\varepsilon + \frac{\nabla_x p^\varepsilon}{\rho_p}) \cdot u_p \, f^\varepsilon \, du_p de_p, \tag{7.105}$$

$$B_2^\varepsilon = \iint_{u_p, e_p} m_p \phi^\varepsilon \, f^\varepsilon \, du_p de_p. \tag{7.106}$$

In this section, we present the computations which enable to pass to the limit at the formal level in eq. (7.99) – (7.106), when $\varepsilon \to 0$. These formal computations are based on the same principle as the traditional passage from the Boltzmann eq. towards fluid mechanics: we first take moments of eq. (7.102), and then close the corresponding equations thanks to the study (in section 7.2.3) of the solutions of $Q(f,f) = 0$ (more precisely, of the large time behavior of the solutions of the spatially homogeneous equation $\partial_t f = Q(f,f)$). We define the following quantities associated with the moments of order zero (mass), one (momentum), two (energy, pressure (Reynolds') tensor) and three (flux of energy) of the fluid of particles:

$$(1-\alpha)\rho = \iint_{u_p, e_p} f m_p \, du_p de_p, \quad (1-\alpha)\rho v = \iint_{u_p, e_p} f m_p u_p \, du_p de_p,$$

$$(1-\alpha)\rho\, e_c = \iint_{u_p, e_p} \frac{1}{2} f m_p |u_p|^2 \, du_p de_p, \quad (1-\alpha)\rho\, e = \iint_{u_p, e_p} f m_p e_p \, du_p de_p,$$

$$(1-\alpha)\rho\, E = \iint_{u_p, e_p} f \left\{ \frac{1}{2} m_p |u_p|^2 + m_p e_p \right\} du_p de_p,$$

$$(1-\alpha)P' = \iint_{u_p,e_p} f m_p (v-u_p)\otimes(v-u_p)\, du_p de_p,$$

$$(1-\alpha)q = \iint_{u_p,e_p} f m_p (v-u_p)^2 (u_p-v)\, du_p de_p.$$

Note that the pressure tensor P' will appear in our set of equations because the fluid of droplets does not "see" the same pressure as the gas. This extra term of pressure, sometimes called interfacial pressure, appears (usually in a non tensorial form) in many works concerned with the modeling of two-phase flows (see [Sai95] and [GHS04] for example). This pressure tensor vanishes when all the droplets have the same velocity (in the limit $\varepsilon \to 0$).

We now integrate the Boltzmann equation against $m_p du_p de_p$ (mass conservation), $m_p u_p du_p de_p$ (momentum conservation), and $m_p[\frac{1}{2}|u_p|^2 + e_p]\, du_p de_p$. We use properties (7.87), (7.88) and (7.89) of the collision kernel. This leads to

$$\partial_t(1-\alpha) + \nabla_x\cdot((1-\alpha)v) = 0.$$

since ρ is constant for the particles,

$$\partial_t((1-\alpha)\rho v) + \nabla_x\cdot((1-\alpha)\rho v\otimes v) + (1-\alpha)\nabla_x p + \nabla_x\cdot\left((1-\alpha)P'\right) = -\iint_{u_p,e_p} D\,(u_p-u_g) f\, du_p de_p,$$

and

$$\partial_t\left((1-\alpha)\rho E\right) + \nabla_x\cdot\left((1-\alpha)\rho\left(E+\frac{p}{\rho}\right)v\right) + p\partial_t(1-\alpha) + \nabla_x\cdot((1-\alpha)(P'v+q)) = -\iint_{u_p,e_p} D\,(u_p-u_g)\cdot u_p f\, du_p de_p + \iint_{u_p,e_p}\Phi\,(T_g-T_p) f\, du_p de_p. \quad (7.107)$$

We now close the equations by formally letting ε go to 0 in (7.99) – (7.106) According to the results of subsection 7.2.3, we know (at the formal level) that $f^\varepsilon \to f$, with

$$f(t,x,u_p,e_p) = G(t,x)\,\delta_{u_p=v(t,x)}(u_p)\,\delta_{e_p=e(t,x)}(e_p). \quad (7.108)$$

We end up with a system of 6 equations which write (remember that $e_g = E_g - \frac{1}{2}u_g^2$ and $e = E - \frac{1}{2}v^2$).

$$\partial_t(\alpha\rho_g) + \nabla_x \cdot (\alpha\rho_g u_g) = 0, \tag{7.109}$$

$$\partial_t((1-\alpha)\rho) + \nabla_x \cdot ((1-\alpha)\rho v) = 0, \tag{7.110}$$

$$\partial_t(\alpha\rho_g u_g) + \nabla_x \cdot (\alpha\rho_g u_g \otimes u_g) + \alpha\nabla_x p = -\tilde{A}, \tag{7.111}$$

$$\partial_t((1-\alpha)\rho v) + \nabla_x \cdot ((1-\alpha)\rho v \otimes v) + (1-\alpha)\nabla_x p = \tag{7.112}$$

$$\tilde{A}, \tag{7.113}$$

$$\partial_t(\alpha\rho_g E_g) + \nabla_x \cdot \left(\alpha\rho_g \left(E_g + \frac{p}{\rho_g}\right) u_g\right) + p\partial_t\alpha = -\tilde{B_1} - \tilde{B_2}, \tag{7.114}$$

$$\partial_t\left((1-\alpha)\rho E\right) + \nabla_x \cdot \left((1-\alpha)\rho \left(E + \frac{p}{\rho}\right) v\right) + p\partial_t(1-\alpha) = \tilde{B_1} + \tilde{B_2}, \tag{7.115}$$

where $\tilde{A}$, $\tilde{B_1}$ and $\tilde{B_2}$ are defined in the introduction, the functions $\tilde{D}$ and $\tilde{\Phi}$ being the same as D, Φ, but taken at points v, e instead of u_p, e_p. We recall the equations of state which complete this system:

$$p = P_1(\rho_g, e_g), \quad T_g = T_1(\rho_g, e_g), \tag{7.116}$$

$$\rho = \rho_p, \quad T = T_2(e). \tag{7.117}$$

7.2.5 Conclusion and perspectives

We now wish to briefly comment some of the issues related to this paper.

Firstly, we wish to explain what can be the extensions of the asymptotics presented in this work: the presence of (molecular or turbulent) diffusion in the gas equations does not change the computations. It is also possible in principle to take into account chemistry terms (e.g. combustion terms) in the equations: this leads however to serious complications. Finally, it is known that polydispersion plays a decisive role in the construction of macroscopic models starting from spray equations (Cf. [DMV03]). In general, it is not possible to guess the evolution of droplets w.r.t. radius, and one has to cut into "sections" the various possible radiuses r. It however sometimes happens that processes of coagulation/breakup lead to such specific profiles (Cf. for example [AB79]). In such (unfortunately unrealistic, at least when sprays are concerned) situations, two-phase macroscopic equations can be obtained (at the formal level) by an asymptotics.

Secondly, we would like to emphasize the extreme difficulty of making rigorous the passage to the limit that we propose (even in a "small time" setting). This is related to the very bad mathematical behavior of the limiting eq. (7.75) – (7.82). Those equations are not written in conservative form and have a domain of non hyperbolicity (Cf. [Ram00]). Moreover, the set of eq. (7.64) – (7.74) has not yet been studied from the mathematical point of view. It might indeed present a behavior as bad as the limiting system [though this guess is not yet sustained by convincing arguments]. One possibility could be to try to pass to the limit in an analogous system, where the molecular viscosity of the gas is not neglected (then the limiting equations are better behaved, Cf. [Ram00]).

7.3 Another model for inelastic collisions in sprays

Later on, after the hydrodynamic limit was obtained, we tried to simplify our model of inelastic collisions for having a gain in terms of numerical costs during the thesis of A. Champmartin (CMLA, ENS Cachan)

We consider droplets are characterized by their radius $r > 0$, their position $x \in \Omega$ (domain of computation), their velocity $v \in \mathbb{R}^3$, and their internal energy (by unit of mass) $e > 0$. [some other parameters are sometimes taken into account, like the distortion of the droplets, Cf. [AOB89]; [ORo81], etc.]. We restrict ourselves in this paper to so-called monodisperse sprays, where all droplets have the same radius $r > 0$.

During a collision, two droplets are in contact and therefore exchange some internal energy. Moreover, the droplets being macroscopic objects, part of the kinetic energy (in the center of mass reference frame) is transformed in internal energy (that is, the collisions are inelastic).

A standard model for inelastic collisions (Cf. [BCG00]; [BGP04]; [Vil06] for example in the context of granular gases) consists in writing

$$v' = \tfrac{v+v^*}{2} + \tfrac{1-\gamma}{4}(v - v^*) + \tfrac{1+\gamma}{4}|v - v^*|\sigma, \tag{7.118}$$

$$v'^* = \tfrac{v+v^*}{2} - \tfrac{1-\gamma}{4}(v - v^*) - \tfrac{1+\gamma}{4}|v - v^*|\sigma, \tag{7.119}$$

where $v, v^* \in \mathbb{R}^3$ are precollisional velocities, $v', v'^* \in \mathbb{R}^3$ are postcollisional velocities, $\gamma \in [0, 1]$ is the inelasticity parameter, and σ is parametrizing the sphere S^2.

The kinetic energy lost (by unit of mass) in (7.118), (7.119) is given by

$$\Delta E_c' = (1 - \gamma^2)\frac{|v - v^*|^2}{8} - \frac{1 - \gamma^2}{8}|v - v^*| < \sigma, v - v^* > . \tag{7.120}$$

The exchange of internal energy is then simply modelled by the equations

$$e' = \tfrac{2-a}{2}e + \tfrac{a}{2}e^* + \tfrac{1}{2}\,\Delta E_c', \tag{7.121}$$

$$e'^* = \tfrac{a}{2}e + \tfrac{2-a}{2}e^* + \tfrac{1}{2}\,\Delta E_c', \tag{7.122}$$

where $e, e^* > 0$ are precollisional internal energies, $e', e'^* > 0$ are postcollisional internal energies, and $a \in [0, 1]$ is the parameter which characterizes the typical time scale of the exchange.

Note that the kinetic energy lost in (7.118), (7.119) is equally distributed between the energies e' and e'^*.

In all generality, both γ and a are functions of $|v - v^*|$ which sometimes can be assessed (Cf. [Mat06]; [DM10]).

The corresponding Boltzmann operator Q can be written in weak form according to the following formula (for all function ψ for which the integrals make sense)

$$\int_v \int_e Q(f, f)(v, e)\, \psi(v, e) dv de \tag{7.123}$$

$$= \int_v \int_e \int_{v^*} \int_{e^*} \int_\sigma f(v, e) f(v^*, e^*)\, [\psi(v', e') - \psi(v, e)] r^2 \tilde{S}(|v - v^*|) dv de dv^* de^* d\sigma, \tag{7.124}$$

where

$$\tilde{S}(w) = w \tag{7.125}$$

corresponds to the cross section of hard spheres, and $r > 0$ is the radius of the droplets.

Note that by taking $\psi(v,e) = 1; v_i; \frac{|v|^2}{2} + e$, we obtain the conservation of mass, (ith component of the) momentum, and total (kinetic + internal) energy:

$$\int_v \int_e Q(f,f) \begin{pmatrix} 1 \\ (v_i)_{i=1,2,3} \\ \frac{|v|^2}{2} + e \end{pmatrix} dvde = 0. \tag{7.126}$$

We also briefly indicate here the strong formulation of Q [in the case of hard spheres], which makes explicit the Jacobian of the transformation $\mathcal{T} : (v, v^*, e, e^*) \mapsto (v', v'^*, e', e'^*)$, but which is not used in the sequel (cf. [Vil06] for more on the Jacobian):

$$\begin{aligned} &Q(f,f)(v,e) = \\ &\iiint_{v,e,\sigma} \left(J_{\mathcal{T}} \, \tfrac{|'v - 'v^*|}{|v - v^*|} \, f('v^*,'e^*) f('v,'e) - f(v^*,e^*) f(v,e) \right) r^2 |v - v^*| d\sigma dv de \\ &= \iiint_{v,e,\sigma} \left(\tfrac{1}{\gamma^2} \tfrac{1}{1-a} \, f('v^*,'e^*) f('v,'e) - f(v^*,e^*) f(v,e) \right) r^2 |v - v^*| d\sigma dv de. \end{aligned} \tag{7.127}$$

The Jacobian $J_{\mathcal{T}}$ is composed of a part $(\frac{1}{\gamma^2} \frac{|v-v^*|}{|'v-'v^*|})$ which is typical of the inelastic collision kernels ([GPV04]; [Vil02]), and of another part $(\frac{1}{1-a})$ which comes from the exchanges of internal energies. In (7.127) is used the following shorthand (related to precollisional velocities, Cf. [Mat06]; [DM10])

$$'v = \tfrac{v+v^*}{2} - \tfrac{1-\gamma}{4\gamma}(v - v^*) + \tfrac{1+\gamma}{4\gamma}|v - v^*|\sigma, \tag{7.128}$$

$$'v^* = \tfrac{v+v^*}{2} + \tfrac{1-\gamma}{4\gamma}(v - v^*) - \tfrac{1+\gamma}{4\gamma}|v - v^*|\sigma, \tag{7.129}$$

$$'e = \tfrac{2-a}{2-2a} e - \tfrac{a}{2-2a} e^* + \tfrac{1}{2}\Delta' E_c, \tag{7.130}$$

$$'e^* = -\tfrac{a}{2-2a} e + \tfrac{2-a}{2-2a} e^* + \tfrac{1}{2}\Delta' E_c, \tag{7.131}$$

$$\Delta' E_c = \frac{1-\gamma^2}{8\gamma^2}|v - v^*|^2 - \frac{1-\gamma^2}{8\gamma^2}|v - v^*| < \sigma, v - v^* > . \tag{7.132}$$

In many instances, the Knudsen number related to the droplets in a spray is small (Cf. [Mat06]; [DM10]), so that the number of collisions to perform in a computation is quite high, and the treatment of Q sometimes requires a large part of the time spent in the computation (up to an increase of more than 100%).

As a consequence, one needs simplified models of collision, which leads to less expensive computations, but keep some of the main features of the original model (7.127) – (7.132).

This problem has already been studied by many authors in the case of the elastic Boltzmann operator for rarefied gases, and has led to various models, among which the BGK model (Cf. [BGK54]) and the ESS model (Cf. [Low66]). These models have been adapted to the case of inelastic Boltzmann kernels for granular media (Cf. [J M00], [San03]), and to the case of Boltzmann kernels taking into account chemical reactions (Cf. [CGS07], [GK02], [MG99]).

The simplified model that we propose writes

$$\partial_t f + \nabla_v \cdot \big(c_1 f(v - v_{avr})\big) + \partial_e(c_2 f) + \partial_e(c_3(e - e_{avr})f) + \partial_e(c_4|v - v_{avr}|^4 \partial_e f) = -\nu(f - f_0), \quad (7.133)$$

where v_{avr} is the mean velocity

$$v_{avr} = \frac{\int_v \int_e f(t,v,e) v dv de}{\int_v \int_e f(t,v,e) dv de}, \quad (7.134)$$

e_{avr} is the mean internal energy

$$e_{avr} = \frac{\int_v \int_e f(t,v,e) e de dv}{\int_v \int_e f(t,v,e) de dv}, \quad (7.135)$$

f_0 is the Maxwellian function of v with the same parameters as f

$$f_0(t,v,e) = \Big(\frac{1}{2\pi T(t)}\Big)^{3/2} e^{-\frac{|v-v_{avr}|^2}{2T(t)}} \int_w f(t,w,e) dw, \quad (7.136)$$

and T is the statistical temperature:

$$T(t) = \frac{1}{3} \frac{\int_v \int_e f(t,v,e)|v - v_{avr}|^2 dv de}{\int_v \int_e f(t,v,e) dv de}. \quad (7.137)$$

It combines:

- a drift towards the mean velocity $\nabla_v \cdot \big(f(v - v_{avr})\big)$, which enables to model the inelasticity (loss of kinetic energy) coupled with a term which ensures the conservation of total energy $\partial_e(f)$,
- a relaxation towards a Maxwellian distribution $-\nu(f - f_0)$,
- a drift towards the mean internal energy $\partial_e((e - e_{avr})f)$, which models the exchange of internal energies during collisions,
- a diffusive term $\partial_e(|v - v_{avr}|^4 \partial_e f)$ coming from the fact that some diffusion w.r.t. internal energy appears when part of the kinetic energy is transformed into internal energy. Note that the term $|v - v_{avr}|^4$ naturally appears by homogeneity if we want c_4 to be the inverse of a time.

The parameters c_1, c_2, c_3, c_4, ν are defined by

$$c_1 = \frac{3S_1(t)}{8r}\big[-1 + \frac{\gamma}{2} + \gamma^2\big](1 - \alpha), \quad (7.138)$$

$$c_2 = -\frac{9S_1(t)}{8r}\big[-1 + \frac{\gamma}{2} + \gamma^2\big](1 - \alpha)T(t), \quad (7.139)$$

$$c_3 = -\frac{3S_3(t)}{4r} a(2 - a)(1 - \alpha), \quad (7.140)$$

$$c_4 = -\frac{S_4(t)}{32r}(1 - \gamma^2)^2(1 - \alpha), \quad (7.141)$$

$$\nu = \frac{3S_1(t)}{8r}(1+\gamma)^2(1-\alpha), \tag{7.142}$$

where S_1, S_3, S_4 depend on the type of collision kernel:

- In the case of Maxwell molecules (that is, when $\tilde{S}(|v-v_*|) = S$ is a constant in (7.124), we take $S_1(t) = S_3(t) = S_4(t) = S$;
- In the case of hard spheres (that is, when $\tilde{S}(|v-v_*|) = |v-v_*|$), we take

$$S_1 = \sqrt{\frac{3(\tilde{T}_{11}^2 + \tilde{T}_{22}^2 + \tilde{T}_{33}^2) + 2(\tilde{T}_{11}\tilde{T}_{22} + \tilde{T}_{22}\tilde{T}_{33} + \tilde{T}_{11}\tilde{T}_{33})}{9T^2}}\sqrt{6T}, \tag{7.143}$$

$$S_3 = \frac{4\sqrt{T}}{\sqrt{\pi}}, \tag{7.144}$$

$$S_4 = \frac{32\sqrt{T}}{5\sqrt{\pi}}. \tag{7.145}$$

Here, the $\tilde{T}_{ii}$ are the eigenvalues of the matrix made out of the T_{ij}, which are the directional temperatures:

$$T_{ij}(t) = \frac{\int_v \int_e f(v_i - v_{i_{avr}})(v_j - v_{j_{avr}})dvde}{\int_v \int_e f dvde}; \qquad i,j = 1..,3, \tag{7.146}$$

and α is the volume fraction of gas in the spray:

$$1-\alpha(t) = \int_v \int_e f(t,v,e)\,\frac{4}{3}\pi r^3 dvde. \tag{7.147}$$

Those coefficients are chosen in such a way that the main properties of the kernel Q (conservation of mass, momentum, total energy) are satisfied, and that some typical quantities (kinetic energy, directional temperatures, variance of the internal energy) have a behavior which is as close as possible to the original kernel Q.

Their choice can be made in an almost completely rational way when one wishes to mimic a kernel with a cross section of Maxwell molecules type [that is, when one chooses $\tilde{S}$ as a constant function instead of (7.125)]. Unfortunately, in the (much more realistic) case of hard spheres (that is, when $\tilde{S}$ is given by (7.125)), this choice is made after some approximations which are not always valid, and other choices of coefficients are possible.

This work is built as follows: in Section 7.3.1 are computed (the evolution of) some moments of the density function f satisfying the Boltzmann eq. $\partial_t f = Q(f,f)$. This computation is exact (except for the variance of internal energy) when hard spheres are replaced by Maxwell molecules, but can only be an approximation in the realistic case of hard spheres. The difficulties related to the treatment of hard spheres [that is, the link between S_1, S_3, S_4 and $\tilde{S}$] are discussed in article [CDM10].

Then, the same computation is repeated in section 7.3.2 for the simplified model (7.133) – (7.136), with arbitrary coefficients $c_1,.,c_4,\nu$. This enables the identification of the coefficients (formulas (7.138) to (7.142)).

Section 7.3.3 is devoted to the numerical simulations and comparisons between the simplified and original model. In subsection 7.3.3 is presented the numerical (particle Monte Carlo) scheme used to solve (7.133) – (7.136). We only provide some numerical results in subsection 7.3.3 when a and γ depend on $|v - v_*|$. Other cases can be found in the paper.

7.3.1 Evolution of some moments of the solution of Boltzmann equation

We consider in this section a solution f of the spatially homogeneous Boltzmann equation

$$\partial_t f = Q(f, f), \tag{7.148}$$

where Q is the kernel defined in (7.118) – (7.124) [or (7.127) – (7.132)].

We want to track the following moments in order to build our simplified model:

- The directional temperatures T_{ij} defined by (7.146),
- The variance of the internal energy

$$g(t) := \frac{\int_{v,e} f(e - e_{avr})^2 dvde}{\int_{v,e} f dvde}. \tag{7.149}$$

Computation of some moments of the collision kernel in the case of Maxwell molecules

Property 7.3.1. *We note*

$$M_0 = \int_{v,e} m\, f\, dvde \tag{7.150}$$

the total mass of the spray (where m is the mass of a droplet). We consider Q defined in (7.118) – (7.124), in the case when $\tilde{S}(|v - v_*|) := S$ is a constant function of the relative velocity (case of Maxwell molecules). The following identities hold (provided that f is a smooth enough nonnegative function of v)

- *For $i, j = 1, .., 3$, $i \neq j$,*

$$\int_{v,e} Q(f, f) m (v_i - v_{i_{avr}})(v_j - v_{j_{avr}}) dvde = \frac{3S}{r}\big[-\frac{3}{8} + \frac{\gamma}{4}(\frac{\gamma}{2} - 1)\big](1 - \alpha) M_0 T_{ij}, \tag{7.151}$$

- *For $i = 1, .., 3$,*

$$\begin{aligned} \int_{v,e} Q(f, f) m (v_i - v_{i_{avr}})^2 dvde &= \frac{3S}{r}\big[-\frac{3}{8} + \frac{\gamma}{4}(\frac{\gamma}{2} - 1)\big](1 - \alpha) M_0 T_{ii} \\ &+ \frac{3S}{8r}(1 + \gamma)^2 (1 - \alpha) M_0 T, \end{aligned} \tag{7.152}$$

•

$$\begin{aligned}\int_{v,e} Q(f,f)m(e-e_{avr})^2 dvde &= -\frac{3S}{2r}a(2-a)(1-\alpha)M_0 g \\ &+ \pi r^2 \frac{(1-\gamma^2)S}{4}\int_{v,e,v^*,e^*} ff^* m(e+e^*-2e_{avr})|v-v^*|^2 dvdedv_* de_* \\ &+ \pi r^2 \frac{(1-\gamma^2)^2 S}{48}\int_{v,e,v^*,e^*} ff^* m|v-v^*|^4 dvdedv_* de_*.\end{aligned}$$

Eq. (7.153) can be simplified if f is a tensor product (as a function of v and e) in the following way:

$$\begin{aligned}&\int_{v,e} Q(f,f)m(e-e_{avr})^2 dvde = \\ -\ &\frac{3S}{2r}a(2-a)(1-\alpha)M_0 g \\ +\ &\pi r^2 \frac{(1-\gamma^2)^2 S}{48}\int_{v,e,v^*,e^*} ff^* m|v-v^*|^4 dvdedv_* de_*.\end{aligned} \tag{7.153}$$

It can even be further simplified when moreover f is an (isotropic) Gaussian function of v:

$$f(v,e) = \left(\int_v f(w,e)\,dw\right)\frac{1}{(2\pi T)^{3/2}} exp(-\frac{|v-v_{avr}|^2}{2T}). \tag{7.154}$$

In that case, we end up with

$$\begin{aligned}&\int_{v,e} Q(f,f)m(e-e_{avr})^2 dvde = \\ -\ &\frac{3S}{2r}a(2-a)(1-\alpha)M_0 g + \frac{15S}{16r}(1-\gamma^2)^2(1-\alpha)M_0 T^2.\end{aligned} \tag{7.155}$$

From these expressions we were able to compute the evolution of the moments of the Boltzmann equation in the case of Maxwell molecules or hard-spheres (see [CDM10]) so that we could create our simpler model (next subsection).

7.3.2 Establishment of the simplified model

Evolution of the moments of the simplified model with arbitrary coefficients

We introduce here the simplified model [which hopefully mimicks the behavior of (7.127) – (7.128)], with arbitrary coefficients $c_1, .., c_4, \nu$:

$$\begin{aligned}&\partial_t f + \nabla_v \cdot \left(c_1 f(v-v_{avr})\right) + \partial_e(c_2 f + c_3(e-e_{avr})f + c_4|v-v_{avr}|^4 \partial_e f) \\ =\ &-\nu(f-f_0)\end{aligned} \tag{7.156}$$

where v_{avr}, e_{avr}, and f_0 are defined by (7.134), (7.135) and (7.136).

It is possible to compute explicitly the evolution of some moments of the solution of eq. (7.156). Those computations are summarized in the following

Property 7.3.2. *We assume that $c_1, .., c_4, \nu \geq 0$ do not depend on v, e (they can depend on T and t). Then the (smooth) solutions of eq. (7.156) satisfy the following properties:*

- *Conservation of mass and momentum:*

$$\partial_t \int_{v,e} f \begin{pmatrix} 1 \\ v \end{pmatrix} dvde = 0, \tag{7.157}$$

- *Evolution of the total energy:*

$$\partial_t \int_{v,e} m f \left(\frac{|v|^2}{2} + e \right) dvde = [3c_1 T + c_2] M_0, \tag{7.158}$$

- *Evolution of the directional temperatures:*

$$\forall i, j = 1, .., 3, i \neq j, \qquad \partial_t T_{ij} = (2c_1 - \nu) T_{ij}, \tag{7.159}$$

$$\forall i = 1, .., 3, \qquad \partial_t T_{ii} = (2c_1 - \nu) T_{ii} + \nu T, \tag{7.160}$$

- *Evolution of the variance of the internal energy:*

$$\partial_t g = 2c_3 g - \frac{2c_4}{M_0} \int_v \int_e f m |v - v_{avr}|^4 dvde. \tag{7.161}$$

Computation of the coefficients: case of Maxwell molecules

We now write down the constraints on the parameters which enable to identify the behavior of the moments (total energy, g and T_{ij}) for the simplified model and for the original model, in the case of Maxwell molecules (that is, when $\tilde{S}(|v - v_*|) = S$).

In order to recover the conservation of total energy which held in the original model, one needs to ensure (according to (7.158)) that

$$c_2 = -3c_1 T \tag{7.162}$$

In order to mimick the behavior of the directional temperatures when f satisfies the original model, we write the following constraints (corresponding to the cases $i \neq j$ and $i = j$ respectively):

$$2c_1 - \nu = \frac{3S}{r}[-\frac{3}{8} + \frac{\gamma}{4}(\frac{\gamma}{2} - 1)](1 - \alpha), \tag{7.163}$$

$$\nu = \frac{3S}{8r}(1 + \gamma)^2 (1 - \alpha). \tag{7.164}$$

Finally, we wish to mimick the behavior of g. This first leads to

$$c_3 = -\frac{3}{4r} a(2 - a)(1 - \alpha) S. \tag{7.165}$$

It remains to perform the computation of $\int\int_{v,e} f m |v - v_{avr}|^4 dvde$. This is not possible in general, and we retain as an approximate result what is obtained when f is assumed to be an (isotropic)

Gaussian w.r.t. v (that is, f is given by formula (7.154)). In this situation, one is led to

$$\int_{v,e} fm|v - v_{avr}|^4 dvde = 15M_0T^2. \tag{7.166}$$

Then, the identification with the (approximate) ode (**??**) satisfied by $g(t)$ when f is solution of the Boltzmann equation with Maxwell molecules leads to:

$$c_4 = -\frac{1}{32r}(1-\gamma^2)^2(1-\alpha)S. \tag{7.167}$$

Collecting all those identities, we get the equations (7.138) – (7.142) for the parameters of the model described in the introduction (with $S_1(t) = S_3(t) = S_4(t) = S$).

Computation of the coefficients: case of hard spheres

In this subsection, we write down the constraints on the parameters which enable to identify the behavior of the moments (total energy, g and T_{ij}) for the simplified model and for the original model, in the case of hard spheres (that is, $\tilde{S}(|v - v_*|) = |v - v_*|$).

The conservation of total energy still leads to eq. (7.162). Then, it is easy to see that (7.163) – (7.165), (7.167) become

$$2c_1 - \nu = \frac{3S_1}{r}[-\frac{3}{8} + \frac{\gamma}{4}(\frac{\gamma}{2} - 1)](1-\alpha), \tag{7.168}$$

$$\nu = \frac{3S_1}{8r}(1+\gamma)^2(1-\alpha), \tag{7.169}$$

$$c_3 = -\frac{3}{4r}a(2-a)(1-\alpha)S_3, \tag{7.170}$$

$$c_4 = -\frac{1}{32r}(1-\gamma^2)^2(1-\alpha)S_4, \tag{7.171}$$

where S_1, S_3 and S_4 are given by (7.143), (7.144) and (7.145). In the last equation, the same assumptions on $\int_v \int_e fm|v - v_{avr}|^4 dvde$ has been performed as in the case of Maxwell molecules. We end up again with the equations (7.138) – (7.142) for the parameters of the model described in the introduction.

We have thus obtained our simplified model in the case of Maxwell molecules as well as in the case of hard spheres.

Extension of the model when a, γ depend on $|v - v_*|$

We now briefly explain how to extend our analysis when the kernel Q (with hard spheres cross section) defined in (7.127) – (7.132) includes inelasticity and energy exchange parameters a and γ which depend on $|v - v_*|$ instead of being absolute constants, that is, $a := a_1(|v - v_*|)$, $\gamma := \gamma_1(|v - v_*|)$ (Cf. [Mat06]; [DM10]).

Our proposition consists in introducing the simplified model (7.133) – (7.147), where a and γ (appearing in formulas (7.138) – (7.142)) are replaced by $a_1(\sqrt{6T})$ and $\gamma_1(\sqrt{6T})$ respectively [that is, $|v - v_*|$ is replaced by its mean quadratic value].

7.3.3 Numerical simulations

Numerical method

In order to solve (7.133) – (7.147), we use a particle method (with constant weight w): the density f is discretized as

$$f(n\Delta t, v, e) \sim \sum_{i=1}^{N} w\, \delta_{v_i(n\Delta t), e_i(n\Delta t)}.$$

The "Vlasov-Fokker-Planck" part of eq. (7.133) is solved by discretizing (at the first order) the characteristic ODEs for v_i and e_i. Moreover, a realization of the Brownian motion is used for the term proportional to $\partial_e^2 f$. The exact conservation of the momentum and total energy is enforced at the end of this procedure. The "BGK" part of eq. (7.133) [that is, the r.h.s. of the equation] is treated by modifying the velocities of a randomly chosen set of particles (Monte-Carlo method). Once again, the conservation of momentum and kinetic energy (which implies total energy too since the internal energy remains unchanged in that step) is enforced at the end of the time step.

Note also that the numerical results obtained with this discretization of eq. (7.133) – (7.147) are compared with simulations of the original equation (7.148) obtained thanks to a DSMC scheme (the code is a modified version of the code used in [Bar04]; [DM10])

In this document we choose to only present results on velocity-depending parameters (results on Maxwell molecules or hard-spheres can be found in the article [CDM10]).

Numerical experiments; velocity-depending parameters

This subsection is devoted to the presentation of results when both γ and a are functions of $|v - v_*|$ in eq. (7.148), as described in subsection 7.3.2.

More precisely, we consider the following formulas for the parameters γ and a:

$$\tilde{\gamma_1}(|v - v_*|) = exp(-\frac{\gamma_1}{|v - v*|}), \tag{7.172}$$

$$\tilde{a_1}(|v - v_*|) = 1 - exp(-\frac{a_1}{|v - v*|}). \tag{7.173}$$

We compare the results obtained on one hand by using the original Boltzmann equation (with $a := \tilde{a}(|v - v_*|)$ and $\gamma := \tilde{\gamma}(|v - v_*|)$ given by (7.172), (7.173); and with hard spheres), and on the other hand by using our simplified model with $a := \tilde{a}(\sqrt{6T})$, $\gamma := \tilde{\gamma}(\sqrt{6T})$, as proposed in subsection 7.3.2.

We first compare the evolution of the directional temperatures $T_{12}(t)$, $T_{11}(t)$, $T_{22}(t)$, in order to observe the equilibrium of those temperatures (Fig. 7.5). We take two different values for the parameter γ_1 in $\tilde{\gamma}$.

On a longer time scale, we also present results in LogLog scale (Fig. 7.11) for the evolution of the temperature T (that is, we check Haff's law numerically).

We end up this series of simulation by one example of evolution of the variance of internal energy $g(t)$ (Fig. 7.12).

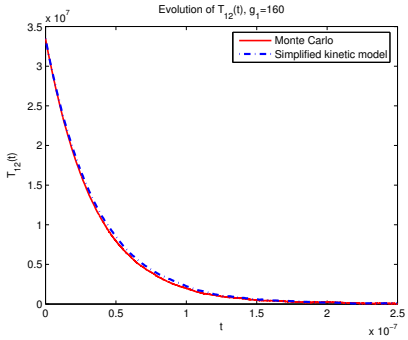

FIGURE 7.3: $\gamma_1 = 160$

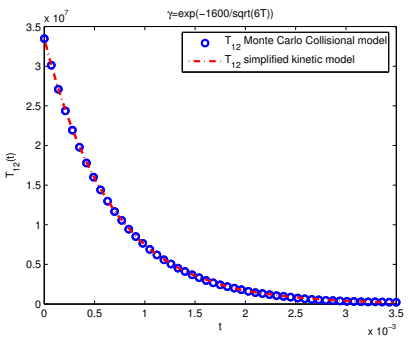

FIGURE 7.4: $\gamma_1 = 1600$

FIGURE 7.5: Evolution of $T_{12}(t)$. γ depending on $|v - v_*|$.

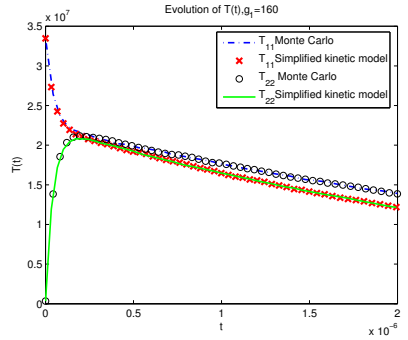

FIGURE 7.6: $\gamma_1 = 160$

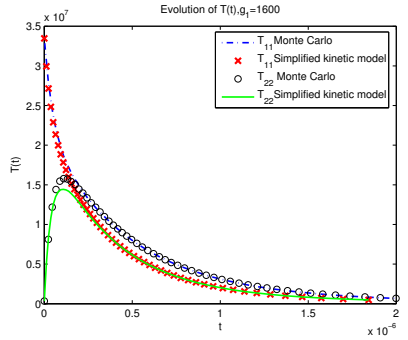

FIGURE 7.7: $\gamma_1 = 1600$

FIGURE 7.8: Evolution of $T_{11}(t)$, $T_{22}(t)$. γ depending on $|v - v_*|$.

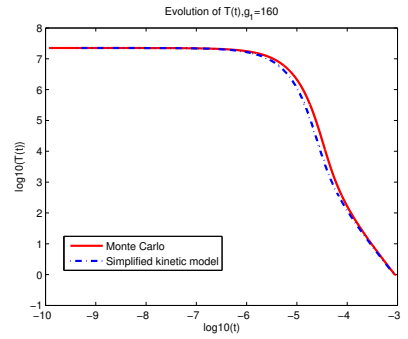

FIGURE 7.9: $\gamma_1 = 160$

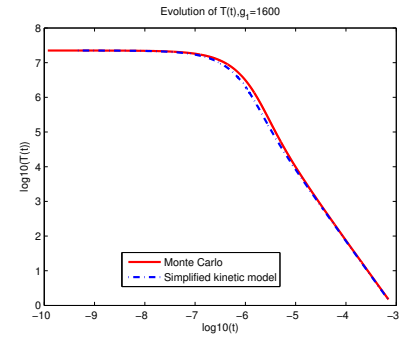

FIGURE 7.10: $\gamma_1 = 1600$.

FIGURE 7.11: Evolution of $T(t)$. γ depending on $|v - v_*|$. Log Log scale

FIGURE 7.12: Evolution of $g(t)$. $\gamma_1 = 160$. $a_1 = 6000$. γ, a depending on $|v - v_*|$.

In our simulations, no sensible degradation was observed w.r.t. the case of hard spheres (with given a, γ).

7.3.4 Conclusion

We introduced in this paper a model of BGK type for the description of the effect of collisions which are inelastic and in which the internal energy of the particles (droplets) is tracked (and can be exchanged during collisions). This model can be obtained almost entirely in a rational way when the collisions occur with a cross section of Maxwell molecules type. In the more realistic case of hard spheres (and even more when the inelasticity and internal energy exchange parameters can depend on the relative velocity of incoming droplets), approximations must be performed. The quality of these approximations were tested at the numerical level.

Chapter 8

Fluid methods for sprays

8.1 Mixing model

We now present another approach to emulate sprays. Due to the cost of Williams equations it seems reasonable to look for other ways to model the problem. Since it is well-known that two-phase flows problems are also difficult to solve, we tried to use another model during the Phd of A. Champmartin ([Cha11]; [Ber+14]). We tried to simplify the model obtained in the hydrodynamic limit ([Mat06]; [DM10]) thanks to the different orders of magnitude of the problem so that we end upwith a more or less classical Euler system. We now present the results that were obtained.

Dispersed flows (*i.e.* droplets in a carrying fluid) as described in [Ish75], are ubiquitous in nature and in industrial applications (see *e.g.* [ORo81]; [Bau+05]; [LO08]; [SM95]; [Gal09]). In the past fifteen years, the continuous increase of computational power triggered the interest of applying computational fluid dynamics to flows involving several phases. However a full description of these flows requires such a tremendous amount of computational power that engineers must resort to simplified models.

These flows are governed by the exchanges that occur between the two phases due to the presence of temperature, pressure or velocity differences. Depending on the degree of equilibrium between the two phases and the degree of complexity that we want to conserve, different types of model are available (*c.f.* [SW84] for a complete review). When the two phases can be followed by equations of fluid mechanics, we have two main classes of models. The first one is the bifluid models in which each phase is described separately. This conducts to a set of 7 (or 6) equations depending on the assumption of equilibrium or non equilibrium in pressure (see *e.g.* [RT04]). Due to the complexity of these models (due to *e.g.* presence of source terms, definition of terms of exchanges at the interface, high number of equations, loss of hyperbolicity in some cases) which entertain numerical difficulties, when the two phases have started to balance (thanks to exchange of momentum and energy), an other class of models is often preferred: the mixture models. These are a good compromise between accuracy and simplicity, since they follow the evolution of mixture quantities between the two phases and allow to deal with less equations due to equilibrium assumptions. This work deals with the description of a model of that type.

The so-called *Homogeneous Equilibrium Model* (HEM) presented in this work is dedicated to two-phase flows where a small volume fraction of solid particles (denoted as the heavy fluid in the following) moves through a continuous fluid phase (either gas or liquid). In that kind of model, the two phases are considered as a mixture [Amb+08]; [Gal09]; [Pan06]: the model is given in the form of a continuity equation for each phase and a single momentum equation, which contains an additional term representing the effect of velocity differences between the phases. A model based

on a force balance for the dispersed phase is required for the computation of the relative velocity (called a drift relation). This formula is obtained either thanks to the experiment as in [HI03], either using simplifying assumptions in order to find an approximate solution on the equation checked by the relative velocity [Mam79]; [GD07]; [Amb+08]. The basic assumption is that a local equilibrium establishes over short times scales and spatial length scales: this leads us to suppose that the movement of the two phases is strongly coupled and can be described by an unique equation in mean velocity with a corrective factor, the relative velocity $\mathbf{m}u_r$. Note that the drift formula obtained depends on the problem considered (in particular of the form of the drag force term) and the assumption that are used to get it.

Typically, we will be interested in the case of tin droplets surrounded by air, with a disequilibrium between the velocities. In our particular applications, the chain of events starts when the particles are released in the gas. During the first stage, where the relative velocity between particles and the surrounding gas may be important, a detailed description of the motion of each particle (*via* a numerical weighting process [ORo81]; [Mat06]; [Duk80]) is possible because the flow is driven by hydrodynamics only. It has been implemented in the so-called "spray" simulation. On the contrary, the last stage involves additional physical phenomena and it becomes computationally out of reach to go on with the detailed description of the particles. One then resorts to a two-fluid simulation (see *e.g.* [Ish75]; [SW84]; [Bes90]; [Ram00]) where the solid particles are averaged out to constitute the heavy fluid (dispersed phase) and thus follow continuous equation of fluid mechanics. During the transition between these two stages, the goal of the HEM model is to keep track of a simplified list of averaged physical quantities and thus to avoid implementing a two-fluid model, while continuing to take into account a disequilibrium in velocity between the two phases. It is initialized at the end of the spray simulation and the output of the HEM simulation is given as an input to the two-phase flow simulation (classical mixture model, *i.e.* HEM model with a relative velocity set to zero). It is assumed that the outcome of the whole simulation is not too sensitive to the transition period where no special physical event should occur.

8.1.1 Model: from two-phase flows towards balanced homogeneous mixture model (HEM)

With our notations, a physical quantity z relative to the heavy fluid (resp. light fluid), or dispersed (resp. continuous) phase, is denoted z^+ (resp. z^-). Then, the averaged volume fraction of both kinds of fluid is noted $\alpha^\pm$, the mass fraction $c^\pm$, the density $\rho^\pm$, the Favre velocity $\mathbf{m}u^\pm$, the specific energy (sum of the specific internal energy and kinetic energy) $E^\pm = e^\pm + 1/2\,\mathbf{m}u^{\pm 2}$, and the total enthalpy $H^\pm$ ($H^\pm := E^\pm + \frac{p}{\rho^\pm}$, where p is the pressure).

In a standard two fluid model, physical quantities for each fluid satisfy two scalar equations (mass conservation and energy conservation) and one vector equation (momentum conservation) [Ish75]; [Mat06]:

$$\partial_t(\alpha^\pm\rho^\pm) + \nabla\cdot(\alpha^\pm\rho^\pm\mathbf{m}u^\pm) = 0, \tag{8.1}$$
$$\partial_t(\alpha^\pm\rho^\pm\mathbf{m}u^\pm) + \nabla\cdot(\alpha^\pm\rho^\pm\mathbf{m}u^\pm\otimes\mathbf{m}u^\pm) + \alpha^\pm\nabla p = \pm\mathbf{m}F_{\mathrm{D,Fluid}} + \alpha^\pm\rho^\pm\,\mathbf{m}g, \tag{8.2}$$
$$\partial_t(\alpha^\pm\rho^\pm E^\pm) + \nabla\cdot(\alpha^\pm\rho^\pm H^\pm\mathbf{m}u^\pm) + p\,\partial_t\alpha^\pm = \pm Q_E + \alpha^\pm\rho^\pm\,\mathbf{m}g\cdot\mathbf{m}u^\pm, \tag{8.3}$$

where Q_E represents the heat exchanges between phases (which depend on the difference of temperature between the two fluids) and $\mathbf{m}g$ is the external gravity acceleration. For our applications, the drag force experienced by the particles, $\mathbf{m}F_{\mathrm{D,Fluid}}$, is mainly due to turbulence. This is why it is quadratic with respect to relative velocity, $\mathbf{m}u_r = \mathbf{m}u^- - \mathbf{m}u^+$, in such a way that

$\mathbf{m}F_{\mathrm{D,Fluid}} = \theta_\rho \frac{C^*}{r^*} \frac{\alpha^+\alpha^-\rho^+\rho^-}{\rho} |\mathbf{m}u_r| \mathbf{m}u_r$ with

$$\theta_\rho = \frac{\alpha^+}{\alpha^-} + \frac{\rho^+}{\rho^-} = \frac{\rho^-}{c^-\rho^+} \tag{8.4}$$

a dimensionless parameter; and $\frac{C^*}{r^*}$ proportional to the ratio between the drag coefficient C_D (see [BDM03] for a definition) and the mean radius of the particle r ($\frac{C^*}{r^*} = \frac{3}{8}\frac{C_\mathrm{D}}{r}$). Moreover, an ideal isobar mixing is assumed throughout this article:

$$\begin{aligned} p &= P^\pm(\rho^\pm, T^\pm), \\ \text{with } T^\pm = T^\pm(\rho^\pm, e^\pm) \text{ and } e^\pm &= E^\pm - 1/2|\mathbf{m}u^\pm|^2. \end{aligned} \tag{8.5}$$

The simplicity conditions placed on the transition model require that the evolution of its averaged physical quantities depends upon only one velocity field: the mixture velocity $\mathbf{m}u = c^+\,\mathbf{m}u^+ + c^-\,\mathbf{m}u^-$. The information about the relative velocity, $\mathbf{m}u_r$, fundamental when dealing with energy budget within the mixed fluid, is then lost in this procedure. It needs to be recovered with a suitable algebraic closure. Let us define two additional quantities: the averaged mixture density ρ

$$\frac{1}{\rho} = \frac{c^+}{\rho^+} + \frac{c^-}{\rho^-}, \tag{8.6}$$

i.e. $\rho = \frac{\rho^+\rho^-}{\rho^- c^+ + \rho^+ c^-}$ [1] and the averaged total energy $E = c^+E^+ + c^-E^-$ [You84]; [You89]; [Gal09] (all the other mean quantities are built on the same model: $z = c^+z^+ + c^-z^-$ using the mass fraction $c^\pm$). We also build relative quantities $z_r := z^- - z^+$ that take into account the disequilibrium between the two phases (*e.g.* c_r the relative concentration and $\frac{1}{\rho_r} := \frac{1}{\rho^-} - \frac{1}{\rho^+}$ the relative density inverse). Starting from the two-fluid model equations (8.1)-(8.3), the evolution of the mixing quantities that have just been defined, can be devised after tedious algebraic manipulations:

$$\partial_t\rho + \nabla\cdot(\rho\,\mathbf{m}u) = 0, \tag{8.7}$$

$$\partial_t(\rho\,c_r) + \nabla\cdot(\rho\,c_r\mathbf{m}u + \rho\,\frac{1-c_r^2}{2}\,\mathbf{m}u_r) = 0, \tag{8.8}$$

$$\partial_t(\rho\,\mathbf{m}u) + \nabla\cdot(\rho\,\mathbf{m}u\otimes\mathbf{m}u + \rho\,\frac{1-c_r^2}{4}\,\mathbf{m}u_r\otimes\mathbf{m}u_r) + \mathbf{m}\nabla\,p = \rho\,\mathbf{m}g, \tag{8.9}$$

$$\partial_t(\rho\,E) + \nabla\cdot(\rho\,H\,\mathbf{m}u + \rho\,(h_r - \frac{c_r}{2}\,\mathbf{m}u_r^2 + \mathbf{m}u\cdot\mathbf{m}u_r)\,\frac{1-c_r^2}{4}\,\mathbf{m}u_r) = \rho\mathbf{m}u\cdot\mathbf{m}g, \tag{8.10}$$

where the averaged specific enthalpy is defined by $H := c^+H^+ + c^-H^- = E + \frac{p}{\rho}$. Due to the relation $c^+ + c^- = 1$, we have: $c^\pm = (1 \mp c_r)/2$. $\mathbf{m}F_\mathrm{D}$ denotes the drag force of the mixture:

$$\mathbf{m}F_\mathrm{D} = \rho\theta_\rho\frac{C^*}{r^*}\frac{1-c_r^2}{4}|\mathbf{m}u_r|\mathbf{m}u_r. \tag{8.11}$$

Combining the equations (8.7)-(8.10) and the next equation above relative velocity (8.13) with the relation check by the mean internal and total energies ($E = e + \frac{1}{2}|\mathbf{m}u|^2 + \frac{1}{2}\frac{1-c_r^2}{4}\mathbf{m}u_r^2$), the last

[1] The mean density ρ (8.6) can be rewritten in terms of an algebraic average of the specific quantity of each phase $\rho = \alpha^+\rho^+ + \alpha^-\rho^-$.

equation (8.10) can equally be replaced by:

$$\partial_t(\rho e) + \nabla \cdot (\rho\,(e\mathbf{m}u + e_r \frac{1-c_r^2}{4}\mathbf{m}u_r)) + p\,(\nabla \cdot \mathbf{m}u + \nabla \cdot (\frac{\rho}{\rho_r}\frac{1-c_r^2}{4}\mathbf{m}u_r)) = \mathbf{m}F_{\mathrm{D}} \cdot \mathbf{m}u_r, \quad (8.12)$$

where $e = c^+e^+ + c^-e^-$ and $\frac{1}{\rho_r} = \frac{1}{\rho^-} - \frac{1}{\rho^+}$ (see [Cha11] §1.1.4 p 45 − 52 for more details on the algebraic manipulations). In these equations, the relative velocity $\mathbf{m}u_r$ satisfies:

$$\partial_t \mathbf{m}u_r + (\mathbf{m}u^- \cdot \mathbf{m}\nabla)\mathbf{m}u^- - (\mathbf{m}u^+ \cdot \mathbf{m}\nabla)\mathbf{m}u^+ + (\frac{1}{\rho^-} - \frac{1}{\rho^+})\mathbf{m}\nabla\, p = -\frac{C^*}{r^*}\theta_\rho\,|\mathbf{m}u_r|\,\mathbf{m}u_r. \quad (8.13)$$

That last equation was brought to the fore in [SEL04]; [You89]; [Gal09]; [GD07] to show that a straightforward algebraic closure of the relative velocity can be found if it is assumed that $\partial_t \mathbf{m}u_r + (\mathbf{m}u^- \cdot \mathbf{m}\nabla)\mathbf{m}u^- - (\mathbf{m}u^+ \cdot \mathbf{m}\nabla)\mathbf{m}u^+$ is negligible compared to the remaining two terms. Neglecting that particular set of terms requires that the time scale of the evolution of the relative velocity and that the length scales characteristic of the fluctuations of $\mathbf{m}u^\pm$ are small enough. If this is justified, the algebraic closure of the relative velocity reads:

$$\mathbf{m}u_r = -\sqrt{\frac{r^*}{C^*\theta_\rho}}\sqrt{\frac{1}{\rho_r}}\frac{\nabla p}{|\nabla p|^{1/2}}. \quad (8.14)$$

In accordance with intuition, the relative velocity should vanish if $\rho^+ = \rho^-$ and it should be along $\mathbf{m}\nabla p$ if $\rho^+ > \rho^-$ (a heavy fluid falls in a lighter fluid) and in the opposite direction if $\rho^+ < \rho^-$ (a light fluid rises in an heavier fluid). More explanations on the obtention of the formula (8.14) can be found in [Ber+14]. The final HEM model is composed of equations (8.7)-(8.9), (8.12) and of the formula (8.14) for the relative velocity. The missing equation in energy is replaced by a unique temperature hypothesis ($T^\pm = T$ in (8.5), which is reasonable in our applications, *c.f.* [Mat07]). The HEM equations are then closed by a closure law which gives both the pressure p and the specific quantities of each fluid: $\rho^\pm$, $e^\pm$ (useful in the HEM equations for the quantities $\frac{1}{\rho_r}$ and e_r), given by the knowledge of ρ, e and c_r: $[p, \rho^\pm, e^\pm] = f(\frac{1}{\rho}, e, c_r)$, the function f depends on the equation of states chosen for the two fluids. Note that due to the use of an algebraic closure for the relative velocity $\mathbf{m}u_r$ instead of equation (8.13), the two systems formulated in total or in internal energy are not equivalent. We choose a model written in internal energy e due to requirements of the study code where the model should be implemented. We do not give the details for the drift formula. They can be found in [Ber+14].

8.1.2 Numerical results

Simulations

The simulations were obtained through a Lagrange-remap solver ([Cha11]). For the discretization of the relative velocity, we use a limiter of MIN-MOD type to limit the pressure gradient. We only show results for the Rayleigh-Taylor instability (other results can be found in [Cha11]).

First case: Rayleigh-Taylor instabilities: We consider an unstable case where a heavy fluid (water) is put on top of a lighter fluid (gas) and submitted to the gravity field. The equation of states (EOS) are those of perfect gas type at standard conditions (compressible for the air and incompressible for the water). We initially perturb the interface between the two fluids and at the beginning, the pressure is uniformly equal to 10^5 (and thus the relative velocity $\mathbf{m}u_r = 0$) and the

mean velocity $\mathbf{m}u$ is also put to 0 (Fig. 8.1). The box is 0.07 m by 0.1 m with $Nx = 56$ and $Ny = 60$ ($\Delta x = Lx/(Nx+1)$, with Nx the number of points of discretization along the x direction). In Fig. 8.2, we observe that the initial perturbation leads to the formation of a Rayleigh-Taylor mushroom. In Fig. 8.3, we can check that these mushrooms originate from initial instabilities of the border.

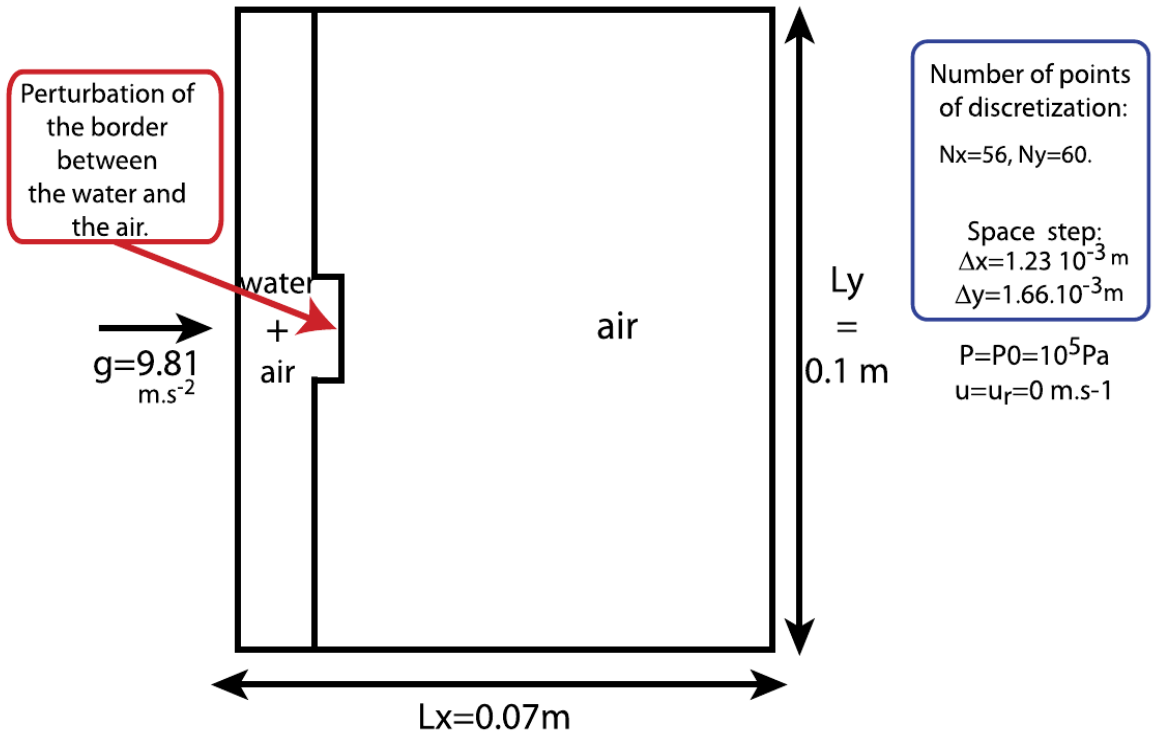

FIGURE 8.1: Test case configuration for the Rayleigh-Taylor instability.

In Fig. 8.2 as well as in Fig. 8.3, the relative velocity is equal to zero at the beginning. Then, due to the instability, the pressure p evolves and the inherent gradient pressure is captured by our HEM model thanks to the relative velocity $\mathbf{m}u_r$. This allows us to see the formation of mushrooms.

8.1.3 Conclusion

We have proposed in this paper an homogeneous mixture model in which we consider the two-phase flows as a mixture. The closure law of $\mathbf{m}u_r$ allows us to take into account relative velocity between the fluids and to avoid the use of two fluids models while being able to tender the drag effects. This model is valid when the velocities of the two fluids are coupled (*i.e.* when the drag force is already acting) and it has been tested on numerical experiments. It would be interesting now to use this model as a transition model during the thermalization in velocity between the two phases, for a complete chain of simulation.

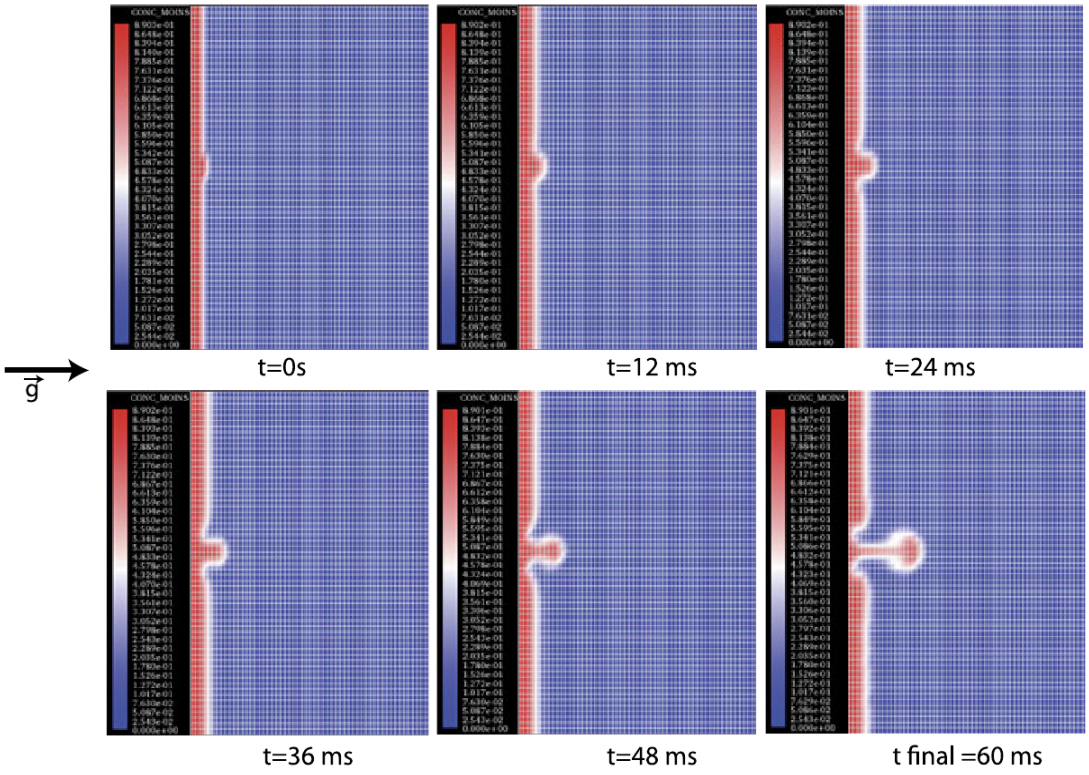

FIGURE 8.2: Heavy fluid (in red) above a lighter one (in blue) with a single initial perturbation of the border (gravity goes from the left to the right).

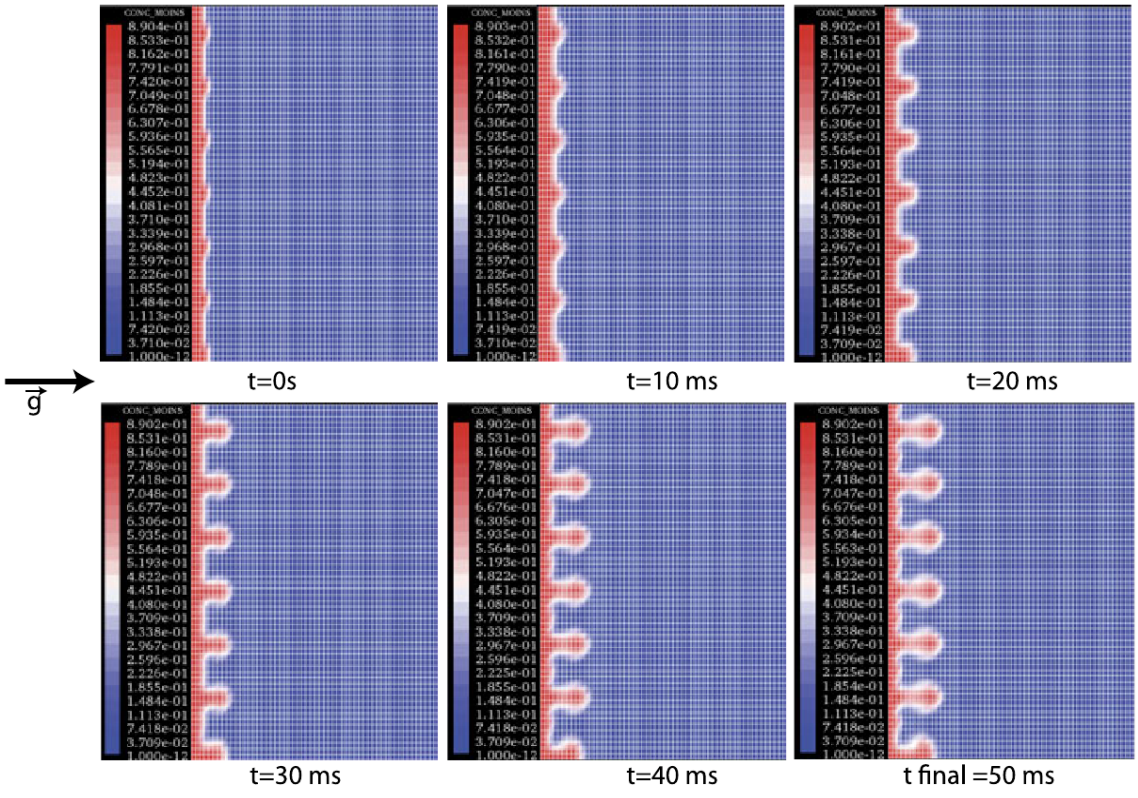

FIGURE 8.3: Heavy fluid (in red) above a lighter one (in blue) with an initial periodic perturbation of the border.

8.2 Simulating pressureless gas

Pressureless gas equation can appear when one wants to use sectional approach for sprays ([DMV03]): using the Eulerian/Eulerian approach for spray is a way to considerably decrease the numerical cost of simulating spray as it has already been mentioned. Although the work that is presented now was not intended for sprays, it can be re-used for them. The work which is presented now comes from the article ([BM12a]] and the proceeding ([BM12b]).

During the last two decades, there have been many contributions on the pressureless gases system, and it seems natural to tackle the question of its discretization. The pressureless gases system appears as a system of conservation laws on the mass and momentum. Hence, it is relevant to wonder if standard numerical schemes for conservation laws, like the upwind scheme, for instance, are fitted to this particular system. However, we emphasize that it is a degenerate hyperbolic system (the Jacobian is not diagonalizable).

Let us now recall the one-dimensional system describing a pressureless gas. Let $T > 0$. The gas density $\rho(t,x) \geq 0$ and the momentum $q(t,x) \in \mathbb{R}$ satisfy the following equations in $(0,T) \times \mathbb{R}$

$$\partial_t \rho + \partial_x(\rho u) = 0, \tag{8.15}$$
$$\partial_t q + \partial_x(q u) = 0. \tag{8.16}$$

One must define the velocity $u(t,x) \in \mathbb{R}$ as a quotient of q by ρ, but this may not be possible, since ρ can be zero. We discuss this issue below, by recalling the notion of duality solutions [BJ98]. As already stated, each equation consists of a conservation law, (8.15) for mass and (8.16) for momentum. We obviously need initial conditions

$$\rho(0,\cdot) = \rho^{\text{in}}, \qquad q(0,\cdot) = q^{\text{in}}, \tag{8.17}$$

in which the condition on the momentum can be replaced by an initial condition on the velocity $u(0,\cdot) = u^{\text{in}}$, and then written again as $q(0,\cdot) = \rho^{\text{in}} u^{\text{in}}$.

The previous system can be seen as a simplified model of the Euler equations, where the pressure has been set to zero. It can describe either cold plasmas or galaxies' dynamics [Zel70]. This system (8.15)–(8.16) and related problems (traffic models, magnetohydrodynamics, astrophysics, pressureless fluid equations...) have been widely studied, see, for instance, [Bou94]; [Gre95]; [ERS96]; [BG98]; [PR97]; [BJ99]; [Bou00]; [Sev01]; [Ber02]; [Pou02]; [LeV04]; [BJM05]; [GS05]; [Cou06]; [Ber+08]; [NT08]. Those references use the same fluid point of view we choose here, or the kinetic one, involving the adhesion dynamics of the so-called sticky particles.

When one studies smooth solutions of the pressureless gases system, (8.16) can be replaced by the standard Burgers equation:

$$\partial_t u + \partial_x\left(\frac{u^2}{2}\right) = \partial_t u + u\partial_x u = 0. \tag{8.18}$$

System (8.15)–(8.16) is then uncoupled, since we obtain u from (8.18), and then ρ from (8.15). On the other hand, it is well-known that smooth initial data can result in mass concentration, for example, when the velocity does not increase. In that case, the velocity cannot satisfy (8.18) anymore.

In [BJ98], Bouchut and James introduced the notion of duality solution for one-dimensional transport equations and conservation laws. In [BJ99], they prove that this framework is fitted to the pressureless gases system. Let us briefly recall the results they obtain.

Definition 1. A couple $(\rho, q) \in C(\mathbb{R}_+; \text{w*-}\mathcal{M}_{\text{loc}}(\mathbb{R}))^2$, with $\rho \geq 0$, is a duality solution to (8.15)–(8.16), if there exists a bounded Borel function a and $\alpha \in L^1_{\text{loc}}(\mathbb{R}_+^*)$ such that

$$\partial_x a \leq \alpha, \qquad q = a\rho, \qquad \text{in } \mathbb{R}_+^* \times \mathbb{R},$$

and, in the duality sense on $(t_1, t_2) \times \mathbb{R}$, for any $0 < t_1 < t_2$,

$$\partial_t \rho + \partial_x(\rho a) = 0, \qquad \partial_t q + \partial_x(q a) = 0.$$

In that setting, u is defined ρ-almost everywhere, and we have $u = a$ ρ-a.e. Bouchut and James prove that duality solutions are stable, and also entropic, *i.e.* the following inequality holds, in the distributional sense,

$$\partial_t(\rho S(u)) + \partial_x(\rho u S(u)) \leq 0, \tag{8.19}$$

for any convex function S. Using those properties and the sticky particles dynamics, they obtain the following existence result.

Theorem 8.2.1. *Let $\rho^{\text{in}}, q^{\text{in}} \in \mathcal{M}_{\text{loc}}(\mathbb{R})$, with $\rho^{\text{in}} \geq 0$ and $|q^{\text{in}}| \leq U\rho^{\text{in}}$, $U \geq 0$. Then there exists a duality solution to (8.15)–(8.17), and we have $\|a\|_\infty \leq U$ and $\alpha(t) = 1/t$.*

As proven in [Hof83], the one-sided Lipschitz (OSL) condition on the expansion rate $\partial_x a \leq 1/t$, also known as the Oleinik entropy condition, is optimal for a convex scalar conservation law. In the proof of Theorem 8.2.1, it is clear that the standard convex entropy condition (8.19) is not enough, and the OSL condition is really required. Note that, when the solutions are smooth, this estimate can easily be proven, since the Burgers equation (8.18) lies in the class of convex scalar conservation laws [BO88]; [LeV92].

Eventually, Bouchut and James also obtain uniqueness when ρ^{in} is nonatomic (essentially meaning that ρ^{in} is smooth).

In this work, we also consider the viscous pressureless gases system. In this system, as explained in [Bou00], (8.16) is replaced by an equation on the velocity itself. Let us choose $\varepsilon > 0$. The gas density $\rho(t,x) > 0$ and the velocity $u(t,x) \in \mathbb{R}$ satisfy, in $(0,T) \times \mathbb{R}$, Equation (8.15) and

$$\partial_t u + u\partial_x u = \frac{\varepsilon}{\rho}\partial^2_{xx} u, \tag{8.20}$$

with the same set of initial conditions (8.17). That writing imposes that ρ remains nonnegative, which is true if ρ^{in} is also nonnegative, see [Bou00]. Note that (8.20) is equivalent, when ε is fixed, to

$$\partial_t u + \partial_x\left(\frac{u^2}{2}\right) = \frac{\varepsilon}{\rho}\partial^2_{xx} u, \tag{8.21}$$

if we take into account the smoothness of the viscous velocity given in [Bou00].

In fact, (8.20) or (8.21) can also be rewritten as an equation on the momentum, with a viscosity term $\varepsilon\partial^2_{xx}u$ on the right-hand side,

$$\partial_t(\rho u) + \partial_x(\rho u^2) = \varepsilon\partial^2_{xx} u,$$

which yields (8.16) when ε goes to 0. In [Bou00], the author proved the existence, in the sense of distributions, of solutions to the viscous system (8.15), (8.17) and (8.21), and that the expansion rate is upper-bounded: $\partial_x u \leq A/(At+1)$, when $A = \max(\operatorname{ess\,sup} \partial_x u^{\text{in}}, 0)$ is finite. He also obtains the convergence of the viscous solutions towards the duality solutions to the pressureless gases system when ε vanishes. More precisely, the following convergence result holds.

Theorem 8.2.2. *Let* $(\rho_\varepsilon^{\text{in}})$, $(u_\varepsilon^{\text{in}})$ *such that, for any* $\varepsilon > 0$,

$$\rho_\varepsilon^{\text{in}} > 0, \qquad \rho_\varepsilon^{\text{in}} \in L^\infty(\mathbb{R}), \qquad \|1/\rho_\varepsilon^{\text{in}}\|_{L^\infty(\mathbb{R})} \leq C\varepsilon^{-1/4},$$

$$u_\varepsilon^{\text{in}} \in L^1 \cap \text{Ł}^\infty(\mathbb{R}), \qquad \|u_\varepsilon^{\text{in}}\|_{L^\infty(\mathbb{R})} \leq C,$$

$$\partial_x u_\varepsilon^{\text{in}} L^1 \cap L^2(\mathbb{R}), \qquad \operatorname{ess\,sup} \partial_x u_\varepsilon^{\text{in}} \leq C\varepsilon^{-1/2}.$$

We assume that $(\rho_\varepsilon^{\text{in}}) \rightharpoonup \rho^{\text{in}}$ *and* $(\rho_\varepsilon^{\text{in}} u_\varepsilon^{\text{in}}) \rightharpoonup q^{\text{in}}$ *in* w*-$\mathcal{M}_{\text{loc}}(\mathbb{R})$. *Then, up to a subsequence,* $(\rho_\varepsilon, \rho_\varepsilon u_\varepsilon)$, *given by the solutions to* (8.15) *and* (8.21), *with initial datum* $(\rho_\varepsilon^{\text{in}}, \rho_\varepsilon^{\text{in}} u_\varepsilon^{\text{in}})$, *converges in* $C_t(\text{w*-}\mathcal{M}_{\text{loc}}(\mathbb{R}))$ *towards the duality solution* (ρ, q) *of* (8.15)–(8.17).

Both viscous and inviscid systems can also be studied in a periodic framework, *i.e.* we focus on the closed interval $[0,1]$ and impose that all the physical quantities have the same values at both $x = 0$ and $x = 1$, so that the solutions are 1-periodic.

This work is dedicated to the numerical approximation of the pressureless gases system (8.15)–(8.16), where the latter may be replaced by (8.21). For readability reasons, we choose the periodic framework.

There are two methods to get *a priori* relevant schemes. The first one is to use the natural kinetic framework which underlies the pressureless gas dynamics, with kinetic schemes, as in [Bou94]; [BJL03], or with particle methods [CKR07]. The second one is related to the discretization of hyperbolic conservation laws. Gosse and James [GJ00] point out the relevance of two families of numerical schemes: the upwind schemes and the Lax-Friedrichs schemes. In [BBT06], Berthon *et al.* investigate a relaxation scheme for the pressureless gases system in one and two-dimensional settings.

As we already pointed out, the key condition to obtain the duality solution is that the velocity expansion rate must be upper-bounded by $1/t$. Brenier and Osher [BO88] obtained the relevance of the OSL condition in a discrete framework for the convex scalar conservation laws. In this work, we first investigate the upwind scheme associated to (8.15)–(8.16), and prove that it fails to ensure the OSL condition. Subsequently, we try the upwind diffusive scheme associated to (8.15) and (8.21), and explain how we can obtain a good numerical approximation of the duality solution to the inviscid pressureless gases system using this scheme. We do not study the Lax-Friedrichs schemes described in [GJ00]. Indeed, the numerical dissipation induced by those first order schemes is too significant. Since it is then natural to use higher order schemes, we recover the same kind of problems as in the diffusive upwind scheme we here propose, involving second order terms.

In the remainder, let Δt, $\Delta x > 0$ such that $N = T/\Delta t \in \mathbb{N}^*$ and $I = 1/\Delta x \in \mathbb{N}^*$, and set $\lambda = \Delta t/\Delta x$. We respectively denote ρ_i^n, q_i^n and u_i^n the approximate values of ρ, q and u at time $n\Delta t \in [0,T]$ and coordinate $(i+1/2)\Delta x \in [0,1)$, for $0 \leq n \leq N$ and $0 \leq i < I$. Since we use a periodic framework, we define ρ_i^n, q_i^n and u_i^n for any $i \in \mathbb{Z}$, by

$$\rho_{i+pI}^n = \rho_i^n, \qquad q_{i+pI}^n = q_i^n, \qquad u_{i+pI}^n = u_i^n, \qquad 0 \leq i < I, \quad p \in \mathbb{Z}^*.$$

For the sake of readability, in the previous notations, we may drop the time iteration index n and replace $n+1$ by a prime symbol " $'$ ". For instance, the velocity at time $(n+1)\Delta t$ and coordinate $(i+1/2)\Delta x$ can be written as u_i' or u_i^{n+1}.

Apart from the density, momentum and velocity, the quantity of interest, which we name the numerical expansion rate, is, for each time and space indices n and i,

$$w_i^n := n\lambda(u_{i+1}^n - u_i^n).$$

Indeed, the OSL condition at time $n\Delta t$ then reads $\max_i w_i^n \leq 1$.

8.2.1 Upwind scheme

Let us first denote the positive and negative parts of $a \in \mathbb{R}$

$$a^+ = \max(0, a), \qquad a^- = \min(0, a).$$

The upwind scheme writes, for any $0 \leq i < I$,

$$\begin{aligned}
\rho_i' &= \rho_i - \lambda\left[\rho_i(u_i)^+ - \rho_{i-1}(u_{i-1})^+\right] - \lambda\left[\rho_{i+1}(u_{i+1})^- - \rho_i(u_i)^-\right], \\
q_i' &= q_i - \lambda\left[q_i(u_i)^+ - q_{i-1}(u_{i-1})^+\right] - \lambda\left[q_{i+1}(u_{i+1})^- - q_i(u_i)^-\right], \\
u_i' &= \frac{q_i'}{\rho_i'}, \qquad \text{if } \rho_i' > 0,
\end{aligned}$$

and u_i' is not defined if $\rho_i' = 0$. It is quite clear that the previous schemes on both ρ and q are monotonic, if the standard Courant-Friedrichs-Lewy (CFL) condition $\lambda \max|u| \leq 1$ is satisfied. Hence, we only choose positive initial data to study positive velocities. The scheme then becomes, for any $0 \leq i < I$,

$$\rho_i' = (1 - \lambda u_i)\rho_i + \lambda u_{i-1}\rho_{i-1}, \tag{8.22}$$

$$q_i' = (1 - \lambda u_i)q_i + \lambda u_{i-1}q_{i-1}, \tag{8.23}$$

$$u_i' = \frac{q_i'}{\rho_i'}. \tag{8.24}$$

As we already stated, this last equality allows to define u_i' only when $\rho_i' > 0$. This fits the mathematical setting of the pressureless gases system, since u can only be defined ρ-almost everywhere. Nevertheless, it is not satisfying from a numerical viewpoint, since the computations stop whenever the density becomes equal to 0. We can impose whichever value we want, for instance, $u_i' = 0$, when $\rho_i' = 0$. Indeed, we do not care about the value of the velocity at a point where is there is no matter. But we must keep in mind not to use those artificial nil values of u_i' to study the numerical expansion rate.

Thanks to (8.24), we immediately have

$$\rho_i'\rho_{i+1}'(u_{i+1}' - u_i') = \rho_i' q_{i+1}' - \rho_{i+1}' q_i',$$

which implies

$$\rho_i'\rho_{i+1}'\frac{w_i'}{(n+1)\lambda} = (1 - \lambda u_{i+1})\rho_{i+1}\rho_i'\frac{w_i}{n\lambda} + \lambda u_{i-1}\rho_{i-1}\rho_{i+1}'\frac{w_{i-1}}{n\lambda}.$$

Under the CFL condition $\lambda \max|u| \leq 1$, if $(w_i)_{0\leq i<I}$ are negative, and if $(\rho_i')_{0\leq i<I}$ are nonnegative, it is clear that the quantities (w_i') also remain negative. Unfortunately, if w_j is nonnegative for a given j, the OSL condition $w_i' \leq 1$ for all i may not be satisfied.

Property 8.2.1. *Let $0 < \lambda < 1$ and U such that $0 < \lambda U < 1$, and choose an integer $I > 2 + 1/\lambda$. We consider the following initial data*

$$\rho_i^0 = 1, \quad 0 \le i \le I-1, \qquad u_0^0 = U, \quad u_i^0 = 0, \quad 1 \le i \le I-1. \tag{8.25}$$

Then the upwind scheme (8.22)–(8.24) does not satisfy the OSL condition. More precisely, we have

$$\max_i w_i^{I-2} > U. \tag{8.26}$$

The assumption on the Courant number $0 < \lambda < 1$ is standard and is a natural consequence of the CFL condition $\lambda U \le 1$ when U is large. The initial data can of course be defined without the discretization grid: we have $\rho^{\text{in}} \equiv 1$ and $u^{\text{in}} \equiv 0$ except in 0 where $u^{\text{in}}(0) = U$.

Remark 8.2.1. As we already pointed out, the standard numerical version of the OSL condition reads $\max_i w_i^n \le 1$. It may have been relaxed into $\max_i w_i^n \le K$, where K is a nonnegative constant, which does not depend on the initial data. But (8.26) implies that the quantity $\max_i w_i^{I-2}$ can be as large as we want, depending on the value of U.

Proposition 8.2.1 means in particular that, if the space step ∂_x is refined enough, the numerical OSL condition cannot be satisfied anymore, with initial data given by (8.25). Moreover, we must point out that, whatever the final time is, one can find a discretization for which the upwind scheme cannot satisfy the OSL condition, because I does not depend on T.

The initial datum u^{in} in the previous proposition is not smooth. Nevertheless, even with smooth (and periodic) initial data, the upwind scheme does not necessarily provide a solution satisfying the OSL condition, see 8.2.2.

8.2.2 Adding an artificial viscosity

As it was done in [Bou00], we now add a small viscosity term in (8.16) to obtain (8.21), and we study the numerical approximation of (8.15) and (8.21). We still deal with arbitrary 1-perodic initial data $u^{\text{in}} \ge 0$, $\rho^{\text{in}} \ge 0$.

In what follows, we consider a fixed $\varepsilon > 0$, small enough. If necessary, we regularize both u^{in} and ρ^{in} so that (keeping the same notations for both, even if they depend on ε) u^{in}, $\rho^{\text{in}} \in C^1(\mathbb{R}; \mathbb{R}_+^*)$, remain periodic and satisfy the assumptions of Theorem 8.2.2, which can be written as

$$\rho^{\text{in}}(x) \ge C\varepsilon^{1/4}, \qquad u^{\text{in}}(x) \le C, \qquad (u^{\text{in}})'(x) \le \frac{C}{\sqrt{\varepsilon}}, \qquad \forall x \in [0,1], \tag{8.27}$$

where C is a constant which does not depend on ε. The regularized ρ^{in} must lie in $\mathbb{R}_+^*$, since the continuous diffusive model involves a division by ρ.

In the following, we set

$$U = \max_{[0,1]} u^{\text{in}} > 0, \qquad V = \min_{[0,1]} u^{\text{in}} > 0,$$
$$A = \max(0, \max_{[0,1]} (u^{\text{in}})') \ge 0, \qquad R = \min_{[0,1]} \rho^{\text{in}} > 0.$$

The previous quantities can depend on ε, and must satisfy properties which come from (8.27), *i.e.*

$$R \geq C\varepsilon^{1/4}, \qquad V \leq U \leq C, \qquad A \leq \frac{C}{\sqrt{\varepsilon}}, \tag{8.28}$$

where C does not depend on ε.

Then we consider $\Delta t, \Delta x > 0$, and set

$$\lambda = \frac{\Delta t}{\Delta x}, \qquad \sigma = \frac{\Delta t}{\Delta x^2}.$$

In the remainder, we make the following assumptions on the time and space steps:

$$0 < \quad \Delta x \quad \leq \frac{2V}{1+A}, \tag{8.29}$$

$$0 < \quad \Delta t \quad \leq \min\left(\frac{1}{4A+1}, \frac{1}{4U}\Delta x, \frac{R}{4\varepsilon(1+AT)}\Delta x^2\right). \tag{8.30}$$

In fact, (8.29) and (8.30) are not so restrictive, since, eventually, Δx and Δt will go to 0, ε being fixed. From now on, even if we do not write the dependence on ε, we must keep in mind, in the numerical examples, that U, V, A and R can depend on ε and must satisfy (8.28), at least for ε small enough. That dependence implies that, at most, Δx is of order $\sqrt{\varepsilon}$ and Δt of order $\sqrt[4]{\varepsilon}$. Note that it cannot prevent Δt and Δx from going to 0 while ε remains fixed.

With the same notations for quantities at times $n\Delta t$ and $(n+1)\Delta t$ as in Section 8.2.1, we now focus on the following scheme, corresponding to the discretization of (8.15) and (8.21).

$$u_i' = u_i - \lambda\left(\frac{{u_i}^2}{2} - \frac{{u_{i-1}}^2}{2}\right) + \frac{\varepsilon\sigma}{\rho_i}(u_{i-1} + u_{i+1} - 2u_i), \tag{8.31}$$

$$\rho_i' = (1 - \lambda u_i')\rho_i + \lambda u_{i-1}'\rho_{i-1}. \tag{8.32}$$

Note that (8.31) is obtained from (8.21), which is written under a conservative form, as suggested in [BO88].

If we choose $u^{\text{in}} \equiv 1$, we can note that both upwind and diffusive schemes give $u_i^n = 1$ for any i and n, which is reassuring: in that case, and when ρ remains nonnegative, the velocity satisfies the Burgers equation, which implies, at least formally, that u remains constant.

Remark 8.2.2. The velocity terms which appear in (8.32) are the ones at time $(n+1)\Delta t$. They must not be at time $n\Delta t$ to ensure the lower bound on ρ, as we shall see in the proof of Theorem 8.2.3 below.

Numerical strategy. Let us here sum up the strategy used to build a relevant numerical solution to the pressureless gases system.

1. Consider 1-periodic initial data.
2. Fix $\varepsilon > 0$ small enough.
3. Regularize ρ^{in}, u^{in} so that they become $C^1(\mathbb{R}; \mathbb{R}_+^*)$ and satisfy (8.27).
4. Fix Δx and Δt satisfying (8.29)–(8.30).
5. Use the numerical scheme (8.31)–(8.32).

The previous strategy holds for two reasons. First, the following theorem states that the scheme (8.31)–(8.32) is L^∞-stable, consistent, monotonic, and that it satisfies the OSL condition. Consequently, (ρ_i^n) and (u_i^n) converge towards to ρ and u, solutions to the viscous pressureless gases system when both Δt and Δx go to 0, ε being fixed. Second, thanks to Theorem 8.2.2, the scheme eventually provides a good approximation of a solution to the inviscid pressureless gases system, if one chooses ε small enough, and regularized initial data in $C^1(\mathbb{R};\mathbb{R}_+^*)$ close to the original ones and satisfying (8.27). The error between the diffusive numerical and the duality solutions is currently under study, see [BM12b].

Theorem 8.2.3. *We assume that* (8.29)–(8.30) *hold. Then we have, for any i and $n \geq 0$,*

$$V \leq u_i^n \leq U, \tag{8.33}$$

$$u_i^n - u_{i-1}^n \leq \frac{A\Delta x}{1 + An\Delta t}, \tag{8.34}$$

$$\rho_i^n \geq \frac{R}{1 + An\Delta t} \geq \frac{R}{1 + AT} > 0. \tag{8.35}$$

Moreover, the discrete total mass is conserved, i.e., *for any $n \geq 0$,*

$$\sum_i \rho_i^n \Delta x = \sum_i \rho_i^0 \Delta x. \tag{8.36}$$

Finally, when $\varepsilon > 0$ is fixed, the scheme (8.31)–(8.32) *is consistent with* (8.15) *and* (8.21)*, is first order accurate in time and space, and is monotonic.*

Equations (8.33) and (8.35) respectively correspond to the maximum principles on the velocity and the density, (8.34) stands for the discrete version of the OSL condition.

Remark 8.2.3. The assumptions (8.30) on Δt ensure the stability of the scheme. More precisely, the second one is induced by the CFL condition and the third one is similar to standard stability conditions for explicit diffusive schemes. The first one is needed for the required properties of the scheme, as it will be detailed in the proof of Theorem 8.2.3.

Remark 8.2.4. Let us check the behavior of the numerical total momentum. Indeed, in its continuous version (8.21), the total momentum is conserved, since all the terms besides the time derivative of ρu are partial derivatives in x. Unfortunately, the scheme does not ensure the exact conservation of the total momentum. Nevertheless, we can write

$$\sum_i q_i' = \sum_i \rho_i u_i' + \lambda \sum_i \rho_i u_i'(u_{i+1}' - u_i'),$$

which implies the following inequalities

$$[1 - \lambda(U - V)] \sum_i \rho_i u_i' \leq \sum_i q_i' \leq \left[1 + \min\left(\frac{1}{n+1}, \lambda(U - V)\right)\right] \sum_i \rho_i u_i'.$$

Then we have to study the behavior of the quantity

$$\sum_i \rho_i u_i' = \sum_i q_i - \frac{\lambda}{2} \sum_i \rho_i ({u_i}^2 - {u_{i-1}}^2),$$

for which we have

$$\sum_i q_i - U \min\left(\frac{1}{n}, \lambda(U - V)\right) \sum_i \rho_i^0 \leq \sum_i \rho_i u_i' \leq \sum_i q_i + \lambda V(U - V) \sum_i \rho_i^0.$$

We eventually can write

$$\begin{aligned}\sum_i q_i' &\geq [1-\lambda(U-V)]\left[\sum_i q_i - U\min\left(\frac{1}{n},\lambda(U-V)\right)\sum_i \rho_i^0\right],\\ \sum_i q_i' &\leq \left[1+\min\left(\frac{1}{n+1},\lambda(U-V)\right)\right]\left[\sum_i q_i + \lambda V(U-V)\sum_i \rho_i^0\right],\end{aligned}$$

which is not really satisfactory. Nevertheless, since the time and space steps satisfy (8.30), we have

$$\lambda \leq \frac{R}{4\varepsilon(1+AT)}\Delta x,$$

which ensures that λ is small when both Δx and Δt go to 0, and $\varepsilon > 0$ is fixed. Of course, that will not prevent the numerical total momentum from varying, but, at least, from one time step to the next one, the variations have to remain small. It is interesting to note that, in the examples of the next section, the total momentum conservation almost holds, meaning that the previous estimates may be improved in some cases.

Numerical examples

As we already pointed out, a significant drawback of our scheme (8.31)–(8.32) is that it does not ensure the exact conservation of the total momentum, since it involves a scheme on the velocity and not on the momentum. Moreover, initial data with vacuum need to be regularized since our scheme cannot stand nil values of ρ. In this section, apart from checking that the OSL condition is satisfied (or not, if studying the behavior of the upwind scheme), we shall also study the numerical total momentum.

Of course, we choose the time and space steps in the following tests such that the CFL condition is satisfied when using the upwind scheme, and (8.29)–(8.30) when using the diffusive scheme.

Nil velocity almost everywhere

This test is the one described in Proposition 8.2.1 to prove that the OSL condition was eventually not satisfied by the upwind scheme. We choose $\varepsilon = 10^{-6}$. The (regularized) initial data are given by $\rho^{\text{in}} \equiv 1$ and

$$u^{\text{in}}(x) = \begin{cases} \dfrac{U+\varepsilon}{2} + \dfrac{U-\varepsilon}{2}\cos\left(\dfrac{\pi x}{\sqrt{\varepsilon}}\right) & \text{if} \quad 0 \leq x \leq \sqrt{\varepsilon},\\ \varepsilon & \text{if} \quad \sqrt{\varepsilon} \leq x \leq 1-\sqrt{\varepsilon},\\ \dfrac{U+\varepsilon}{2} - \dfrac{U-\varepsilon}{2}\cos\left[\dfrac{\pi}{\sqrt{\varepsilon}}\left(x-1+\sqrt{\varepsilon}\right)\right] & \text{if} \quad 1-\sqrt{\varepsilon} \leq x \leq 1,\end{cases}$$

We immediately check that $\min u^{\text{in}} = \varepsilon$, $\max u^{\text{in}} = U$, $\max(u^{\text{in}})' \leq \dfrac{U\pi}{2\sqrt{\varepsilon}}$ and $\min \rho^{\text{in}} = 1$. We numerically choose $U = 1$. The space step is set to $\Delta x = 10^{-4}$ on $[0,1]$, *i.e.* $I = 10^4$, and the Courant number to $\lambda = 0.25$, so that $\Delta t = 2.5\ 10^{-5}$. We perform 100 iterations in time, *i.e.* $T = 2.5\ 10^{-3}$ s. Eventually, it is clear, on Figure 8.4, that the diffusive scheme is more efficient than the upwind one regarding the OSL condition.

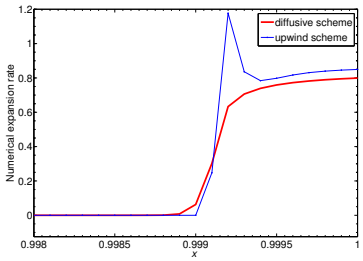

FIGURE 8.4: Positive part of the numerical expansion rate near 1 at final time T

Piecewise linear velocity

There are other situations when the upwind scheme does not satisfy the OSL condition. For instance, let us consider the following set of initial data

$$\rho^{\text{in}}(x) = 1, \qquad u^{\text{in}}(x) = 1 - x \geq 0, \qquad \forall x \in [0,1), \tag{8.37}$$

extended by 1-periodicity on $\mathbb{R}$. In both tests, we choose $T = 1.2$ and $\Delta x = 10^{-4}$.

Using the upwind scheme Using the upwind scheme implies choosing the Courant number λ so that the CFL condition holds. We set $\lambda = 0.1$, which ensures $\lambda \max u < 1$. Then, on Figure 8.5, the positive part of the numerical expansion rate w is plotted on $[0,1]$.

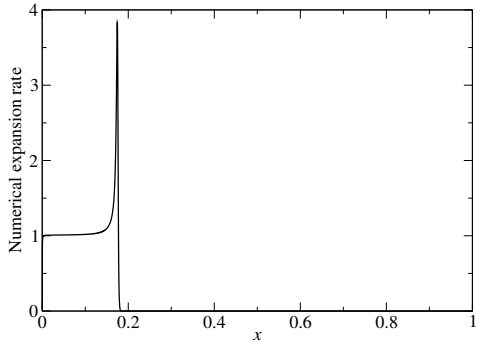

FIGURE 8.5: "Upwind" plot of w^+ at $t = 0.2\,\text{s}$ with initial data (8.37)

It is then clear that there are some values of i such that $w_i > 1$, and, in anticipation of the next paragraph, we must point out that, of course, choosing a lower Courant number does not have any effect on the behavior of the numerical expansion rate.

Using the diffusive scheme We choose $\varepsilon = 0.001$. As explained in Section 8.2.2, the initial data must be regularized: both ρ^{in} and u^{in} must be $C^1(\mathbb{R};\mathbb{R}_+^*)$, and u^{in} is regularized near 0 in order to have a reasonable periodic agreement with the value in 1, and satisfy (8.27). Since (8.29)–(8.30) must hold, it is possible to check that ($\lambda = 0.01$, $\Delta t = 10^{-6}$) is a relevant choice.

This time, the OSL condition is satisfied, as one can see on Figure 8.6 at $x = 0.1$, where the upwind scheme experiences trouble with the expansion rate for times smaller than 0.2.

Eventually, to investigate the total numerical momentum, on Figure 8.7, we show its behavior with respect to t, till T, and the result is quite convincing. On the same figure, we also show the total numerical mass, which is of course exactly conserved.

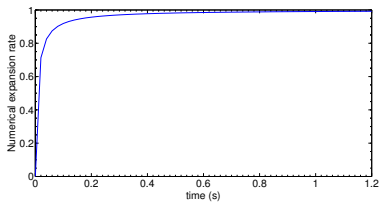

FIGURE 8.6: "Diffusive" plot of w^+ at $x = 0.1$ with regularized initial data (8.37)

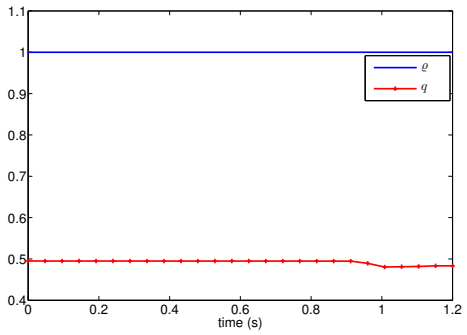

FIGURE 8.7: Numerical total mass and momentum

Chapter 9

Conclusions and Perspectives

The works presented are not the most recent: we have started studies on particles-fluid interactions when the fluid is at a supersonic regime, especially on break-up (Phd of G. Marois) and first results should soon be available: a numerical code has been developed to capture the interaction of a shock with droplets for different Mach numbers and study the influence of the break-up model on the behavior of the shock.

Bibliography

[AB79] Michael Aizenman and Thor A. Bak. "Convergence to equilibrium in a system of reacting polymers". In: *Comm. Math. Phys.* 65.3 (1979), pp. 203–230. ISSN: 0010-3616. URL: http://projecteuclid.org/getRecord?id=euclid.cmp/1103904874.

[AG91] S. Alinhac and P. Gérard. *Opérateurs pseudo-différentiels et théorème de Nash-Moser*. Interéditions/Editions du CNRS, 1991.

[Amb+08] Annalisa Ambroso et al. "The drift-flux asymptotic limit of barotropic two-phase two-pressure models." English. In: *Commun. Math. Sci.* 6.2 (2008), pp. 521–529.

[And+00a] P. Andries et al. *Numerical comparison between the Boltzmann and ES-BGK models for rarefied gases*. Tech. rep. INRIA, 2000.

[And+00b] P. Andries et al. "The Gaussian-BGK model of Boltzmann equation with small Prandtl number". In: *Eur. J. Mech. B-Fluids* (2000), pp. 813–830.

[And+00c] P. Andriès et al. "The Gaussian-BGK model of Boltzmann equation with small Prandtl number." In: *Eur. J. Mech. B/Fluids* (2000).

[And06] J. D. Anderson. *Hypersonic and high-temperature gas dynamics second edition*. American Institute of Aeronautics and Astronautics, 2006.

[AO89] A.A. Amsden and P.J. O'Rourke. *The T.A.B. method for numerical calculation of spray droplet breakup*. Tech. rep. Los Alamos National Laboratory, 1989.

[AOB89] A.A. Amsden, P.J. O'Rourke, and T.D. Butler. *Kiva II, a computer program for chemical reactive flows with spray*. Tech. rep. Los Alamos National Laboratory, 1989.

[Aok+17] Kazuo Aoki et al. "Slip Boundary Conditions for the Compressible Navier–Stokes Equations". In: *Journal of Statistical Physics* 169.4 (Nov. 2017), pp. 744–781. ISSN: 1572-9613. DOI: 10.1007/s10955-017-1886-8. URL: https://doi.org/10.1007/s10955-017-1886-8.

[Arn+89] D. Arnett et al. In: *Ann. Rev. Astron. Astrophys.* 27 (1989), p. 629.

[Aup15a] B Aupoix. "Improved heat transfer predictions on rough surfaces". In: *International Journal of Heat and Fluid Flow* 56 (2015), pp. 160–171.

[Aup15b] B Aupoix. "Roughness Corrections for the k–ω Shear Stress Transport Model: Status and Proposals". In: *Journal of Fluids Engineering* 137.2 (2015), p. 021202.

[Bar+13] C. Baranger et al. "Locally Refined Discrete Velocity Grids for Stationary Rarefied Flow Simulations". In: *Journal of Computational Physics* 257 (Oct. 2013), pp. 572–593.

[Bar+18] C. Baranger et al. "A BGK model for high temperature rarefied gas flows". In: *Work in progress* (2018).

[Bar04] C. Baranger. "Modelling of oscillations, breakup and collisions for droplets: the establishment of kernels for the T.A.B. model". In: *Math. Models Methods Appl. Sci.* 14.5 (2004), pp. 775–794. ISSN: 0218-2025.

[Bau+05] M. Baudin et al. "A relaxation method for two-phase flow models with hydrodynamic closure law". In: *Numer. Math.* 99.3 (2005). cite dans darcy law for the drift par guillard duval comme exemple de modeles de drift (A voir si il faut le mettre ou pas!), pp. 411–440. ISSN: 0029-599X. DOI: http://dx.doi.org/10.1007/s00211-004-0558-1.

[BB90] Barrett Stone Baldwin and Timothy J Barth. *A one-equation turbulence transport model for high Reynolds number wall-bounded flows*. National Aeronautics and Space Administration, Ames Research Center, 1990.

[BBT06] C. Berthon, M. Breuss, and M.-O. Titeux. "A relaxation scheme for the approximation of the pressureless Euler equations". In: *Numer. Methods Partial Differential Equations* 22.2 (2006), pp. 484–505. ISSN: 0749-159X. DOI: 10.1002/num.20108. URL: http://dx.doi.org/10.1002/num.20108.

[BC16] M. Bisi and M.J. Cáceres. "A BGK relaxation model for polyatomic gas mixtures". In: *Commun. Math. Sci.* 14.2 (Oct. 2016), pp. 297–325.

[BCG00] A. V. Bobylev, J. A. Carrillo, and I. M. Gamba. "On some properties of kinetic and hydrodynamic equations for inelastic interactions". In: *J. Statist. Phys.* 98.3-4 (2000), pp. 743–773. ISSN: 0022-4715.

[BD06] C. Baranger and L. Desvillettes. "Coupling Euler and Vlasov equations in the context of sprays : local smooth solutions." In: *J. Hyperbolic Differ. Equ.* 3 (2006), pp. 1–26.

[BDM03] L. Boudin, L. Desvillettes, and R. Motte. "A modeling of compressible droplets in a fluid". In: *Commun. Math. Sci.* 1.4 (2003), pp. 657–669. ISSN: 1539-6746.

[Ber+08] F. Berthelin et al. "A model for the formation and evolution of traffic jams". In: *Arch. Ration. Mech. Anal.* 187.2 (2008), pp. 185–220. ISSN: 0003-9527. DOI: 10.1007/s00205-007-0061-9. URL: http://dx.doi.org/10.1007/s00205-007-0061-9.

[Ber+14] A. Bernard-Champmartin et al. "Modelling of an Homogeneous Equilibrium Mixture Model (HEM)". In: *Acta Appl. Math.* 129.1 (Feb. 2014), pp. 1–21. ISSN: 0167-8019. DOI: 10.1007/s10440-013-9827-2. URL: http://dx.doi.org/10.1007/s10440-013-9827-2.

[Ber02] F. Berthelin. "Existence and weak stability for a pressureless model with unilateral constraint". In: *Math. Models Methods Appl. Sci.* 12.2 (2002), pp. 249–272. ISSN: 0218-2025. DOI: 10.1142/S0218202502001635. URL: http://dx.doi.org/10.1142/S0218202502001635.

[Bes90] D. Bestion. "The physical closure laws in the CATHARE code". In: *Nuclear Engineering and Design* 124.3 (1990), pp. 229–245. ISSN: 0029-5493. URL: http://www.sciencedirect.com/science/article/B6V4D-4816XBY-JG/2/fad4eddadd415877372936d641e67

[BG98] Y. Brenier and E. Grenier. "Sticky particles and scalar conservation laws". In: *SIAM J. Numer. Anal.* 35.6 (1998), 2317–2328 (electronic). ISSN: 0036-1429. DOI: 10.1137/S0036142997317353.

[BGK54] P.L. Bhatnagar, E.P. Gross, and M. Krook. "A model for collision processes in gases. I: Small amplitude processes in charged and neutral one-component systems." English. In: *Phys. Rev., II. Ser.* 94 (1954), pp. 511–525.

[BGP04] A. V. Bobylev, I. M. Gamba, and V. Panferov. "Moment inequalities and high-energy tails for the Boltzmann equations with inelastic interactions". In: *J. Statist. Phys.* 116.5-6 (2004), pp. 1651–1682.

[Bir94] G.A. Bird. *Molecular gas dynamics and the direct simulation of gas flows*. Oxford Science publications, 1994.

[BJ98] F. Bouchut and F. James. "One-dimensional transport equations with discontinuous coefficients". In: *Nonlinear Anal.* 32.7 (1998), pp. 891–933. ISSN: 0362-546X. DOI: 10.1016/S0362-546X(97)00536-1. URL: http://dx.doi.org/10.1016/S0362-546X(97)00536-1.

[BJ99] F. Bouchut and F. James. "Duality solutions for pressureless gases, monotone scalar conservation laws, and uniqueness". In: *Comm. Partial Differential Equations* 24.11-12 (1999), pp. 2173–2189. ISSN: 0360-5302. DOI: 10.1080/03605309908821498. URL: http://dx.doi.org/10.1080/03605309908821498.

[BJL03] F. Bouchut, S. Jin, and X. Li. "Numerical approximations of pressureless and isothermal gas dynamics". In: *SIAM J. Numer. Anal.* 41.1 (2003), 135–158 (electronic). ISSN: 0036-1429. DOI: 10.1137/S0036142901398040. URL: http://dx.doi.org/10.1137/S0036142901398040.

[BJM05] F. Bouchut, F. James, and S. Mancini. "Uniqueness and weak stability for multidimensional transport equations with one-sided Lipschitz coefficient". In: *Ann. Sc. Norm. Super. Pisa Cl. Sci. (5)* 4.1 (2005), pp. 1–25. ISSN: 0391-173X.

[BL75] Claus Borgnakke and Poul S. Larsen. "Statistical collision model for Monte Carlo simulation of polyatomic gas mixture". In: *Journal of Computational Physics* 18.4 (1975), pp. 405–420. ISSN: 0021-9991. DOI: DOI:10.1016/0021-9991(75)90094-7.

[BM12a] Laurent Boudin and Julien Mathiaud. "A numerical scheme for the one-dimensional pressureless gases system". In: *Numerical Methods for Partial Differential Equations* 28.6 (Sept. 2012), pp. 1729–1746. DOI: 10.1002/num.20700. URL: https://hal.archives-ouvertes.fr/hal-00537145.

[BM12b] Laurent Boudin and Julien Mathiaud. "Asymptotic behavior of a diffusive scheme solving the inviscid one-dimensional pressureless gases system". In: *HYP'2012 - Fourteenth International Conference on Hyperbolic Problems*. Vol. 8. AIMS Series on Applied Mathematics - Hyperbolic Problems: Theory, Numerics, Applications. Padova, Italy: AIMS, June 2012, p. 1066. URL: https://hal.inria.fr/hal-00765620.

[BO88] Y. Brenier and S. Osher. "The discrete one-sided Lipschitz condition for convex scalar conservation laws". In: *SIAM J. Numer. Anal.* 25.1 (1988), pp. 8–23. ISSN: 0036-1429. DOI: 10.1137/0725002. URL: http://dx.doi.org/10.1137/0725002.

[Bol64] L. Boltzmann. *Lectures on Gas Theory*. University of California Press, 1964. URL: https://books.google.fr/books?id=jUobO7s879EC.

[Bou+94] J.-F. Bourgat et al. "Microreversible collisions for polyatomic gases and Boltzmann's theorem". In: *Eur. J. Mech. B/Fluids* 13.2 (1994), pp. 237–254.

[Bou00] L. Boudin. "A solution with bounded expansion rate to the model of viscous pressureless gases". In: *SIAM J. Math. Anal.* 32.1 (2000), 172–193 (electronic). ISSN: 0036-1410. DOI: 10.1137/S0036141098346840. URL: http://dx.doi.org/10.1137/S0036141098346840.

[Bou94] F. Bouchut. "On zero pressure gas dynamics". In: *Advances in kinetic theory and computing*. Vol. 22. Ser. Adv. Math. Appl. Sci. World Sci. Publ., River Edge, NJ, 1994, pp. 171–190.

[Bou98] M. Boucker. "Modélisation numérique multidimensionnelle d'écoulements diphasiques liquide-gaz en régimes transitoire et permanent: méthodes et applications". PhD thesis. CMLA, Ecole normale supérieure de Cachan, 1998.

[Bre83] H. Brezis. *Analyse fonctionnelle*. Masson, 1983.

[BT85] N. Bellomo and G. Toscani. "On the Cauchy problem for the nonlinear Boltzmann equation: global existence, uniqueness and asymptotic stability". In: *J. Math. Phys.* 26.2 (1985), pp. 334–338. ISSN: 0022-2488.

[CC70] S. Chapman and T.G. Cowling. *The mathematical theory of non uniform gases*. Cambridge Mathematical Library, 1970.

[CCC09] Eric A. Carlen, José A. Carrillo, and Maria C. Carvalho. "Strong convergence towards homogeneous cooling states for dissipative Maxwell models". In: *Ann. Inst. H. Poincaré Anal. Non Linéaire* 26.5 (2009), pp. 1675–1700. ISSN: 0294-1449. DOI: 10.1016/j.anihpc.2008.10.005. URL: http://dx.doi.org/10.1016/j.anihpc.2008.10.005.

[CDM10] Aude Champmartin, Laurent Desvillettes, and Julien Mathiaud. "A BGK-type model for inelastic Boltzmann equations with internal energy." In: *Rivista di Matematica della Università di Parma* 1.2 (Dec. 2010). final version available on Riv. Mat. Univ. Parma,

Volume 1 - Number 2 - 2010., pp. 271–305. URL: https://hal.archives-ouvertes.fr/hal-00589307.

[Cer88] C. Cercignani. *The Boltzmann Equation and its Applications*. Springer-Verlag, 1988.

[CF88] P. Constantin and C. Foias. *Navier Stokes equations*. The University of Chicago Press, 1988.

[CGS07] G.L. Caraffini, M. Groppi, and G. Spiga. "On BGK approximation for reactive and nonreactive flows." English. In: *Transp. Theory Stat. Phys.* 36.4-6 (2007), pp. 475–494. DOI: 10.1080/00411450701468332.

[Cha11] Anne Champmartin. "Modeling and numerical study of two phases flow". Theses. École normale supérieure de Cachan - ENS Cachan, Feb. 2011. URL: https://tel.archives-ouvertes.fr/tel-00598571.

[CIP94] C. Cercignani, R. Illner, and M. Pulvirenti. *The mathematical theory of dilute gases*. Vol. 106. Applied Mathematical Sciences. New York: Springer-Verlag, 1994, pp. viii+347. ISBN: 0-387-94294-7.

[CKR07] A. Chertock, A. Kurganov, and Yu. Rykov. "A new sticky particle method for pressureless gas dynamics". In: *SIAM J. Numer. Anal.* 45.6 (2007), 2408–2441 (electronic). ISSN: 0036-1429. DOI: 10.1137/050644124. URL: http://dx.doi.org/10.1137/050644124.

[Col37] Colebrook. "Experiments with fluid friction in roughened pipes". In: *Proceedings of the Royal Society of London A: Mathematical, Physical and Engineering Sciences* 161.906 (1937), pp. 367–381. ISSN: 0080-4630. DOI: 10.1098/rspa.1937.0150. eprint: http://rspa.royalsocietypublishing.org/content/161/906/367.full.pdf. URL: http://rspa.royalsocietypublishing.org/content/161/906/367.

[Cou06] J.-F. Coulombel. "From gas dynamics to pressureless gas dynamics". In: *Proc. Amer. Math. Soc.* 134.3 (2006), 683–688 (electronic). ISSN: 0002-9939. DOI: 10.1090/S0002-9939-05-08087-1. URL: http://dx.doi.org/10.1090/S0002-9939-05-08087-1.

[Cou89] J. Cousteix. *Turbulence et couche limite*. Cepadues, Sept. 1989.

[DAA13] G. Duffa, American Institute of Aeronautics, and Astronautics. *Ablative Thermal Protection Systems Modeling*. AIAA education series. American Institute of Aeronautics and Astronautics, Incorporated, 2013. ISBN: 9781624101717. URL: https://books.google.fr/books?id=0MvjMgEACAAJ.

[DC91] J. Delery and M.-C. Coet. "Experiments on Shock-Wave/Boundary-Layer Interactions Produced by Two-Dimensional Ramps and Three-Dimensional Obstacles". In: *Hypersonic Flows for Reentry Problems*. Ed. by Jean-Antoine Désidéri, Roland Glowinski, and Jacques Périaux. Berlin, Heidelberg: Springer Berlin Heidelberg, 1991, pp. 97–128. ISBN: 978-3-642-76527-8.

[Des97a] L. Desvillettes. "Sur un modèle de type Borgnakke-Larsen conduisant à des lois d'énergie non linéaires en température pour les gaz parfaits polyatomiques". In: *Ann. Fac. Sci. Toulouse Math. (6)* 6.2 (1997), pp. 257–262. ISSN: 0240-2955.

[Des97b] Laurent Desvillettes. "Sur un modèle de type Borgnakke—Larsen conduisant à des lois d'énergie non linéaires en température pour les gaz parfaits polyatomiques". fre. In: *Annales de la Faculté des sciences de Toulouse : Mathématiques* 6.2 (1997), pp. 257–262. URL: http://eudml.org/doc/73419.

[DL13] Giacomo Dimarco and Raphaël Loubere. "Towards an ultra efficient kinetic scheme. Part I: Basics on the BGK equation". In: *Journal of Computational Physics* 255 (2013), pp. 680–698. ISSN: 0021-9991. DOI: https://doi.org/10.1016/j.jcp.2012.10.058. URL: http://www.sciencedirect.com/science/article/pii/S0021999112006870.

[DL89] R. J. DiPerna and P.-L. Lions. "On the Cauchy problem for Boltzmann equations: global existence and weak stability". In: *Ann. of Math. (2)* 130.2 (1989), pp. 321–366. ISSN: 0003-486X.

[DLY99] S. B. Dalziel, P. F. Linden, and D. L. Youngs. "Self-similarity and internal structure of turbulence induced by Rayleigh-Taylor instability". In: *J. Fluid Mech.* 399 (1999), pp. 1–48. ISSN: 0022-1120.

[DM10] Laurent Desvillettes and Julien Mathiaud. "Some Aspects of the Asymptotics Leading fromGas-Particles Equations Towards Multiphase Flows Equations". In: *Journal of Statistical Physics* 141.1 (Oct. 2010), pp. 120–141. ISSN: 1572-9613. DOI: 10.1007/s10955-010-0044-3. URL: https://doi.org/10.1007/s10955-010-0044-3.

[DM99] B. Dubroca and L. Mieussens. "A conservative and entropic discrete-velocity model for rarefied polyatomic gases". In: *ESAIM Proceedings* 10 (CEMRACS 1999), pp. 127–139.

[DMS05] L. Desvillettes, R. Monaco, and F. Salvarani. "A kinetic model allowing to obtain the energy law of polytropic gases in the presence of chemical reactions". In: *European Journal of Mechanics - B/Fluids* 24.2 (2005), pp. 219–236. ISSN: 0997-7546. DOI: http://dx.doi.org/10.1016/j.euromechflu.2004.07.004. URL: http://www.sciencedirect.com/science/article/pii/S0997754604000858.

[DMV03] G. Dufour, M. Massot, and P. Villedieu. "Étude d'un modèle de fragmentation secondaire pour les brouillards de gouttelettes". In: *C. R. Math. Acad. Sci. Paris* 336.5 (2003), pp. 447–452. ISSN: 1631-073X.

[DR99] K. Domelevo and J-M. Roquejoffre. "Existence and stability of travelling wave solutions in a kinetic model of two-phase flows". In: *Comm. Partial Differential Equations* 24.1-2 (1999), pp. 61–108. ISSN: 0360-5302.

[Duf05] G. Dufour. "Modélisation multi-fluide eulérienne pour les écoulements diphasiques à inclusions dispersées". PhD thesis. Université Paul Sabatier Toulouse III, 2005.

[Duk80] John K. Dukowicz. "A particle-fluid numerical model for liquid sprays". In: *Journal of Computational Physics* 35.2 (1980), pp. 229–253. ISSN: 0021-9991. DOI: DOI:10.1016/0021-9991(80)90087-X. URL: http://www.sciencedirect.com/science/article/B6WHY-4DDR2JN-42/2/5187f201a834708d01db14da4b1deba1.

[ERS96] W. E, Yu. G. Rykov, and Ya. G. Sinai. "Generalized variational principles, global weak solutions and behavior with random initial data for systems of conservation laws arising in adhesion particle dynamics". In: *Comm. Math. Phys.* 177.2 (1996), pp. 349–380. ISSN: 0010-3616. URL: http://projecteuclid.org/getRecord?id=euclid.cmp/1104286332.

[FM05] N. Fournier and S. Mischler. "A spatially homogeneous Boltzmann equation for elastic, inelastic and coalescing collisions". In: *J. Math. Pures Appl. (9)* 84.9 (2005), pp. 1173–1234. ISSN: 0021-7824.

[Gal09] Thomas Galié. "Couplage interfacial de modèles en dynamique des fluides. Application aux écoulements diphasiques." PhD thesis. U, Mar. 2009.

[GBK54] E.P. Gross, P.L. Bhatnagar, and M. Krook. "A model for collision processes in gases." In: *Physical review* 94.3 (1954), pp. 511–525.

[GD07] H. Guillard and F. Duval. "A Darcy law for the drift velocity in a two-phase flow model". In: *Journal of Computational Physics* 224.1 (2007), pp. 288–313. ISSN: 0021-9991. DOI: DOI:10.1016/j.jcp.2007.02.025. URL: http://www.sciencedirect.com/science/article/B6WHY-4N7RWF1-1/2/5337b6f7c2474dc9ac6a7ee9c7b575cf.

[GHP91] E. Guyon, J.-P. Hulin, and L. Petit. *Hydrodynamique physique*. Intereditions,Editions du C.N.R.S., 1991.

[GHS04] T. Gallouët, J-M. Hérard, and N. Seguin. "Numerical modeling of two-phase flows using the two-fluid two-pressure approach". In: *Math. Models Methods Appl. Sci.* 14.5 (2004), pp. 663–700. ISSN: 0218-2025.

[GJ00] L. Gosse and F. James. "Numerical approximations of one-dimensional linear conservation equations with discontinuous coefficients". In: *Math. Comp.* 69.231 (2000),

pp. 987–1015. ISSN: 0025-5718. DOI: 10.1090/S0025-5718-00-01185-6. URL: http://dx.doi.org/10.1090/S0025-5718-00-01185-6.

[GJ12] Hossein Gorji and Patrick Jenny. "A Kinetic Model for Gas Mixtures Based on a Fokker-Planck Equation". In: *Journal of Physics: Conference Series* 362.1 (2012), pp. 012042–.

[GJ13] M. Hossein Gorji and Patrick Jenny. "A Fokker-Planck based kinetic model for diatomic rarefied gas flows". In: *Physics of fluids* 25.6 (June 2013), pp. 062002–.

[GJV02] Thierry Goudon, Pierre-Emmanuel Jabin, and Alexis Vasseur. "Limites hydrodynamiques pour les équations de Vlasov-Stokes". In: *Journées "Équations aux Dérivées Partielles" (Forges-les-Eaux, 2002)*. Nantes: Univ. Nantes, 2002, Exp. No. VII, 15.

[GK02] M. Groppi and W. Koller. "Kinetic calculations for chemical reactions and inelastic transitions in a gas mixture". In: *Zeitschrift fur Angewandte Mathematik und Physik (ZAMP)* 5 (Sept. 2002), pp. 855–876. DOI: 10.1007/s00033-002-8186-z. URL: http://www.springerlink.com/content/D79AWDNJNYU45BGG.

[GO01] C. Garcia Vazquez and F. Ortegon Gallego. "Sur un problème elliptique non linéaire avec diffusion singulière et second membre dans L1". In: *C.r. Acad. sci.* 332 (2001), pp. 145–150.

[Gol05] François Golse. "The Boltzmann equation and its hydrodynamic limits". In: *Evolutionary equations. Vol. II*. Handb. Differ. Equ. Elsevier/North-Holland, Amsterdam, 2005, pp. 159–301.

[GPV04] I. M. Gamba, V. Panferov, and C. Villani. "On the Boltzmann equation for diffusively excited granular media". In: *Comm. Math. Phys.* 246.3 (2004), pp. 503–541. ISSN: 0010-3616.

[Gre95] E. Grenier. "Existence globale pour le système des gaz sans pression". In: *C. R. Acad. Sci. Paris Sér. I Math.* 321.2 (1995), pp. 171–174. ISSN: 0764-4442.

[Gri92] Christopher Grigson. "Drag losses of new ships caused by hull finish". In: *Journal of Ship Research* 36.2 (1992). cited By 28, pp. 182–196.

[GS04] François Golse and Laure Saint-Raymond. "The Navier–Stokes limit of the Boltzmann equation for bounded collision kernels". In: *Inventiones mathematicae* 155.1 (Jan. 2004), pp. 81–161. ISSN: 1432-1297. DOI: 10.1007/s00222-003-0316-5. URL: https://doi.org/10.1007/s00222-003-0316-5.

[GS05] I. Gallagher and L. Saint-Raymond. "On pressureless gases driven by a strong inhomogeneous magnetic field". In: *SIAM J. Math. Anal.* 36.4 (2005), 1159–1176 (electronic). ISSN: 0036-1410. DOI: 10.1137/S0036141003435540. URL: http://dx.doi.org/10.1137/S0036141003435540.

[GTJ11] M.H. Gorji, M. Torrilhon, and Patrick Jenny. "Fokker–Planck model for computational studies of monatomic rarefied gas flows". In: *Journal of fluid mechanics* 680 (Aug. 2011), pp. 574–601.

[Guo02] Y. Guo. "The Landau equation in a periodic box". In: *Comm. Math. Phys.* 231.3 (2002), pp. 391–434. ISSN: 0010-3616.

[Guo03] Y. Guo. "Classical solutions to the Boltzmann equation for molecules with an angular cutoff". In: *Arch. Ration. Mech. Anal.* 169.4 (2003), pp. 305–353. ISSN: 0003-9527.

[Haf83] P.K. Haff. "Grain flow as a fluid mechanical phenomenon". In: *J. Fluid. Mech.* 134 (1983).

[Ham98] K. Hamdache. "Global existence and large time behavior of solutions for the Vlasov-Stokes equations". In: *Japan J. Indust. Appl. Math. 15,1* (1998).

[Han60] C. F. Hansen. "Approximations for the thermodynamic and transport properties of high-temperature air". In: *Nasa* (1960).

[HF92] L.P. Hsiang and G.M. Faeth. "Near-limit drop deformation and secondary breakup". In: *International Journal of Multiphase Flow* 18.5 (1992), pp. 635–652.

[HF95] L.P. Hsiang and G.M. Faeth. "DROP DEFORMATION AND BREAKUP DUE TO SHOCK-WAVE AND STEADY DISTURBANCES". In: *International Journal of Multiphase Flow* 21.5 (1995), pp. 545–560.

[HI03] Takashi Hibiki and Mamoru Ishii. "One-dimensional drift-flux model and constitutive equations for relative motion between phases in various two-phase flow regimes". In: *International Journal of Heat and Mass Transfer* 46.25 (2003), pp. 4935–4948. ISSN: 0017-9310. DOI: DOI:10.1016/S0017-9310(03)00322-3. URL: http://www.sciencedirect.com/science/article/B6V3H-497H7J5-3/2/e082d5822e325e6e14160ac3cb77bdea.

[Hof83] D. Hoff. "The sharp form of Oleinik's entropy condition in several space variables". In: *Trans. Amer. Math. Soc.* 276.2 (1983), pp. 707–714. ISSN: 0002-9947. DOI: 10.2307/1999078. URL: http://dx.doi.org/10.2307/1999078.

[HVW80] J Hill, R Voisinet, and D Wagner. "Measurements of surface roughness effects on the heat transfer to slender cones at Mach 10". In: *18th Aerospace Sciences Meeting*. 1980, p. 345.

[Hyl99] J. Hylkema. "Modélisation cinétique et simulation numérique d'un brouillard dense de gouttelettes. Application aux propulseurs à poudre". PhD thesis. Ecole nationale supérieure de l'aéronautique et de l'espace (Toulouse), 1999.

[IH06] Mamoru Ishii and Takashi Hibiki. *Thermo-fluid dynamics of two-phase flow*. With a foreword by Lefteri H. Tsoukalas. New York: Springer, 2006, pp. xvi+462. ISBN: 978-0-387-28321-0; 0-387-28321-8.

[IS84] R. Illner and M. Shinbrot. "The Boltzmann equation: global existence for a rare gas in an infinite vacuum". In: *Comm. Math. Phys.* 95.2 (1984), pp. 217–226. ISSN: 0010-3616.

[Ish75] M. Ishii. *Thermo-fluid dynamic theory of two-phase flow*. Eyrolles, Paris, 1975, p. 248.

[J M00] A. Santos J. Maria Montanero. "Computer simulation of uniformly heated granular fluids". In: *Granular Matter* 2 (mai 2000), pp. 53–64.

[JTH10] Patrick Jenny, Manuel Torrilhon, and Stefan Heinz. "A solution algorithm for the fluid dynamic equations based on a stochastic model for molecular motion". In: *Journal of computational physics* 229.4 (2010), pp. 1077–1098.

[KMC90] R. I. Klein, C. F. McKee, and P. Colella. "In The Evolution of Interstellar Medium". In: *L. Blitz, Ed., Astronomical Society of the Pacific Conference Series* 12 (1990), p. 117.

[KMC94] R. I. Klein, C. F. McKee, and P. Colella. "The Hydrodynamic Interaction of Shock Waves with Interstellar Clouds. I. Nonradiative Shocks in Small Clouds." In: *Ap. J.* 420 (1994), p. 213.

[KMN79] S. Kawashima, A. Matsumura, and T. Nishida. "On the fluid-dynamical approximation to the Boltzmann equation at the level of the Navier-Stokes equation". In: *Comm. Math. Phys.* 70.2 (1979), pp. 97–124. ISSN: 0010-3616.

[Kum+89] T. Kumagai et al. "Gamma-Rays, X-Rays and Optical Light from the Cobalt and the Neutron Star in SN 1987A". In: *Ap. J.* 345 (1989), pp. 412–422.

[Lap+98] Bernard Lapeyre et al. *Méthodes de Monte-Carlo pour les équations de transport et de diffusion*. Mathématiques et applications. Cet ouvrage est une version remaniée des notes d'un cours présenté par les auteurs en préliminaire au 25e Congrès d'analyse numérique, les 22 et 23 mai 1993. Berlin: Springer, 1998. ISBN: 3-540-63393-6. URL: http://opac.inria.fr/record=b1080218.

[Las05] S. Lasserre. "Contribution à l'étude mathématique et numérique des solutions à support compact pour les modèles de turbulence compressible". PhD thesis. University of Paris VI, 2005.

[Lau02] F. Laurent. "Modélisation mathématique et numérique de la combustion de brouillards de gouttes polydispersés". PhD thesis. Université Claude Bernard (Lyon), 2002.

[LB03] A. Llor and P. Bailly. "A new turbulent two-field concept for modeling Rayleigh-Taylor, Richtmyer-Meshkov, and Kelvin-Helmholtz mixing layers". In: *Laser and particle beams* 21-3 (2003), pp. 305–315.

[Lev+17] C. Levet et al. "Microstructure and gas-surface interaction studies of a 3D carbon/carbon composite in atmospheric entry plasma". In: *Carbon* 114.Supplement C (2017), pp. 84–97. ISSN: 0008-6223. DOI: https://doi.org/10.1016/j.carbon.2016.11.054. URL: http://www.sciencedirect.com/science/article/pii/S0008622316310284.

[LeV04] R. J. LeVeque. "The dynamics of pressureless dust clouds and delta waves". In: *J. Hyperbolic Differ. Equ.* 1.2 (2004), pp. 315–327. DOI: 10.1142/S0219891604000135.

[Lev17] Cyril Levet. "Ablation of carbonaceous materials under high flux : multi physics study of the interaction between the material and the flow". Theses. Université de Bordeaux, Apr. 2017. URL: https://tel.archives-ouvertes.fr/tel-01528576.

[LeV92] R. J. LeVeque. *Numerical methods for conservation laws*. Second. Lectures in Mathematics ETH Zürich. Basel: Birkhäuser Verlag, 1992, pp. x+214. ISBN: 3-7643-2723-5.

[Lew93] R. Lewandowski. "Modèles de turbulence et équations paraboliques". In: *C. R. Acad. Sci. Paris* 317.Série I (1993), pp. 835–840.

[Lio94] P.-L. Lions. "Compactness in Boltzmann's equation via Fourier integral operators and applications. III". In: *JMKU* 48 (3 1994), pp. 539–584.

[Lio96] P.-L. Lions. *Mathematical topics in fluid mechanics . vol. 1 , Incompressible models*. Clarendon Press, 1996.

[LM93] R. Lewandowski and B. Mohammadi. "Existence and positivity results for the ϕ-θ and a modified k-ϵ two-equation turbulence models". In: *Math. Models Methods Appl. Sci.* 3.2 (1993), pp. 195–215. ISSN: 0218-2025.

[LO08] P. Worth Longest and Michael J. Oldham. "Numerical and experimental deposition of fine respiratory aerosols: Development of a two-phase drift flux model with near-wall velocity corrections". In: *Journal of Aerosol Science* 39.1 (2008), pp. 48–70. ISSN: 0021-8502. DOI: DOI:10.1016/j.jaerosci.2007.10.001. URL: http://www.sciencedirect.com/science/article/B6V6B-4PW05FC-1/2/c927591111db765030760eae4dbada5

[Low66] Jr. Lowell H. Holway. "New Statistical Models for Kinetic Theory: Methods of Construction". In: *Physics of Fluids* 9.9 (1966), pp. 1658–1673. DOI: 10.1063/1.1761920. URL: http://link.aip.org/link/?PFL/9/1658/1.

[LS72] B.E. Launder and D.B. Spalding. *Mathematical models of turbulence*. Academic press, 1972.

[Maj84] A. Majda. *Compressible fluid flow and systems of conservation laws in several space variables*. Springer-Verlag, 1984.

[Mam79] Novak Zuber Mamoru Ishii. "Drag coefficient and relative velocity in bubbly, droplet or particulate flows". In: *AIChE Journal* 25 , Issue 5 (1979), pp. 843–855.

[Mas96] M. Massot. "Modélisation mathématique et numérique de la combustion des mélaanges gazeux". PhD thesis. Université Claude Bernard (Lyon), 1996.

[Mat03] J. Mathiaud. "Différents aspects du modèle k-epsilon". MA thesis. ENS Lyon, 2003.

[Mat06] J. Mathiaud. "Etude de système de type gaz-particules." PhD thesis. CMLA, Ecole normale supérieure de Cachan, 2006.

[Mat07] Julien Mathiaud. *Ordres de grandeur pour le passage d'un modèle gaz-particules vers un modèle HEM*. Tech. rep. CEA DAM DIF, 2007.

[Mat08] Julien Mathiaud. "Local smooth solutions of the incompressible K-ε model and the low turbulent diffusion limit". In: *Communications in Mathematical Sciences* 6.2 (2008), pp. 361–383.

[Mat10] Julien Mathiaud. "Local smooth solutions of a thin spray model with collisions". In: *Mathematical Models and Methods in Applied Sciences* 20.02 (2010), pp. 191–221. DOI: 10.1142/S0218202510004192. eprint: http://www.worldscientific.com/doi/pdf/

10.1142/S0218202510004192. URL: http://www.worldscientific.com/doi/abs/10.1142/S0218202510004192.

[Men92] F. R. Menter. "Improved two-equation k-omega turbulence models for aerodynamic flows". In: *NASA STI/Recon Technical Report N* 93 (Oct. 1992), p. 22809.

[MG99] M.Groppi and G.Spiga. "Kinetic approach to chemical reactions and inelastic transitions in a rarefied gas". In: *Journal of Mathematical Chemistry* 26-Issue1 (1999), pp. 197–219. DOI: 10.1023/A:1019194113816. URL: http://www.springerlink.com/content/U324087V545141GQ.

[Mie00] L. Mieussens. "Discrete-velocity Models and Numerical Schemes for the Boltzmann-BGK Equation in plane and axisymmetric geometries". In: *Journal of Computational Physics* 162 (2000), pp. 429–466.

[Mie99] L. Mieussens. "Modèles à Vitesses Discrètes et Méthodes Numériques pour l'Equation de Boltzmann-BGK". Thèse. Université de Bordeaux I, 1999.

[ML82] Finson M.L. *Study of turbulent boundary layers over rough surfaces, with emphasis on the effects of roughness character and mach number*. Tech. rep. DTIC, 1982.

[MM06] S. Mischler and C. Mouhot. "Cooling process for inelastic Boltzmann equations for hard spheres. II. Self-similar solutions and tail behavior". In: *J. Stat. Phys.* 124.2-4 (2006), pp. 703–746. ISSN: 0022-4715. DOI: 10.1007/s10955-006-9097-8. URL: http://dx.doi.org/10.1007/s10955-006-9097-8.

[MM16] J. Mathiaud and L. Mieussens. "A Fokker–Planck Model of the Boltzmann Equation with Correct Prandtl Number". In: *Journal of Statistical Physics* 162.2 (Jan. 2016), pp. 397–414. ISSN: 1572-9613. DOI: 10.1007/s10955-015-1404-9. URL: https://doi.org/10.1007/s10955-015-1404-9.

[MM17] J. Mathiaud and L. Mieussens. "A Fokker–Planck Model of the Boltzmann Equation with Correct Prandtl Number for Polyatomic Gases". In: *Journal of Statistical Physics* 168.5 (Sept. 2017), pp. 1031–1055. ISSN: 1572-9613. DOI: 10.1007/s10955-017-1837-4. URL: https://doi.org/10.1007/s10955-017-1837-4.

[MM18] J. Mathiaud and L. Mieussens. "Vibrational models of Boltzmann equation with correct second principle: BGK and Fokker-Planck". In: *Work in progress* (2018).

[MMR06] S. Mischler, C. Mouhot, and M. Rodriguez Ricard. "Cooling process for inelastic Boltzmann equations for hard spheres. I. The Cauchy problem". In: *J. Stat. Phys.* 124.2-4 (2006), pp. 655–702. ISSN: 0022-4715. DOI: 10.1007/s10955-006-9096-9. URL: http://dx.doi.org/10.1007/s10955-006-9096-9.

[Mon+88] J.L. Montagné et al. "Hypersonic Blunt Body Computations Including Real Gas Effects". In: *NASA Technical Memorandum* 100074 (Mar. 1988).

[MP94] B. Mohammadi and O. Pironneau. *Analysis of the k-ε Turbulence Model*. Masson, 1994.

[MP97] S. Mischler and B. Perthame. "Boltzmann equation with infinite energy: renormalized solutions and distributional solutions for small initial data and initial data close to a Maxwellian". In: *SIAM J. Math. Anal.* 28.5 (1997), pp. 1015–1027. ISSN: 0036-1410.

[MR16] Julien Mathiaud and Xavier Roynard. "Local Smooth Solutions of the Incompressible k-ω Model". In: *Acta Applicandae Mathematicae* 146.1 (Dec. 2016), pp. 1–16. DOI: 10.1007/s10440-016-0054-5. URL: https://doi.org/10.1007/s10440-016-0054-5.

[MV01] M. Massot and P. Villedieu. "Modélisation multi-fluide eulérienne pour la simulation de brouillards denses polydispersés". In: *C. R. Acad. Sci. Paris Sér. I Math.* 332.9 (2001), pp. 869–874. ISSN: 0764-4442.

[NBK86] W.-F. Ng, T.J. Benson, and W.G. Kunik. "Real gas effects on the numerical simulation of a hypersonic inlet". In: *Journal of Propulsion and Power* 2.4 (1986), pp. 381–382.

[Nik50] Johann Nikuradse. *Laws of flow in rough pipes*. National Advisory Committee for Aeronautics Washington, 1950.

[NT08] T. Nguyen and A. Tudorascu. "Pressureless Euler/Euler-Poisson systems via adhesion dynamics and scalar conservation laws". In: *SIAM J. Math. Anal.* 40.2 (2008), pp. 754–775. ISSN: 0036-1410. DOI: 10.1137/070704459. URL: http://dx.doi.org/10.1137/070704459.

[Ola+17] M Olazabal-Loumé et al. "Study on k-ω shear stress transport model corrections applied to rough wall turbulent hypersonic boundary layers". In: (2017).

[ORo81] P. O'Rourke. "Collective drop effects on vaporizing liquid sprays". PhD thesis. Princeton University, 1981.

[OZS09] Peter J. O'Rourke, Paul (Pinghua) Zhao, and Dale Snider. "A model for collisional exchange in gas/liquid/solid fluidized beds". In: *Chemical Engineering Science* 64.8 (2009), pp. 1784–1797. ISSN: 0009-2509. DOI: DOI:10.1016/j.ces.2008.12.014.

[Pan06] Roxana Panescu. "Modélisation Eulerienne d'écoulements diphasiques à phase dispersée et simulation numérique par une méthode volumes - éléments finis". PhD thesis. Université de Nice Sophia Antipolis, 2006.

[Pou02] F. Poupaud. "Diagonal defect measures, adhesion dynamics and Euler equation". In: *Methods Appl. Anal.* 9.4 (2002), pp. 533–561. ISSN: 1073-2772.

[PR04] L. Pareschi and G. Russo. *An introduction to the numerical analysis of the Boltzmann equation in Summer School on methods and models of kinetic theory*. Rivista di Matematica della Università di Parma, 2004.

[PR97] F. Poupaud and M. Rascle. "Measure solutions to the linear multi-dimensional transport equation with non-smooth coefficients". In: *Comm. Partial Differential Equations* 22.1-2 (1997), pp. 337–358. ISSN: 0360-5302. DOI: 10.1080/03605309708821265. URL: http://dx.doi.org/10.1080/03605309708821265.

[Ram00] D. Ramos. "Quelques résultats mathématiques et simulations numériques d'écoulements régis par des modèles bifluides". PhD thesis. CMLA, Ecole normale supérieure de Cachan, 2000.

[Rov06] J.M. Rovarch. "Un solveur volume fini 3D pour les écoulements diphasiques". PhD thesis. CMLA, Ecole normale supérieure de Cachan, 2006.

[RS16] B. Rahimi and H. Struchtrup. "Macroscopic and kinetic modelling of rarefied polyatomic gases". In: *Journal of Fluid Mechanics* 806 (2016), pp. 437–505.

[RT04] E. Romenski and E. F. Toro. *Compressible Two-Phase Flows: Two-Pressure Models and Numerical Methods*. Tech. rep. C'est à citer pour un aperçu des différents types de modèles bifuides existants à deux pressions. Laboratory of Applied Mathematics, Faculty of Engineering, 38050, University of Trento, Italy: Isaac Newton Institute for Mathematical Sciences,Cambridge University, UK, 2004.

[SA92] PHILLIPE R Spalart and Steven R Allmaras. "A one-equation turbulence model for aerodynamic flows". In: (1992).

[Sai03] Laure Saint-Raymond. "Convergence of Solutions to the Boltzmann Equation in the Incompressible Euler Limit". In: *Archive for Rational Mechanics and Analysis* 166.1 (Jan. 2003), pp. 47–80. ISSN: 1432-0673. DOI: 10.1007/s00205-002-0228-3. URL: https://doi.org/10.1007/s00205-002-0228-3.

[Sai95] L. Sainsaulieu. *Contribution à la modélisation mathématique et numérique des écoulements diphasiques constitués d'un nuage de particules dans un écoulement de gaz. Habilitation à diriger des recherches*. Université Paris VI. 1995.

[San03] A. Santos. "Transport coefficients of d-dimensional inelastic Maxwell models". In: *Physica A: Statistical Mechanics and its Applications* 321.3-4 (2003), pp. 442–466. ISSN: 0378-4371. DOI: DOI:10.1016/S0378-4371(02)01005-1. URL: http://www.sciencedirect.com/science/article/B6TVG-464P5B9-K/2/27b0df17b06d8b2fcbee66d236a09a9f.

[Sch37] Hermann Schlichting. "Experimental investigation of the problem of surface roughness". In: (1937).

[SEL04] A. Sokolichin, G. Eigenberger, and A. Lapin. "Simulation of buoyancy driven bubbly flow: Established simplifications and open questions." In: *AIChE Journal* 50 (2004), pp. 24–45. DOI: 10.1002/aic.10003.

[Ser96a] D. Serre. *Systèmes de lois de conservation I*. Diderot, 1996.

[Ser96b] D. Serre. *Systèmes de lois de conservation II*. Diderot, 1996.

[Sev01] M. Sever. "An existence theorem in the large for zero-pressure gas dynamics". In: *Differential Integral Equations* 14.9 (2001), pp. 1077–1092. ISSN: 0893-4983.

[SM95] C. M. Sheppard and S. D. Morris. "Drift-flux correlation disengagement models: Part I – Theory: Analytic and numeric integration details". In: *Journal of Hazardous Materials* 44.2-3 (1995), pp. 111–125. ISSN: 0304-3894. DOI: DOI:10.1016/0304-3894(95)00051-U. URL: http://www.sciencedirect.com/science/article/B6TGF-3YS900C-1/2/f2b05505adde8f0881a91617db5fc725.

[SW84] H.B. Stewart and B. Wendroff. "Two-phase flow: Models and methods". In: *J. Comput. Phys.* 56:3 (1984), pp. 363–409.

[Tay96a] M. Taylor. *Partial differential equations, basic theory*. Springer, 1996.

[Tay96b] M. Taylor. *Partial differential equations III, non linear equations*. Springer, 1996.

[Tha+00] F. Thais et al. *The Astrolab experiment: Rayleigh-Taylor instabilities in supernova*. Elsevier, 2000.

[UA82] S. Ukai and K. Asano. "On the Cauchy problem of the Boltzmann equation with a soft potential". In: *Publ. Res. Inst. Math. Sci.* 18.2 (1982), 477–519 (57–99). ISSN: 0034-5318.

[VH97] P. Villedieu and J. Hylkema. "Une méthode particulaire aléatoire reposant sur une équation cinétique pour la simulation numérique des sprays denses de gouttelettes liquides". In: *C. R. Acad. Sci. Paris Sér. I Math.* 325.3 (1997), pp. 323–328. ISSN: 0764-4442.

[Vig+10] G. L. Vignoles et al. "Effective Surface Recession Laws for the Physico-Chemical Ablation of C/C Composite Materials". In: *Mechanical Properties and Performance of Engineering Ceramics and Composites V*. John Wiley and Sons, Inc., 2010, pp. 351–360. ISBN: 9780470944127. DOI: 10.1002/9780470944127.ch33. URL: http://dx.doi.org/10.1002/9780470944127.ch33.

[Vil02] C. Villani. *A review of mathematical topics in collisional kinetic theory*. Elsevier Science, 2002.

[Vil06] C. Villani. "Mathematics of Granular Materials". In: *Journal of Statistical Physics* 124 (2006), pp. 781–822.

[Wil08] David C Wilcox. "Formulation of the kw Turbulence Model Revisited". In: *AIAA journal* 46.11 (2008), pp. 2823–2838.

[Wil93] D.C. Wilcox. "A two-equation turbulence model for wall-bounded and free-shear flows". In: *1993 AIAA 24 th Fluid Dynamics Conference*. 1993.

[Wil94] D.C. Wilcox. *Turbulence Modeling for CFD*. DCW Industries, Incorporated, 1994.

[You84] David L. Youngs. "Numerical simulation of turbulent mixing by Rayleigh-Taylor instability". In: *Physica D: Nonlinear Phenomena* 12.1-3 (1984), pp. 32–44. ISSN: 0167-2789. DOI: DOI:10.1016/0167-2789(84)90512-8. URL: http://www.sciencedirect.com/science/article/B6TVK-46M72XV-6/2/3f43e8860d1777f1cc7109e5e3ce2462.

[You89] David L. Youngs. "Modelling turbulent mixing by Rayleigh-Taylor instability". In: *Physica D: Nonlinear Phenomena* 37.1-3 (1989), pp. 270–287. ISSN: 0167-2789. DOI: DOI:10.1016/0167-2789(89)90135-8. URL: http://www.sciencedirect.com/science/article/B6TVK-46TYX7P-1B/2/a575aa77acf01c919da34f80ca6a11f9.

[Zel70] Ya.B. Zel'dovich. "Gravitational instability: An approximate theory for large density perturbations". In: *Astron. and Astrophys.* 5 (1970), pp. 84–89.

List of Figures